CHALMERS
UNIVERSITY OF TECHNOLOGY

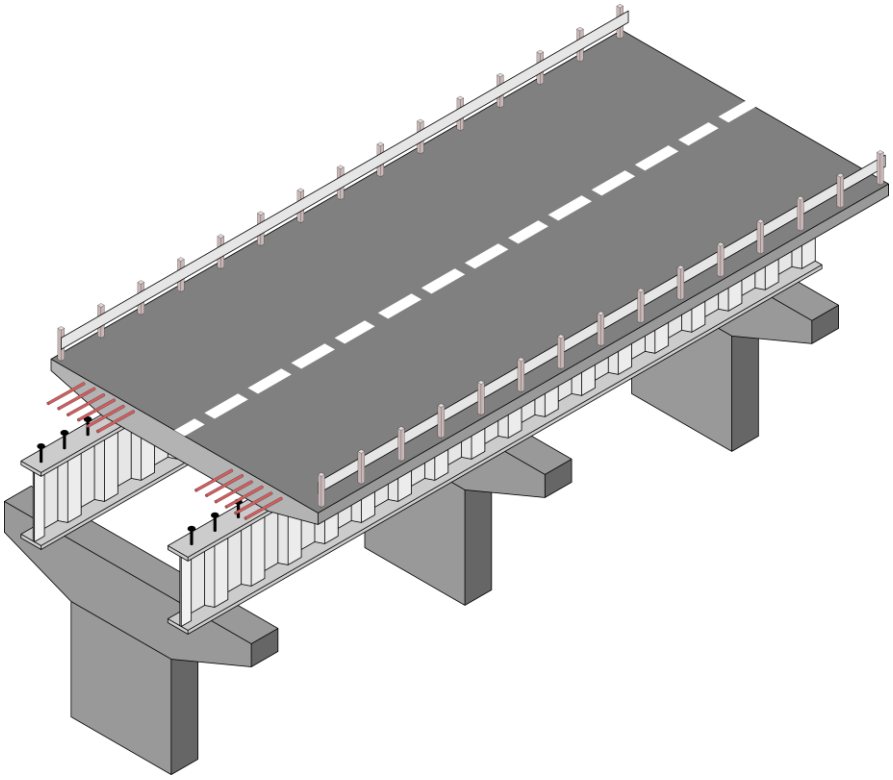

Design of Continuous Composite Road Bridges

Bridge girders with corrugated webs in stainless steel

Master's thesis in the Master's program Structural engineering and building technology

JULIA STEFFNER
MICHAELA ÖMAN

DEPARTMENT OF ARCHITECTURE AND CIVIL ENGINEERING
DIVISION OF STRUCTURAL ENGINEERING

CHALMERS UNIVERSITY OF TECHNOLOGY
Gothenburg, Sweden 2021
www.chalmers.se

Master's thesis ACEX30

Design of Continuous Composite Road Bridges

Bridge girders with corrugated webs in stainless steel

JULIA STEFFNER
MICHAELA ÖMAN

CHALMERS
UNIVERSITY OF TECHNOLOGY

Department of Architecture and Civil engineering
Division of Structural Engineering
Lightweight structures
Chalmers University of Technology
Gothenburg, Sweden 2021

Design of Continuous Composite Road Bridges
Bridge girders with corrugated webs in stainless steel

JULIA STEFFNER
MICHAELA ÖMAN

Supervisor: Phd. Mohsen Heshmati, Bridge and Hydraulic department at WSP
Examiner: Associate Professor Mohammad al-Emrani, Department of Architecture and Civil Engineering

Department of Architecture and Civil Engineering
Division of Structural Engineering
Lightweight structures
Chalmers University of Technology
SE-412 96 Gothenburg
Telephone +46 31 772 1000

Cover: Illustration of a continuous steel/concrete composite bridge with corrugated webs.

Department of Architecture and Civil Engineering
Gothenburg, Sweden 2021

Design of Continuous Composite Road Bridges
Bridge girders with corrugated webs in Stainless Steel
JULIA STEFFNER
MICHAELA ÖMAN
Department of Architecture and Civil Engineering
Chalmers University of Technology

Abstract

Continuous steel/concrete composite bridges are a commonly used bridge solution normally designed with steel girders with flat webs in carbon steel. Carbon steel is susceptible to corrosion and demands repeated maintenance. By using stainless steel instead, the maintenance can be reduced. Due to higher material cost for stainless steel it is of importance to use innovative methods to minimize the material consumption. Girders with corrugated webs provide higher shear capacity than conventional beams with flat-webs which can be interpreted as reduction in web thickness and number of vertical stiffeners. As a result, the weight of the girders and the associated production costs could be reduced.

The aim of the study is to investigate the possibilities to optimize the design of continuous composite stainless steel/concrete girders using corrugated webs and to show possible material savings that can be obtained using this concept. The savings are investigated in terms of investment costs, maintenance costs and environmental impact. In order to investigate the different concepts, finite element models are created in Brigade/Plus. The models are based on Python-scripts that are built up as a general design tool in order to generate different design concepts. Two case studies are performed in order to compare the concepts with girders with flat webs in carbon steel to girders with corrugated webs in stainless steel.

The results indicate that both the higher material strength of stainless steel and the increased load-bearing capacity of girders with corrugated webs contribute to up to 19% material savings in the studied cases. According to the case studies, higher beams lead to larger material savings since the corrugation can be better utilized. For lower beams the material savings are more dependent on the material strength than the corrugation.

Comparing the concept of flat webs with carbon steel to corrugated webs in stainless steel showed that the investment cost is only marginally higher for the concept with stainless steel. The total cost including both investment and maintenance cost are on the other hand lower for the design with corrugated webs in stainless steel. This is due to the high maintenance costs for carbon steel bridges.

The calculated carbon emissions are higher for the bridges designed with flat webs in carbon steel compared to corrugated webs in stainless steel. This is mainly due to higher material consumption for the designs with flat webs in carbon steel.
Keywords: Composite bridges, Continuous bridges, Stainless steel, Corrugated web.

Design av kontinuerliga komposit vägbroar
Brobalkar med korrugerade liv i rostfritt stål
JULIA STEFFNER
MICHAELA ÖMAN
Institutionen för Arkitektur och Samhällsbyggnadsteknik
Chalmers Tekniska Högskola

Sammanfattning

Kontinuerliga kompositbroar i stål och betong är ett vanligt förekommande brokoncept som ofta konstrueras med stålbalkar med platta liv i kolstål. Kolstål är rostbenäget och kräver därför underhållsarbete. Genom att istället använda rostfritt stål kan underhållet minskas. Rostfritt stål har dock höga materialkostnader och det är därför viktigt att använda innovativa lösningar för att minska materialförbrukningen. Balkar med korrugerade liv har högre tvärkraftskapacitet än de traditionella balkarna med platta liv vilket kan leda till minskning av livtjockleken och antalet vertikala livavstyvare.

Syftet med studien är att undersöka möjligheten att optimera kontinuerliga kompositbroar i rostfritt stål och betong med korrugerade liv och visa på potentiella materialbesparingar som det här konceptet kan möjliggöra. Besparingarna är utryckta i investeringskostnader, underhållskostnader och miljöpåverkan. För att jämföra de olika koncepten kommer FE-modeller att upprättas i Brigade/Plus. Modellerna är baserade på Python-script som är uppbyggda som ett generellt verktyg som kan generera olika brokoncept. För att jämföra konceptet med att använda platta liv i kolstål med korrugerade liv i rostfritt stål är två fallstudier utförda.

Resultatet visade att både den högre hållfastheten för rostfritt stål och den högre kapaciteten på stålbalkar med korrugerade liv bidrog till viktbesparingar på upp till 19%. Fallstudierna visade att högre balkar i kombination med korrugerade liv i rostfritt stål bidrog till större viktbesparingar. För lägre balkar hade materialhållfastheten en större påverkan på viktbesparingarna än korrugeringen.

Jämförelsen mellan en bro med platta liv i kolstål med en bro med korrugerade liv i rostfritt stål visade att investeringskostnaderna var marginellt högre för konceptet med rostfritt stål. Den totala kostnaden som inkluderade både investerings- och underhållskostnader var dock lägre för bron i rostfritt stål. Detta beror på den höga underhållskostnaden för broarna i kolstål.

De framräknade koldioxidutsläppen var högre för broarna med platta liv i kolstål i jämförelse med bron med korrugerade liv i rostfritt stål. Detta beror främst på den större mängd material som behövdes för platta liv i kolstål.

Keywords: Kompositbroar, Kontinuerliga broar, Rostfritt stål, Korrugerade liv.

Acknowledgements

This Master's thesis was conducted at WSP's Bridge and Hydraulic department in Gothenburg together with the Department of Architecture and Civil Engineering, Chalmers University and Technology. The study is a part of an ongoing industrial research project, SUNLIGHT, examine the ability to build maintenance-free steel bridges.

In order to perform this thesis we have received valuable help and guidance from several people in the industry that we would like to thank.

We would like to send our biggest gratitude to our supervisor Phd. Mohsen Heshmati. Without your wide knowledge, inspiring enthusiasm and generosity with your time we would not have been able to perform this study. Independent of time and day, you have always been supporting us. Additionally, we would like to thank Phd. Poja Shams Hakimi for your helpful comments and input throughout the project.

Furthermore, we want to thank our examiner Associate Professor Mohammad al-Emrani for your expertise and encouraging support. We are thankful that you were able to join us during this spring. We also would like to thank Senior Lecturer Mozhdeh Amani for your help in the early stage of the project.

Lastly, we would like to send our gratitude to Lars-Åke Persson at Stål & Rörmontage AB, Joakim Hedegård at Swerim AB and Paul Janiak at Outokumpu R&D who helped us performing cost estimations. We also want to thank Fu-siang Syu for the collaboration providing us with your valuable environmental results.

Julia Steffner and Michaela Öman, Gothenburg, June 2021

Contents

List of Figures

List of Tables

Nomenclature

Abbreviations

CSC	Cross-section class
FAT	Fatigue limit state
LCA	Life cycle analysis
LCC	Life cycle cost
$LM1$	Load model 1
$LM2$	Load model 2
NA	National Annex
SLS	Serviceability limit state
$TSFS$	Transportstyrelsens föreskrifter och allmäna råd om tillämpning av eurokoder
ULS	Ultimate limit state

Greek letters

α	Corrugation angle
α_T	Thermal coefficient
ε	Cross-section classification factor
ε_{cs}	Total shrinkage strain
γ_d	Partial safety factor
$\varphi_{\infty,cs}$	Final creep value for shrinkage loads
$\varphi_{\infty,long}$	Final creep value for long-term loads
$\psi_{L.cs}$	Additional creep factor for shrinkage loads
$\psi_{L.long}$	Additional creep factor for long-term loads

Roman lower case letters

a_1	Flat-fold length of corrugation
a_2	Length of angled part of corrugation
a_3	Corrugation depth
a_4	Transverse length of a_2
$b_{eff.deck}$	Effective width of concrete deck
f_y	Yield strength
f_u	Ultimate strength
n_0	Modular ratio between steel and concrete
$n_{L.short}$	Modular ratio for short-term loads
$n_{L.long}$	Modular ratio for long-term loads
$n_{L.cs}$	Modular ratio for shrinkage loads
r_c	Factor for increased length due to corrugation
t_{deck}	Thickness of concrete deck
$z_{tp.comp}$	Center of gravity of the composite cross-section from the top of the concrete deck
$z_{tp.steel}$	Center of gravity of the steel cross-section from the top of the concrete deck

Roman upper case letters

A_{comp}	Area of composite section
A_{steel}	Area of steel section
A_{re}	Area of reinforcement within the effective concrete width
$E_{s,ser}$	Secant modulus for non-linear material
E_s	Modulus of elasticity for steel
E_{cm}	Modulus of elasticity for concrete
$I_{y.comp}$	Moment of inertia for composite cross-section around strong axis
$I_{y.steel}$	Moment of inertia for steel cross-section around strong axis
$I_{z.comp}$	Moment of inertia for composite cross-section around weak axis
$I_{z.steel}$	Moment of inertia for steel cross-section around weak axis
ΔT_{NS}	Temperature difference in concrete deck from primary effects of shrinkage
ΔT_{MS}	Temperature difference in concrete deck for calculation of second order effects of creep

Terminology

Brigade/Plus	Finite element software for bridge-design
Composite bridge	Bridge solution with steel girders connected to a concrete deck where the advantages of the of the materials are utilized in bending
Fatigue limit state	If exceeded, failure due to fatigue will occur
Mathcad Prime	Calculation software
Navier's formula	Formula for calculations of stresses
Python	Programming language
Serviceability limit state	If exceeded, problems during usage will occur
Ultimate limit state	Maximum capacity of a structure, beyond this point collapse or failure will occur

1
Introduction

This chapter aims to give a background to the thesis and present the method used for the research. Limitations of the study are also introduced together with an overview of the report.

Composite bridges are well-known bridge types, usually designed with steel girders with flat webs connected to a concrete deck using shear connectors. This enables composite action and the advantages of the two materials can be optimally utilized (Collin et al., 2008). The steel girders normally consists of traditional carbon steel which is susceptible to corrosion and demands repeated maintenance in forms of surveillance, repainting and replacement during its service life (Stålbyggnadsintitutet, 2017). In order to decrease the maintenance, stainless steel which is more corrosion resistant material can be used instead. This would lower the costs throughout the service life. However, the material costs are still higher for stainless steel compared to conventional carbon steel, which is why the material consumption is of great economical advantage.

In order to decrease the amount of steel used in bridge girders, the cross-sections needs to be as material efficient as possible. By using a corrugated web with high out of plane stiffness, the web thickness can be kept to a minimum and the need of longitudinal and transversal stiffeners can be eliminated (Boutillon et al., 2015). Thereby, the cross-section can be optimized resulting in lower material consumption.

Concluded from the Master thesis *Design of Composite Steel-Concrete Bridges using Stainless Steel Girders with Corrugated Webs* by Henrysson & Yman (2020), large material savings can be achieved using corrugated webs in stainless steel when designing simply supported bridges. Unlike simply supported bridges, continuous bridges are statically indeterminate which influence the load distribution and demands a more extensive system analysis. Continuous bridges are also exposed to second order effects due to creep and shrinkage causing internal forces which require additional capacity of the structure (Vayas and Iliopoulos, 2014).

This study is conducted at WSP's Bridge and Hydraulic department in Gothenburg and is a part of an ongoing industrial research project. This thesis is a sequel of the master thesis *Design of Composite Steel-Concrete Bridges using Stainless Steel Girders with Corrugated Webs* conducted by Henrysson & Yman (2020).

1.1 Aim

The aim of the thesis is to investigate the possibility to optimize the design of continuous composite steel girders using corrugated webs in stainless steel. The goal is to show possible material savings by using this design compared to the conventional design with flat webs in carbon steel. The material savings will be investigated in terms of investment costs, maintenance costs and environmental impact.

1.2 Method

The execution of the thesis is divided into five main steps:

1. Perform a literature study with the purpose of gaining knowledge in design methodology for continuous composite bridges with corrugated webs in stainless steel.
2. Structure Python-scripts to create a general design tool for different design concepts and cross-sectional dimensions.
3. Implement the scripts in the finite element program Brigade/Plus to perform system analyses and optimize the bridge designs.
4. Execute two case studies comparing the concepts of bridges with flat webs in carbon steel to bridges with corrugated webs in stainless steel.
5. Estimate the optimized designs in terms of investment and maintenance cost together with environmental impact.

1.3 Limitations

Limitations for the thesis:

- The design and optimization of the bridge will only be conducted on the steel girders while the concrete deck is not re-designed.
- The thesis will only focus on composite bridges with twin-girders. Box-girders will not be considered.
- Trapezoidal shaped corrugation is used for the web design. Other corrugation forms are not studied.
- Road bridges will be the focus in this study.
- For design with stainless steel, the only material considered is Duplex steel 1.4162.
- The height of the bridge girder will be kept constant along the whole bridge. Material savings due to varying cross-section height in span and support will not be investigated.

1.4 Thesis outline

The report consists of 7 chapters in total. A brief description of the chapters is presented below:

Chapter 1 - Introduction, gives a background of the thesis and states the aim, limitations and method for the study.

Chapter 2 - Theory, consists of a literature study that presents the fundamental theory of continuous composite bridges, corrugated webs and stainless steel.

Chapter 3 - Design methodology, describes the design procedure for continuous composite bridges with both flat/corrugated webs in carbon/stainless steel. The differences in the calculation procedure for the different concepts are highlighted and further investigated.

Chapter 4 - Finite element model, explains how the concepts are modelled in Brigade/Plus and how the different loads are implemented in the models.

Chapter 5 - Case studies, presents the results from the two case studies performed in the thesis. The material savings are presented in economical and environmental terms and the load effects are compared for the different designs.

Chapter 6 - Discussion, presents a discussion on the results obtained from the performed case studies. The discussion focus on the differences of using flat/corrugated webs as well as using carbon/stainless steel.

Chapter 7 - Conclusion, concludes the results obtained from the project work and connects the results with the aim of the thesis. A discussion on further research are also included in this chapter.

2
Theory

This chapter aims to give an overview of the theory for continuous composite bridges with corrugated webs. The main parts covered in this chapter is the structure of continuous and composite bridges, corrugated webs and the application and properties of stainless steel.

2.1 Continuous bridges

A continuous bridge consists of a continuous load bearing segment in two or several spans. This type of bridge is a cost-effective solution when longer spans are needed. It is also an advantage when a simply supported system would imply difficult serviceability verifications and demand an extensive use of steel (Vayas and Iliopoulos, 2014). A stiffer system is thereby preferable and a continuous composite bridge is a commonly used solution which provides higher redundancy, limited deformability and capability of redistribution.

Continuous bridges demand heavier cross sections over the internal supports due to the interaction between strong negative bending moment and shear forces (Vayas and Iliopoulos, 2014). This results in varying stiffness of the girders along the bridge affecting the load distribution.

2.2 Composite bridges

For composite bridges, the main idea is to make different construction parts work as one unit (Utsi and Lagerqvist, 2012). One commonly used solution is steel girders combined with a concrete deck where the advantages of the materials can be utilized in bending. Concrete is used to handle compression stresses while the steel handles the tensile stresses.

2.2.1 Design concepts

There are several design concepts for composite bridges. Two examples are the box girder and the double-girder (Vayas and Iliopoulos, 2014). Double-girder bridges can be designed with two identical main girders, this concept is called twin-girder

bridge. A typical cross section for a twin-girder bridge is illustrated in Figure 2.1.

Figure 2.1: Conceptual design of a twin-girder cross section.

One of the biggest advantages with composite bridges is the low self-weight of the superstructure (Utsi and Lagerqvist, 2012). This results in cheaper foundation and bearings. By utilizing the different materials, the construction height can also be decreased which is favourable when the free height underneath the bridge is limited. Furthermore, there are several erection methods available for composite bridges. These methods can be customized for the given conditions providing an effective construction phase (Vayas and Iliopoulos, 2014). The construction methods are further explained in Section 2.2.4.

2.2.2 Design of cross section

For continuous systems, varying height of the cross section is favorable in order to fulfill the bearing capacity but still maintain the aesthetics and secure good clearance (Vayas and Iliopoulos, 2014). Due to the interaction of high negative bending moment and shear force over the internal supports, the cross section will be heavier in these regions compared to those in the span. The negative moment will cause tension in the concrete deck over the supports and reinforcement will therefore be necessary in order to deal with the tensile stresses (Utsi and Lagerqvist, 2012). Since the steel girders will be subjected to compression in these regions, the bending and deformation capacity will be influenced by stability issues which needs to be accounted for.

2.2.3 Connectors between the materials

In order to obtain full composite action between the concrete and the steel, connectors are needed. This in order to transfer the shear flow between the materials (Utsi and Lagerqvist, 2012). There are several connectors available, but the most common one and the one handled in the standards is welded shear studs. The studs are welded to the upper steel flange and would enable composite action when the

concrete has hardened. This is illustrated in Figure 2.2.

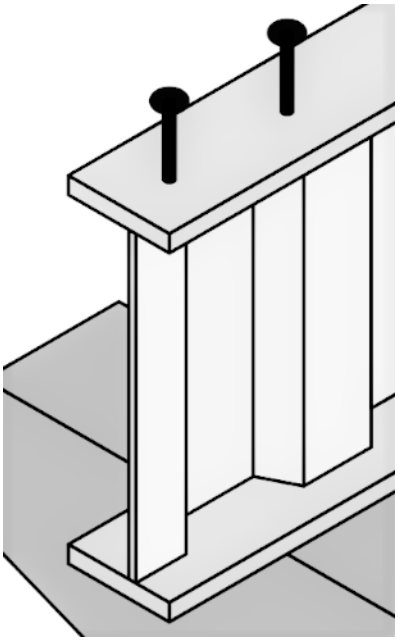

Figure 2.2: Shear studs welded to the upper steel flange on the main girder.

2.2.4 Construction methods

The construction phase sets the load history for the bridge since stresses and deformations are influenced. To secure a cost-efficient construction with a desired geometry and bearing capacity it is important to choose an appropriate erection method (Vayas and Iliopoulos, 2014). For the erection of the bridge structure, the steel girders are the first part mounted on site which can either be lifted into place or launched from one end to another using hydraulic rams. Temporary supports might be needed in order to limit the length of the cantilevers and decrease the stresses. If bigger elements are used, the parts can be welded together on site. Thereafter, the concrete is casted on top of the girders by using temporary form-work. Before the concrete has hardened, the steel girders need to carry the load without contribution from the concrete. Therefore, cross-bracing is commonly needed in order to minimize the risk of *lateral torsional buckling* (LT-buckling) before composite action is achieved.

The casting of the concrete deck is usually divided into different stages in order to limit the negative bending moment and to minimize the tension stresses in the concrete. For shorter spans, the casting is normally executed from one end to another since the hogging moment is not a big issue. Although, for larger spans the hogging moment is more critical and the span regions are first casted followed by the internal support areas (Vayas and Iliopoulos, 2014).

2.3 Stainless steel

Carbon steel is the conventionally used material when it comes to bridge design (Vayas and Iliopoulos, 2014). Although, carbon steel is sensitive to corrosion and can increase the maintenance cost since the need of expensive and time-consuming repainting is substantial. Another available steel type is stainless steel which usually have higher initial investment costs compared to carbon steel but has a substantially higher resistance against corrosion (Stålbyggnadsintitutet, 2017). Due to the high investment costs, the profitability of using stainless steel rather develops throughout the service life since the material demands less maintenance and possesses a longer service period. This can result in economical savings comparing the entire life cycle cost of a bridge in stainless steel to a bridge in carbon steel.

Since the investment costs for stainless steel is comparatively high, it is of considerably importance to optimize the cross section in order to minimize the material usage. The main parameter that governs the bridge design is not the choice of material but rather the cross-sectional design (Schedin and Backhouse, 2019).

2.3.1 Manufacturing

The material properties of stainless steel are highly influenced by the production process (Stålbyggnadsintitutet, 2017). Stainless steel manufactured by annealing is the most common type on the market. Another production method is cold-forming, where the material obtains higher strength but at the same time loses some of its ductility. However, this loss in ductility is normally negligible due to the high initial ductility. Cold-forming also makes the material work differently in tension and compression because of different stress-strain behavior for the material in different directions. However, cold-formed stainless steel is slightly more expensive compared to annealed stainless steel.

2.3.2 Properties

Steel with a minimum of 10.5% chromium is defined as stainless steel which is divided into four different categories with different properties (Stålbyggnadsintitutet, 2017). Duplex stainless steel is a mixture of the two categories austhenitic- and ferritic stainless steel. The composition of the Duplex steel gives high strength and good resistance to corrosion. This makes Duplex steel useful in heavy structures that are exposed to corrosion.

The difference in material composition for stainless steel and carbon steel gives different properties for the materials (Stålbyggnadsintitutet, 2017). One of the largest differences is the stress-strain relation. In Figure 2.3, stress-strain curves for different steel types are presented. The figure shows that carbon steel has a linear behavior up to the yield limit, while stainless steel does not show any precise yield point.

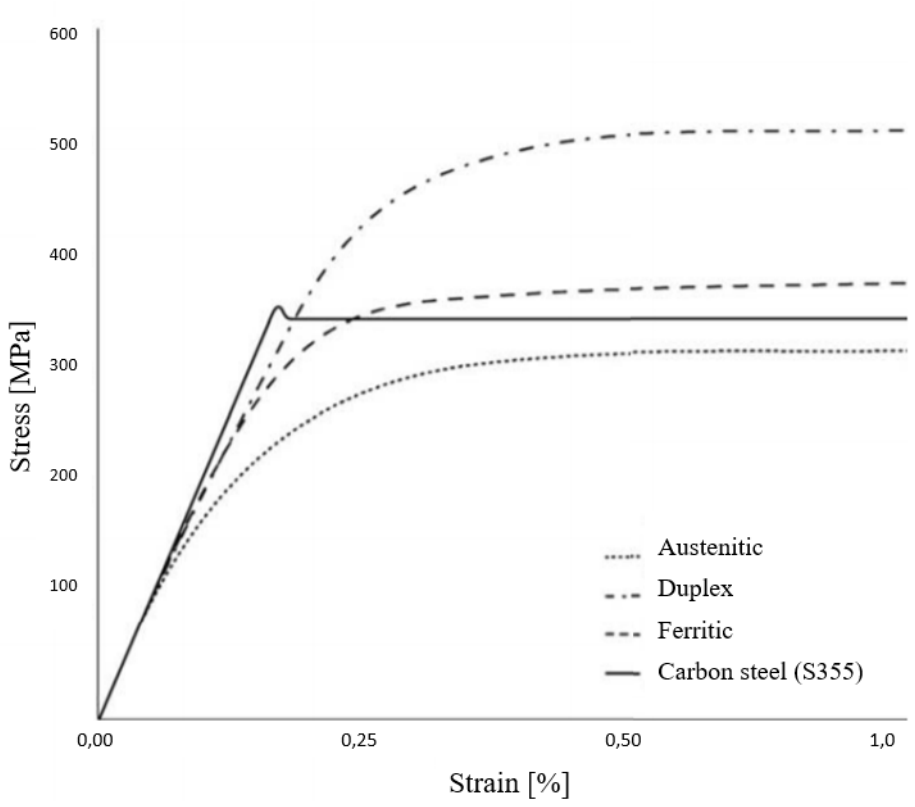

Figure 2.3: Stress-strain relation for stainless and carbon steel (Stålbyggnadsintitutet, 2017).

2.3.2.1 Modulus of elasticity for stainless steel

Because of the non-linear behavior of stainless steel, different modulus of elasticity needs to be used for calculations in *Ultimate limit state* (ULS) compared to calculations in *Serviceability limit state* (SLS). In ULS calculations, the elastic modulus can be set to a constant value of $E = 200$ GPa according to SS-EN 1993-1-4 2.1.3(1). For calculations in SLS, the non-linear behavior of stainless steel must be accounted for. According to SS-EN 1993-1-4 4.2, a secant modulus of elasticity can be used for this purpose, see Equation 2.1. This secant modulus is applicable as long as the maximum stresses does not exceed 65% of the 0.2-limit (Stålbyggnadsintitutet, 2017). When the stresses are too high, the deflection calculations will be too conservative.

$$E_{s,ser} = \frac{E_{s,1} + E_{s,2}}{2} \tag{2.1}$$

Where,

$E_{s,ser}$ is the secant modulus of elasticity
$E_{s,1}$ is the secant modulus corresponding to the stress σ_1 in the tension flange
$E_{s,2}$ is the secant modulus corresponding to the stress σ_2 in the compression flange

The values for $E_{s,1}$ and $E_{s,2}$ are calculated according to Equation 2.2.

$$E_{s,i} = \frac{E}{1 + 0.002\frac{E}{\sigma_{i,Ed,ser}}(\frac{\sigma_{i,Ed,ser}}{f_y})^n} \tag{2.2}$$

Where,

E	is the modulus of elasticity
i	is either 1 or 2 dependent on if the flange is in tension or compression
$\sigma_{i,Ed,ser}$	is the maximum stress in SLS
f_y	is the yield strength
n	is the Ramberg-Osgood parameter

The value of n varies for different steel grades and depends on the level of non-linearity. The higher level of non-linearity, the lower value of n (Stålbyggnadsintitutet, 2017).

2.3.3 Stainless steel in composite bridges

Stainless steel is a very ductile material and therefore behaves differently compared to carbon steel (Shamass and Cashell, 2018b). The rigid-plastic theory gives good predictions of the behavior of carbon steel, which has an elastic response up to a specific yield point. For stainless steel there is no specific yield point and the response shows a non-linear behaviour, as could be seen in Figure 2.3. The strain hardening of stainless steel under plastic deformation is thus not included when following the general design codes for composite bridges, which are developed for carbon steel. By excluding the strain hardening effect, the calculated moment capacity will be incorrectly estimated in a conservative manner. Accordingly, the calculations will be on the safe side using the existing design codes, but the optimization of the material use can be underestimated since the effect of strain hardening would probably increase the material savings. However, for girders where stability is governing the design (cross section class 3 and 4) the stresses won't exceed the yield limit thus, the design rules won't be affected by the different post-yielding behavior of stainless steel.

2.3.3.1 Simplified analytical method

Eurocode does not include any different approach for calculating the bending moment capacity of a composite bridge with stainless steel compared to carbon steel. To account for this, Shamass & Cashell (2018) have developed a method were the bending moment capacity for a composite beam in stainless steel is calculated more precisely. The internal forces in the cross section depends on the position of the neutral axis. Therefore, an iterative method must be used in order to find these forces. The numerical integrations needed for the calculations are time consuming and requires a lot of software, consequently a simplified method was developed as well.

The simplified analytical method is useful when calculating the plastic bending moment capacity for larger constructions with stainless steel (Shamass and Cashell, 2018a). The plastic bending capacity of regular carbon steel is built on the assumption in Eurocode that the effective area of the steel girder is stressed to its yield strength. The simplified method accounts for the non-linear behavior and strain-hardening effect of stainless steel by assuming that the effective area is stressed to a value equal to the stress level at 60% of the steel girder height instead.

2.3.3.2 Stainless steel as reinforcement

The use of stainless steel as reinforcement in concrete decks makes it possible to reduce the thickness of the concrete cover (Dahlström and Persson, 2018). This is feasible due to its higher resistance to corrosion compared to conventional carbon steel. The reduction in concrete cover would reduce the concrete consumption and also decrease the required reinforcement amount since the self-weight of the structure would be reduced.

Another advantage of using stainless steel instead of carbon steel as reinforcement is the better strength properties and the ability to exceed crack widths limitations (Dahlström and Persson, 2018). The limitation of crack widths in the design codes are necessary in order to protect the reinforcement from corrosion. This demands a large number of reinforcement bars to keep the reinforcement ratio high. If stainless steel would be used instead, the reinforcement ratio could be reduced since the protective concrete layer would be less important. This enables better material utilization and larger material saving.

2.3.3.3 Studs, screws and bolts

If different steel materials are used for the connectors and the steel girders, problems with galvanic corrosion can occur due to the fact that one of the materials is more noble than the other one (Dahlström and Persson, 2018). This phenomenon increases the corrosion rate for the less noble steel material. To avoid this, the same steel material should be used for the main girders as for the studs, screws and bolts. It is also stated in SS-EN 1993-1-4, A.6.2 that carbon steel fasteners should not be used together with stainless steel.

The capacity of studs in composite bridges should be designed according to SS-EN 1994-2, 6.6.3. This standard only accounts for studs in carbon steel and not for calculations using studs in stainless steel. The capacity of studs in composite bridges is dependent on the ultimate capacity, f_u, but limited to 500 MPa. The ultimate capacity for Duplex stainless steel exceeds this limit and therefore, the calculations according to Eurocode is conservative when using studs in stainless steel.

2.4 Corrugated webs

In today's bridge design one of the main structural elements is I-shaped girders with flat webs. In order to withstand the bending moment in the structure, the girders are normally designed with deep cross sections and slender webs (Elkawas et al., 2018). The high slender web-plates demands several transverse stiffeners due to the weak out-of-plane bending stiffness. This increases the material consumption and the risk of fatigue damage due to the extensive number of welds. Another design solution for the girders is to use a corrugated web instead with an increased bending stiffness in the lateral direction in order to improve the buckling stability (Hassanein et al., 2017). This results in decreased material consumption since the need of transverse and longitudinal stiffeners is limited or even eliminated and the web thickness can be kept to a minimum. As an example, by implementing a corrugated web, the weight of the structure can be decreased with up to 15% compared to a ordinary concrete box-girder bridge (Boutillon et al., 2015).

2.4.1 Manufacturing

There are two main designs of corrugated webs, sinusnodal and trapezoidal webs (Karlsson, 2018). One of the advantages with trapezoidal webs is that they can be customized thanks to its simple production method. The conventional shape parameters illustrated in Figure 2.4 can be optimized for each individual girder. The corrugated webs are usually processed using cold bending which prevents reduction of the steel ductility and surface cracking (Boutillon et al., 2015).

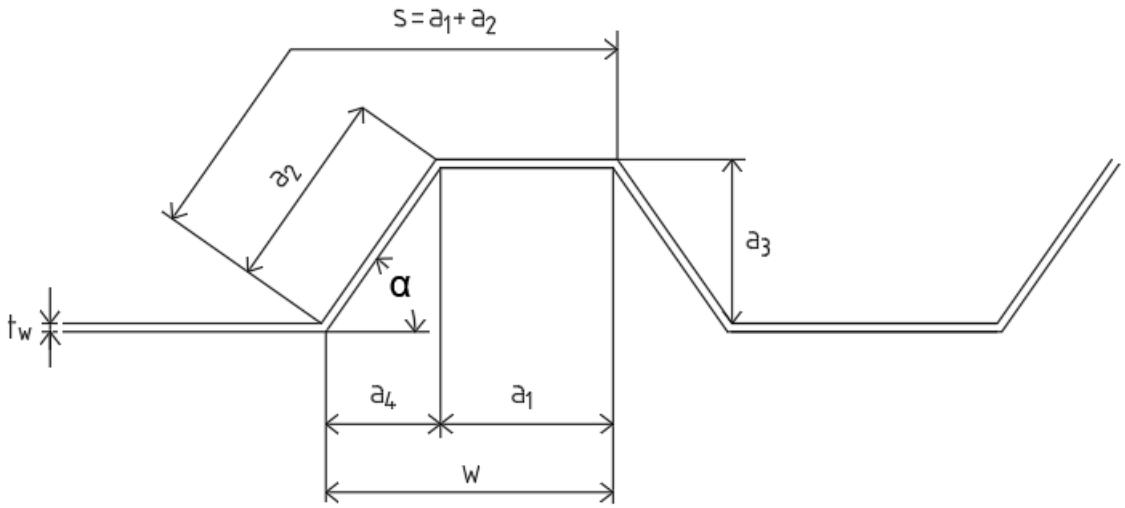

Figure 2.4: Corrugation parameters for a trapezoidal shaped plate (Karlsson, 2018).

2.4.2 Design capacity

Girders with corrugated webs are designed for the web to withstand the shear force and the flanges to withstand the bending moment. Due to the accordion effect as a result of the corrugation, the webs are easily deformed in the axial direction and do not attract demanding axial stresses (Boutillon et al., 2015). The web will therefore transfer only pure shear and normal fillet welds can be used to transfer the forces between the steel components.

For this type of web design, the main shear failure modes are local, global and interactive buckling (Hassanein et al., 2017). Conducted by Karlsson (2018), some of the design parameters of the corrugated web, illustrated in Figure 2.4, has an extensive influence on the buckling behaviour and therefore need to be chosen wisely in order to optimize the design and achieve desired capacity. The corrugation angle, α, and the flat fold length, a_1, were established having the biggest influence on the ultimate shear capacity and the buckling behaviour, together with the thickness, t_w, and height, h_w, of the web. For each unique beam, there is an optimal design of α and a_1 in order to optimize the shear capacity.

When calculating the bending moment resistance of a girder with corrugated web, the influence of the web is neglected according to SS-EN 1993-1-5, Annex D due to the accordion effect. In order to compensate for the loss in stiffness, the web height can be increased in order to withstand higher bending moment (Henrysson and Yman, 2020). Although, this is not always feasible since the free height underneath the bridge is usually governing for the design.

3
Design Methodology

Chapter 3 aims to explain how to design continuous composite bridges and how it is affected by using different materials and different web designs. Focus will mainly be on the various capacity checks needed to design the main steel girders and how material choice, web design and number of spans influence the different checks.

3.1 Guidance in design process

In Sweden, there is mainly one guideline to be followed when designing new bridges, *Krav brobyggande*, which provides general regulations and instructions. This document mainly refers to the *Eurocodes*, a collection of ten different standards, providing additional regulations regarding various materials, constructions and capacity checks. The standards used in this master's thesis are listed in Table 3.1.

Table 3.1: The Swedish European standards used in the design process

Eurocode	**Standard**
SS-EN 1990	Basis of structural design
SS-EN 1991	Actions on structures
	Part 1-1: General actions
	Part 1-4: Wind actions
	Part 1-5: Thermal actions
	Part 2: Traffic loads on bridges
SS-EN 1992	Design of concrete structures
	Part 1-1: General rules
	Part 2: Concrete bridges
SS-EN 1993	Design of steel structures
	Part 1-1: General rules and rules for buildings
	Part 1-4: Stainless steel
	Part 1-5: Plated structural elements
	Part 1-8: Design of joints
	Part 1-9: Fatigue
	Part 2: Steel bridges
SS-EN 1994	Design of composite steel and concrete structures
	Part 2: General rules and rules for bridges

According to Krav Brobyggande, the *National Annex* (NA) named *Transportstyrelsens föreskrifter och allmänna råd om tillämpning av eurokoder* (TSFS 2018:57), should always override the Eurocodes if there are any inconsistencies.

3.2 Material

The calculations will be made for composite bridges consisting of a concrete deck and two girders in both stainless steel and in carbon steel. The treated materials with associated material parameters are presented in the following sections.

3.2.1 Steel

Stainless steel and carbon steel have different material properties and thereby different capacities. The type of stainless steel handled in this thesis is Duplex stainless steel with material parameters according to Table 3.2. The types of carbon steel included in the study are S355 and S460 with material parameters presented in Table 3.3.

Table 3.2: Material parameters for stainless steel, SS-EN 1993-1-4:2006/A1:2015

Steel grade	**Thickness** [mm]	f_y [MPa]	f_u [MPa]	E_s [GPa]
1.4162	$t \leq 6.4$*	530	700	See Section 2.3.2.1
	$6.4 < t \leq 10$	480	680	
	$10 < t \leq 75$	450	650	

* Below 6.4mm cold formed plates can be used possessing higher material strength

Table 3.3: Material parameters for carbon steel, SS-EN 10025-4:2019

Steel grade	**Thickness** [mm]	f_y [MPa]	f_u [MPa]	E_s [GPa]
S355	$t \leq 16$	355	490	210
	$16 < t \leq 40$	345	470	
	$40 < t \leq 63$	335	470	
S460	$t \leq 16$	460	540	210
	$16 < t \leq 40$	440	540	
	$40 < t \leq 63$	430	530	

3.2.2 Concrete

The reinforced concrete deck connecting the steel girders can be designed with different material properties depending on chosen concrete class. The class used for this thesis is C35/45 with material parameters according to Table 3.4. The reinforcement data is presented in Table 3.5.

Table 3.4: Material parameters for concrete, SS-EN 1992-1-1 Table 3.1

Concrete class	f_{ck} [MPa]	f_{cm} [MPa]	f_{ctm} [MPa]	$f_{ctk,0.05}$ [MPa]	E_{cm} [GPa]
C35/45	35	43	3.2	2.2	34

Table 3.5: Material parameters for reinforcement

Material	f_y [MPa]	E_s [GPa]
B500B	500	*

*Chosen equal as for the used structural steel, SS-EN 1994-2 3.2(2)

3.2.3 Modular ratios due to creep

In the analysis, the concrete deck is transformed to an equivalent steel cross section which is done using modular ratios calculated according to Equation 3.1.

$$n_0 = \frac{E_s}{E_{cm}} \tag{3.1}$$

Where,

n_0 is the modular ratio between steel and concrete
E_s is the modulus of elasticity for steel
E_{cm} is the modulus of elasticity for concrete

The concrete will be subjected to creep causing a stiffness redistribution which is accounted for including the creep factor in the modular ratio, SS-EN 1994-2 5.4.2.2. This redistribution of stresses leads to increased stresses in the steel section and decreased stresses in the concrete. For composite bridges, an additional creep factor is included accounting for the loading duration. Although, the creep will not have an influence on the short-term loads and therefore the modular ratio excluding the creep factor will be used when considering these loads. The modular ratios for short-term, shrinkage, and long-term loads are presented in Equation 3.2 - 3.4. The stress redistribution dependant on the modular ratios due to creep are referred to as the *primary effects of creep.*

$$n_{L.short} = n_0 \tag{3.2}$$

$$n_{L.cs} = n_0 \cdot (1 + \psi_{L.cs} \cdot \varphi_{\infty,cs}) \tag{3.3}$$

$$n_{L.long} = n_0 \cdot (1 + \psi_{L.long} \cdot \varphi_{\infty,long}) \tag{3.4}$$

Where,

$n_{L.short}$	is the modular ratio for short-term loads
$n_{L.cs}$	is the modular ratio for shrinkage loads
$\psi_{L.cs}$	= 0.55, the additional creep factor for shrinkage loads
$\varphi_{\infty,cs}$	is the final creep value for shrinkage loads
$n_{L.long}$	is the modular ratio for long-term loads
$\psi_{L.long}$	= 1.1, the additional creep factor for long-term loads
$\varphi_{\infty,long}$	is the final creep value for long-term loads

3.2.3.1 Second order effects of creep

For continuous bridges, the system is statically indeterminate and the deflections due to the primary effects of creep are restrained. Creep arise in the compressed concrete resulting in an additional rotation over the internal support (Vayas and Iliopoulos, 2014). Thereby, an extra moment is developed over the support which compensates for the additional rotation, see Figure 3.1. This is referred to as the *secondary effects of creep*. The moment due to the secondary effects of creep can be high and it is therefore important to consider it in the capacity calculations. The second order effects of creep give a favorable effect in the span and an unfavorable effect over the internal supports. Therefore, only the unfavorable effect will be included in the load effects for the capacity calculations. This is needed in order to secure sufficient capacity of the girders even before the effect of creep has developed.

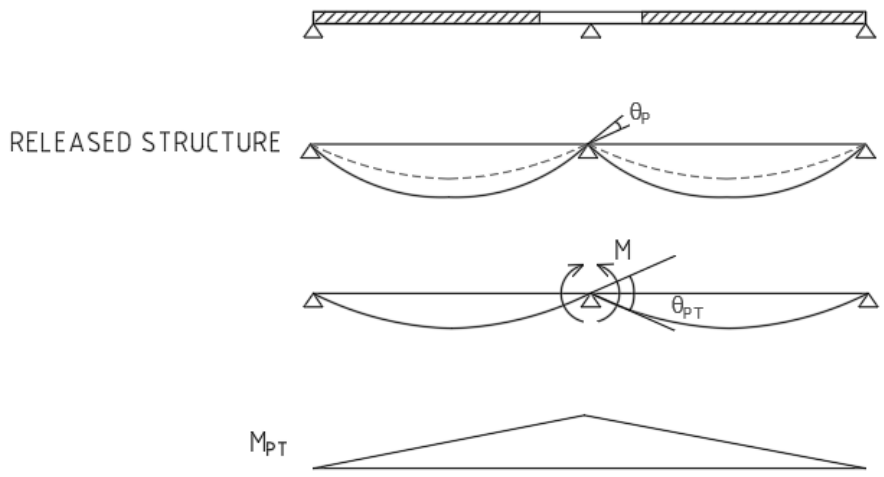

Figure 3.1: Additional rotation due to creep resulting in an extra moment over the internal support. Figure redrawn from Vayas and Iliopoulos (2014).

3.3 Structural system

The study will be conducted on a continuous twin-girder bridge where the steel girders constitute the primary system transferring the loads in the longitudinal direction. The top flanges will be connected by a concrete deck, which constitutes the secondary system, transferring the loads in the transverse direction to the steel girders. When composite action is obtained, the concrete deck contributes to the longitudinal bearing capacity.

3.3.1 Steel girders

Composite action between the steel and the concrete is obtained first when the concrete has hardened, and therefore the analysis of the steel girders needs to be developed into two parts, *construction stage* and *service stage*. In the construction stage, the cross section includes the steel girders only while in the service stage a transformed cross section considering both the concrete and the steel is analysed. The concrete will be subjected to creep which will only be included in the service stage when the concrete is accounted for. In order to consider shear lag between the steel and the concrete in the steel girders, the width of the upper steel flange might need to be reduced according to SS-EN 1993-1-5 3.1.

3.3.1.1 Cross section classification

The cross section classes for the compressed parts need to be checked according to SS-EN 1993-1-1 5.5. The purpose of the cross section classification is to investigate if the full capacity of the different structural parts can be utilized in bending or if the capacity of the cross section needs to be reduced due to buckling. The cross section class is dependent on the c/t-ratio were t is the thickness and c is the height or the width of the studied part.

The different limits for the cross section classes are dependent on if the part is an internal part (web) or outstand part (flange) as well as the stress distribution, according to SS-EN 1993-1-1 5.5. The stress limits for the cross section classes differ between carbon and stainless steel due to the factor ε. For carbon steel, this factor is calculated according to Equation 3.5 which depends only on the yield strength of the material. When it comes to stainless steel, this factor is also influenced by the modulus of elasticity E_s, see Equation 3.6. If any part of the cross section ends up in class 4, reduction due to buckling is accounted for by calculating the effective width of the specific part. For girders with flat webs, the cross section class for both the flanges and the web needs to be controlled. For a girder with corrugated web, the bending capacity is only utilized in the flanges and therefore the cross section classification of the web is unnecessary.

$$\varepsilon = \sqrt{\frac{235}{f_y}} \tag{3.5}$$

$$\varepsilon = \sqrt{\frac{235}{f_y} \cdot \frac{E_s}{210}} \tag{3.6}$$

Where,

f_y is the yield strength [MPa]
E_s is the modulus of elasticity of steel [GPa]

When classifying the flanges for a girder with corrugated web, SS-EN 1993-1-5 Annex D states that the outstand part of the flange should be taken as the maximum distance between the flange end and the corrugation. This is a conservative assumption and an alternative approach is suggested. Instead of using the maximum distance, the average width between the flange end and the corrugation can be used if the criteria in Equation 3.7 is fulfilled (B.Johansson et al., 2007). This approach is also investigated further by Henrysson & Yman (2020) showing that when using an average width for the outstand part of the flange, the reduction factor is not affected by a deeper corrugation as Eurocode states. This allows wider flanges with higher bending capacity before the need of reduction due to buckling.

$$\frac{(a_{c1} + a_{c4}) \cdot a_{c3}}{(a_{c1} + 2 \cdot a_{c4}) \cdot b_f} < 0.14 \tag{3.7}$$

Where,

a_{c1}, a_{c3}, a_{c4} are corrugation parameters, see Figure 3.7
b_f is the width of the compressed flange

3.3.2 Concrete deck

To consider shear lag for the concrete deck, an effective width can be used, see Figure 3.2. The effective width is calculated according to SS-EN 1994-2, 5.4.1.2 where the widths differ for different regions along the bridge, see Figure 3.3. The choice of material and web design does not have an influence on the effective width of the concrete deck.

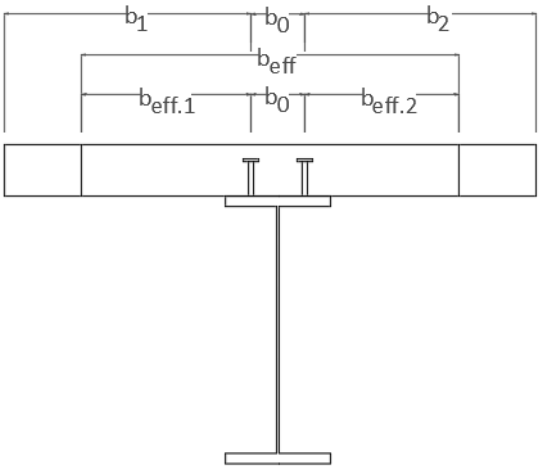

Figure 3.2: Transverse effective width of the concrete deck.

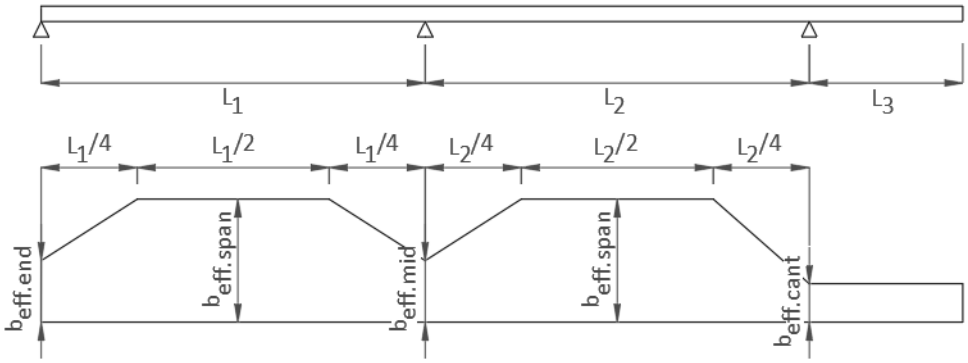

Figure 3.3: Longitudinal variation in effective width of the concrete deck.

3.3.3 Composite action

During the service stage, composite action is obtained between the concrete deck and the steel girders where the concrete deck is remained uncracked. However, according to SS-EN 1994-2, 5.4.2.3, 15% of the span length on either side of the internal support can be assumed as fully cracked region. This enables composite action between the reinforcement and the steel girders instead. This assumption also applies for the cantilever parts in both ends of the bridge. In the rest of the span the concrete is assumed to be uncracked. In Figure 3.4, the filled areas illustrate the uncracked regions while the residual parts are considered as cracked.

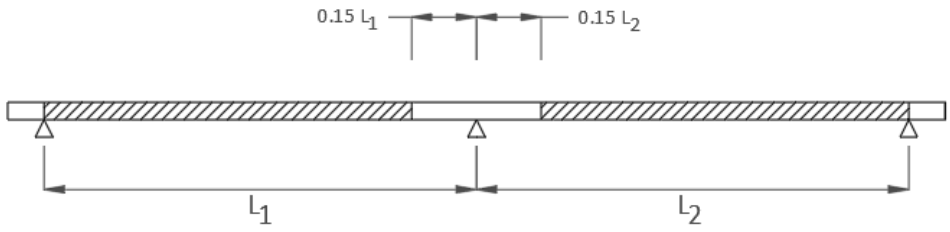

Figure 3.4: Cracked and uncracked regions along the bridge.

3.3.3.1 Uncracked regions

For the uncracked regions, the composite cross section is transformed into an equivalent steel section using the effective widths of the concrete deck, see Section 3.3.2 and the modular ratios calculated in Section 3.2.3. Since the modular ratio is different for when considering different loads, the area of the composite section in Equation 3.8 will change as well. When a corrugated web is considered, the contribution from the web is neglected in the area and stiffness calculations due to the accordion effect (Boutillon et al., 2015).

$$A_{comp.i} = A_{steel} + t_{deck} \cdot \frac{b_{eff.deck}}{n_{L.i}} \tag{3.8}$$

Where,

i	is the index referring the considered phase
$A_{comp.i}$	is the area of the composite cross section
A_{steel}	is the area of the steel girder
t_{deck}	is the thickness of the concrete deck
$b_{eff.deck}$	is the effective width of the concrete deck, calculated in Section 3.3.2
$n_{L.i}$	is the modular ratio for the considered phase

The center of gravity for the composite cross section is calculated according to Equation 3.9, relative to the top of the concrete deck.

$$z_{tp.comp.i} = \frac{A_{steel} \cdot z_{tp.steel} + t_{deck} \cdot \frac{b_{eff.deck}}{n_{L.i}} \cdot \frac{t_{deck}}{2}}{A_{comp.i}} \tag{3.9}$$

Where,

$z_{tp.comp.i}$	is the center of gravity of the composite cross section calculated from the top of the concrete deck for the specific phase
$z_{tp.steel}$	is the center of gravity of the steel-girder calculated from the top of the concrete deck

The moment of inertia around the strong axis (y-axis) and around the weak axis (z-axis) are calculated according to Equation 3.10 and 3.11 respectively for the uncracked regions.

$$I_{y.comp.i} = I_{y.steel} + A_{steel} \cdot (z_{tp.steel} - z_{tp.comp.i})^2 + \frac{\frac{b_{eff.deck}}{n_{L.i}} \cdot t_{deck}^3}{12} + \frac{b_{eff.deck}}{n_{L.i}} \cdot t_{deck} \cdot (z_{tp.comp.i} - \frac{t_{deck}}{2})^2 \tag{3.10}$$

Where,

$I_{y.comp.i}$	is the moment of inertia for the composite cross section around the y-axis for the specific phase
$I_{y.steel}$	is the moment of inertia for the steel girder around the y-axis

$$I_{z.comp.i} = I_{z.steel} + \frac{\frac{b_{eff.deck}}{n_{L.i}}^3 \cdot t_{deck}}{12} \tag{3.11}$$

Where,

$I_{z.comp.i}$	is moment of inertia for the composite cross section around the z-axis for the specific phase
$I_{z.steel}$	is moment of inertia for the steel girder around the z-axis

3.3.3.2 Cracked regions

For the regions where the concrete deck is considered as cracked, the reinforcement area within the effective concrete width is included in the composite cross section. Here, the cross-sectional constants are not dependent on the studied phase since creep will not have an influence. Therefore, the area of the composite cross sections in the cracked regions, calculated according to Equation 3.12, is only dependent on the amount of reinforcement in the concrete deck. As in the uncracked regions, the web contribution is neglected in the area and the stiffness calculations for a corrugated web.

$$A_{comp} = A_{steel} + A_{re} \tag{3.12}$$

Where,

A_{comp}	is the area of the composite cross section
A_{steel}	is the area of the steel girder
A_{re}	is the total reinforcement area within the effective concrete width

Regarding the center of gravity, the calculation for the cracked regions is performed in the same manner as for the uncracked ones. This since the reinforcement is assumed to be located in the center of the concrete deck, see Equation 3.13.

$$z_{tp.comp} = \frac{A_{steel} \cdot z_{tp.steel} + A_{re} \cdot \frac{t_{deck}}{2}}{A_{comp}} \tag{3.13}$$

Where,

$z_{tp.comp}$ is the center of gravity of the composite cross section calculated from the top of the concrete deck for the specific phase
$z_{tp.steel}$ is the center of gravity of the steel girder calculated from the top of the concrete deck

The moment of inertia around the strong axis (y-axis) and around the weak axis (z-axis) are calculated according to Equation 3.14 and 3.15 respectively for the cracked regions.

$$I_{y.comp} = I_{y.steel} + A_{steel} \cdot (z_{tp.steel} - z_{tp.comp})^2 + \\ + A_{re} \cdot (z_{tp.comp} - \frac{t_{deck}}{2})^2 \tag{3.14}$$

Where,

$I_{y.comp}$ is the moment of inertia for the composite cross section around the y-axis
$I_{y.steel}$ is the moment of inertia for the steel girder around the y-axis

$$I_{z.comp} = I_{z.steel} \tag{3.15}$$

Where,

$I_{z.comp}$ is the moment of inertia for the composite cross section around the z-axis
$I_{z.steel}$ is the moment of inertia for the steel girder around the z-axis

3.4 Loads

The loads acting on the structure are divided into permanent loads and variable loads based on the loading duration. These loads are further described in the following sections.

3.4.1 Permanent loads

The permanent loads acting on the structure is the self-weight from the structural components and the shrinkage load. These loads are presented in Table 3.6. Since the consideration of creep will influence the stiffness, the permanent loads are divided into different phases. The creep is included in the long-term and shrinkage phase but not during construction.

Table 3.6: Permanent loads

Load	**Phase**
Form work	Construction
Steel girders	Construction & Long-term
Concrete deck	Construction & Long-term
Edge beams	Construction & Long-term
Coating	Long-term
Shrinkage	Shrinkage

3.4.1.1 Self-weight of steel girders

The self-weight of the steel girders is calculated using the density of the relevant steel material multiplied with the volume of the girder and the gravitation constant $g = 9.81 m/s^2$. The corrugated web has an additional length due to its corrugation. To consider this, the factor r_c giving the relation between the flat and the curved parts of the web according to Equation 3.16 is multiplied with the total length of the girder. The self-weight of the girder is thereby dependent on both the type of steel and the type of web design.

$$r_c = \frac{a_1 + a_2}{a_1 + a_4} \tag{3.16}$$

Where,

r_c is the factor for increased length due to corrugation
a_1 is the flat fold length
a_2 is the inclined length of the corrugation depth
a_4 is the straight length of a_2

3.4.1.2 Self-weight of concrete deck

The load from the reinforced concrete deck will also be calculated dependent on its volume and density. Before the concrete has hardened the weight of the concrete is higher due to the larger amount of water. When the concrete dries the weight decreases. It is important to take this into consideration when calculating the stresses in the construction stage before the concrete has hardened.

3.4.1.3 Shrinkage

The shrinkage force in the concrete comes from both autogenous shrinkage and drying shrinkage. The main part of the autogenous shrinkage strain arises during the first days after casting. Drying shrinkage on the other hand, comes from the water leaving the concrete which is a slow process. The total shrinkage can be calculated according to SS-EN 1992-1-1 3.1.4.

The shrinkage causes the concrete to contract but because of its interaction with the steel girder the contraction is restrained. This leads to an internal tension force in the concrete deck and an equal compression force in the composite section. In the cracked regions, the concrete can shrink freely and no tensile forces within the concrete deck are developed. Thereby, these normal forces are neglected over the internal supports. The force couple is balanced by an additional bending moment acting in the composite section. These forces and moment are referred to as the *primary effect of shrinkage*.

The shrinkage forces in continuous bridges leads to lower stiffness in the span were the concrete is uncracked. This results in an additional rotation over the internal support, similar to the effects of creep. A counteracting bending moment is thereby developed which is referred to as the *second order effects of shrinkage*. The secondary effects of shrinkage give favorable effect in the spans and unfavorable effect over the internal supports. In the capacity calculations, only the unfavorable effect over the internal support will be included. If all parts of the steel girders are in cross section class 1 or 2, the second order effects of shrinkage can be neglected in the capacity calculations in ULS. Although, the effects should still be included in SLS regardless of the cross section class (Vayas and Iliopoulos, 2014).

3.4.2 Variable loads

The bridge is exposed to several variable loads arising from traffic, temperature variations and wind, see Table 3.7. The variable loads are considered as short-term loads.

Table 3.7: Variable loads

Load	**Value**	**Reference**
Traffic load	$Q_{1k} = 300kN\ q_{1k} = 9kN/m^2$ $Q_{2k} = 200kN\ q_{2k} = 2.5kN/m^2$	SS-EN 1991-2
	$A = 180kN\ B = 300kN\ q = 5kN$	TFSF 2018:57
Acceleration/ braking load	$Q_{lk} = 0.6\alpha_{Q1}2Q_{1k} + 0.1\alpha_{q1}q_{1k}w_l L$ $180\alpha_{Q1}kN \leq Q_{lk} \leq 900kN$	SS-EN 1991-2
	$Q_{lk} = min(0.35B, 500kN)$	TFSF 2018:57
Side force from braking	$Q_{trk} = 0.25 \cdot Q_{lk}$	SS-EN 1991-2
Wind load	Dependent on location	TFSF 2018:57
Temperature load	See Section 3.4.2.2	

3.4.2.1 Traffic load

Both traffic loads according to Eurocode and Trafikverket are taken into account. The traffic loads in Eurocode that are considered are Load model 1 (LM1) and Load model 2 (LM2). These are combined and handled according to SS-EN 1991-2, 4.3.2

and SS-EN 1991-2, 4.3.3. Load model 3 and 4 are not relevant for the analyses in this thesis. The traffic loads according to Trafikverket are axial- and boogie-loads with A-/B-values according to TSFS 2018:57.

3.4.2.2 Temperature load

Temperature variations create forces that either makes the bridge extract or contract. The size and direction of these forces are dependent on whether the outside temperature varies or if the temperature between the concrete deck and the steel girders differ.

The temperature variations in the ambient air, also referred to as the uniform temperature component, are dependent on the geographic location of the bridge. The minimum and maximum temperature variations for the considered location are extracted from TSFS 2018:57, 8 ch 2 §.

There are two available methods to calculate the effect of temperature variations between the concrete deck and the steel girders. In this thesis, Method 2 according to SS-EN 1991-1-5 6.1.4.2 is used. This method includes the nonuniform temperature component and can be applied with a simplified approach were the temperature in the steel and concrete are considered not to vary inside the separate materials. Instead, the variation is applied between the materials, see Figure 3.5. The temperature variation in the steel is set equal to 0 while the variation in the concrete is set to $\Delta T = 10$ if the top surface is warmer and $\Delta T = -10$ if the top surface is colder, SS-EN 1991-1-5 Figure 6.2b.

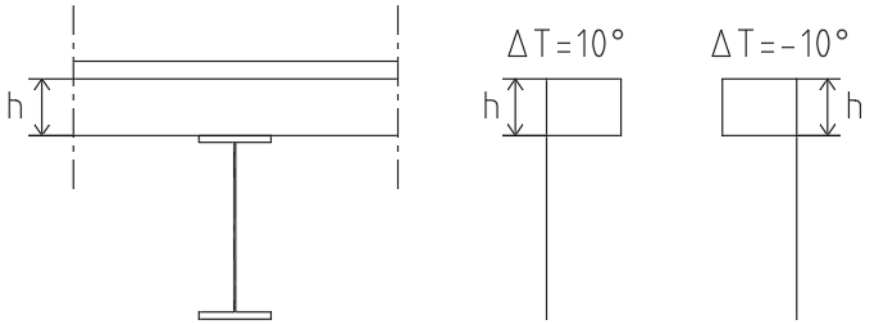

Figure 3.5: Simplified method for temperature variations in composite bridges. Redrawn from SS-EN 1991-1-5.

For a composite bridge in carbon steel the effect of different thermal expansion coefficients for steel and concrete can be neglected, SS-EN 1991-1-5 Table C1 (6). Thereby, the linear coefficient for thermal expansion for carbon steel can then be assigned the same value as for concrete, $\alpha_T = 10 \cdot 10^{-6}/°C$. When using stainless steel, the thermal coefficient is higher compared to carbon steel causing load effects necessary to include in the global analysis in ULS. The different linear coefficients

for thermal expansion are presented in Table 3.8.

Table 3.8: Linear coefficients for thermal expansion

Material	α_T $(\cdot 10^{-6}/°C)$	**Reference**
Concrete	10	SS-EN 1991-1-5 Table C1
Carbon steel	12	SS-EN 1991-1-5 Table C1
Carbon steel in composite bridges	10	SS-EN 1991-1-5 Table C1 (6)
Duplex stainless steel	13	prEN 1993-1-4:2020 (E) Final draft

3.4.2.3 Wind load

The wind load acting on the bridge is calculated for two cases, one when the wind load is acting only on the bridge structure and one when it is acting only on the vehicles. These cases are then combined in order to consider the worst effect for the bridge structure. The values for the reference wind are retrieved from TSFS 2018:57 and SS-EN 1991-1-4.

3.4.3 Load combinations

The loads during *Ultimate limit state* (ULS) are combined with safety factors to ensure that the structure does not collapse or deform until failure. Structures are divided into different safety classes with corresponding partial safety factors dependent on the consequence of a collapse. TSFS 2018:57 states recommended safety classes with related partial safety factors dependent on the span length according to Table 3.9.

Table 3.9: Safety classes and safety partial factors for bridge design

Safety class	**Partial safety factor,** γ_d	**Comment**
2	0.91	Length of span $\leq$ 15m
3	1.0	Length of span $>$ 15m

The loads acting on the structure are combined according to two different load cases, one when the permanent loads are the main load, see Table 3.10 and Table 3.11, and one when the variable loads are the main load, see Table 3.12 and Table 3.13. The load cases are according to SS-EN 1990 and TSFS 2018:57. The combination factors are, in some cases, dependent on the cross section classes of the structure. In SS-EN 1994-2 5.4.2.2 (6) it is described that creep and shrinkage loads can be neglected if all parts in the bridge are in cross section class 1 or 2.

Table 3.10: STR/GEO 6.10a - ULS, cross section in CSC 1 or 2

Permanent loads	**sup**	**inf**	**Unfavorable**	**Favorable**
Self-weight	1.0	1.0	$\gamma_d \cdot 1.35 \cdot sup$	$1.0 \cdot inf$
Surfacing	1.1	0.9	$\gamma_d \cdot 1.35 \cdot sup$	$1.0 \cdot inf$
1st Shrinkage	1.0	1.0	$\gamma_d \cdot 1.35 \cdot sup$	$1.0 \cdot inf$
2nd Shrinkage	1.0	1.0	$\gamma_d \cdot 0.0 \cdot sup$	$0.0 \cdot inf$
2nd Creep	1.0	1.0	$\gamma_d \cdot 0.0 \cdot sup$	$0.0 \cdot inf$
Variable loads	Ψ_0		**Main load**	**Other load**
Traffic loads	0.75		$\gamma_d \cdot 1.5 \cdot \Psi_0$	$\gamma_d \cdot 1.5 \cdot \Psi_0$
Acceleration	0.75		$\gamma_d \cdot 1.5 \cdot 0.6 \cdot \Psi_0$	$\gamma_d \cdot 1.5 \cdot \Psi_0$
Temperature	0.6		$\gamma_d \cdot 1.5 \cdot \Psi_0$	$\gamma_d \cdot 1.5 \cdot \Psi_0$

Table 3.11: STR/GEO 6.10a - ULS, cross section in CSC 3 or 4

Permanent loads	**sup**	**inf**	**Unfavorable**	**Favorable**
Self-weight	1.0	1.0	$\gamma_d \cdot 1.35 \cdot sup$	$1.0 \cdot inf$
Surfacing	1.1	0.9	$\gamma_d \cdot 1.35 \cdot sup$	$1.0 \cdot inf$
1st Shrinkage	1.0	1.0	$\gamma_d \cdot 1.35 \cdot sup$	$1.0 \cdot inf$
2nd Shrinkage	1.0	1.0	$\gamma_d \cdot 1.0 \cdot sup$	$1.0 \cdot inf$
2nd Creep	1.0	1.0	$\gamma_d \cdot 1.35 \cdot sup$	$1.0 \cdot inf$
Variable loads	Ψ_0		**Main load**	**Other load**
Traffic loads	0.75		$\gamma_d \cdot 1.5 \cdot \Psi_0$	$\gamma_d \cdot 1.5 \cdot \Psi_0$
Acceleration	0.75		$\gamma_d \cdot 1.5 \cdot 0.6 \cdot \Psi_0$	$\gamma_d \cdot 1.5 \cdot \Psi_0$
Temperature	0.6		$\gamma_d \cdot 1.5 \cdot \Psi_0$	$\gamma_d \cdot 1.5 \cdot \Psi_0$

Table 3.12: STR/GEO 6.10b - ULS, cross section in CSC 1 or 2

Permanent loads	**sup**	**inf**	**Unfavorable**	**Favorable**
Self-weight	1.0	1.0	$\gamma_d \cdot 0.89 \cdot 1.35 \cdot sup$	$1.0 \cdot inf$
Surfacing	1.1	0.9	$\gamma_d \cdot 0.89 \cdot 1.35 \cdot sup$	$1.0 \cdot inf$
1st Shrinkage	1.0	1.0	$\gamma_d \cdot 0.89 \cdot 1.35 \cdot sup$	$0.0 \cdot inf$
2nd Shrinkage	1.0	1.0	$\gamma_d \cdot 0.0 \cdot sup$	$0.0 \cdot inf$
2nd Creep	1.0	1.0	$\gamma_d \cdot 0.0 \cdot sup$	$0.0 \cdot inf$
Variable loads	Ψ_0		**Main load**	**Other load**
Traffic loads	0.75		$\gamma_d \cdot 1.5$	$\gamma_d \cdot 1.5 \cdot \Psi_0$
Acceleration	0.75		$\gamma_d \cdot 1.5 \cdot 0.6$	$\gamma_d \cdot 1.5 \cdot \Psi_0$
Temperature	0.6		$\gamma_d \cdot 1.5$	$\gamma_d \cdot 1.5 \cdot \Psi_0$

Table 3.13: STR/GEO 6.10b - ULS, cross section in CSC 3 or 4

Permanent loads	**sup**	**inf**	**Unfavorable**	**Favorable**
Self-weight	1.0	1.0	$\gamma_d \cdot 0.89 \cdot 1.35 \cdot sup$	$1.0 \cdot inf$
Surfacing	1.1	0.9	$\gamma_d \cdot 0.89 \cdot 1.35 \cdot sup$	$1.0 \cdot inf$
1st Shrinkage	1.0	1.0	$\gamma_d \cdot 0.89 \cdot 1.35 \cdot sup$	$1.0 \cdot inf$
2nd Shrinkage	1.0	1.0	$\gamma_d \cdot 1.0 \cdot sup$	$1.0 \cdot inf$
2nd Creep	1.0	1.0	$\gamma_d \cdot 0.89 \cdot 1.35 \cdot sup$	$1.0 \cdot inf$
Variable loads	Ψ_0		**Main load**	**Other load**
Traffic loads	0.75		$\gamma_d \cdot 1.5$	$\gamma_d \cdot 1.5 \cdot \Psi_0$
Acceleration	0.75		$\gamma_d \cdot 1.5 \cdot 0.6$	$\gamma_d \cdot 1.5 \cdot \Psi_0$
Temperature	0.6		$\gamma_d \cdot 1.5$	$\gamma_d \cdot 1.5 \cdot \Psi_0$

The loads during *Serviceability limit state* (SLS) are combined with safety factors regarding discomfort, such as deformations. The load combinations used for SLS are presented in Table 3.14, according to SS-EN 1990 and TSFS 2018:57. When calculating the load effects, the effects of creep and shrinkage should not be neglected irrespective of the design limit-state.

Table 3.14: Frequent 6.15b - SLS

Permanent loads	**sup**	**inf**		**Unfavorable**	**Favorable**
Self-weight	1.0	1.0		$1.0 \cdot sup$	$1.0 \cdot inf$
Surfacing	1.1	0.9		$1.0 \cdot sup$	$1.0 \cdot inf$
1st Shrinkage	1.0	1.0		$1.0 \cdot sup$	$1.0 \cdot inf$
2nd Shrinkage	1.0	1.0		$1.0 \cdot sup$	$1.0 \cdot inf$
2nd Creep	1.0	1.0		$1.0 \cdot sup$	$1.0 \cdot inf$
Variable loads	Ψ_0	Ψ_1	Ψ_2	**Main load**	**Other load**
Traffic loads	0.75	0.75	0	Ψ_1	Ψ_2
Acceleration	0.75	0.75	0		
Temperature	0.6	0.6	0.5	Ψ_1	Ψ_2

3.5 Capacity checks

The design procedure for calculating a simply supported composite bridge with corrugated web in stainless steel is explained in detail in the Master Thesis *Design of Composite Steel-Concrete Bridges using Stainless Steel Girders with Corrugated Webs* by Henrysson & Yman (2020). Compared to simply supported bridges, there are several additional capacity checks that needs to be performed for continuous girders. Those checks are mainly performed close to the internal supports. The capacity checks needed for a continuous bridge regarding the main girders are further described in following sections. The influence of material choice and web design on the calculation procedure is identified and explained.

3.5.1 Ultimate limit state (ULS), Construction stage

During construction phase, composite action between the concrete and the steel is not yet fulfilled and the steel girders are thereby carrying the loads without contribution from the deck. In Table 3.15, the different capacity checks that needs to be performed during construction stage are summarized. The table also shows how the calculation procedure differs if the continuous bridge is designed with a flat or a corrugated web and if it is designed in stainless or carbon steel. Notice that Table 3.15 only presents where there is a difference in the calculation procedure and not if there is a difference in material parameters. The differences in the calculations are described further in the following subsections.

Table 3.15: Capacity checks during construction stage, ULS

Capacity check	**Carbon steel**	**Stainless steel**	**Flat web**	**Corrugated web**
LT-buckling	Buckling curve dependent on thickness & steel strength	Buckling curve d	Contribution from flanges and web	Contribution from web neglected
Stresses			Contribution from flanges and web	Contribution from web neglected

3.5.1.1 LT-buckling

The bottom flange over the internal support and the top flange in span needs to be controlled against LT-buckling during construction stage. This is needed since the flanges might buckle between the transverse stiffeners. If the compressed flange is in cross section class 4, the width needs to be reduced due to the risk of plate buckling. When calculating LT-buckling for a girder with flat web, 1/3 of the compressed part of the web can be accounted for in the stiffness. For a corrugated web, the contribution from the web is neglected, according to SS-EN 1993-1-5 Annex D.

The choice of material also influences the LT-buckling. For stainless steel, buckling curve d is always used, see SS-EN 1993-1-4 5.4.2. For carbon steel on the other hand, the choice of buckling curve depends on the thickness and steel strength of the compressed flange. See SS-EN 1993-1-1 6.3.1.2.

3.5.1.2 Stresses

The stresses arising during construction stage are calculated in the top and bottom flange in the steel section. The stresses are compared to the ultimate strength for the steel material to assure that the steel girders alone can withstand the stresses.

3.5.2 Ultimate limit state (ULS), Service stage

In the service stage, composite action is established and the capacity checks that needs to be performed on the composite cross section are further presented in the following subsections. A summary of the different capacity checks performed in service stage and which calculations that are influenced by the web design or material choice are presented in Table 3.16.

Table 3.16: Capacity checks during service stage, ULS

Capacity check	**Carbon steel**	**Stainless steel**	**Flat web**	**Corrugated web**
LT-buckling	Buckling curve dependent on thickness & steel strength	Buckling curve d	Contribution from both flanges and web	Contribution from web neglected
Bending moment			Both the web and the flanges contribute to the capacity	Only the flanges contribute to the capacity
Shear capacity	For flat webs, different limit for control of buckling	For flat webs, different limit for control of buckling		Different buckling behavior
Interaction				Not checked since no contribution from web
Studs				
Stiffeners				Stiffeners only needed on one side of the web
Cross-beams				Larger distance between cross-beams
Welds				

3.5.2.1 LT-buckling

The bottom flange over the internal support needs to be controlled against LT-buckling in service stage in the same manner as in construction stage, SS-EN 1994-2, 6.2.1.5 (6). The compressed top flange in span does not need to be controlled against LT-buckling since composite action is established and the top flanges in span are considered as rigid, hence no risk of buckling exists.

3.5.2.2 Bending moment capacity

The bending moment capacity of a composite cross section is calculated according to SS-EN 1994-2, 6.2. For a corrugated web, the steel flanges are designed to withstand the bending moment alone while the calculations for a flat web also includes contribution from the web. If the compressed flange is in cross section class 4, the width of the flange might need to be reduced due to the risk of buckling. The stresses arising in the steel cross section due to the different loads are summarized and calculated for the top and bottom flange of the girder, both in span and over the internal supports.

3.5.2.3 Shear capacity

The steel girders are designed for the web to withstand the shear force. The shear capacity of the web is calculated differently for a corrugated web compared to a flat web, where the choice of material also influences the calculations of the last-mentioned one.

Starting with the influence of different web designs where the main difference is the buckling behavior. For corrugated webs, both global and local buckling modes are considered which are calculated according to SS-EN 1993-1-5, Annex D. The lowest of the two reduction factors are used for the reduction of the shear capacity.

For the design of flat webs, the resistance to shear buckling needs to be controlled. The calculation is performed differently if the flat web is designed in stainless steel or carbon steel. For stainless steel, the control is made according to SS-EN 1993-1-4, 5.6(2) and for carbon steel according to SS-EN 1993-1-5, 5.1(2). These two standards provide limits for when the influence of shear buckling needs to be considered. When shear buckling is considered, the shear capacity of the web is reduced. For both stainless steel and carbon steel the reduction in shear capacity depends on whether the end-supports are rigid or non-rigid. If the shear capacity from the web is adequate to withstand the shear force, contribution from the flanges can be neglected.

3.5.2.4 Interaction moment and shear

When performing capacity calculations for continuous girders with flat webs, the interaction between bending moment and shear needs to be calculated according to SS-EN 1993-1-5, 7.1. This, because the capacity of the web is included both in

the bending capacity and the shear capacity. Both the shear force and the negative bending moment will be large over the internal supports hence the interaction needs to be controlled at this location. For corrugated webs, the web does not contribute to the bending capacity due to the accordion effect. This means that the check of interaction between bending moment and shear force is unnecessary for this type of girder.

3.5.2.5 Studs

To get full composite action between the steel girder and the concrete deck, the studs must be designed to transfer the shear flow between the two materials, SS-EN 1994-2, 6.6.3. The loads causing the shear flow are the permanent loads as well as the variable loads (traffic and temperature) and the horizontal braking/acceleration loads. Over the supports, the shear flow is higher compared to the rest of the bridge due to the shear force which demands an increased number of studs in these regions.

3.5.2.6 Stiffeners on main girders

Stiffeners are placed on the main girders to prevent buckling of the web plate and to connect the cross-beams. The transverse stiffeners over the supports are exposed to high reaction forces and therefore capacity checks of the stiffeners need to be performed in order to ensure enough stiffness. For corrugated webs, stiffeners needs to be placed only at one side of the web for the connection to the cross-beams. However, it is most common to place the stiffeners on both sides of the girders with flat webs due to its lower out-of-plane stiffness.

3.5.2.7 Cross-beams

The cross-beams will resist the wind load acting on the bridge and also distribute the lifting force during bearing change. The capacity of the cross-beams needs to be calculated and checked against bending moment, shear force, buckling of cross-beam at bearing change and buckling of stiffener on cross-beams. Additionally, the load-transferring welds and the joints between the cross-beams and the main girder needs to be controlled. Due to the corrugated web, the distance between the cross-beams can be increased.

3.5.2.8 Welds

The welds in the cross section needs to be controlled regarding design resistance in ULS and in *Fatigue limit state* (FAT). The purpose of the welds is to transfer shear flow between the different components. The fillet welds should be controlled according to SS-EN 1993-1-8, 4.5.3.2. The design resistance of welds is dependent on the correlation factor, β_w, which is dependent on the material of the weld. For carbon steel, β_w is found in SS-EN 1993-1-8, Table 4.1, and for stainless steel β_w=1.0 according to SS-EN 1993-1-4, 6.3(1).

3.5.3 Serviceability limit state (SLS)

The checks performed in SLS are different for the span and the support regions. Over the supports, the top part of the composite section will be in tension and the maximum stresses in the reinforcement steel needs to be controlled according to SS-EN 1994-2, 7.2.2. In span, the deflections need to be calculated together with the web breathing.

3.5.3.1 Deflection

The deflection of the bridge structure in SLS due to traffic loads should be limited according to *Krav brobyggande*, B.3.4.2.2. Stainless steel has a nonlinear behaviour before it reaches yielding, and therefore the modulus of elasticity does not follow a linear approach. A secant modulus of elasticity can be calculated instead which is dependent on the current applied stress, see 2.3.2.1.

3.5.3.2 Web breathing

The slenderness of the web plate should be limited since large deformations in plane can cause damaging breathing. If the web fulfils the limits according to SS-EN 1993-2 7.4, the check against web breathing is unnecessary.

3.5.4 Fatigue limit state (FAT)

The fatigue calculations are based on the lambda-method and carried out according to SS-EN 1993-2 and SS-EN 1993-1-9. The governing construction details of the steel girders needs to be located in order to perform a fatigue analysis. Additionally, for continuous bridges, the reinforcing steel will be in tension over the internal support and therefore the reinforcement should also be analysed in FAT. Due to the continuous girders, further critical details need to be studied over the internal support as well. Since the varying behaviour of the girder will demand different cross sections along its length, it is important to investigate the fatigue capacity at the locations where there will be a change in cross-sectional dimensions. The details controlled for FAT in this thesis are:

- Weld between bottom flange and web over support
- Joint between bottom flanges on main girders
- Joint between bottom flanges on main girders where there is also a change in cross section
- Weld between bottom flange and stiffener
- Effect of studs on the top flange on the main girder

4

Finite Element Model

When designing bridges, it is important to choose an appropriate software in order to capture the structural behaviour. Continuous bridges are statically indeterminate and the difference in stiffness along the bridge girders will influence the load distribution. Therefore, a more complex software is required for the system analysis for this type of bridges. Following chapter will explain how the bridges are modelled in the software, how the loads are considered and how the results are extracted and analysed.

The finite element model is created in order to calculated load effects both for twin-girder composite bridges with corrugated webs and with flat webs. The model is generalized which enables usage for bridges in two or more spans with different geometric dimensions and material parameters. Thereby, the model can be used for girders in both stainless steel and in carbon steel.

4.1 Structure of the design procedure

In this thesis, the FE-program Brigade/Plus is used in order to simulate the structural behaviour of composite bridges and calculate sectional forces, moments and displacements. The model is built up using Python-scripts and the retrieved load effects are used for the capacity controls carried out in Mathcad Prime. In Figure 4.1 the main structure of the design process is presented together with used programs.

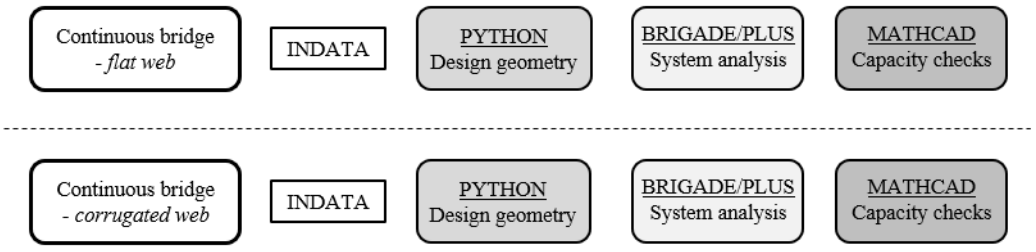

Figure 4.1: Structure of design procedure including the used programs.

Two separate systems are created, one for a continuous bridge with flat webs and one for a continuous bridge with corrugated webs. This, because the stiffness calculations differ between the two designs as mentioned in Section 3.3.3. There are six models created for each web design; one for construction loads, one for short-term loads, one for long-term loads, one for creep loads, one for shrinkage loads and one for temperature loads. The reason for using several models is because different loads should be applied during different phases dependent on if creep should be considered or not. Another reason is that some of the loads should be applied in the concrete deck and the steel girders separately. Each model in Brigade/Plus consists of nine Python-scripts that generates the design geometry, material parameters and the considered loads. The required information regarding dimensions and material data for the bridge is inserted in the INDATA-file before generating the models. For the system with flat webs, the required information for the analysis is presented in Appendix A. For the system with corrugated webs, the required information is presented in Appendix B. The dimensions and geometry are extracted from the Python-scripts and the load effects are extracted from the system analysis in Brigade/Plus. This data is implemented in the capacity calculations conducted in Mathcad Prime for both Construction stage and Service stage. Figure 4.2 shows a detailed structure of the system used for the design process.

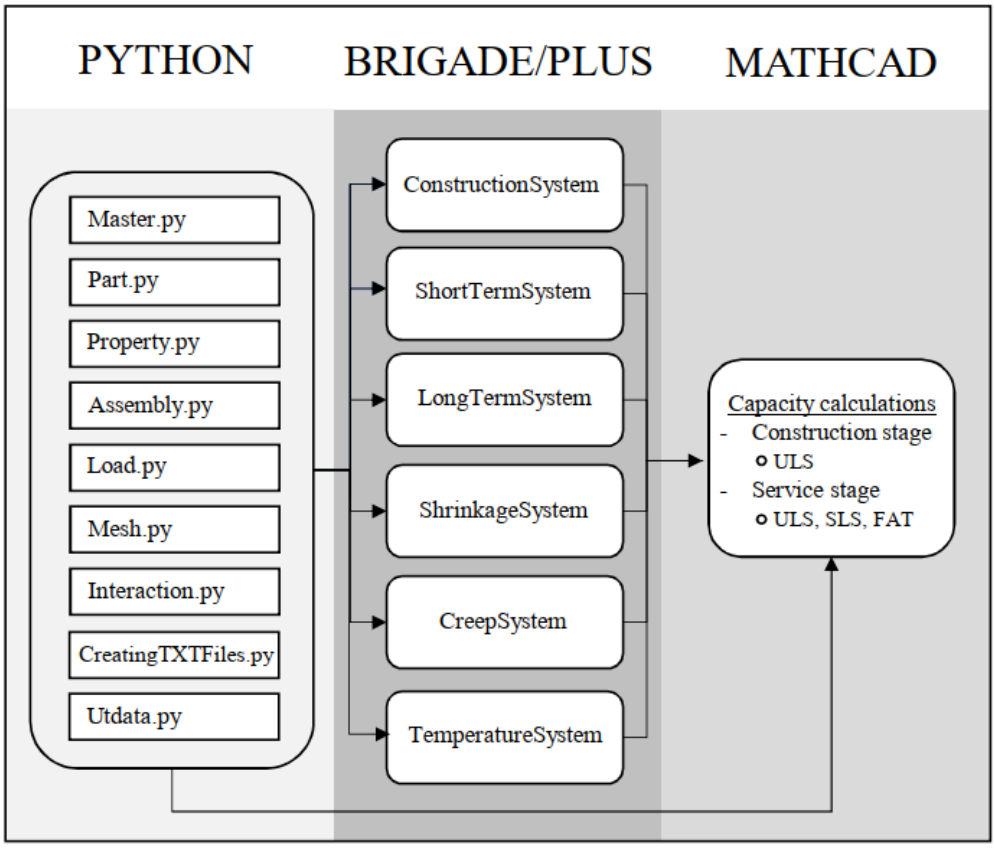

Figure 4.2: Detailed structure of the design process.

4.2 Setting up the models

Different models will be set up in Brigade/Plus in order to apply the loads and to take creep into account in a correct way. A summary of the different models is presented in Figure 4.3. It is explained for which models the composite action is modelled and for which ones the concrete deck and the steel girders are modelled separately. In the figure, it is also stated how the interaction between the structural parts is modelled and which loads that are applied. How the different sections with associated interactions are modelled in Brigade/Plus are further described in Section 4.2.3 & 4.2.4. How the loads are applied are explained in Section 4.3.

MODEL	SECTION	INTERACTION	LOADS
ConstructionSystem	Steel section	Constrained in z-direction	Self-weight of structure Form-work Wind loads
ShortTermSystem	Composite section Short-term constants	Constrained in z-direction	Traffic loads Wind load
LongTermSystem	Composite section Long-term constants	Constrained in z-direction	Self-weight of structure Coating
ShrinkageSystem	Steel/concrete section	Constrained in all directions	Shrinkage load
CreepSystem	Composite section Long-term constants	Constrained in z-direction	Creep load
TemperatureSystem	Steel/concrete section	Constrained in all directions	Temperature load

Figure 4.3: Summary of the different models for the system analysis.

4.2.1 Model orientation

The bridge is modelled in 3D to consider the load distribution both in transverse and longitudinal direction. The global and local coordinate system for the model is defined according to Figure 4.4. Origo for the global system is located in the center line on top of the concrete, see Figure 4.5.

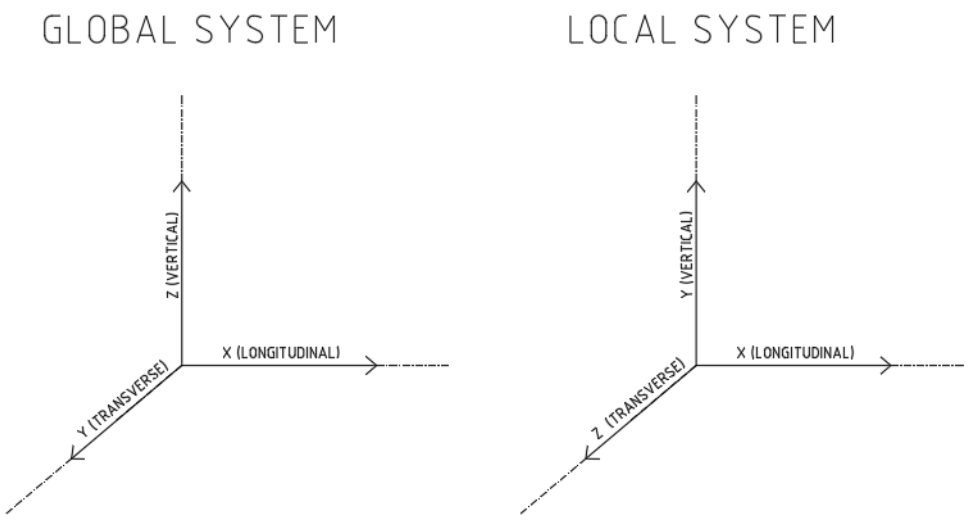

Figure 4.4: Coordinate system for global and local system.

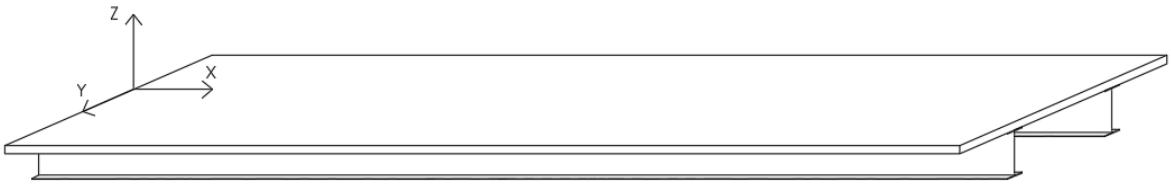

Figure 4.5: Location of origo for global system.

4.2.2 Boundary conditions

The boundary conditions are dependent on the number of spans. For a two-span continuous bridge, the boundary conditions for the supports are defined according to Figure 4.6 and Table 4.1 with coordinates in accordance to the global system. The internal support is prevented from movement in both longitudinal and transverse direction while the end supports only prevents movement in the transverse direction. In order to stabilize the model, the rotation in x-direction is constrained for each support.

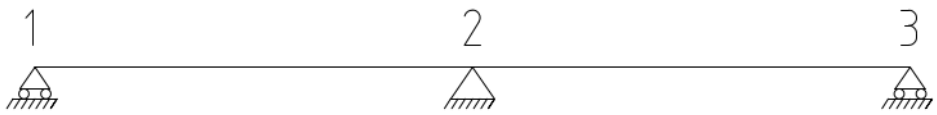

Figure 4.6: Boundary conditions for a 2-span bridge.

Table 4.1: Boundary conditions for a 2-span bridge

Support	X	Y	Z	RX	RY	RZ
1		X	X	X		
2	X	X	X	X		
3		X	X	X		

For a multiple span bridge, the boundary conditions are defined according to Figure 4.7 and Table 4.2 with coordinates in accordance to the global system. Here, one of the end supports prevents movement in both longitudinal and transverse direction while the rest of the supports only prevent movement in the transverse direction. In conformity with the two-span model, the rotation in x-direction is constrained for each support.

Figure 4.7: Boundary conditions for a bridge with multiple spans.

Table 4.2: Boundary conditions for a multiple span bridge

Support	X	Y	Z	RX	RY	RZ
1	X	X	X	X		
2		X	X	X		
3		X	X	X		
... n		X	X	X		

4.2.3 Modelling composite sections

In Brigade/Plus, structural elements can be modelled using different element types. How the elements are modelled effects the results from the simulations which is why extra care needs to be taken when setting up the models. Figure 4.8 shows how composite sections are modelled. The composite sections are further described in the following sections.

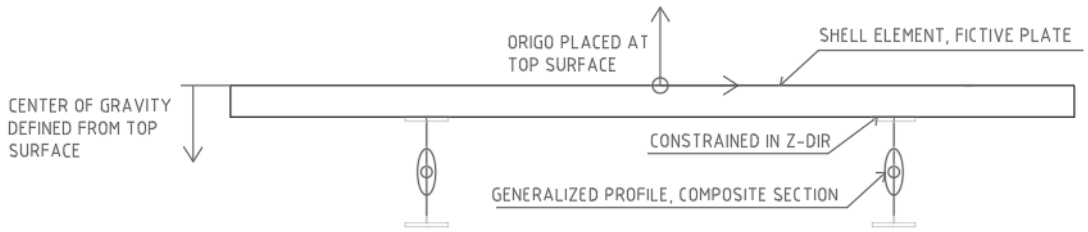

Figure 4.8: Structure of model with composite section.

4.2.3.1 Shell element

The concrete deck is modelled as a fictive shell element in order to distribute the loads applied on the deck to the beams in the transverse direction. In order to enable the load distribution, the modulus of elasticity is set equal to the considered concrete class. For the composite sections, the shell element is not supposed to contribute to the bearing capacity in the longitudinal direction since the contribution from the concrete deck is included in the beams instead.

4.2.3.2 Beam elements with generalized profiles

The girders are modelled as beam sections with generalized profiles with material properties defined as those for the steel girders. Generalized profiles do not have a specific shape as the standard profiles provided in Brigade/Plus. Instead, the input needed for this profile type is the cross-sectional area, the stiffness in the strong and the weak direction and the center of gravity. This enables the ability to consider composite action by implementing the cross-sectional constants for the composite sections, $A_{comp.i}$, $I_{y.comp.i}$, $I_{z.comp.i}$ and $z_{tp.comp.i}$ calculated according to Section 3.3.3.

As a simplification, the effective width of the concrete deck due to shear lag calculated in Section 3.3.2 is assumed as a uniform effective width for the internal spans and support regions (Vayas and Iliopoulos, 2014). The effective concrete width considered in the model is illustrated in Figure 4.9. The cross-sectional constants can then be applied to the right sections of the beam elements along the bridge. During *construction stage*, no composite action is established and therefore the beam elements will be modelled without considering the contribution from the concrete deck.

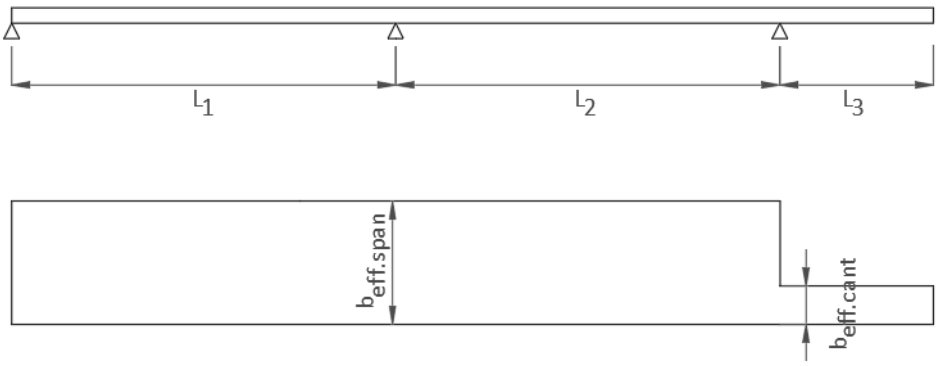

Figure 4.9: Effective width of the concrete deck considered in the models.

Another reason for using generalized profiles instead of predefined profiles in Brigade/-Plus is because the cross-sectional dimensions can easily be changed. When using the model to analyse a composite bridge with corrugated webs the cross-sectional constants can be changed instead of using a completely different profile.

4.2.3.3 Interaction between elements

The interaction between the shell element and the beam elements are modelled with a connection constrained in z-direction. This allows the loads to be transferred from the deck to the girders. The reason for not using moment stiff connections is that the stiffness of the concrete deck is already included in the beam elements. Using moment stiff connections would result in additional stiffness in the longitudinal direction from the shell element which is already accounted for.

4.2.4 Modelling steel/concrete sections

The shrinkage and temperature loads should be applied on the concrete deck and the steel girders separately. The previous described model with composite section is therefore not suitable for these types of loads and a new section is set up. Figure 4.10 shows how this section is modelled. A more detailed description of how the different elements are composed are described in the following sections.

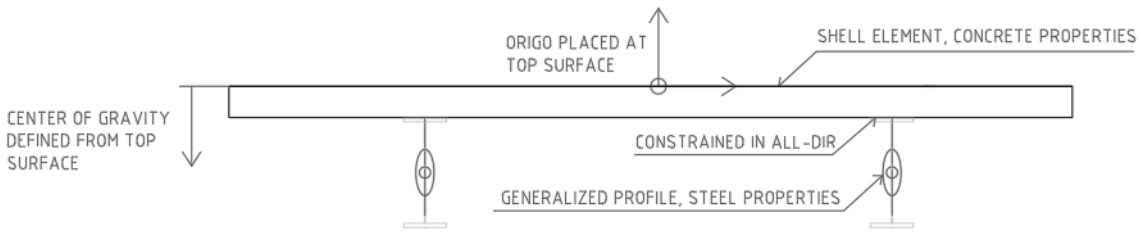

Figure 4.10: Structure of model with steel/concrete section.

4.2.4.1 Shell element

The concrete deck is modelled as a shell element with real concrete parameters. The thermal expansion factor for the concrete is included in the property manual in order to apply temperature loads on the shell element.

4.2.4.2 Beam elements with generalized profiles

The beam elements are modelled as generalized profiles but unlike the composite section, only cross-sectional constants and properties for the steel girders are applied. No contribution from the concrete deck is included in the beam elements since the shell is modelled with real concrete deck parameters.

4.2.4.3 Interaction between elements

The interaction between the shell element and the beam elements are modelled as tied in all directions and the connection is regarded as moment stiff. Thereby, the contribution from the concrete deck can be included in the total bearing capacity in the longitudinal direction.

4.3 Loads

The loads included in the analysis with associated magnitude are presented in Section 3.4. It is described in the following section how these loads are applied in the FE-model and when they are considered.

4.3.1 Construction loads

During construction stage, the steel girders will carry the loads arising from the casting of the concrete deck. These loads are modelled according to Table 4.3. The self-weight of the steel girders is modelled as *transverse line loads* which is dependent on the cross-sectional dimensions. The self-weight from the concrete deck is modelled as a *pressure load* with the density for wet concrete. The load from the form work and the additional construction loads are divided equally between the two girders and modelled as transverse line loads along the beams. The wind load is recalculated to vertical force components applied as transverse line loads along the beams, for more detailed description see Section 4.3.3.3.

Table 4.3: Construction loads in Brigade/Plus

Load	**Load type in Brigade/Plus**
Form work	Transverse line load
Construction load	Transverse line load
Steel girders	Transverse line load
Wet concrete	Pressure load
Edge beam	Shell edge load
Wind load	Transverse line load

4.3.2 Permanent loads

The permanent loads included in the model are defined in Section 3.4.1. These loads are applied in the long-term model and how they are modelled is presented in Table 4.4.

Table 4.4: Permanent loads in Brigade/Plus

Load	**Load type in Brigade/Plus**
Steel girder	Transverse line load
Reinforced concrete	Pressure load
Edge beam	Shell edge load
Coating	Transverse line load
Shrinkage	Temperature field
Creep (2nd order)	Temperature field

The self-weight of the reinforced concrete is applied as a pressure load spread across the fictive deck. The steel girders will have different cross-sectional area along the bridge due to cross-sectional changes which will affect the self-weight. Therefore, the self-weight of the steel girders will be modelled as transverse line loads along the beams with varying amplitude for different sections. The load from the coating is also applied in the model as transverse line loads along the beams. The self-weight of the edge beams including the rails are modelled as uniform *shell edge loads* along both edges of the shell element.

4.3.2.1 Shrinkage

The shrinkage force acting on the concrete leads to both primary and secondary effects, see Section 3.4.1.3. In the shrinkage model, the primary effects are modelled as a uniform temperature difference in the concrete deck calculated according to Equation 4.1 (Vayas and Iliopoulos, 2014). The modulus of elasticity, E_{cm}, of the modelled concrete deck is reduced by the creep factor $n_{L.cs}$.

$$\Delta T_{NS} = \frac{\varepsilon_{cs}}{\alpha_T} \tag{4.1}$$

Where,

ε_{cs} is the total shrinkage strain
α_T is the linear coefficient for thermal expansion for concrete

The temperature difference results in a moment $M_{s.cs}$ in the steel section. This moment, from the primary effects of shrinkage, is extracted from the results and recalculated for composite cross-section, see Equation 4.2 and Figure 4.11.

$$M_{comp.cs} = M_{s.cs} \cdot \frac{I_{y.steel}}{I_{y.comp.cs}} \tag{4.2}$$

Where,

$M_{comp.cs}$ is the moment acting in the composite section from primary effects of shrinkage
$M_{s.cs}$ is the moment acting in the steel section from primary effects of shrinkage
$I_{y.steel}$ is the moment of inertia for the steel section
$I_{y.comp.cs}$ is the moment of inertia for shrinkage composite section

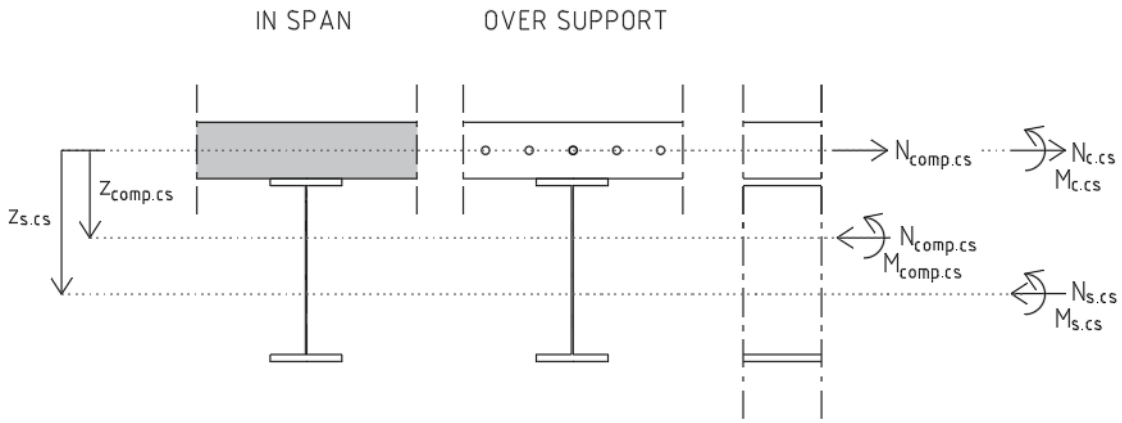

Figure 4.11: Primary effects of shrinkage. Figure redrawn from Vayas and Iliopoulos (2014).

The second order effect of shrinkage can also be modelled as a temperature difference applied along the beam elements in the non-cracked regions (Vayas and Iliopoulos, 2014). The temperature difference is calculated according to Equation 4.3 using the moment arising from the primary order effects of shrinkage. This moment varies along the whole bridge, although a simplification is made where an average of the moment in span is applied along the beam elements. The modulus of elasticity, E_{cm}, for the modelled concrete deck is reduced by the creep factor $n_{L.cs}$ similarly as for the primary effects. The temperature difference, ΔT_{MS}, results in an additional moment M_{PT} over the internal support, see Figure 4.12.

$$\Delta T_{MS} = \frac{M_{comp.cs}}{E_s \cdot I_{y.comp.cs}} \cdot \frac{h_{beam}}{\alpha_s} \tag{4.3}$$

Where,

ΔT_{MS}	is the temperature difference applied in the model
$M_{comp.cs}$	is the moment acting on the composite section from primary effects of shrinkage
E_s	is the module of elasticity for steel
$I_{y.comp.cs}$	is the moment of inertia for shrinkage composite section
h_{beam}	is the total height of the steel cross section
α_s	is the thermal expansion coefficient for steel

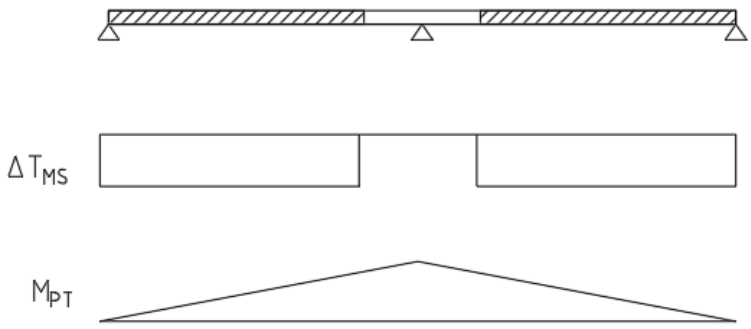

Figure 4.12: Second order effects of shrinkage. Figure redrawn from Vayas and Iliopoulos (2014).

4.3.2.2 Creep

The primary effects of creep are taken into account by changing the modular ratios for different phases, see Section 3.2.3. The second order effects on the other hand, leading to an additional unfavorable moment over the internal supports, are implemented as a temperature difference applied at the uncracked regions of the beams. This temperature is calculated according to Equation 4.4 (Vayas and Iliopoulos, 2014).

$$\Delta T_{MP} = \frac{M_0}{E_s \cdot h_{beam}} \cdot \left(\frac{1}{I_{y.comp.long}} - \frac{1}{I_{y.comp.short}}\right) \tag{4.4}$$

Where,

ΔT_{MP}	is the temperature difference due to creep applied in the model
M_0	is the moment acting on the short-term composite section from permanent loads
E_s	is the modulus of elasticity for steel
$I_{y.comp.long}$	is the long-term moment of inertia for the composite section
$I_{y.comp.short}$	is the short-term moment of inertia for the composite section
h_{beam}	is the total height of the steel beam
α_s	is the thermal expansion coefficient for steel

The moment acting on the short-term composite section from permanent loads must be calculated separately before it can be implemented in the temperature difference

for creep. This moment varies along the bridge but as a simplified approach the largest moment in span is extracted and a uniform temperature difference is applied along the uncracked regions, see Figure 4.13.

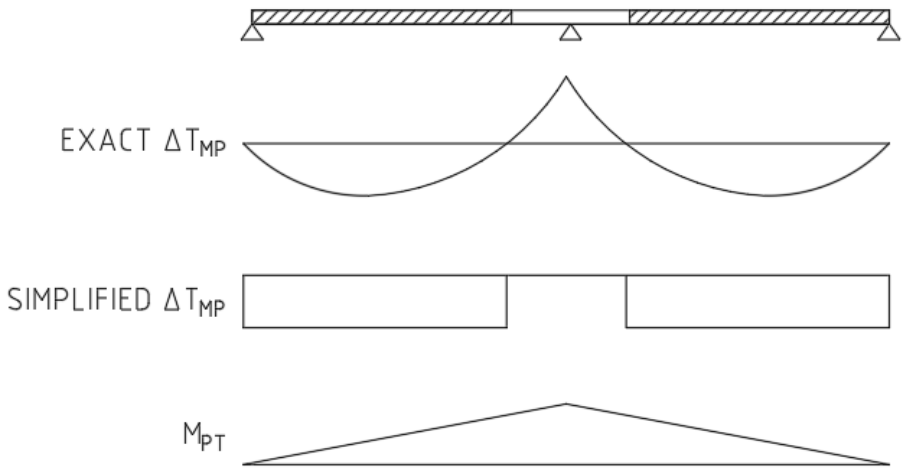

Figure 4.13: Second order effects of creep. Figure redrawn from Vayas and Iliopoulos (2014).

4.3.3 Variable loads

The variable loads applied on the bridge are defined in Section 3.4.2. How these loads are modelled is presented in Table 4.5 and described further in following sections.

Table 4.5: Variable loads in Brigade/Plus

Load	**Load type in Brigade/Plus**
Traffic loads	Live loads 4.3.3.1
Braking/Acceleration	Normal line load
Wind load	Transverse line load
Side force	Transverse line load
Temperature load	Temperature field

4.3.3.1 Traffic loads

The traffic loads applied in the model are presented in Section 3.4.2. All vehicle loads are imported to Brigade/Plus from Design code *TDOK 2016:0204 version 3.0 med TSFS 2018:57*, that includes vehicle loads defined in both Eurocode and in TSFS 2018:57. The traffic loads are modelled as *live loads*.

In order to find the worst position for the traffic loads, six different lane positions are analysed according to Figure 4.14. The number of lanes is limited in order to decrease the simulation time. The lanes are modelled as a line in the center of the lane width which is equal to 3m. Two lanes with a center distance of 3m are combined in Brigade/Plus simultaneously, both exposed to uniformly distributed loads and traffic loads according to the design codes.

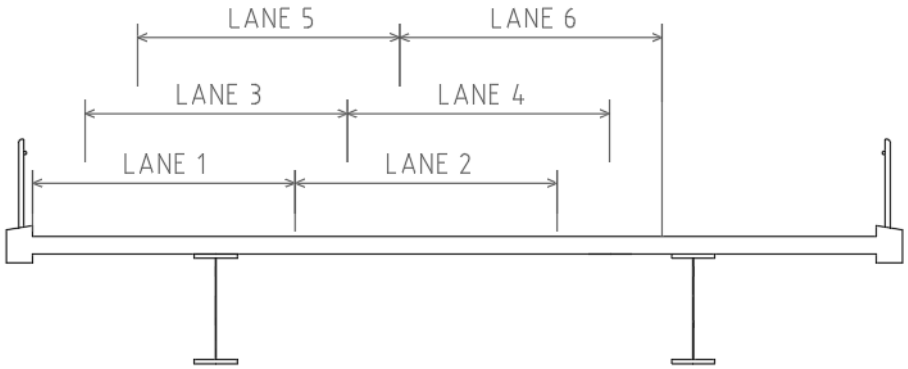

Figure 4.14: Lane positions modelled for analysis in the model.

4.3.3.2 Braking/acceleration force

The braking/acceleration force should be applied at the top of the coating in the longitudinal direction according to SS-EN 1991-2 4.4.1. In order to apply this force at the right position, two fictive beams are modelled above the steel girders at the level of the coating surface, see figure 4.15. The beam elements should only transfer the braking/acceleration force to the main girders and therefore the material properties are set to fictive values. The connections to the main girders are moment stiff enabling the load distribution. The braking/acceleration force is implemented as *normal line loads* along the fictive beams with opposite directions.

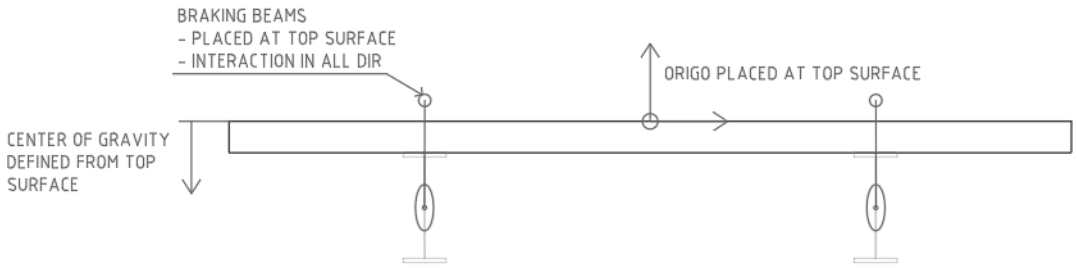

Figure 4.15: Structure of model including braking beams.

4.3.3.3 Wind load

The wind load acting on the bridge is calculated for two cases, one when the wind load is acting only on the bridge structure and one when it is acting only on the

vehicles. The two cases are combined in Brigade/Plus in order to find the worst combination. The wind load is recalculated to a moment applied at the top of the concrete deck and then divided with the center distance between the two girders in order to get two vertical force components, according to Figure 4.16. The vertical components are modelled as transverse line loads along the two main girders. The wind load is applied in the short-term model with wind load acting both on the traffic and on the bridge structure. It is also included in the construction model, although the wind load is then only considered on the bridge structure.

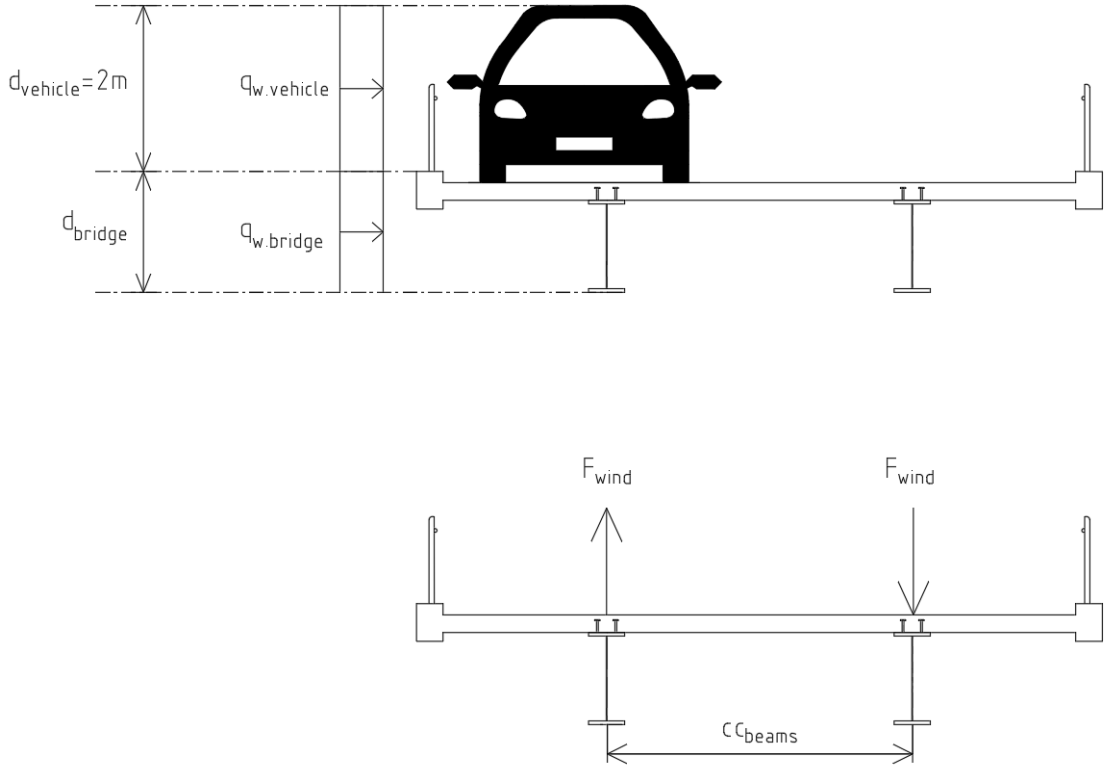

Figure 4.16: Wind load acting on the bridge.

4.3.3.4 Side force

The horizontal side force from braking is modelled in the same manner as the wind load with two vertical components applied as transverse line loads along the main girders. The side force is recalculated as a moment working in the level of the concrete deck and then divided with the center distance of the main girders in order to obtain the vertical force components.

4.3.3.5 Temperature load

The temperature loads are defined in Section 3.4.2.2. The uniform temperature component is modelled as a constant temperature difference for the whole structure, making the bridge expand or contract. The non-uniform temperature compo-

nent is modelled as temperature differences between the materials where a constant temperature difference is set for the steel and concrete elements respectively.

4.4 Verification

In order to verify the reliability of the model, both a convergence study and a verification comparing the results to hand-calculations are carried out.

4.4.1 Convergence study

A convergence study is conducted in order to establish a correct mesh size to be used for the model. A uniformly distributed load is applied on the concrete deck and the maximum span moment is calculated for each mesh size. The result from the convergence study is presented in Figure 4.17. A too coarse mesh could lead to inaccurate results and a too fine mesh could lead to unnecessary long computational time. The convergence study shows that there is just a small difference in maximum span moment between the different mesh sizes thus the mesh size of 0.14 mm is applied for the model. This in order to provide accurate results with a reasonable computational time.

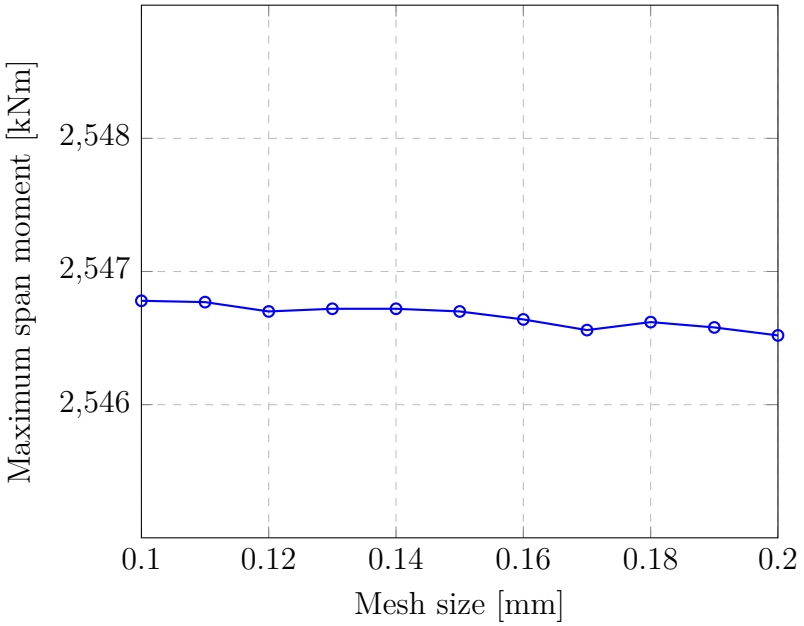

Figure 4.17: Convergence study comparing maximum span moment for several mesh sizes.

4.4.2 Result verification

The models are verified by hand-calculations. The support reactions and support moments are calculated by hand and compared to results obtained in Brigade/Plus.

The margin of error for the reaction forces is between 0-1 % and for bending moment over the internal support between 5-6 %. This applies for all models which is concluded as reasonable.

4.5 Extracting results

From the model, sectional forces and moments, displacements and reaction forces are retrieved for the capacity calculations. These results are taken along the governing main girder. The names of the different outputs are defined in Figure 4.18.

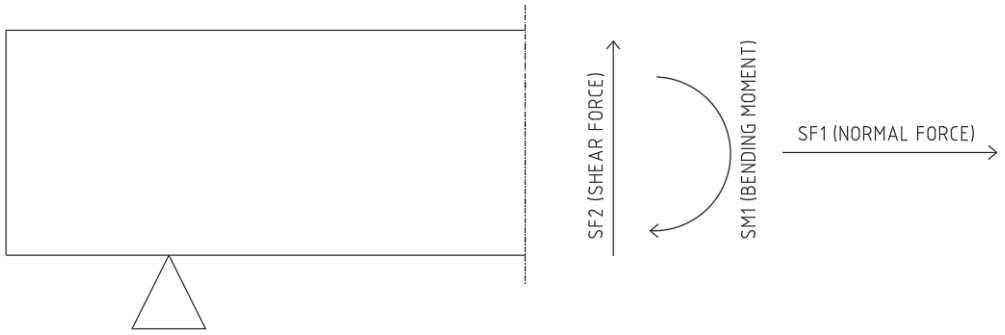

Figure 4.18: Name of output parameters in Brigade/Plus.

All data is extracted from the system analysis in Brigade/Plus and converted to text-files using Python-scripts. The text-files are imported to Mathcad Prime were the capacity checks are carried out according to the methodology described in Section 3.5. In order to combine the results retrieved from the different models, the moments are recalculated to stresses using *Navier's formula*.

5
Case Studies

In this chapter, the two performed case studies will be presented. The procedure of conducting the case studies will be explained together with the retrieved results. The chapter will also include important limitations and assumptions made in order to perform the studies and to draw reasonable conclusions.

For the first case study, a continuous composite bridge in two spans was investigated with three designs using different choices for material and web form. Two design concepts consisted of girders with flat webs in different types of carbon steel, S355 and S460. The third design concept included girders with corrugated webs in stainless steel (Duplex 1.4162). The capacity calculations for the flat webs in S355 are presented in Appendix C. The same calculation procedure is used for the flat webs in S460 with different material parameters. The capacity calculations for the corrugated webs in stainless steel are presented in Appendix D.

The second case study was performed in the same manner as the first one using the same design concepts. However, the beam heights were increased with 500mm resulting in new cross sectional dimensions. This was done in order to investigate the influence of the increased beam height on the material savings.

The possible material savings between the designs with flat webs in carbon steel compared to the corrugated webs in stainless steel were investigated. For the designs in case study 2, the savings were also investigated in terms of investment cost, maintenance cost and environmental impact. The bridges were designed using the Python-scripts and FE-models described in Chapter 4. The capacity calculations were performed according to the capacity checks presented in Section 3.5. Since the system was statically indeterminate, the design process was iterative and numerous system analyses had to be performed in order to obtain desired cross-sectional designs.

In order to limit the case studies and to get comparable results, following assumptions and limitations were made for the analyses:

- The redesign only included the main girders. No capacity controls were conducted for the remaining parts such as cross-beams, stiffeners, studs, welds and the reinforced concrete deck. According to Henrysson & Yman (2020), the material savings achieved by redesigning and optimizing these structural elements were very small compared to the savings on the main girders. There-

fore, these controls were considered less relevant for the purpose of the study.

- The total height of the girders together with the web thickness was kept constant along the whole bridge.

- The cross sections were limited to be in CSC 1-3. This is because the capacity calculations would be more time consuming for effective cross sections in CSC 4 due to additional eccentricities.

- The casting loads were applied for two different cases during construction stage. One case when the casting loads were applied in one span, resulting in larger span moment, and one case when the casting loads were applied in both spans, resulting in larger moment over the internal support.

5.1 Design loads

The same loads were used for both case studies except for the self-weight of the girders which is dependent on the cross-sectional design. The permanent loads are presented in Table 5.1 and the variable loads are presented in Table 5.2. How these loads were applied in Brigade/Plus are described in Section 4.3. The temperature and the wind load are both dependent on the location of the bridge. For the case studies, the bridges were assumed to be located in the municipality of Borås in the south west part of Sweden.

The shrinkage load and the second order effect of creep was calculated and included in the case studies according to the procedure in Section 4.3.

Table 5.1: Permanent loads used for the case studies

Load	**Value**	**Reference**
Form work	1600 kg/m	*
Steel girder		
Carbon steel	7.85 kg/dm^3	SS-EN 10025-1:2004
Stainless steel	7.7 kg/dm^3	SS-EN 10088-1:2014
Reinforced concrete		
*Wet concrete***	26 kN/m^3	SS-EN 1991-1-1
Hardened concrete	25 kN/m^3	SS-EN 1991-1-1
Edge beam	25 kN/m^3	SS-EN 1991-1-1
Railing	0.5 kN/m	*
Coating	22 kN/m^3	Krav Brobyggande

* Values taken from previous bridge design calculations
** Used for construction stage

Table 5.2: Variable loads used for the case studies

Load	**Value**	**Reference**
Traffic load	$Q_{1k} = 300kN\ q_{1k} = 9kN/m^2$ $Q_{2k} = 200kN\ q_{2k} = 2.5kN/m^2$ $A = 180kN\ B = 300kN\ q = 5kN$	SS-EN 1991-2 TFSF 2018:57
Acceleration/ braking load	$Q_{lk} = 0.6\alpha_{Q1}2Q_{1k} + 0.1\alpha_{q1}q_{1k}w_lL$ $180\alpha_{Q1}kN \leq Q_{lk} \leq 900kN$ $Q_{lk} = min(0.35B, 500kN)$	SS-EN 1991-2 TFSF 2018:57
Side force from braking	$Q_{trk} = 0.25 \cdot Q_{lk}$	SS-EN 1991-2
Wind load*	$q_{wind.structure} = 0.185kN/m$ $q_{wind.vehicle} = 0.492kN/m$	TFSF 2018:57
Temperature load	$T_{min} = -35°C$ $T_{max} = 35°C$	TSFS 2018:57

* Negligible effect on design of main girders and therefore kept equal for all designs regardless of beam height

5.2 Case study 1

The bridge studied in case study 1 was inspired by an existing bridge in order to choose reasonable values regarding dimensions of the structure. Three different redesigns were carried out in order to compare the savings with respect to web design and material choice. The three analysed designs were one with flat webs in S355, one with flat webs in S460 and one with corrugated webs in stainless steel.

5.2.1 Structural system

The considered bridge concept was a continuous composite bridge in two spans with span lengths equal to 28.3m. The bridge was a twin-girder bridge with two identical main girders. Since the load effects demand different capacities of the structure in span and over the internal support, different cross-sectional designs had to be used for these regions. Therefore, two types of beams were designed for the longitudinal girders where beam type 1 was located in the span and beam type 2 was located over the internal support, see Figure 5.1. The cross-sectional changes were located 5.66m from both sides of the internal support. The remaining global dimensions that were chosen for the studied bridge are presented in Table 5.3.

Table 5.3: Global dimensions of the studied bridge in case study 1

Part	Dimension
Total length	59.4m
Span lengths	28.3m
Console length	1.4m
Beam height	1.25m
Deck thickness	0.32m
Bridge width	9.5m
Coating thickness	0.1m

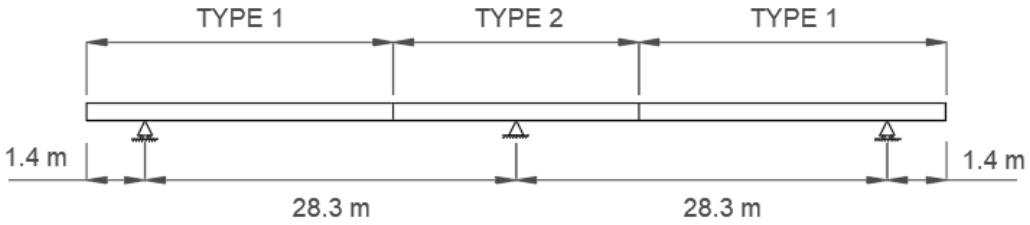

Figure 5.1: Longitudinal system of the studied bridge in case study 1.

5.2.2 Governing utilization ratios

In order to make the different designs comparable, the beam types were designed to have governing utilization ratios between 95% - 100%. Table 5.4 - 5.6 presents the governing capacity controls with corresponding utilization ratios for the three different bridge designs, both for the beams in span and for the beams over the internal support. Since the change in web thickness had such an impact on the shear capacity, the desired utilization ratio of 95% - 100% for the web could not be achieved for all bridge designs. Instead a utilization ratio >90% was aimed for.

Table 5.4: Governing utilization ratios for design with flat web in S355, h=1250mm

Part	Capacity control	Flat web, S355
Span		
Top flange	ULS, LT-buckling in construction phase	95%
Bottom flange	ULS, bending in service phase	96%
Support		
Top flange	ULS, bending in construction phase	99%
Bottom flange	ULS, bending in service phase	100%
Web	ULS, Shear capacity	96%

Table 5.5: Governing utilization ratios for design with flat web in S460, h=1250mm

Part	**Capacity control**	**Flat web, S460**
Span		
Top flange	ULS, LT-buckling in construction phase	96%
Bottom flange	FAT, stiffener to bottom flange	99%
Support		
Top flange	ULS, bending in construction phase	96%
Bottom flange	ULS, bending in service phase	95%
Web	ULS, Shear capacity	93%

Table 5.6: Governing utilization ratios for design with corrugated web in stainless steel, h=1250mm

Part	**Capacity control**	**Corrugated web**
Span		
Top flange	ULS, LT-buckling in construction phase	100%
Bottom flange	FAT, stiffener to bottom flange	100%
Support		
Top flange	ULS, bending in construction phase	100%
Bottom flange	ULS, LT-buckling in service phase	96%
Web	ULS, Shear capacity	96%

5.2.3 Cross-sectional dimensions

The chosen cross-sectional dimensions for beam type 1 and beam type 2 are presented in Table 5.7 & 5.8 for all three designs. Thinner webs could be used for the corrugated webs in stainless steel compared to the designs with flat webs in carbon steel. This is because of the higher shear capacity achieved by the corrugation. The flanges on the other hand had to be larger for the corrugated webs compared to the flat webs. This is due to the contribution from the webs which could not be accounted for when calculating the bending capacity for the design with corrugated webs, according to SS-EN 1993-1-5 Annex D. Comparing the corrugated webs in stainless steel with the flat webs in S355, the cross sectional area of the flanges could be smaller for the corrugated webs. This is due to the higher steel strength of stainless steel compared to S355.

Table 5.7: Sectional dimensions for beam type 1 in case study 1

Sectional constants	Flat web S355 [mm]	Flat web S460 [mm]	Corrugated web stainless steel [mm]
b_{tf}	490	400	460
t_{tf}	32	36	30
h_w	1178	1174	1180
t_w	16	15	9
b_{bf}	720	630	770
t_{bf}	40	40	40

Table 5.8: Sectional dimensions for beam type 2 in case study 1

Sectional constants	Flat web S355 [mm]	Flat web S460 [mm]	Corrugated web stainless steel [mm]
b_{tf}	500	350	380
t_{tf}	25	25	30
h_w	1185	1189	1183
t_w	16	15	9
b_{bf}	740	590	640
t_{bf}	40	36	37

In order to optimize the design of the bridge with corrugated webs, the corrugation parameters were chosen in order to avoid large reduction in capacity against shear buckling. The corrugation parameters that were used in the case study are presented in Table 5.9, with notations according to Figure 2.4.

Table 5.9: Corrugations parameters used for the case study 1

Corrugation parameter	$[mm]$
a_{c1}	70
a_{c2}	68
a_{c3}	40
a_{c4}	55
s_c	138
w_c	125
α	36$[deg]$

5.2.4 Material savings

Due to the corrugated webs and the stainless steel, the design of the steel girders could be optimized. The material savings considering the total amount of material used for the two main girders in each design concept are presented in Table 5.10. The savings between the bridge designed with corrugated webs in stainless steel and

flat webs in S355 are due to both the corrugation and the higher material strength. The material savings obtained when comparing the corrugated webs in stainless steel and the flat webs in S460 on the other hand is mainly due to the corrugation. This is because stainless steel and S460 have similar strength properties.

Table 5.10: Material savings for the design with corrugated web in stainless steel compared to the designs with flat web in carbon steel for case study 1

Material	**Material saving in** [%]	**Material saving in** $[kg]$
S355	15%	$8.78 \cdot 10^3 kg$
S460	3%	$1.66 \cdot 10^3 kg$

5.2.5 Load effects

The support moments retrieved from the system analysis in ULS during service stage are presented in Figure 5.2 for the three girder designs. The load effects from the different loads are plotted separately. The moments are re-calculated to act on the steel sections and includes both safety factors and load combination factors according to combination 6.10b, see Section 3.4.3.

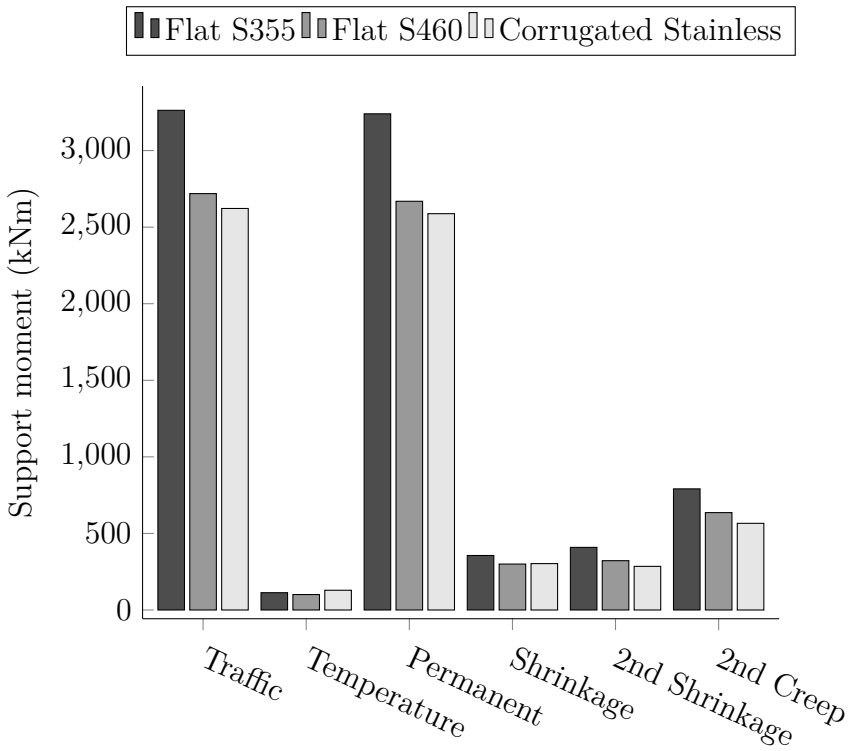

Figure 5.2: Support moments working on the steel section in case study 1.

The resulting moments from each load type are higher for the flat web girders in carbon steel compared to the corrugated web girders in stainless steel. Although, with the exception from the temperature loads which are higher for the latter. It is also visible that all the resulting support moments are higher for the girders in S355 compared to the ones in S460.

In Appendix E, the corresponding stresses in the top and bottom flanges due to the support moments in Figure 5.2 are presented. Here, also the normal forces considered over the internal support are included. The contribution to the total stresses from the different loads are illustrated in Figure 5.3 for the top flange and Figure 5.4 for the bottom flange. The traffic loads and the permanent loads had almost the same influence on the total load effect for all the designs, both for the top and the bottom flanges. These loads were governing for the cross-sectional design. The biggest difference regarding the influence on the total load effect between the designs was the temperature load. The temperature load was higher for the girders in stainless steel resulting in a bigger influence on the total load effect.

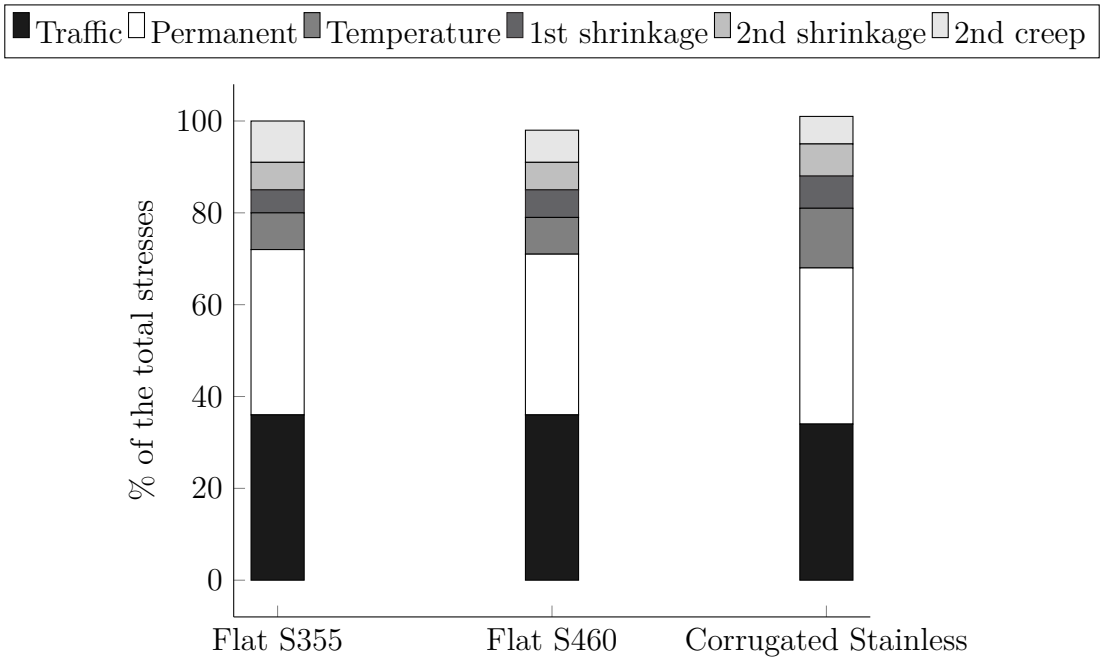

Figure 5.3: Contribution from the different loads to the stresses in top flange for the designs in case study 1.

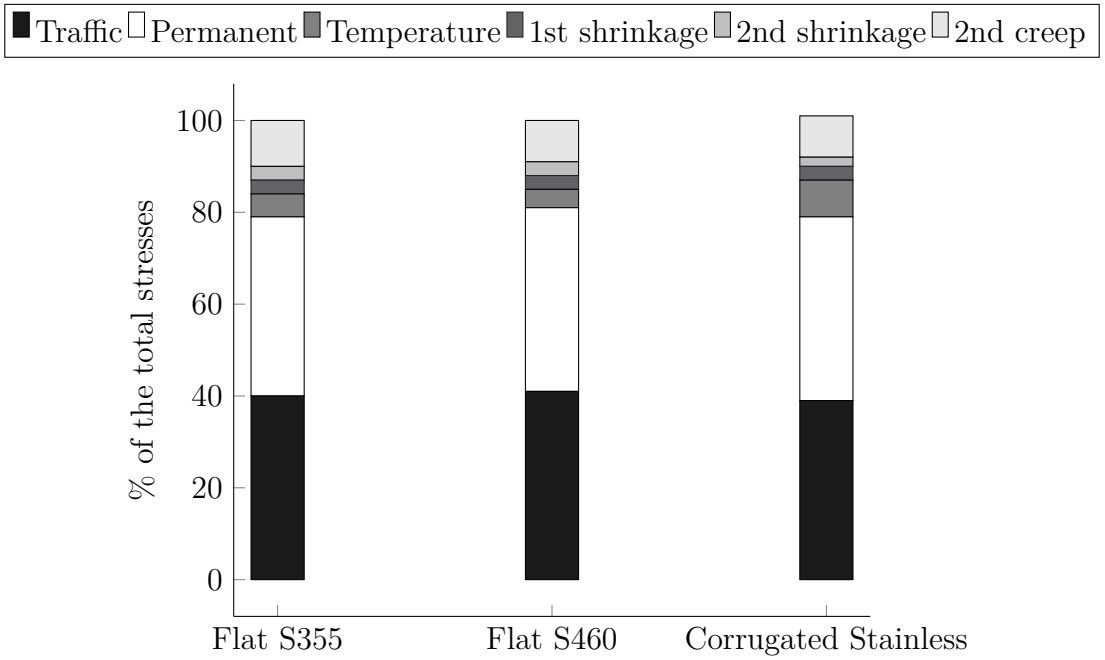

Figure 5.4: Contribution from the different loads to the stresses in bottom flange for the designs in case study 1.

5.3 Case study 2

Similarly, as for the case study 1, a continuous twin-girder composite bridge in two spans was considered in case study 2. The study included three different girder designs, one with flat webs in S355, one with flat webs in S460 and one with corrugated webs in stainless steel.

5.3.1 Structural system

All global dimensions were kept the same as for case study 1 except for the height of the girders which was increased with 500mm. The global dimensions for the bridge studied in case study 2 are presented in Table 5.11. The locations of beam type 1 and beam type 2 are presented in Figure 5.5.

Table 5.11: Global dimensions of the studied bridge in case study 2

Part	**Dimension**
Total length	59.4m
Span lengths	28.3m
Console length	1.4m
Beam height	1.75m
Deck thickness	0.32m
Bridge width	9.5m
Coating thickness	0.1m

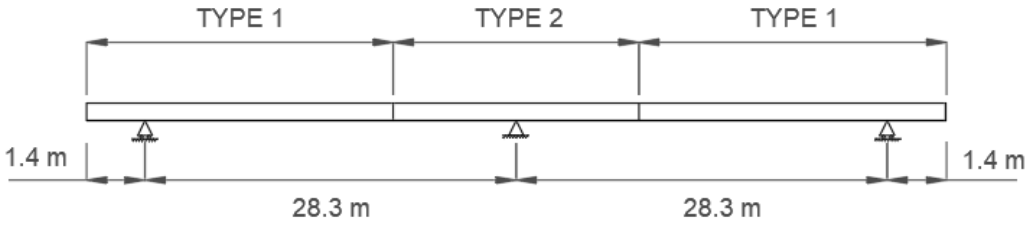

Figure 5.5: Longitudinal system of the studied bridge in case study 2.

5.3.2 Governing utilization ratios

The beam types were designed to have governing utilization ratios between 95% - 100%. Table 5.12 - 5.14 presents the governing capacity controls for the three bridge designs, both for the beams in span and over the internal support. As for case study 1, the desired utilization ratio of 95% - 100% could not be achieved for all designs regarding the web. Instead a utilization ratio >90% was aimed for.

Table 5.12: Governing utilization ratios for flat web bridge in S355, h=1750mm

Part	**Capacity control**	**Flat web, S355**
Span		
Top flange	ULS, LT-buckling in construction phase	96%
Bottom flange	ULS, bending in service phase	97%
Support		
Top flange	ULS, bending in construction phase	96%
Bottom flange	ULS, bending in service phase	96%
Web	ULS, Shear capacity	94%

Table 5.13: Governing utilization ratios for flat web bridge in S460, h=1750mm

Part	**Capacity control**	**Flat web, S460**
Span		
Top flange	ULS, LT-buckling in construction phase	98%
Bottom flange	FAT, stiffener to bottom flange	100%
Support		
Top flange	ULS, LT-buckling in construction phase	98%
Bottom flange	ULS, LT-buckling in service phase	97%
Web	ULS, Shear capacity	92%

Table 5.14: Governing utilization ratios for corrugated web bridge in stainless steel, h=1750mm

Part	Capacity control	Corrugated web
Span		
Top flange	ULS, LT-buckling in construction phase	96%
Bottom flange	FAT, stiffener to bottom flange	97%
Support		
Top flange	ULS, bending in construction phase	99%
Bottom flange	ULS, LT-buckling in service phase	99%
Web	ULS, Shear capacity	93%

5.3.3 Cross-sectional dimensions

The chosen cross-sectional dimensions for beam type 1 and beam type 2 are presented in Table 5.15 & 5.16 for all three designs. For case study 2, the thickness of the webs for the design with corrugated webs in stainless steel could be reduced further due to the increased height. For both designs with flat webs in carbon steel the increased height did not result in any reduction in web thickness. The flange dimensions could be reduced for all three designs due to the higher bending stiffness obtained by to the increased height.

Table 5.15: Sectional dimensions for beam type 1 in case study 2

Sectional constants	Flat web S355 [mm]	Flat web S460 [mm]	Corrugated web stainless steel [mm]
b_{tf}	430	440	440
t_{tf}	28	22	25
h_w	1690	1698	1688
t_w	16	15	6
b_{bf}	550	550	700
t_{bf}	32	30	37

Table 5.16: Sectional dimensions for beam type 2 in case study 2

Sectional constants	Flat web S355 [mm]	Flat web S460 [mm]	Corrugated web stainless steel [mm]
b_{tf}	300	260	350
t_{tf}	19	19	23
h_w	1694	1704	1694
t_w	16	15	6
b_{bf}	550	480	540
t_{bf}	37	27	33

The corrugation parameters were chosen in order to avoid reduction in capacity against shear buckling. The corrugation parameters that were used in this case study are presented in Table 5.17, with notations according to Figure 2.4.

Table 5.17: Corrugations parameters used for the case study 2

Corrugation parameter	$[mm]$
a_{c1}	55
a_{c2}	92
a_{c3}	54
a_{c4}	74
s_c	147
w_c	129
α	$36[deg]$

5.3.4 Material savings

As a result of higher shear-strength of beams with corrugated webs and higher strength of stainless steel, the weight of the steel girders could be reduced. The material savings are presented in Table 5.18 considering the total material consumption of the two main girders for each design. The material saving could be achieved due to both the corrugation and the higher strength of stainless steel. Below 6,4mm, cold-formed stainless steel has an increased steel strength, see Table 3.2. This type of steel was used for the web plate which resulted in higher capacity compared to S460. The material choice therefore had a larger impact for comparison between the corrugated webs in stainless steel and the flat webs in S460 in case study 2 than in case study 1.

Table 5.18: Material savings for the design with corrugated web in stainless steel compared to the designs with flat webs in carbon steel for case study 2

Material	**Material saving in** [%]	**Material saving in** $[kg]$
S355	19%	$9.86 \cdot 10^3 kg$
S460	9%	$4.34 \cdot 10^3 kg$

5.3.5 Load effects

The support moments retrieved from the system analysis in ULS during service stage are presented in Figure 5.6 for the three designs. The load effects from the different loads are plotted separately. The moments are re-calculated to act on the steel sections and includes both safety factors and load combination factors according to combination 6.10b, see Section 3.4.3.

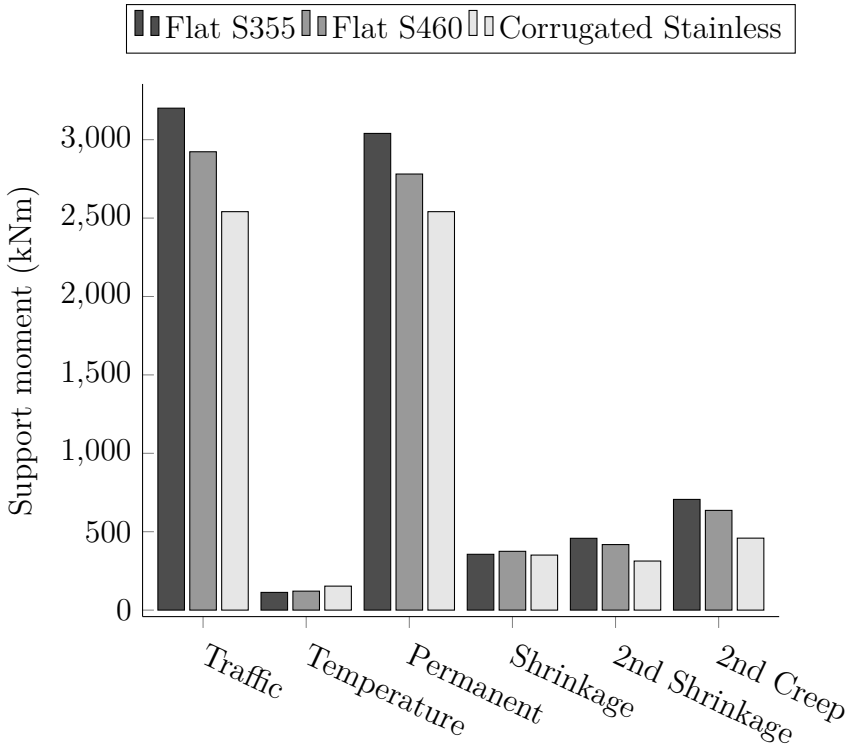

Figure 5.6: Support moments working on the steel sections in case study 2.

The resulting moments from each load type were higher for the flat web girders in carbon steel compared to the corrugated web girders in stainless steel. Although, with the exception from the temperature load which was higher for the last mentioned one. The resulting support moments were also higher for the girders in S355 compared to the ones in S460.

In Appendix E, the corresponding stresses in the top and bottom flanges due to the support moments in Figure 5.6 are presented. Here, also the normal forces considered over the internal support are included. The contribution to the total stresses from the different loads are illustrated in Figure 5.7 for the top flange and Figure 5.8 for the bottom flange. Same as for case study 1, the traffic loads and permanent loads were the governing load types studying the resulting stresses for all three designs. The largest difference in load effect between the designs were the temperature load which was higher for the girder in stainless steel.

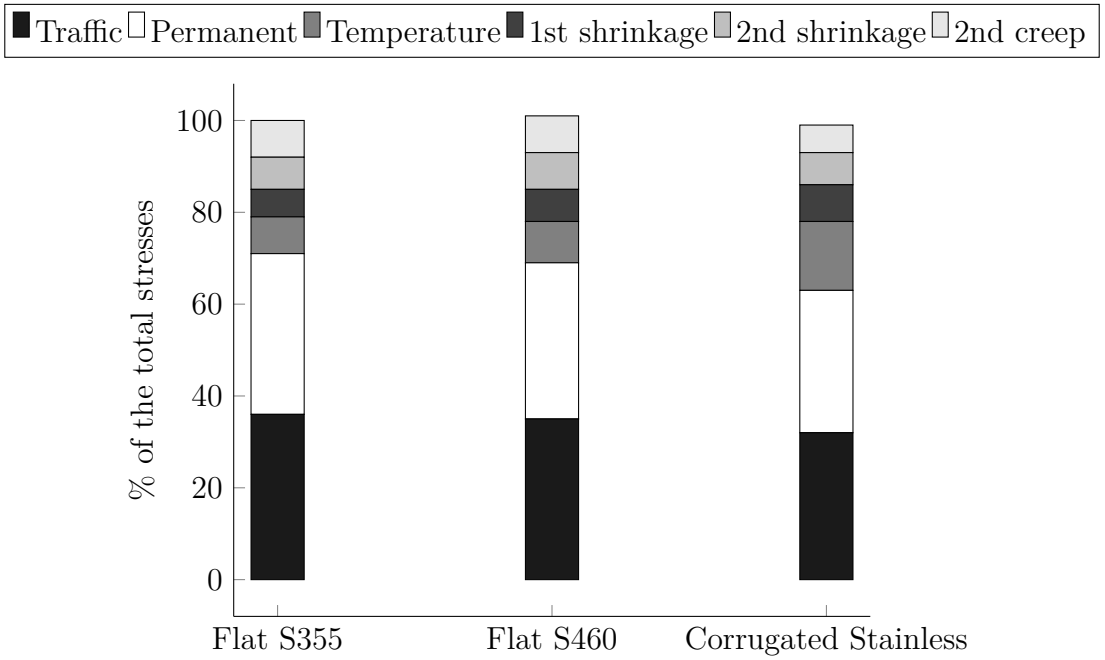

Figure 5.7: Contribution from the different loads to the stresses in top flange for the designs in case study 2.

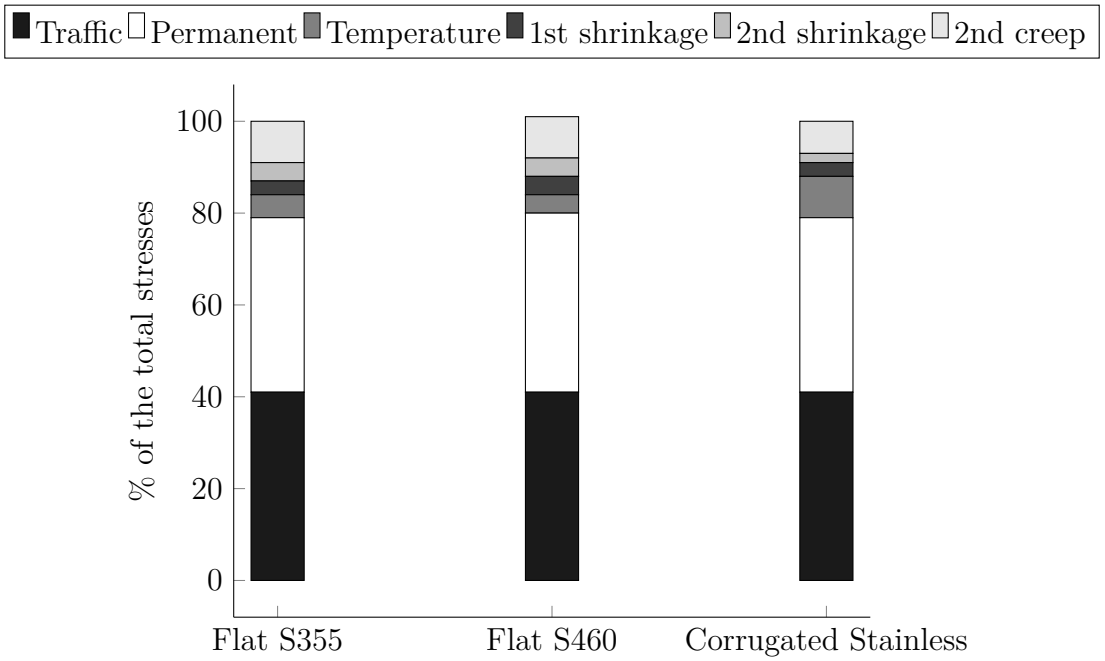

Figure 5.8: Contribution from the different loads to the stresses in bottom flange for the designs in case study 2.

5.3.6 Economic evaluation

A cost estimation was performed in collaboration with *Stål & Rörmontage AB*. The economic evaluation included the investment costs for the designs and an estimation of the maintenance costs during the bridge's service life. In the cost estimation, only the two main girders and stiffeners were included. In Table 5.19 the total weight of the designs are presented. The assumed market prices for the materials used in the cost estimation are presented per kilo in Table 5.20.

Table 5.19: Total weight of the steel girders for each design

Flat web S355	**Flat web S460**	**Corrugated web stainless steel**
54 500 kg	48 943 kg	46 000 kg

Table 5.20: Material cost per kilo for the considered materials according to Stål & Rörmontage AB (Personal communication, May 19, 2021)

S355	**S460**	**Stainless 1.4162**
12 SEK/kg	16 SEK/kg	30 SEK/kg

In Table 5.21 the investment costs for the designs are presented. The total investment cost is divided in three subcategories; Material cost, Production cost and Treatment cost. The material cost is higher for the bridge in stainless steel compared to the other ones. This is due to the considerably higher price per kilo for stainless steel as could be seen in Table 5.20.

Table 5.21: Investment costs in SEK for the bridge designs in case study 2 according to Stål & Rörmontage AB (Personal communication, May 18, 2021)

	Flat web S355	**Flat web S460**	**Corrugated web stainless steel**
Material cost	892 000	1 027 000	1 700 000
Production cost	2 158 000	3 923 000	2 015 000
Treatment cost	550 000	550 000	135 000
Total	**3 600 000**	**5 500 000**	**3 850 000**

Summarizing the investment costs, the flat web in S460 is the most expensive one while the other two are more equal in price. There are several reasons why the carbon steel bridges are more expensive regarding the production and treatment costs compared to the one in stainless steel. Following reasons are presented by Stål & Rörmontage AB (Personal communication, May 19, 2021):

- **Welding**
  The welding labour have a considerable influence on the costs, standing for approximately 70% of the total production cost for all the designs. Since stainless steel is more resistant to heat and the corrugated web possesses support during mounting of the flange plate, no temporary stiffeners are needed during welding. On the contrary, this is not the case for the flat web girders in carbon steel which therefore demands several stiffeners during welding to prevent deformations. This obstructs the welding procedure increasing the welding labour. Additionally, the fillet welds were chosen to 7mm in the flat web girders and 5mm in the corrugated web girder. This results in longer welding time even though the welding length is actually longer for the corrugated web. According to Table 5.21, the production cost is considerably higher for the bridge in S460 compared to the other two. According to Stål & Rörmontage AB the plates in S460 used for this cost estimation needs to be preheated before welding. This results in increased energy consumption and additional labour which substantially increase the production costs.

- **Surface treatment**
  In order to prevent corrosion, the carbon steel bridges need a surface treatment in terms of painting in the factory. This is not necessary for the bridge in stainless steel. Although, instead it needs to be pickled after welding. This surface treatment is however less demanding in comparison with the required painting work for carbon steel bridges resulting in higher treatment costs for the latter cases.

- **Work on site**
  The girders are long and therefore need to be transferred to the building site in two parts. For the girders in carbon steel, this demands additional painting work that needs to be conducted on site. This work is more demanding compared to the pickling of the stainless steel girders resulting in higher costs.

In Table 5.22 the maintenance costs for the bridge designs in carbon steel are presented. The maintenance calculations were performed by *Stål & Rörmontage AB*, using a calculation tool based on publications provided by *the Swedish Transport Administration*. Only the costs arising from the painting work was included in the cost estimations. Thereby, the maintenance cost for the web in stainless steel was equal to zero since no additional painting was required during its service life. The type of painting work and action time from the start of service life is presented in Table 5.22. The cost estimation includes the net present value considering an interest rate of 3.5% which is in line with the Swedish Transport Administration.

Table 5.22: Maintenance costs in SEK for the carbon steel bridges in case study 2 according to Stål & Rörmontage AB (Personal communication, May 18, 2021)

Action time [*years*]	**Activity**	**Cost estimation**	**Net present value** [*Interest rate 3.5%*]
10	Paint improvement	427 700	303 205
20	Partial repainting	685 000	330 688
30	Paint improvement	427 000	152 380
40	Repainting	1 513 400	382 243
50	Paint improvement	427 700	76 581
60	Partial repainting	658 000	83 523
70	Paint improvement	427 700	38 487
		4 540 200	**1 367 107**

A summation of the investment and the maintenance costs for the designs are presented in Table 5.23. The flat webs in carbon steel both had a considerably higher total cost compared to the corrugated webs in stainless steel. This is mainly due to the fact that carbon steel demands repeated painting work in order to prevent corrosion while this type of work is not required for structures in stainless steel.

Table 5.23: Total costs in SEK considering investment and maintenance for the bridge design in case study 2 according to Stål & Rörmontage AB (Personal communication, May 18, 2021)

	Flat web S355	**Flat web S460**	**Corrugated web stainless steel**
Investment cost	3 600 000	5 500 000	3 850 000
Maintenance cost	1 367 107	1 367 107	-
Total cost	**4 967 107**	**6 867 107**	**3 850 000**

As stated previously, the cost-estimation for the design in S460 is conducted with the assumption that preheating is required for welding. As a result, the investment cost for this solution in Table 5.23 is considerably higher compared to the other two designs. The need for preheating may differ depending on the chosen welding method and additives, as well as the material composition, even though the same steel grade is considered. This is because the same steel grade can have different material compositions. The required preheating temperature is dependent on the carbon equivalent of the steel, the lower equivalent the lower is the need for preheating (Stemne, 2021). The preheating temperature can be calculated according to SS-EN 1011-2 if the material composition is known together with the thicknesses of the considered steel parts and the welding method. Concluded from this standard is that preheating could be avoided for the designed steel girders in S460 provided that appropriate material consumption and welding method is chosen. As can be seen in Table 5.24, this can lead to a drastic change of the production costs, and thereby the investment costs. In Table 5.25 the total cost for the three designs are presented where preheating of S460 is neglected. The result still indicates that the

design with corrugated webs in stainless steel results in lower total cost compared to the other two designs.

Table 5.24: Investment costs in SEK for the bridge designs in case study 2 without the need for preheating of S460

	Flat web S355	**Flat web S460**	**Corrugated web stainless steel**
Material cost	892 000	1 027 000	1 700 000
Production cost	2 158 000	2 423 000*	2 015 000
Treatment cost	550 000	550 000	135 000
Total	**3 600 000**	**4 000 000**	**3 850 000**

*Production cost for the design in S460 without the need for preheating before welding

Table 5.25: Total costs in SEK considering investment and maintenance costs for the bridge designs in case study 2 without the need for preheating of S460

	Flat web S355	**Flat web S460**	**Corrugated web stainless steel**
Total cost	4 967 107	5 367 107*	3 850 000

* Total cost for the design in S460 without the need for preheating before welding

5.3.7 Environmental evaluation

A simplified LCA was performed in collaboration with the master thesis *Comparative life cycle analysis for bridges made of conventional steel and stainless steel in the early design phases: Developing a parametric multi-perspective approach* written by Syu (2021). The results from the analysis were obtained from F. Syu (Personal communication, May 21, 2021), see Appendix E. The analysis included the production of the material, transportation to building site, service life maintenance and end of life stage. The environmental impact is expressed in *Global warming potential* (GWP) by using CO_2-equivalents. The system boundaries are presented in Figure 5.9, were the stages included in the analysis are marked in grey.

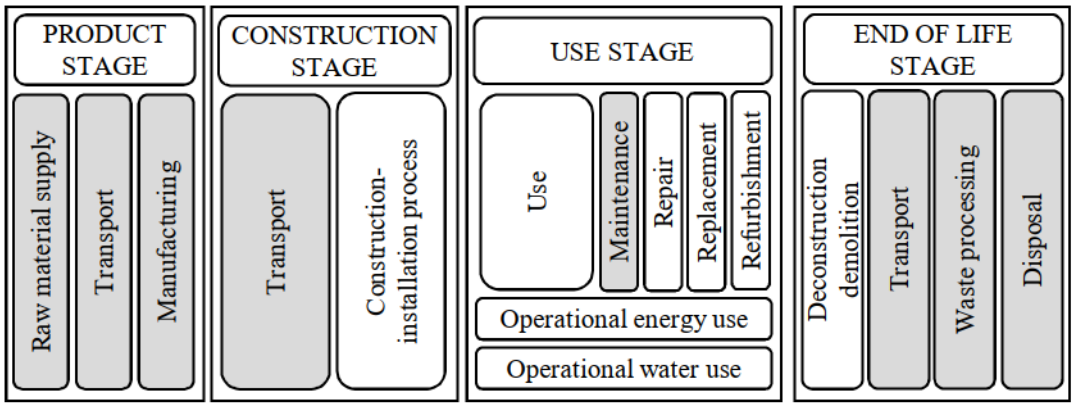

Figure 5.9: System boundaries included in the simplified LCA, definitions according to SS-EN 15978:2011.

The system boundaries and assumptions made for the simplified LCA were:

- **Product stage**
  Includes emissions from production of the materials and the welding labour.

- **Construction stage**
  Includes emissions from transportation of the materials to the building site. The transportation distance is assumed to be the same for all three concepts.

- **Use stage**
  Includes maintenance of carbon steel in terms of repainting, partial repainting and paint improvement.

- **End-of life stage**
  Includes transport of the material from the site, waste processing and disposal.

The emission factors that gave the largest impact are presented in Table 5.26. The emission factors are presented as the average kilo carbon dioxide emitted for every kilo steel produced. The total carbon emissions from the concepts in the different stages are presented in Figure 5.10. The reason for the higher emissions from carbon steel bridges is due to the need of heavier girders. This also increased the carbon emissions from transportation compared to the bridge in stainless steel.

Table 5.26: Important emission factors

Material	**Emission factor** $[kgCO_2e/kg]$	**Data source**
Carbon steel	2.71	SSAB, 2020
Stainless steel	2.74	Outokumpu, 2019

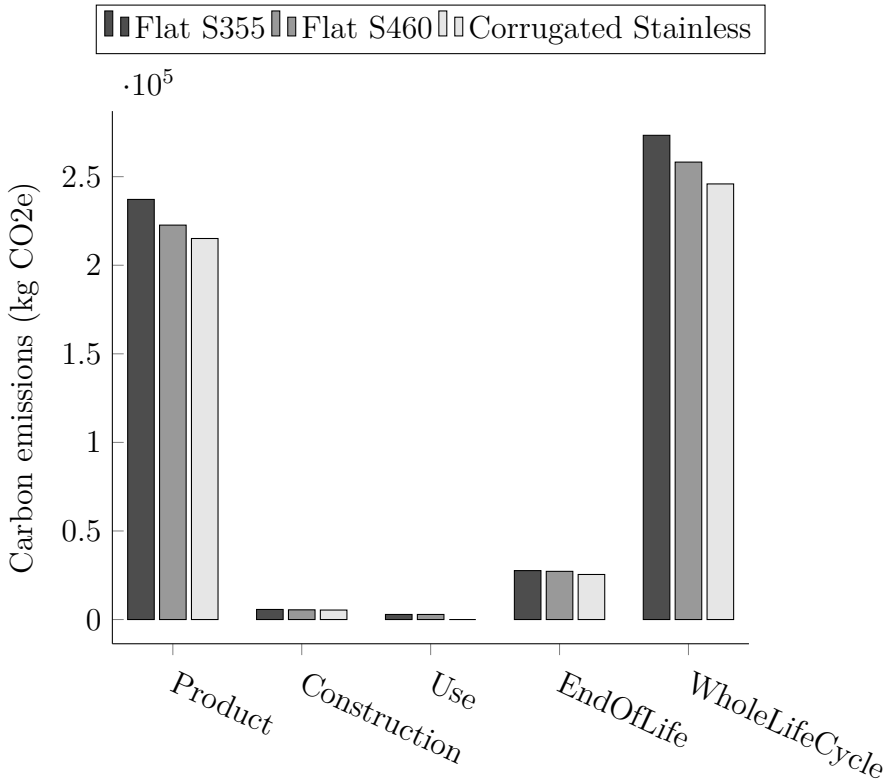

Figure 5.10: Carbon emissions during the life cycle for the girder designs (Syu, 2021).

The CO_2-equivalent on the materials can be different dependent on which company that is manufacturing the material. A sensitivity analysis was conducted in order to see the influence of the choice of CO_2-equivalent, see Figure 5.11 (Syu, 2021).

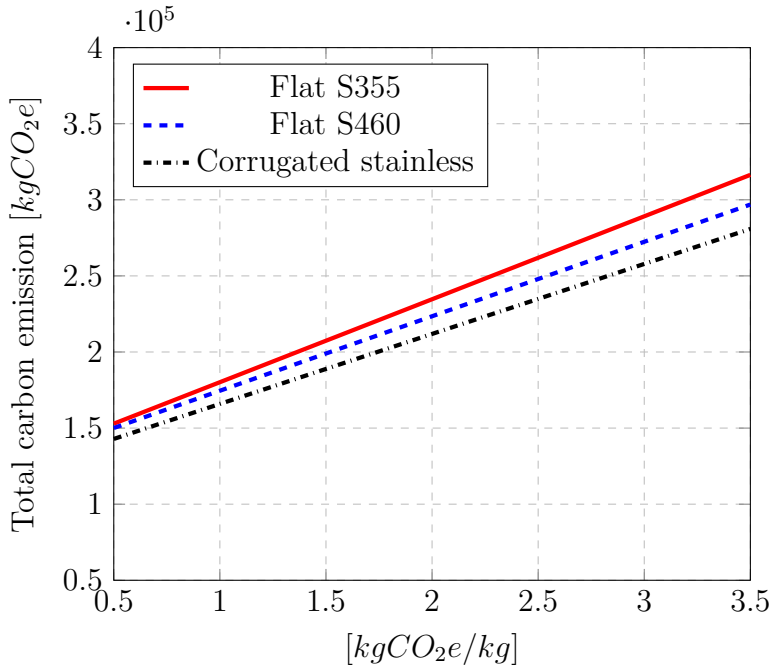

Figure 5.11: Sensitivity analysis on the simplified LCA indicating the influence of different CO_2-equivalent on the total carbon emissions.

6
Discussion

Chapter 6 will present discussions about the results obtained from the case studies in Chapter 5. The discussion will focus on the similarities and differences by using different web designs and materials.

6.1 Material savings

Concluded from the case studies, material savings could be obtained for the girders with corrugated webs in stainless steel. When increasing the beam height in case study 2, the beams achieved higher bending capacity and optimization of the flanges could be performed. Thereby, all the designs decreased in weight. Moving to a higher web was also accompanied by a reduction of the thickness of the corrugated webs whereas the thickness of the flat webs had to be kept unchanged to compensate for its lower shear-buckling strength. When using deeper flat webs, the reduction due to shear buckling is increased. In order to enable thinner webs, additional stiffeners would be essential. Since the design of stiffeners was neglected in this thesis, the web thickness had to be maintained. For the corrugated webs, the corrugation could be optimized limiting the reduction due to local and global buckling. Thereby, the web thickness could be reduced and larger material savings could be obtained compared to the other designs in case study 2.

Another aspect that influenced the material savings between case study 1 and 2 was the material strength. Since the web thickness for the corrugated webs could be decreased to 6mm, the higher material strength of 530 MPa according to Table 3.2 could be utilized for the webs. For the flat webs in carbon steel, the yield strength was considerably lower which demanded thicker webs. Although, it is important to emphasise that it was due to the corrugation that the web thickness could be reduced which in turn made it possible to utilize the higher yield strength.

The material strength was also the reason why the savings were larger for the corrugated webs in stainless steel in comparison with the flat webs in S355. According to Table 3.2 & 3.3, the material properties for S460 and stainless steel are more equal while S355 has a considerably lower strength. Therefore, a heavier cross section was needed for this type of beam and the material consumption increased.

6.2 Load effects

Comparing the support moments from the different loads in Figure 5.2 & 5.6 respectively, the moments were larger for the flat webs compared to the corrugated webs. This applied for all loads except for the temperature load which was strongly dependent on the thermal coefficient of the material, see discussion in Section 6.2.1. The reason for the larger moments for flat webs was due to the higher axial stiffness compared to the corrugated webs. This resulted in larger forces working on the cross sections.

6.2.1 Influence of temperature load

When comparing the stresses retrieved in both case studies, the biggest difference between the designs was the temperature load. The stress distribution in the steel cross section due to the temperature load is illustrated in Figure 6.1 for all the designs.

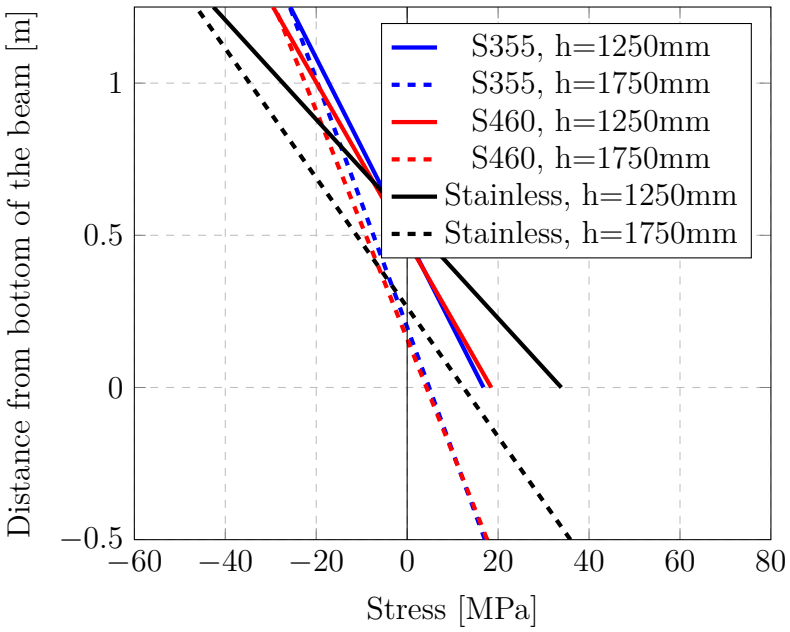

Figure 6.1: Stress distribution in the steel cross section over the internal support due to temperature loads.

It is visible, studying the temperature stresses, that the influence of the increased beam height is negligible while the difference in material has a considerable impact. The stresses are significantly higher for the corrugated webs in stainless steel compared to the other two designs. This is due the thermal coefficient which is higher for stainless steel compared to traditional carbon steel.

When designing composite bridges in carbon steel, the thermal coefficient for the steel girders can be chosen equal to the one for concrete. Thereby, the strain difference between the materials is equal to zero and the concrete deck and the steel

girders will contract and extract in the same rate. Taking this into account, only the temperature difference between the materials are of interest for the composite bridges in carbon steel. For the bridges in stainless steel on the other hand, also the maximum temperatures in the ambient air contributes with additional stresses. The strain difference between the stainless-steel girders and the concrete deck is the reason for the higher temperature stresses in the steel cross section.

In order to investigate the influence of the thermal coefficient, the stress distribution within the steel cross section was studied over the internal support. For the comparison, only the thermal coefficient of the steel girder was changed, all other dimensions and constants were kept the same. The result of the study is presented in Figure 6.2 where the stress distribution is illustrated for several values of the thermal coefficient. It is important to note that maximum tensile stresses in the top flange are obtained when the concrete deck is colder than the steel girders while the maximum compression stresses in the bottom flange are obtained when the concrete deck is warmer than the steel girders. The maximum tensile and compression stresses illustrated in Figure 6.2 will therefore not occur at the same time and it only shows the worst case for respective flange.

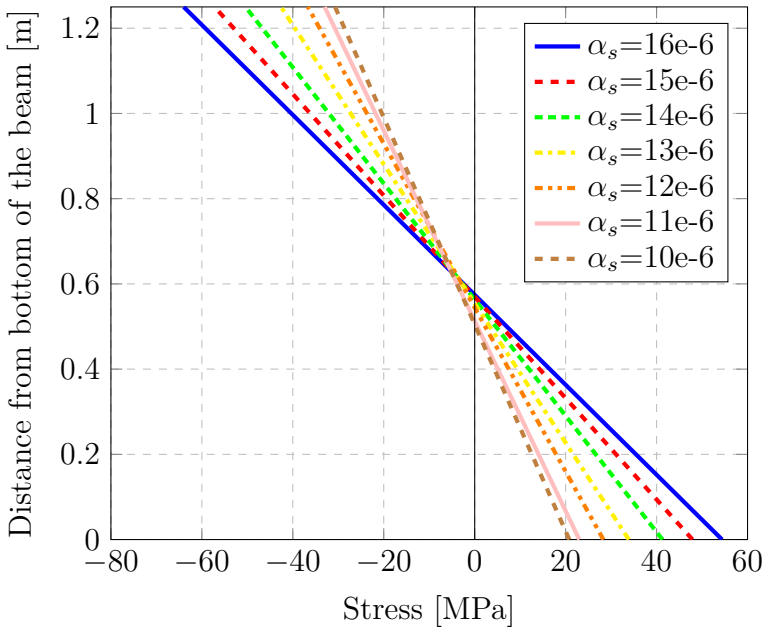

Figure 6.2: Temperature stresses in the steel cross section over the internal support for different thermal coefficients.

According to Figure 6.2, the choice of thermal coefficient for the steel girders has a great impact on the resulting temperature stresses. In the current version of SS-EN 1991-1-5, the thermal coefficient for all type of stainless steel is equal to α_s=16e-6. Although, according to prEN 1993-1-4:2020 (E) final draft, for Duplex stainless steel α_s=13e-6. This is the value used for the case studies in Chapter 5. By lowering the thermal coefficient, the stresses in the steel can be decreased with approximately

40%. This will influence the design of the girders and it is therefore important to use appropriate values for the thermal coefficients.

6.2.2 Influence of second order effects

The contribution from the second order effects to the total stresses in ULS is presented in Table 6.1 and 6.2. The presented stresses in the top and bottom flanges are summations of the second order effects from shrinkage and creep over the internal support.

Table 6.1: Contribution from second order effects in case study 1

Case study 1	**Top flange [MPa]**		**Bottom flange [MPa]**	
Flat web S355	-48.6	15%	44.7	13%
Flat web S460	-51.8	14%	52.1	12%
Corrugated web stainless steel	-46.1	13%	47.5	11%

Table 6.2: Contribution from second order effects in case study 2

Case study 2	**Top flange [MPa]**		**Bottom flange [MPa]**	
Flat web S355	-46.7	15%	42.5	13%
Flat web S460	-47	16%	52.8	13%
Corrugated web stainless steel	-40.9	13%	41.2	9%

From the summations it is visible that the second order effects have a significant influence on the total stresses and should therefore not be neglected in the calculations. The contribution from the second order effects are higher in the top flanges than in the bottom flanges for all design concepts. The design of the bottom flanges is governed by the stresses in service stage and the second order effect will thereby influence the design of the bottom flanges. Although, the governing utilization ratios for the top flanges are rather the stress-limitations in construction stage which occur before the second order effects has developed. The difference in percentage between the designs are small and it rather depends on the optimization procedure discussed in Section 6.5 than the choice of material and web design.

It is important to note that the calculation procedure for the second order effects in this thesis is based on a simplified approach, see Section 4.3.2.1 and Section 4.3.2.2. This is a conservative simplification which can result in higher stresses from the second order effects than what will occur in reality.

According to SS-EN 1994-2 5.4.2.2(8), the primary effects of shrinkage can be neglected in the cracked regions if the secondary effects of shrinkage is included in the

calculations. In this thesis, both the primary and secondary effects of shrinkage are included in the calculations to investigate their respective contribution to the overall stresses. This is a conservative approach, especially since the first order effects are in the same level as the second order effects. For the calculations it would therefore be enough to only include the load effects from either the primary or the secondary effects and still get reliable results.

6.3 Economic evaluation

The economic evaluation performed for the bridge designs in case study 2, showed that the bridge with corrugated webs in stainless steel resulted in lower total cost compared to the flat webs in carbon steel. This was mainly because of the less demanding maintenance work. According to Stål & Rörmontage AB (Personal communication May 18, 2021), bridges in stainless steel are never designed for a service life shorter than 120 years. Although, all the designs are calculated for a service life of 80 years. If the bridges would have been designed for a longer service life, additional painting for the carbon steel bridges would have been required. This would increase the maintenance costs accordingly. Thereby, the economic savings achieved from using corrugated webs in stainless steel could have been even higher.

Noticed during the cost estimation was that the welding stood for approximately 70% of the production costs for all three designs. During the study, the welds were not optimized and the size of the welds were chosen based on existing similar bridges. Since the size of the welds had such an impact on the final result, it would be necessary to investigate the welds further to optimize them considering the production cost.

Concluded in Section 5.3.6, the choice of welding method and steel composition together with the thickness of the considered parts will influence the need for preheating of S460. In the cost estimations done by Stål & Rörmontage AB the parts needed to be preheated prior to welding as a consequence of their choice of steel composition and welding method. Concluded from SS-EN 1011-2, the same steel grade with another material composition and welding method might not demand preheating. It is important to note that the possible differences in material price due to their composition has not been taken into account in the conducted cost estimations. However, as it is apparent in Table 5.23 and 5.25 material cost deviations would be negligible in comparison to the additional induced production costs due to the preheating. Therefore, the choice of steel supplier and welding methods during the production phase is of utmost importance that should not be undervalued. A comparison should then be made whether it is more profitable using cheaper steel that requires preheating compared to possibly slightly more expensive steel without this requirement. Equally important is that the production factories choose the welding method and additives for the specific project and material, and not just by following what the common practice at the workshop dictates.

Summarizing the economic evaluation it is important to emphasize some important aspects influencing the results. The costs were based only on Stål & Rörmontage AB's data and estimations leading to case specific results. If an additional firm would have been included in the analysis, other assumptions and cost estimations could have been made. In reality, when collecting offers for new bridges, competing manufactures are included pressing the prices further. Thereby, the holistic perspective on the costs for new bridges was excluded. Moreover, several aspects throughout the service life was neglected in the estimations and the results does not include a complete cost estimation. In summary, the purpose of the cost estimations was to compare the different concepts to each other, rather than present the actual cost for a specific bridge design.

6.4 Environmental evaluation

The simplified LCA clearly showed that the carbon emissions were directly related to the amount of material used in the different designs. A comparison of the total carbon emissions from the different bridges showed that the design with corrugated webs in stainless steel had the lowest impact on the environment in terms of carbon emissions. This was due to the lower amount of steel in the girders. It is important to note that another environmental indicator or impact category could have resulted in other conclusions regarding the environmental impact for the different designs.

In comparison with the economic evaluation where the use stage had a considerable impact on the total costs, the contribution from the use stage to the total carbon emissions were very low. This was because the production stage had such an impact on the total emissions resulting in a negligible influence from the use stage.

The sensitivity analysis presented in Figure 5.11 showed that the carbon emissions from the bridge in stainless steel is always lower than the carbon steel bridges as long as the CO_2-equivalent is chosen similar to one another. Although, since various references can be used for the different materials the result could change drastically. The result is therefore highly dependent on the data sources used for the analyses.

The purpose with the simplified LCA was to show the difference in carbon emission between the studied concepts. The system boundaries were therefore set to include only the main aspects that influenced the carbon emissions for the different concepts.

6.5 Optimization procedure

The resulting load effects and material savings are dependent on the design choices. Since the system was statically indeterminate the load distribution depended on the stiffness distribution along the girders. A higher stiffness in a certain region attracted more loads than the other regions which influenced the final load effects.

Therefore, there was not just one optimal design in order to achieve governing utilization ratios close to 100% for the girders.

The optimization of the designs was also dependent on the relation between thickness and width for the different parts in the cross section. More slender flanges can result in larger savings as long as they do not exceed the limits for CSC 4. This means that the flanges could be optimized further by changing the thickness/width ratio even if they reached a governing utilization ratio of 100%. These savings are however small in relation to the overall savings achievable by decreasing the web thickness.

The optimization was conducted on girders divided into two different beam types, beam type 1 located in the spans and beam type 2 located over the internal support. These beam types were designed for maximum stresses in the span and over the internal support respectively. This means that the beams possess unnecessary additional capacity in the intermediate regions with lower stresses. In order to further optimize the designs and achieve high utilization ratios along the whole bridge, the bridge girders could have been divided into additional sections and beam types. The cross sections could thereby be designed based on the maximum stresses in the considered region resulting in more optimized designs. This would however result in additional connections which would demand further design work and material. Since the connections would no longer only be placed close to the zero moment areas, more heavy and expensive connections would be essential in order to transfer the loads.

7
Conclusion

The aim of the thesis was to investigate the capability to optimize the design of continuous composite steel girders using corrugated webs in stainless steel. The goal was to show possible material savings by using this design compared to the conventional design with flat webs in carbon steel. Concluded in the studied cases, savings in terms of investment cost, maintenance cost and environmental impact were possible for bridges designed with corrugated webs in stainless steel.

7.1 Concluding remarks

Concluding remarks of the performed study are:

- In the two case studies performed, material savings using corrugated webs in stainless steel were obtained. The comparison with flat webs in S355/S460 resulted in material savings up to 19%/9%.

- It was showed that by increasing the height of the girders the material savings due to the corrugation increased. The corrugation also enables higher strength of stainless steel to be used. This showed that large material savings can be obtained when combining these two effects.

- Investigating the load effects showed that all loads resulted in larger moments and forces for the flat webs except for the temperature loads. This was due to the larger thermal expansion coefficient for stainless steel resulting in higher stresses in the steel section. Additionally, the system analysis showed that the second order effects contribute to approximately 10% of the total stresses over the internal support and should therefore not be neglected in design calculations.

- The investment cost was only marginally higher for the design in stainless steel compared to the designs in carbon steel, despite the fact that stainless steel material costs nearly three times more than carbon steel. In addition, the total costs including both investment costs and maintenance costs were considerably higher for the bridges in carbon steel. This cost estimation was case specific and additional partners should be consulted in order to strengthen the results.

- The simplified LCA showed that the designs with carbon steel had higher carbon emissions than the bridge in stainless steel. This was mainly due to the higher amount of material used in these designs which increased the emissions from product stage.

7.2 Further studies

This section presents further research that is relevant to perform in order to investigate additional optimization possibilities and to strengthen the results obtained in the thesis. Further studies should investigate:

- Continuous composite bridges with varying beam height along the whole length of the bridge. As shown in the calculations, a higher cross section was needed over the internal supports in order to handle the shear forces. In the spans on the other hand, where the shear forces were closer to zero, the height of the girders could be reduced accordingly. The material savings arising from a reduced web height in the spans should be investigated further.
- How the concrete deck should be designed in order to optimize the design of the steel girders. As stated in Section 2.3.3.2, by using stainless steel as reinforcement the concrete cover and the self-weight of the concrete deck could be reduced. This reduction in load effect could lead to further savings on the steel girders.
- How support settlements and movements will influence the design of the main girders and if this will influence the material savings.
- How the calculation procedure of the second order effects of creep and shrinkage effects the final results. In this thesis, a simplified method was used for the calculations. Further studies should aim to investigate how conservative this approach is regarding the final load effects and if a more precise calculation procedure should be used instead.
- The behavior of continuous bridge girders in CSC 4. In this thesis only bridge girders in CSC 3 and lower have been investigated. A further study should aim to investigate the capability of additional material savings for a girder in CSC 4.
- How much the location of the transition of the cross sections influence the results. Further studies should also investigate if additional beam types along the bridge could be used in order to further optimize the design.
- The influence of using additional manufacturing partners in the cost estimations in order to get a diverse assessment representing several parties.

References

B.Johansson, Maquoi, R., Sedlacek, G., Müller, C., & Beg, D. (2007). *Commentary and worked examples to en 1993-1-5, "plated structural elements"*.

Boutillon, L., Combault, J., Ikeda, S., Imberty, F., Mori, T., Nagamoto, N., Novak, B., & Saito, K. (2015). *Corrugated-steel-web bridges*. Fèdération internationale du béton.

Collin, P., Johansson, B., & Sundquist, H. (2008). *Steel concrete composite bridges*. Stockholm: Royal Institute of Technology, Luleå Technical University.

Dahlström, S. E., & Persson, J. (2018). *Implementation of stainless steel reinforcement in concrete bridges.* (Master thesis, Chalmers University of Technology). Chalmers Open Digital Repository. https://hdl.handle.net/20.500.12380/255636

Elkawas, A., Hassanein, M., & Elchalakani, M. (2018). Lateral-torsional buckling strength and behaviour of high-strength steel corrugated web girders for bridge construction. *Thin-walled structures*, *122*, 112–123.

Hassanein, M., Elkawas, A., El Hadidy, A., & Elchalakani, M. (2017). Shear analysis and design of high-strength steel corrugated web girders for bridge design. *Engineering Structures*, *146*, 18–33.

Henrysson, A., & Yman, E. (2020). *Design of composite steel-concrete bridges using stainless steel girders with corrugated webs* (Master thesis, Chalmers University of Technology). Chalmers Open Digital Repository. https://hdl.handle.net/20.500.12380/301009

Karlsson, E. (2018). *Stainless steel bridge girders with corrugated webs* (Master thesis, Chalmers University of Technology). Chalmers Open Digital Repository. https://hdl.handle.net/20.500.12380/255630

Outokumpu. (2019). *Hot rolled stainless steel*. [EPD]. https://www.outokumpu.com/en/sustainability/sustainable-solutions/environmental-product-declarations

Schedin, E., & Backhouse, A. Stainless steel composite bridge study. In: Outokumpu, 2019.

Shamass, R., & Cashell, K. (2018a). Analysis of stainless steel-concrete composite beams. *Journal of Constructional Steel Research*, *152*, 132–142.

Shamass, R., & Cashell, K. (2018b). Bending moment capacity of stainless steel-concrete composite beams. *Proceedings of the 12th International Conference on Advances in Steel-Concrete Composite Structures. ASCCS 2018*, 145–151.

SSAB. (2020). *Hot rolled steel plates*. [EPD]. https://www.ssab.com/download-center?dcFilter=environmentalpr&dcSearch#sort=%5C%40customorder%5C%20descending&f:document=[3f0a0e364ca54f74a30faff866bd87ff]

Stålbyggnadsintitutet. (2017). *Dimensionering av konstruktioner i rostfritt stål* (4th ed.). Stockholm.

Stemne, D. (2021). Förhöjd arbetstemperature vid svetsning - varför och hur utförs den. *Nyheter om stålbyggnad, Nr 2*, 33–34. https://www.stalbyggnad.se/tidning/tidningen-stalbyggnad-nummer-2-2021/

Swedish Standards Institute. (2001). *SS-EN 1011-2 Welding - recommendations for welding of metallic materials, Part 2: Arc welding of ferritic steels.* https://www.sis.se/

Swedish Standards Institute. (2002). *SS-EN 1990 basis of structural design.* https://www.sis.se/

Swedish Standards Institute. (2003). *SS-EN 1991 Actions on structures.* https://www.sis.se/

Swedish Standards Institute. (2005a). *SS-EN 1993-1-1 Design of steel structures, Part 1-1 general rules and rules for buildings.* https://www.sis.se/

Swedish Standards Institute. (2005b). *SS-EN 1993-1-8 Design of steel structures, Part 1-8 design of joints.* https://www.sis.se/

Swedish Standards Institute. (2005c). *SS-EN 1993-1-9 Design of steel structures, Part 1-9 fatigue.* https://www.sis.se/

Swedish Standards Institute. (2005d). *SS-EN 1994-2 Design of composite steel and concrete structures, Part 2 General rules and rules for bridges.* https://www.sis.se/

Swedish Standards Institute. (2006a). *SS-EN 1993-1-4 Design of steel structures, Part 1-4 General rules - supplementary rules for stainless steels.* https://www.sis.se/

Swedish Standards Institute. (2006b). *SS-EN 1993-1-5 Design of steel structures, Part 1-5 Plated structural elements.* https://www.sis.se/

Swedish Standards Institute. (2011). *SS-EN 15978:2011 Sustainability of construction works - assessment of environmental performance of buildings - calculations method.* https://www.sis.se/

Swedish Standards Institute. (2020). *prEN 1993-1-4:2020 (E) Final draft - Design of steel structures, Part 1-4 General rules - supplementary rules for stainless steels.*

Syu, F.-s. (2021). *Comparative life cycle analysis for bridges made of conventional steel and stainless steel in the early design phases: Developing a parametric multi-perspective approach* (Master thesis, Chalmers University of Technology). Chalmers Open Digital Repository.

Trafikverket. (2019a). *Krav brobyggande.*

Trafikverket. (2019b). *Råd brobyggande.*

Transportstyrelsen. (2018). *Transportstyrelsens föreskrifter och allmäna råd om tillämpning av eurokoder.*

Utsi, S., & Lagerqvist, O. (2012). *Samverkanskonstruktioner stål-betong* (1st ed.). Stålbyggnadsinstitutet.

Vayas, I., & Iliopoulos, A. (2014). *Design of steel-concrete composite bridges to eurocodes.* CRC Press.

A

Indata for flat web in carbon steel for Brigade/Plus

```python

# -*- coding: utf-8 -*-
"""
Created on Mon Feb 22 08:23:00 2021

@author: SEMO20559
"""
#=============================================================================
# INDATA
#=============================================================================
modelName='Bro_test'
g=9.82                                  # Gravity constant
RH=80.0                                 # Relative humidity in the ambient air

# ------ Dimensions ------ #

lengthBridge=59.4                       # Total length of the main beams [m]
supports=[1.4, 29.7, 58.0]              # Coordinates of the supports [m]
ccBeams=5.3                             # CC distance between the beams [m]
zAvgBeams=1.0                           # Average distance to beams cg [m]

Type1 = {'bft':0.490, 'tft':0.032, 'bfb':0.720, 'tfb':0.040, 'hw':1.178, 'tw':0.016}
Type2 = {'bft':0.500, 'tft':0.025, 'bfb':0.740, 'tfb':0.040, 'hw':1.185, 'tw':0.016}

beams=[(0.0, 24.04, Type1),
       (24.04, 35.36, Type2),
       (35.36, lengthBridge, Type1)]      # This matrix should allways end at
                                            # the end of the bridge
#Deck
widthDeck=9.5                           # Width of the deck [m]
thicknessDeck=0.32                      # Average thickness of deck [m]
ccStuds=0.27                            # CC distance between studs [m]

b1=2.515                                # Outstand part of the deck [m]
b2=1.865                                # Internal part of the deck [m]

# Edge beams
heightEdgeBeam=0.7                      # Total height of edge beam [m]
widthEdgeBeam=0.32                      # Total width of edge beam [m]

#Transversal beams
l_cr_support=4.0                        # Distance of cross beams close to
                                            # the internal support [m]
l_cr_span=6.0                           # Distance of cross beams in span [m]

# Welds
a_wt=0.007                                # a-value weld (top) [m]
a_wb=0.007                                # a-value weld (bottom) [m]

# Reinforcement
layersRein=2.0                          # Reinforcement layers over support
fiRein=0.016                            # Diameter of reinforcement bars [m]
sRein=0.106                             # Center distance between bars [m]
f_yk=500.0e6                            # Yield strength [Pa]

# Covering
thicknessCov=0.10                       # Thickness of covering [m]
ro_cov=23000.0                          # Weight of covering material [N/m3]


# ------ Material indata ------ #

# Steel
v=0.3                                    # Poisssons ratio [-]
```

```
E_s=210.0e9                          # Modulus of elasticity, steel [Pa]
G_s=E_s/(2.0*(1.0+v))                # Shear modulus, steel [Pa]
ro_s=7850.0                          # Density, steel
[kg/m3]
thermalExp_s=10.0e-6                 # Thermal coefficient, steel

# Concrete
E_cm=34.0e9                          # Modulus of elasticity, concrete [Pa]
f_cm=43.0e6                          # Men compression strenght [Pa]
f_ck=35.0e6                          # Char. compression strength [Pa]
f_ctm=3.2e6                          # Mean tensile strength [Pa]
f_ctk0_05=2.2e6                      # Lower char. tensile strength[Pa]
ro_c=25000.0                         # Weight of concrete [N/m3]
ro_cw=26000.0                        # Weight of wet concrete [N/m3]
thermalExp_c=10.0e-6                 # Thermal coefficient, concrete


# ------ Loads ------ #

qBrakeTP=3111.0                     # Breaking force, TP vehicles [N/m]
qStructureWind=185.0                # Vertical component wind load
                                        # on structure [N/m]
qTrafficWind=492.0                  # Vertical component wind load
                                        # on traffic [N/m]
qForm=1600.0                        # Form work load [kg/m]
qConstruction=750.0                 # Construction load [N/m2]
qRailing=500.0                      # Load from railing [N/m]

#Parameters for creep calculation
M_0=3719480.0                       # Maximum span moment calculated for
                                        # short-term system with
                                        # permanent loads [Nm]

#Parameters for shrinkage calculation
epsilon_cs=2.5e-4                   # Final shrinkage strain [-]
M_as=281666.0                       # Average span moment due to primary
                                        # effects of shrinkage [Nm]
# Parameters for temperature load
Temin=-31
Temax=39


segment='0.5'
increments='2,2'
```

B

Indata for corrugated web in stainless steel for Brigade/Plus

```python
# -*- coding: utf-8 -*-
"""
Created on Mon Feb 22 08:23:00 2021

@author: SEMO20559
"""
#=============================================================================
# INDATA
#=============================================================================
modelName='Bro_test'
g=9.82                                  # Gravity constant
RH=80.0                                 # Relative humidity in the ambient air

#Beams
lengthBridge=59.4                       # Total length of the main beams [m]
supports=[1.4, 29.7, 58.0]              # Coordinates of the supports [m]
ccBeams=5.3                             # CC distance between the beams [m]
zAvgBeams=1.0                           # Average distance to beams cg [m]

Type1 = {'bft':0.460, 'tft':0.030, 'bfb':0.770, 'tfb':0.040, 'hw':1.180, 'tw':0.009}
Type2 = {'bft':0.380, 'tft':0.030, 'bfb':0.640, 'tfb':0.037, 'hw':1.183, 'tw':0.009}

beams=[(0.0, 24.04, Type1),
       (24.04, 35.36, Type2),
       (35.36, lengthBridge, Type1)]     # This matrix should allways end at
                                            # the end of the bridge
#Deck
widthDeck=9.5                           # Width of the deck [m]
thicknessDeck=0.32                      # Average thickness of deck [m]
ccStuds=0.27                            # CC distance between studs [m]

b1=2.515                                # Outstand part of the deck [m]
b2=1.865                                # Internal part of the deck [m]

# Edge beams
heightEdgeBeam=0.7                      # Total height of edge beam [m]
widthEdgeBeam=0.32                      # Total width of edge beam [m]

#Transversal beams
l_cr_support=4.0                        # CC distance of cross beams close to
                                            # the internal support [m]
l_cr_span=6.0                           # CC distance of cross beams in span [m]

# Welds
a_wt=0.007                              # a-value weld (top) [m]
a_wb=0.007                              # a-value weld (bottom) [m]

#Corrugation parameters
a_c1=0.070                              # Flat fold length [m]
alph_c=36.0                             # Corrugation degree [deg]
a_c3=0.040                              # Corrugation depth [m]

# Reinforcement
layersRein=2.0                          # Reinforcement layers over support
fiRein=0.016                            # Diameter of reinforcement bars [m]
sRein=0.106                             # Center distance between bars [m]
f_yk=500.0e6                            # Yield strength [Pa]

# Covering
thicknessCov=0.1                        # Thickness of covering [m]
ro_cov=23000.0                          # Weight of covering [N/m3]


# ------ Material indata ------ #
```

```
65
66  # Steel
67  v=0.3                                  # Poisson ratio [-]
68  E_s=200.0e9                            # Modulus of elasticity, steel [Pa]
69  G_s=E_s/(2.0*(1.0+v))                  # Shear modulus, steel [Pa]
70  ro_s=7700.0                            # Density, teel
    [kg/m3]
71  thermalExp_s=13.0e-6                   # Thermal coefficient, steel
72
73  # Concrete
74  E_cm=34.0e9                            # Modulus of elasticity, concrete [Pa]
75  f_cm=43.0e6                            # Men compression strenght [Pa]
76  f_ck=35.0e6                            # Char. compression strength [Pa]
77  f_ctm=3.2e6                            # Mean tensile strength [Pa]
78  f_ctk0_05=2.2e6                        # Lower char. tensile strength[Pa]
79  ro_c=25000.0                           # Weight of concrete [N/m3]
80  ro_cw=26000.0                          # Weight of wet concrete [N/m3]
81  thermalExp_c=10.0e-6                   # Thermal coefficient, concrete
82
83  # ------ Loads ------ #
84
85  qBrakeTP=3111.0                      # Breaking force, TP vehicles [N]
86  qStructureWind=185.0                 # Vertical component wind load
87                                           # on structure [N/m]
88  qTrafficWind=492.0                   # Vertical component wind load
89                                           # on traffic [N/m]
90  qForm=1600.0                         # Form work load [kg/m]
91  qConstruction=750.0                  # Construction load [N/m2]
92  qRailing=500.0                       # Load from railings [N/m]
93
94  #Parameters for creep calculation
95  M_0=3732270.0                        # Maximum span moment calculated for
96                                           # short-term system with
97                                           # permanent loads [Nm]
98  #Parameters for shrinkage calculation
99  epsilon_cs=2.5e-4                    # Final shrinkage strain [-]
100 M_as=213508.5                        # Average span moment due to primary
101                                          # effects of shrinkage [Nm]
102 # Parameters for temperature load
103 Temin=-31
104 Temax=39
105
106
107 segment='0.5'
108 increments='2,2'
109
110
111
```

C

Case study 1: Design with flat web in carbon steel, S355

1 Material

1.1 Carbon steel girder

$SteelType := \text{“CarbonSteel”}$

The choosen steel grade is S355. Material strengths are presented below for different thicknesses.

$f_{y\_w16mm_1} = 355\ MPa$ Proof strength for $t \leq 16\ mm$ - SS- EN 1993-1-1 Table 3.1

$f_{u\_w16mm_1} = 490\ MPa$ Ultimate strength for $t \leq 16\ mm$ - SS- EN 1993-1-1 Table 3.1

$f_{y\_tf40mm_1} = 345\ MPa$ Proof strength for $t \leq 40\ mm$ - EN 1993-1-1 Table 3.1

$f_{u\_tf40mm_1} = 470\ MPa$ Ultimate strength for $t \leq 40\ mm$ - SS- EN 1993-1-1 Table 3.1

$f_{y\_bf63mm_1} = 335\ MPa$ Proof strength for $t \leq 63\ mm$ - SS- EN 1993-1-1 Table 3.1

$f_{u\_bf63mm_1} = 470\ MPa$ Ultimate strength for $t \leq 63\ mm$ - SS- EN 1993-1-1 Table 3.1

$f_{ytf} := f_{y\_tf40mm}$ $f_{utf} := f_{u\_tf40mm}$ Choosen strength in top flange

$f_{ybf} := f_{y\_bf40mm}$ $f_{ubf} := f_{u\_bf40mm}$ Choosen strength in bottom flange

$f_{yw} := f_{y\_w16mm}$ $f_{uw} := f_{u\_w16mm}$ Choosen strength in web

$$\varepsilon_{ft} := \sqrt{\frac{235}{\frac{f_{ytf}}{MPa}}}$$ SS-EN 1993-1-5 4.4

$$\varepsilon_{fb} := \sqrt{\frac{235}{\frac{f_{ybf}}{MPa}}}$$ SS-EN 1993-1-5 4.4

$$\varepsilon_{w} := \sqrt{\frac{235}{\frac{f_{yw}}{MPa}}}$$ SS-EN 1993-1-5 4.4

$E_s = 210\ GPa$ Modulus of elasticity - SS-EN 1993-1-1 3.2.6 (1)

$\gamma_{M0} := 1.0$ Partial coefficient considering the resistance of the cross-section -TSFS 18 ch 2 §

$\gamma_{M1} := 1.0$ Partial coefficient considering the resistance of members to instability -TSFS 18 ch 2 §

$\gamma_{M2} := 1.2$ Partial coefficient considering the resistance of the cross-section in tension to fracture -TSFS 18 ch 2 §

$\alpha_s = 10 \cdot 10^{-6}$ Thermal expansion coefficient for carbon steel in composite bridges

1.2 Concrete slab

The design of the concrete slab is neglected in this master thesis. In order to calculate loads from shrinkage and creep some material parameters are included.

1.2.1 Concrete

The choosen concrete class is C35/45.

$f_{ck} = 35\ MPa$	Compressive strength - SS- EN 1992-1-1 Table 3.1
$f_{cm} = 43\ MPa$	Mean compressive strength - SS- EN 1992-1-1 Table 3.1
$f_{ctm} = 3.2\ MPa$	Mean tensile strength - SS- EN 1992-1-1 Table 3.1
$f_{ctk.0.05} = 2.2\ MPa$	5% fractile tensile strength - SS- EN 1992-1-1 Table 3.1
$E_{cm} = 34\ GPa$	Youngs modulus - SS- EN 1992-1-1 Table 3.1
$\gamma_c := 1.5$	Partial safety factor concrete (Permanent and variable loads) - SS- EN 1992-1-1 Table .2.1N
$\gamma_{cE} := 1.2$	Partial safety factor concrete (Accidental loads) - SS- EN 1992-1-1 Table 2.1N
$\alpha_{cc} := 1.0$	Accounting for longterm effects on the compressive strength - TSFS 2018:57 14 ch 3 §
$\alpha_{ct} := 1.0$	Accounting for longterm effects on the tensile strength - TSFS 2018:57 14 ch 3 §
$f_{cd} := \alpha_{cc} \cdot \frac{f_{ck}}{\gamma_c} = 23.3\ MPa$	Design compressive stength
$f_{ctd} := \alpha_{ct} \cdot \frac{f_{ctk.0.05}}{\gamma_c} = 1.47\ MPa$	Design tensile stength
$\alpha_c = 10 \cdot 10^{-6}$	Thermal expansion coefficient for concrete

1.2.1.1 Final shrinkage strain

$u := 2\ w_{deck} + 2\ t_{deck} = 19.640\ m$ Is the perimeter of the cross-section in contact with the atmosphere

$A_c = 3.040\ m^2$ Area of full concrete deck section

$h_0 := \frac{2 \cdot A_c}{u} = 310\ mm$ Equivalent thickness

$t_y := 80 years$

$t := 29200\ day$

$f_{cm} = 43\ MPa$ Mean compressive strength

$t_s := 1\ day$

$RH := 80\%$ Krav Brobyggande B.3.1.5

$$\beta_{ds} := \frac{\frac{t - t_s}{day}}{\left(\frac{t - t_s}{day}\right) + 0.04 \cdot \sqrt{\left(\frac{h_0}{1\ mm}\right)^3}} = 0.993$$ SS-EN 1992-1-1 3.1.4 Equation 3.10

$$k_h := \begin{cases} 0.85 - \left(\frac{h_0}{mm} - 200\right) \cdot 0.001 & \text{if } 200\ mm \le h_0 < 300\ mm \\ 0.75 - \left(\frac{h_0}{mm} - 300\right) \cdot 0.0005 & \text{else if } 300\ mm \le h_0 < 500\ mm \\ 0.7 & \text{else if } h_0 \ge 500\ mm \\ 1.0 & \text{else} \end{cases} = 0.75$$ SS-EN 1992-1-1 3.1.4 table 3.3

$RH_0 := 100\%$

$\alpha_{ds1} := 4$ SS-EN 1992-1-1 Appendix B.2 (1), Cementclass N

$\alpha_{ds2} := 0.12$ SS-EN 1992-1-1 Appendix B.2 (1), Cementclass N

$$\beta_{RH} := 1.55 \cdot \left(1 - \left(\frac{RH}{RH_0}\right)^3\right) = 0.76$$ SS-EN 1992-1-1 Appendix B.2 equation B12

$f_{cmo} := 10\ MPa$ SS-EN 1992-1-1 Appendix B.2 (1)

$\varepsilon_{cd.0} := 0.85 \cdot \left(\left(220 + 110 \cdot \alpha_{ds1} \right) \cdot e^{\left(-\alpha_{ds2} \cdot \frac{f_{cm}}{f_{cmo}} \right)} \right) \cdot 10^{-6} \cdot \beta_{RH} = 2.53 \cdot 10^{-4}$ SS-EN 1992-1-1 Appendix B.2 equation B11

$\varepsilon_{cd} := \beta_{ds} \cdot k_h \cdot \varepsilon_{cd.0} = 1.87 \cdot 10^{-4}$ Drying shrinkage - SS-EN 1992-1-1 3.1.4 Equation 3.9

$\varepsilon_{ca0} := 2.5 \cdot \left(\frac{f_{ck} - f_{cmo}}{MPa} \right) \cdot 10^{-6} = 6.3 \cdot 10^{-5}$ SS-EN 1992-1-1 3.1.4 Equation 3.12

$\beta_{as} := 1 - e^{\left(-0.2 \cdot \sqrt{\frac{t - t_s}{day}} \right)} = 1.0$ SS-EN 1992-1-1 3.1.4 Equation 3.13

$\varepsilon_{ca} := \beta_{as} \cdot \varepsilon_{ca0} = 6.25 \cdot 10^{-5}$ Autogenous shrinkage - SS-EN 1992-1-1 3.1.4 Equation 3.11

$\varepsilon_{cs} := \varepsilon_{ca} + \varepsilon_{cd} = 2.5 \cdot 10^{-4}$ Total shrinkage - SS-EN 1992-1-1 3.1.4 Equation 3.8

1.2.1.1 Creep function

$RH := 80$ — [%] - Relative humidity in the ambient air

t_0 — [days] - Time for first loading

$u := 2\ w_{deck} + 2\ t_{deck} = 19.640\ m$ — Is the perimeter of the cross-section in contact with the atmosphere

$A_c = 3.040\ m^2$ — Area of full concrete deck section

$$h_0 := \frac{2 \cdot A_c}{u} = 310\ mm$$ — SS- EN 1992-1-1 B.1 (B.6)

$$\alpha_1 := \left(\frac{35\ MPa}{f_{cm}}\right)^{0.7} = 0.9$$ — SS- EN 1992-1-1 B.1 (B.8c)

$$\alpha_2 := \left(\frac{35\ MPa}{f_{cm}}\right)^{0.2} = 1$$ — SS- EN 1992-1-1 B.1 (B.8c)

$$\varphi_{RH} := \begin{cases} \text{if } f_{cm} > 35\ MPa \\ \quad \left(1 + \dfrac{1 - \frac{RH}{100}}{0.1 \cdot \sqrt[3]{\frac{h_0}{mm}}} \cdot \alpha_1\right) \cdot \alpha_2 \\ \text{else} \\ \quad \left(1 + \dfrac{1 - \frac{RH}{100}}{0.1 \cdot \sqrt[3]{\frac{h_0}{mm}}}\right) \end{cases} = 1.2$$ — SS- EN 1992-1-1 B.1 (B.3a,b)

$$\beta_{fcm} := \frac{16.8}{\sqrt{\frac{f_{cm}}{MPa}}} = 2.6$$ — SS- EN 1992-1-1 B.1 (B.4)

$$\beta_{t0}(t_0) := \frac{1}{0.1 + \left(\frac{t_0}{day}\right)^{0.2}}$$ — SS- EN 1992-1-1 B.1 (B.5)

$\varphi_0(t_0) := \varphi_{RH} \cdot \beta_{fcm} \cdot \beta_{t0}(t_0)$ — Nominal creep value - SS- EN 1992-1-1 B.1 (B.2)

$\varphi_{\infty\_cs} := \varphi_0(1\ day) = 2.81$ — Final creep value for shrinkage (t= 1 day) - SS-EN 1994-2 5.4.2.2 (4)

$\varphi_{\infty\_perm} := \varphi_0(7\ day) = 1.96$ — Final creep value for permanent loads (t= 7 day) - SS-EN 1994-2 5.4.2.2

1.2.2 Reinforcement

The used reinforcement is B500B.

$f_{yk} = 500\ MPa$ — SS- 212540:2014 Table C.2

$E_{rs} := E_s = 210\ GPa$ — SS- EN 1994-2 3.2(2)

$\gamma_s := 1.15$ — Permanent and variable loads SS- EN 1992-1-1 Table 2.1N

$\gamma_{sfat} := 1.15$ — Fatigue loading SS- EN 1992-1-1 Table 2.1N

$\gamma_{sA} := 1.0$ — Accidental loading SS- EN 1992-1-1 Table 2.1N

$f_{yd} := \frac{f_{yk}}{\gamma_s} = 435\ MPa$ — Design yield strength - SS-EN 1990 6.3.3

1.2.3 Modular ratios

Calculated according to SS-EN 1994-2, 5.4.2.2, Equation (5.6).

$n_0 := \frac{E_s}{E_{cm}} = 6.18$ — Modular ratio between stainless steel and concrete

$\varphi_{L\_perm} := 1.1$ — Creep factor depending on the load durance for permanent loads - SS- EN 1994-2 5.4.2.2

$\varphi_{L\_cs} := 0.55$ — Creep factor depending on the load durance for shrinkage - SS- EN 1994-2 5.4.2.2

$n_{L\_short} := n_0 \cdot (1 + 0 \cdot 0) = 6.2$ — Modular ratio for short-term loads and temperature

$n_{L\_perm} := n_0 \cdot (1 + \varphi_{L\_perm} \cdot \varphi_{\infty\_perm}) = 19.5$ — Modular ratio for permanent loads (excl. shrinkage)

$n_{L\_cs} := n_0 \cdot (1 + \varphi_{L\_cs} \cdot \varphi_{\infty\_cs}) = 15.7$ — Modular ratio for shrinkage

$$n_L := \begin{bmatrix} n_{L\_perm} \\ n_{L\_short} \\ n_{L\_cs} \end{bmatrix}$$

2 System

2.1 Primary system - longitudinal

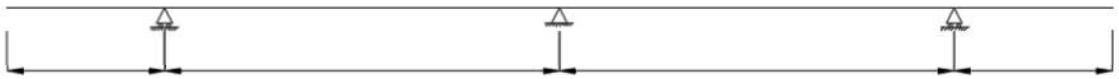

$l_{console.1} = 1.40\ m$ $L_{span_1} = 28.30\ m$ $L_{span_2} = 28.30\ m$ $l_{console.2} = 1.40\ m$

The longitudinal system consists of two steel beams spanning over several spans. The steel girder change in cross-section over the internal supports. The cross section changes are located according to the coordinates below.

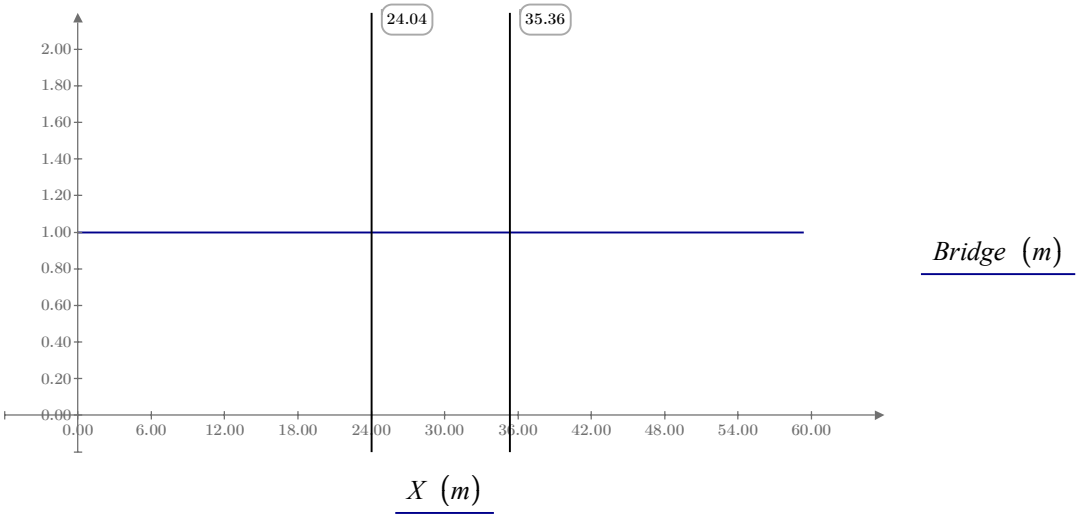

2.1.1 Cross-section dimensions

2.1.1.1 Beam type 1

Steel beam type 1 is located in the spans .

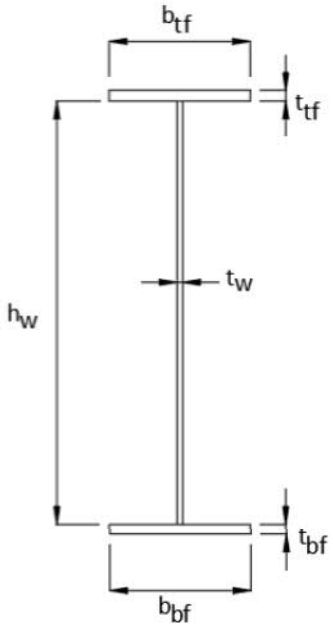

$b_{tf}(X_{span}) = 490\ mm$ Width top flange

$t_{tf}(X_{span}) = 32\ mm$ Thickness top flange

$h_w(X_{span}) = 1178\ mm$ Height web

$t_w(X_{span}) = 16\ mm$ Thickness tweb

$b_{bf}(X_{span}) = 720\ mm$ Width bottom flange

$t_{bf}(X_{span}) = 40\ mm$ Thickness bottom flange

2.1.1.2 Beam type 2

Steel beam type 2 is located over the internal support area.

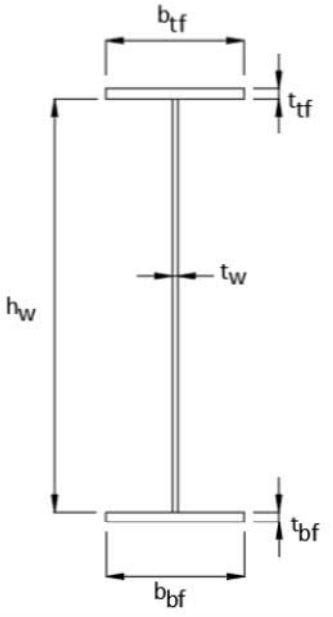

$b_{tf}(X_{support}) = 500\ mm$ Width top flange

$t_{tf}(X_{support}) = 25\ mm$ Thickness top flange

$h_w(X_{support}) = 1185\ mm$ Height web

$t_w(X_{support}) = 16\ mm$ Thickness tweb

$b_{bf}(X_{support}) = 740\ mm$ Width bottom flange

$t_{bf}(X_{support}) = 40\ mm$ Thickness bottom flange

2.2 Secondary system - transversal

The secondary system consists of a reinforced concrete deck with dimensions presented below.

2.2.1 Concrete

$t_{deck} = 0.32\ m$ Height of concrete deck

$w_{deck} = 9.50\ m$ Total width of concrete deck

2.2.2 Reinforcement

The reinforcement is assumed to be located in the center of the concrete deck.

$\phi_{rein} = 16\ mm$ Dimension of reinforcement bar

$s_{rein} = 106\ mm$ CC-distance between bars

$n_{rein} = 2$ Number of layers

3 Loads

Here, the loads inserted in the system analysis in Brigade/Plus are presented.

$L_{bridge} := 59.4\ m$ — Bridge length

$cc_{beams} := 5.3\ m$ — CC-distance between main girders

$h_{girder} := 1.25\ m$ — Height of girder

$t_{deck} := 0.32\ m$ — Thickness of concrete deck

$h_{edgebeam} := 0.7\ m$ — Height of edge beam

$w_{deck} := 9.5\ m$ — Width of bridge deck

3.1 Permanent loads

3.1.1 Steel beams

$\rho_{steel} := 7850\ \frac{kg}{m^3}$ — Density of carbon steel

3.1.2 Concrete deck

$\rho_{con.w} := 26\ \frac{kN}{m^3}$ — Wet concrete used for calculations during construction stage

$\rho_{con} := 25\ \frac{kN}{m^3}$ — Dry concrete used for calculations during service stage

3.1.3 Coating

$t_{cov} := 100\ mm$ — Thickness of coating

$\rho_{cov} := 23\ \frac{kN}{m^3}$ — Weight of coating

$g_{cov} := t_{cov} \cdot \rho_{cov} = 2300\ \frac{N}{m^2}$ — Uniformly distributed load from coating

3.1.4 Rails

$g_{rails} := 0.5 \ \frac{kN}{m}$

Line load due to railings located on the edgebeams

3.1.5 Shrinkage

$\varepsilon_{cs} = 2.50 \cdot 10^{-4}$

Final shrinkage strain

$M_{as} := 281.66 \ kN \cdot m$

Moment working on the steel section due to first order effects of shrinkage

3.1.6 Creep

$M_0 := 3719.48 \ kN \cdot m$

Short term moment in span due to permanent loads

3.2 Variable loads

3.2.1 Braking and acceleration force

Trafikverket vehicles

$A_{tr} := 180 \ kN$

$B_{tr} := 300 \ kN$

$$Br := max\left(\begin{bmatrix} 0.88 \\ 1 \\ 1.1 \\ 1.17 \\ 1.32 \\ 0.44 + 1.32 + 0.44 + 1.32 \\ 0.55 + 1 + 1.32 \\ 0.44 + 1.1 + 1.1 + 0.66 \\ 0.44 + 1.32 + 0.44 + 1.32 \\ 0.55 + 1 + 1.32 \\ 0.44 + 1.1 + 1.1 + 0.66 \\ 0.33 + 1 + 1.32 \\ 0.55 + 0.55 + 0.55 + 0.33 + 0.12 \end{bmatrix} \cdot B_{tr}\right) = 1056.00 \ kN$$

$Q_{1k\_tr} := min\left(0.35 \cdot Br, 500 \ kN\right) = 369.60 \ kN$

$q_{br.tr} := \frac{Q_{1k\_tr}}{2 \cdot L_{bridge}} = 3.11 \ \frac{kN}{m}$

Braking/acceleration load from Trafikverket vehicle

3.2.2 Temperature load

$T_0 := 10$

$T_{min} := -35$ Minimum temperature for Borås kommun, TSFS 2018:57

$T_{max} := 35$ Maximum temperature for Borås kommun, TSFS 2018:57

$T_{e.min} := T_{min} + 4 = -31$

$T_{e.max} := T_{max} + 4 = 39$

3.2.3 Wind load

$h_{vehicle} := 2\ m$

$d_{tot} := h_{girder} + t_{deck} + t_{cov} + h_{vehicle} = 3.67\ m$

$\rho_{air} := 1.25\ \frac{kg}{m^3}$

$v_b := 25\ \frac{m}{s}$

$q_p := 0.79\ \frac{kN}{m^2}$ Terrain category II, assumed height 8m. TSFS 2018:57 Table 7.1

$q_b := \frac{1}{2} \cdot \rho_{air} \cdot v_b^{\ 2} = 0.39\ \frac{kN}{m^2}$ SS-EN 1991-1-4 4.5, Eq.4.10

$c_e := \frac{q_p}{q_b} = 2.02$ SS-EN 1991-1-4 4.5, Eq.4.9

$\frac{w_{deck}}{d_{tot}} = 2.59$

$c_{fx} := 1.65$ SS-EN 1991-1-4, Figure 8.3

$C_w := c_e \cdot c_{fx} = 3.34$ Form factor for force on superstructure in x-direction

Wind load on structure

$d_{bridge} := h_{girder} + h_{edgebeam} + 0.6\ m = 2.55\ m$ SS-EN 1991-1-4, Table 8.1

$F_{w.bridge} := q_p \cdot c_{fx} \cdot d_{bridge} = 3.32\ \frac{kN}{m}$ Horizontal component per meter bridge

$z := d_{bridge} - (h_{girder} + t_{deck}) = 0.98\ m$

$$q_{bridge} := \frac{F_{w.bridge} \cdot \left(\frac{d_{bridge}}{2} - z \right)}{cc_{beams}} = 0.185 \ \frac{kN}{m}$$

Wind load on structure

Wind load on vehicle

$d_{vehicle} := h_{vehicle} = 2.0 \ m$

SS-EN 1991-1-4, Table 8.1

$$F_{w.vehicle} := q_p \cdot c_{fx} \cdot d_{vehicle} = 2.607 \ \frac{kN}{m}$$

$$q_{vehicle} := \frac{F_{w.vehicle} \cdot \left(\frac{d_{vehicle}}{2} \right)}{cc_{beams}} = 0.492 \ \frac{kN}{m}$$

Wind load on vehicle

4 Capacity checks during construction

The capacity check that is carried out in this chapter is bending moment capacity with respect to lateral torsional buckling in the casting stagetogether with the maximum stresses in the cross-section.

Because the checks are performed by using vectors and closed areas, controll-caluclations are showed for the governing coordinates. Critical points are presented in blue below:

$X_{check\_m\_midsup} = 29.7\ m$ Coordinate for control calculations - bending moment over midsupport

$X_{check\_m\_span} = 13.72\ m$ Coordinate for control calculations - bending moment in span

$X_{check\_v\_midsup} = 29.641\ m$ Coordinate for control calculations - shear force midsupport

$X_{check\_v\_endsup} = 1.426\ m$ Coordinate for control calculations - shear force end support

4.1 Load Combinations

The loads should be combined according to STR/GEO and 6.10a or 6.10b dependant on which case gives the worst load effects. The load combinations are presented below.

STR/GEO 6.10a

Permanent loads	**sup**	**inf**	**Unfavorable**	**Favorable**
Self-weight	1.0	1.0	$\gamma_d \cdot 1.35 \cdot sup$	$1.0 \cdot inf$
Surfacing	1.1	0.9	$\gamma_d \cdot 1.35 \cdot sup$	$1.0 \cdot inf$
Variable loads	Ψ_0		**Main load**	**Other load**
Wind loads	1.0		$\gamma_d \cdot 1.5 \cdot \Psi_0$	$\gamma_d \cdot 1.5 \cdot \Psi_0$

STR/GEO 6.10b

Permanent loads	**sup**	**inf**	**Unfavorable**	**Favorable**
Self-weight	1.0	1.0	$\gamma_d \cdot 0.89 \cdot 1.35 \cdot sup$	$1.0 \cdot inf$
Surfacing	1.1	0.9	$\gamma_d \cdot 0.89 \cdot 1.35 \cdot sup$	$1.0 \cdot inf$
Variable loads	Ψ_0		**Main load**	**Other load**
Wind loads	1.0		$\gamma_d \cdot 1.5$	$\gamma_d \cdot 1.5 \cdot \Psi_0$

4.2 Load effects

Load effects are retrieved from Brigade/Plus. During construction stage two different casting scenarios are calculated in order to see the worst effect. One scenario is when the casting load is located in one span and the other with the casting load located in two spans.

Bending moment, casting loads in 1 span

$M_{d.LC1.6.10.a}$ Bending moment from casting loads in 1 span, load combination 6.10a
$M_{d.LC1.6.10.b}$ Bending moment from casting loads in 1 span, load combination 6.10b

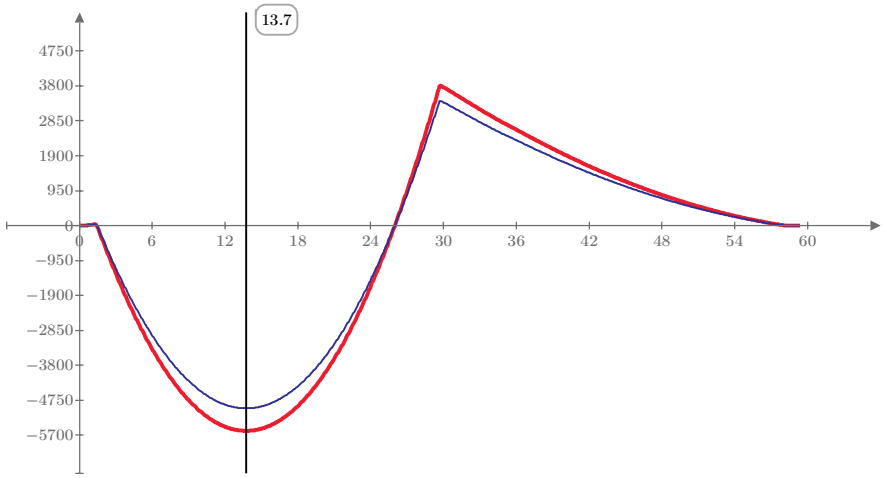

$M_{d.LC1.6.10.a}(X)\ \ (kN \cdot m)$

$M_{d.LC1.6.10.b}(X)\ \ (kN \cdot m)$

$X\ \ (m)$

Bending moment, casting loads in both spans

$M_{d.LC2.6.10.a}$ Bending moment from casting loads in 2 span, load combination 6.10a
$M_{d.LC2.6.10.b}$ Bending moment from casting loads in 2 span, load combination 6.10b

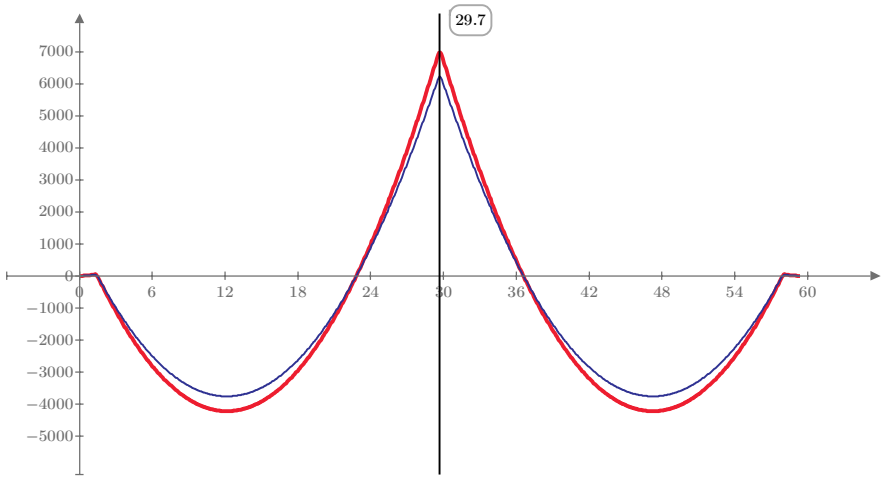

$M_{d.LC2.6.10.a}(X)\ \ (kN \cdot m)$

$M_{d.LC2.6.10.b}(X)\ \ (kN \cdot m)$

$X\ \ (m)$

Shear force, load effect from loads in 1 span

$V_{d.LC1.6.10.a}$ Shear force from casting loads in 1 span, load combination 6.10a
$V_{d.LC1.6.10.b}$ Shear force from casting loads in 1 span, load combination 6.10b

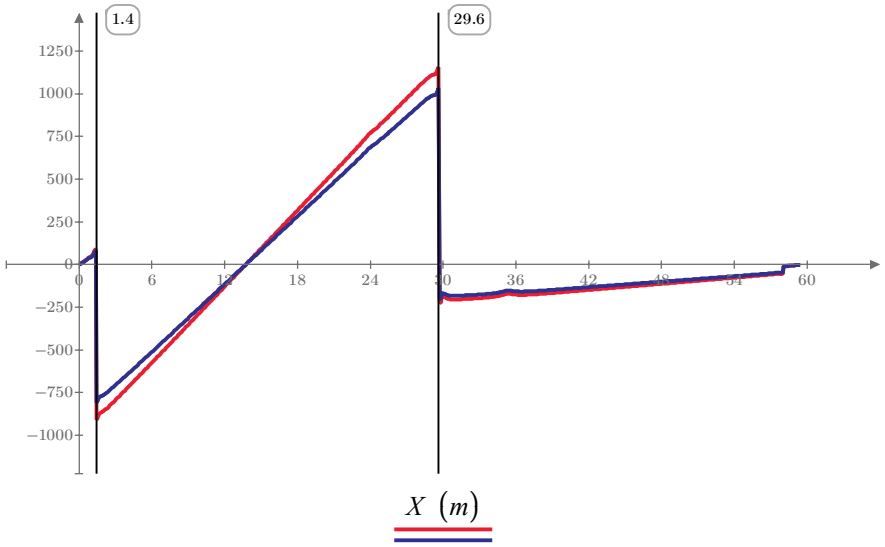

$V_{d.LC1.6.10.a}(X)$ (kN)

$V_{d.LC1.6.10.b}(X)$ (kN)

Shear force, load effect from loads in both spans

$V_{d.LC2.6.10.a}$ Shear force from casting loads in 2 span, load combination 6.10a
$V_{d.LC2.6.10.b}$ Shear force from casting loads in 2 span, load combination 6.10b

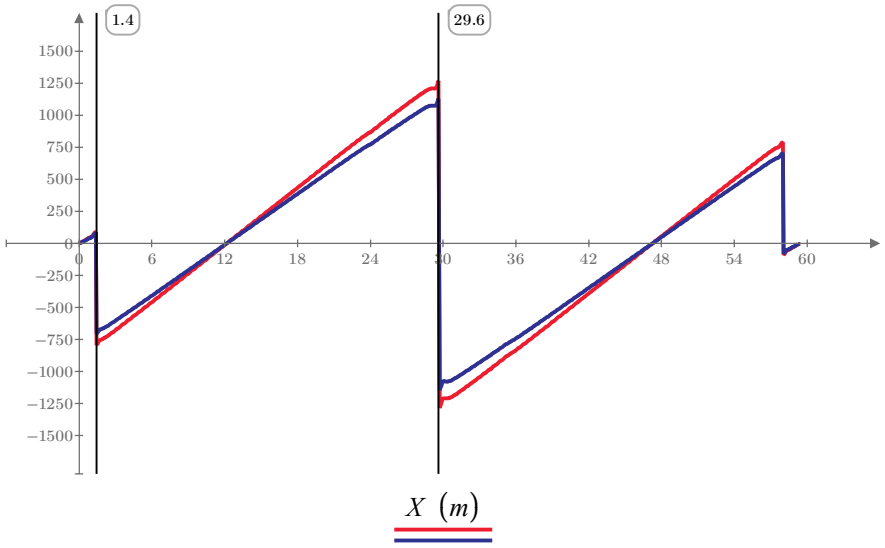

$V_{d.LC2.6.10.a}(X)$ (kN)

$V_{d.LC2.6.10.b}(X)$ (kN)

$LoadComb := \text{“6.10a”}$ Load combination that gives worst load effects

4.3 Cross-section classification

The cross-section classes is determined according to SS-EN 1993-1-1 5.6.

$a_{weld.top} = 7\ mm$ Weld thickness between top flange and web

$a_{weld.bot} = 7\ mm$ Weld thickness between bottom flange and web

$c_w(x) := h_w(x) - \sqrt{2} \cdot a_{weld.top} - \sqrt{2} \cdot a_{weld.bot}$ Distance between welded toes on web.

$c_{tf}(x) := \frac{b_{tf}(x)}{2} - \frac{t_w(x)}{2} - \sqrt{2} \cdot a_{weld.top}$ Length of the outstand part of top flange.

$c_{bf}(x) := \frac{b_{bf}(x)}{2} - \frac{t_w(x)}{2} - \sqrt{2} \cdot a_{weld.bot}$ Length of the outstand part of bottom flange.

Cross-section class, top flange

$E_s = 210\ GPa$ Modulus of elasticity

$f_{ytf}(X_{check\_m\_span}) = 345\ MPa$ Proof strength of top flange

$f_{ytf}(X_{check\_m\_midsup}) = 345\ MPa$ Proof strength of top flange

$\varepsilon_{tf}(X_{check\_m\_span}) = 0.83$

$\varepsilon_{tf}(X_{check\_m\_midsup}) = 0.83$

$$csc_{tf}(x) := \begin{cases} \text{if } \frac{c_{tf}(x)}{t_{tf}(x)} \le 9\ \varepsilon_{tf}(x) \\ \quad \text{“csc1”} \\ \text{else if } 9\ \varepsilon_{tf}(x) < \frac{c_{tf}(x)}{t_{tf}(x)} \le 10\ \varepsilon_{tf}(x) \\ \quad \text{“csc2”} \\ \text{else if } 10\ \varepsilon_{tf}(x) < \frac{c_{tf}(x)}{t_{tf}(x)} \le 14\ \varepsilon_{tf}(x) \\ \quad \text{“csc3”} \\ \text{else} \\ \quad \text{“Not suitable for these calculations”} \end{cases}$$

Cross-section class top flange

$csc_{tf}(X_{check\_m\_span}) = \text{“csc1”}$ Cross-section class at $X_{check\_m\_span} = 13.721\ m$

$csc_{tf}(X_{check\_m\_midsup}) = \text{“csc3”}$ Cross-section class at $X_{check\_m\_midsup} = 29.700\ m$

Cross-section class, bottom flange

$E_s = 210\ GPa$ Modulus of elasticity

$f_{ybf}(X_{check\_m\_span}) = 345\ MPa$ Proof strength of bottom flange

$f_{ybf}(X_{check\_m\_midsup}) = 345\ MPa$ Proof strength of bottom flange

$\varepsilon_{bf}(X_{check\_m\_span}) = 0.83$

$\varepsilon_{bf}(X_{check\_m\_midsup}) = 0.83$

$csc_{bf}(x) :=$ Cross-section class bottom flange

if $\frac{c_{bf}(x)}{t_{bf}(x)} \le 9\ \varepsilon_{bf}(x)$
"csc1"
else if $9\ \varepsilon_{bf}(x) < \frac{c_{bf}(x)}{t_{bf}(x)} \le 10\ \varepsilon_{bf}(x)$
"csc2"
else if $10\ \varepsilon_{bf}(x) < \frac{c_{bf}(x)}{t_{bf}(x)} \le 14\ \varepsilon_{bf}(x)$
"csc3"
else
"Not suitable for these calculations"

$csc_{bf}(X_{check\_m\_span}) =$ "csc3" Cross-section class at $X_{check\_m\_span} = 13.721\ m$

$csc_{bf}(X_{check\_m\_midsup}) =$ "csc3" Cross-section class at $X_{check\_m\_midsup} = 29.700\ m$

Cross-section class, web

$E_s = 210\ GPa$ Modulus of elasticity

$f_{yw}\left(X_{check\_m\_midsup}\right) = 355\ MPa$ Proof strength of web

$\varepsilon_w\left(X_{check\_m\_span}\right) = 0.81$

$\alpha := 0.5$ Safe side

$\psi(x) := \dfrac{\overrightarrow{\sigma_{s.tw}(x)}}{\sigma_{s.bw}(x)}$ Stress distribution in the web

$\psi\left(X_{check\_m\_midsup}\right) = -1.72$

$\psi\left(X_{check\_m\_span}\right) = -1.49$

$csc_w(x) :=$
- if $\dfrac{c_w(x)}{t_w(x)} \le \dfrac{36\ \varepsilon_w(x)}{\alpha}$
  - "csc1"
- else if $\dfrac{36\ \varepsilon_w(x)}{\alpha} < \dfrac{c_w(x)}{t_w(x)} \le \dfrac{41.5\ \varepsilon_w(x)}{\alpha}$
  - "csc2"
- else if $\dfrac{41.5\ \varepsilon_w(x)}{\alpha} < \dfrac{c_w(x)}{t_w(x)} \le 62\ \varepsilon_w(x) \cdot (1 - \psi(x)) \cdot \sqrt{\langle -\psi(x) \rangle}$
  - "csc3"
- else
  - "Not suitable for these calculations"

Cross-section class web

$csc_w\left(X_{check\_m\_midsup}\right) =$ "csc3" Cross-section class at $X_{check\_m\_midsup} = 29.700\ m$

$csc_w\left(X_{check\_m\_span}\right) =$ "csc3" Cross-section class at $X_{check\_m\_span} = 13.721\ m$

4.4 Lateral torsional buckling of compressed flange

Compressed top flange, in span

The buckling capacity of the compressed flange is calculated according to to SS-EN 1993-1-1 6.3.1.2.

$$\alpha_{LT} := \left\| \begin{array}{l} \text{if } t_{tf}(X_{check\_m\_span}) \le 40\ mm \\ \quad \| \ 0.49 \\ \text{else if } t_{tf}(X_{check\_m\_span}) > 40\ mm \\ \quad \| \ 0.76 \end{array} \right\| = 0.49$$

SS-EN 1993-1-1 Table 6.2, buckling around z-z

$l_{cr.span} = 6\ m$ Distance between the cross-beams

$b_f := b_{tf}(X_{check\_m\_span}) = 490\ mm$ Width of top flange

$t_f := t_{tf}(X_{check\_m\_span}) = 32\ mm$ Thickness of top flange

$f_{yt} := f_{ytf}(X_{check\_m\_span}) = 345\ MPa$ Proof strength

$I_{zf} := \frac{b_f^{3} \cdot t_f}{12} = 0.00031\ m^4$ Moment of inertia of the compressed flange

$N_{cr.LT\_t} := \frac{\pi^2 \cdot E_s \cdot I_{zf}}{l_{cr.span}^{2}} = 18062\ kN$

$\lambda_{LT\_t} := \sqrt{\frac{b_f \cdot t_f \cdot f_{ytf}(X_{check\_m\_span})}{N_{cr.LT\_t}}} = 0.547$

$\Phi_{LT\_t} := 0.5 \cdot \left(1 + \alpha_{LT} \cdot (\lambda_{LT\_t} - 0.2) + \lambda_{LT\_t}^{2}\right) = 0.73$

$\chi_{LT\_t} := min\left(\frac{1}{\Phi_{LT\_t} + \sqrt{\Phi_{LT\_t}^{2} - \lambda_{LT\_t}^{2}}}, 1\right) = 0.816$ = $\chi_{LT}(X_{check\_m\_span}) = 0.816$

SS-EN 1993-1-1 6.3.1.2 Equation 6.49

$h_{w\_t} := h_w(X_{check\_m\_span}) = 1178\ mm$ Height of web

$t_b := t_{bf}(X_{check\_m\_span}) = 40\ mm$ Thickness of bottom flange

$k_{fl} := 1.1$ Increase in capacity due to simplified method used, SS-EN 1993-1-1 6.3.2.4 (2)B

$$M_{Rd.t.LT\_t} := \frac{b_f \cdot t_f \cdot k_{fl} \cdot \chi_{LT\_t} \cdot f_{yt}}{\gamma_{M1}} \left(h_{w\_t} + \frac{t_f + t_b}{2}\right) = 5896\ kN \cdot m$$ = $M_{Rd.t.LT}(X_{check\_m\_span}) = 5896\ kN \cdot m$

Compressed bottom flange over support

The buckling capacity of the compressed flange is calculated according to to SS-EN 1993-1-1 6.3.1.2.

$$\alpha_{LT} := \left\| \begin{array}{l} \text{if } t_{bf}\left(X_{check\_m\_midsup}\right) \le 40\ mm \\ \quad \| \ 0.49 \\ \text{else if } t_{bf}\left(X_{check\_m\_midsup}\right) > 40\ mm \\ \quad \| \ 0.76 \end{array} \right\| = 0.49$$

SS-EN 1993-1-1 Table 6.2, buckling around z-z

$l_{cr.support} = 4\ m$ — Distance between the cross-beams

$b_f := b_{bf}\left(X_{check\_m\_midsup}\right) = 740\ mm$ — Width of bottom flange

$t_f := t_{bf}\left(X_{check\_m\_midsup}\right) = 40\ mm$ — Thickness of bottom flange

$E_s = 210\ GPa$ — Modulus of elasticity

$f_{yb} := f_{ybf}\left(X_{check\_m\_midsup}\right) = 345\ MPa$ — Proof strength

$$I_{zf} := \frac{b_f^{\,3} \cdot t_f}{12} = 0.001\ m^4$$

Moment of inertia of the compressed flange

$$N_{crLT} := \frac{\pi^2 \cdot E_s \cdot I_{zf}}{l_{cr.support}^{\,2}} = 174974\ kN$$

Critical buckling load

$$\lambda_{LT\_l} := \sqrt{\frac{b_f \cdot t_f \cdot f_{yb}}{N_{crLT}}} = 0.242$$

$$\Phi_{LT\_l} := 0.5 \cdot \left(1 + \alpha_{LT} \cdot \left(\lambda_{LT\_l} - 0.2\right) + \lambda_{LT\_l}^{\,2}\right) = 0.54$$

$$\chi_{LT\_l} := min\left(\frac{1}{\Phi_{LT\_l} + \sqrt{\Phi_{LT\_l}^{\,2} - \lambda_{LT\_l}^{\,2}}}, 1\right) = 0.979 \quad = \quad \chi_{LT.b}\left(X_{check\_m\_midsup}\right) = 0.979$$

SS-EN 1993-1-1 6.3.1.2 Equation 6.49

$h_{w\_l} := h_w\left(X_{check\_m\_midsup}\right) = 1185\ mm$ — Height of web

$t_t := t_{tf}\left(X_{check\_m\_midsup}\right) = 25\ mm$ — Thickness of top flange

$k_{fl} := 1.1$ — Increase in capacity due to simlified method used, SS-EN 1993-1-1 6.3.2.4 (2)B

$$M_{Rd.b.LT\_l} := \frac{b_f \cdot t_f \cdot k_{fl} \cdot \chi_{LT\_l} \cdot f_{yb}}{\gamma_{M1}} \left(h_{w\_l} + \frac{t_t + t_f}{2}\right) = 13387\ kN \cdot m \quad = \quad M_{Rd.b.LT}\left(X_{check\_m\_midsup}\right) = 13387\ kN \cdot m$$

4.4.1 Check of lateral torsional buckling

$M_{Rd.t.LT}(X)$	Capacity of the top flange against LT- buckling during casting
$M_{Rd.b.LT}(X)$	Capacity of the bottom flange against LT- buckling during casting
$M_{d.ULS.max}(X)$	Load effects during casting
$M_{d.ULS.min}(X)$	Load effects during casting

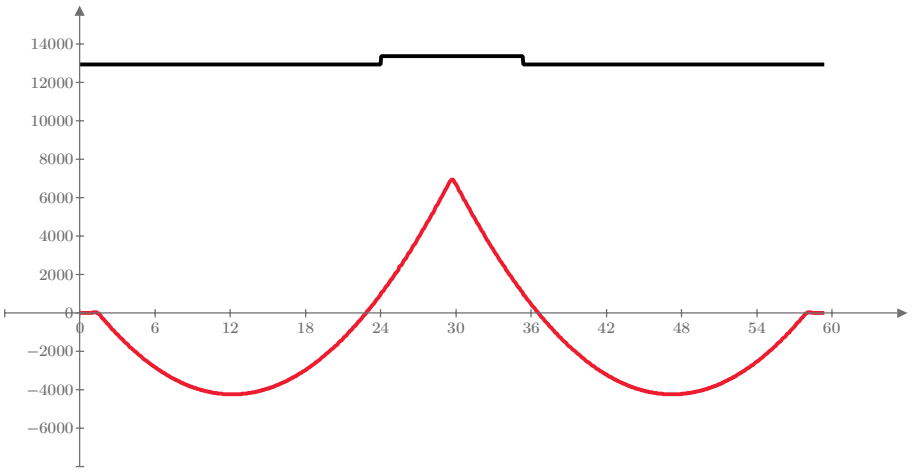

$M_{d.ULS.LC2}(X)\ \ (kN \cdot m)$

$M_{Rd.b.LT}(X)\ \ (kN \cdot m)$

$X\ \ (m)$

$$\eta_{max} := max\left(\frac{M_{d.ULS.LC2}(X)}{M_{Rd.b.LT}(X)}\right) = 52\%$$

Utilization rate of the bottom flange regarding LT-buckling over support during casting

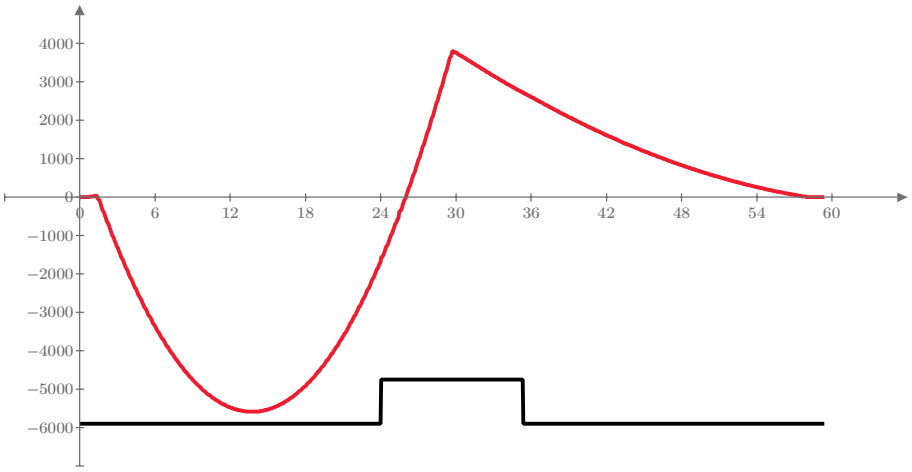

$M_{d.ULS.LC1}(X)\ \ (kN \cdot m)$

$-M_{Rd.t.LT}(X)\ \ (kN \cdot m)$

$X\ \ (m)$

$$\eta_{min} := max\left(\frac{M_{d.ULS.LC1}(X)}{-M_{Rd.t.LT}(X)}\right) = 95\%$$

Utilization rate of the top flange regarding LT-buckling in span during casting

4.5 Stresses in steel cross-section

The stresses in the top and bottom flange from loads during construction are compared to the yield strength of steel girders to verify that the steel girders can withstand the stresses alone before composite action with concrete is achieved.

Top flange, in span

$M := M_{d.ULS.LC1}\left(X_{check\_m\_span}\right) = -5582\ kN \cdot m$ Load effect at midspan

$I := I_{y.steel}\left(X_{check\_m\_span}\right) = 0.018\ m^4$ Moment of inertia at midspan

$z := \left(t_{deck} + \frac{t_{tf}\left(X_{check\_m\_span}\right)}{2}\right) - z_{tp.steel}\left(X_{check\_m\_span}\right) = -0.732\ m$ Centre of gravity at midspan maesured from the top of the concrete deck

$\sigma := \frac{M}{I} \cdot z = 232\ MPa$ = $\sigma_{stf\_ULS\_cast}\left(X_{check\_m\_span}\right) = 232\ MPa$

$\sigma_{stf\_ULS\_cast}(X)$ Stresses in the top flange during casting stage.

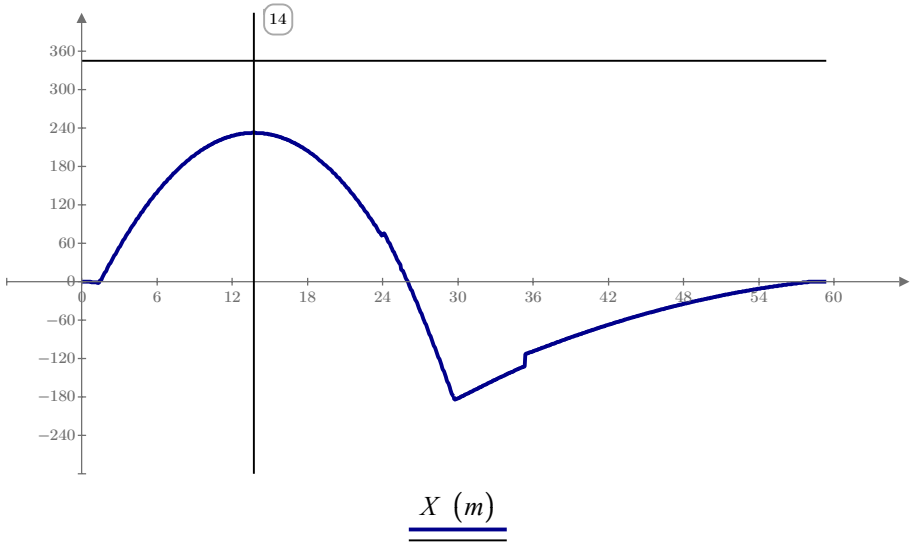

$\eta_{max} := max\left(\frac{\sigma_{stf\_ULS\_cast}(X)}{f_{ytf}(X)}\right) = 67\%$

Bottom flange, in span

$M := M_{d.ULS.LC1}\left(X_{check\_m\_span}\right) = -5582\ kN \cdot m$ Load effect at midspan

$I := I_{y.steel}\left(X_{check\_m\_span}\right) = 0.018\ m^4$ Moment of inertia at midspan

$z := t_{deck} + h_{beam}\left(X_{check\_m\_span}\right) - \frac{t_{bf}\left(X_{check\_m\_span}\right)}{2} - z_{tp.steel}\left(X_{check\_m\_span}\right) = 0.482\ m$ Centre of gravity at midspan measured from the top of concrete deck

$\sigma := \frac{M}{I} \cdot z = -153\ MPa$ = $\sigma_{sbf\_ULS\_cast}\left(X_{check\_m\_span}\right) = -153\ MPa$

$\sigma_{sbf\_ULS\_cast}(X)$ Stresses in the bottom flange during casting stage.

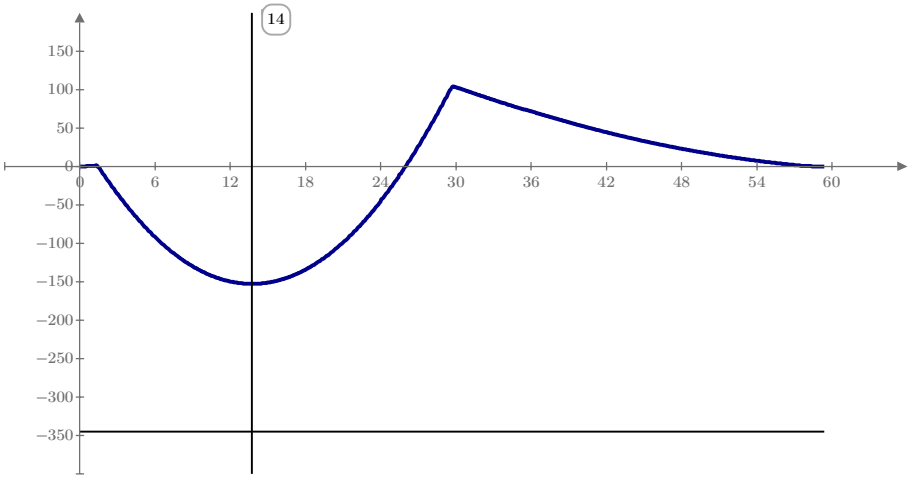

$\sigma_{sbf\_ULS\_cast}(X)\ \ (MPa)$

$-f_{ybf}(X)\ \ (MPa)$

$X\ \ (m)$

$\eta_{max} := max\left(\frac{\sigma_{sbf\_ULS\_cast}(X)}{-f_{ybf}(X)}\right) = 44\%$

Top flange, over midsupport

$M := M_{d.ULS.LC2}\left(X_{check\_m\_midsup}\right) = 6990\ kN \cdot m$ Load effect over midsupport

$I := I_{y.steel}\left(X_{check\_m\_midsup}\right) = 0.016\ m^4$ Moment of inertia at midsupport

$z := \left(t_{deck} + \frac{t_{tf}\left(X_{check\_m\_midsup}\right)}{2}\right) - z_{tp.steel}\left(X_{check\_m\_midsup}\right) = -0.778\ m$ Centre of gravity at midsupport measured from the top of the concrete deck

$\sigma := \frac{M}{I} \cdot z = -338\ MPa$ = $\sigma_{stf\_ULS\_cast}\left(X_{check\_m\_midsup}\right) = -338\ MPa$

$\sigma_{stf\_ULS\_cast}(X)$ Stresses in the top flange during casting stage.

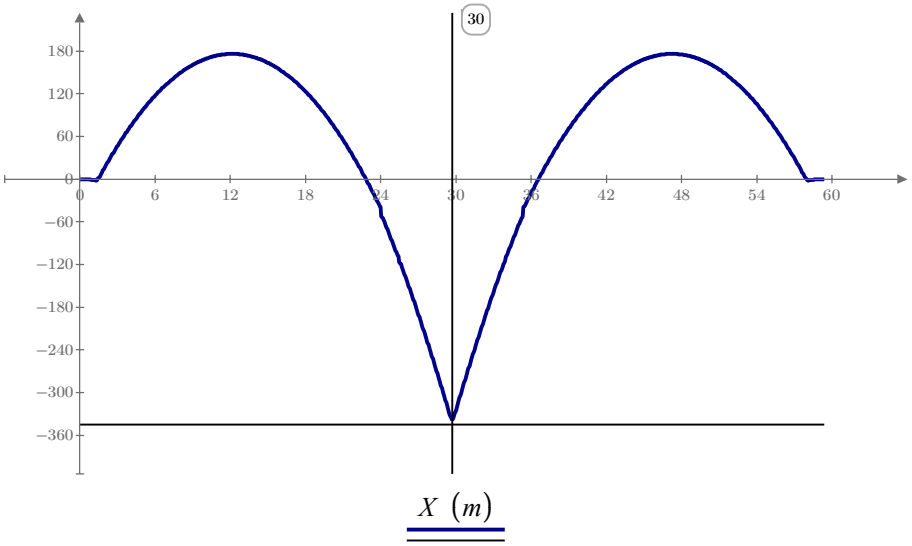

$\sigma_{stf\_ULS\_cast}(X)\ (MPa)$

$-f_{ytf}(X)\ (MPa)$

$\eta_{max} := max\left(\frac{\sigma_{stf\_ULS\_cast}(X)}{-f_{ytf}(X)}\right) = 98\%$

Bottom flange, over midsupport

$M := M_{d.ULS.LC2}\left(X_{check\_m\_midsup}\right) = 6990\ kN \cdot m$ Load effect over midsupport

$I := I_{y.steel}\left(X_{check\_m\_midsup}\right) = 0.016\ m^4$ Moment of inertia at midsupport

$z := t_{deck} + h_{beam}\left(X_{check\_m\_midsup}\right) - \frac{t_{bf}\left(X_{check\_m\_midsup}\right)}{2} - z_{tp.steel}\left(X_{check\_m\_midsup}\right) = 0.439\ m$ Centre of gravity at midsupport measured from the top of the concrete deck

$\sigma := \frac{M}{I} \cdot z = 191\ MPa$ = $\sigma_{sbf\_ULS\_cast}\left(X_{check\_m\_midsup}\right) = 191\ MPa$

$\sigma_{sbf\_ULS\_cast}(X)$ Stresses in the bottom flange during casting stage.

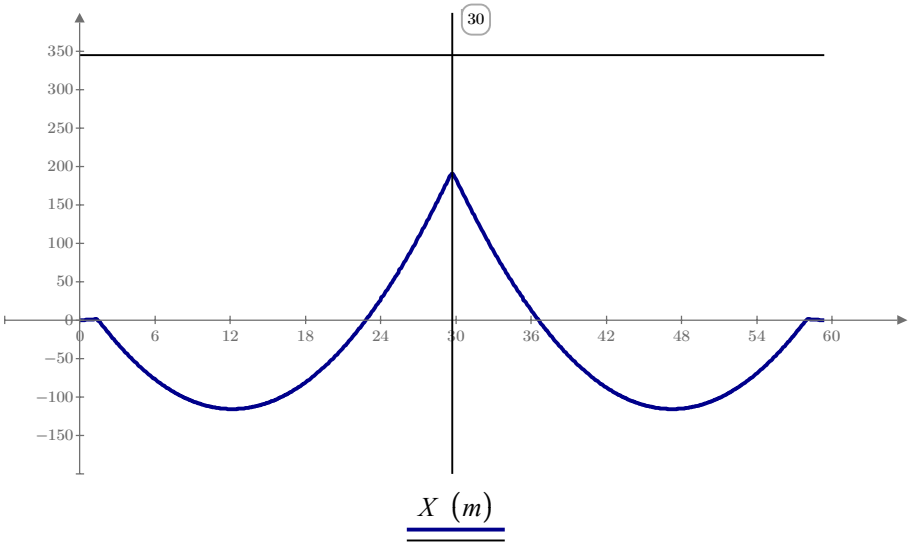

$\sigma_{sbf\_ULS\_cast}(X)\ (MPa)$

$f_{ybf}(X)\ (MPa)$

$\eta_{max} := max\left(\frac{\sigma_{sbf\_ULS\_cast}(X)}{f_{ybf}(X)}\right) = 55\%$

5 Capacity checks - Ultimate limit state, global

The capacity checks that are to be carried out are bending moment capacity, shear capacity and the capacity of welds.
Because the checks are performed by using vectors and closed areas, controll-caluclations are showed for the governing coordinates. Critical points are presented in blue below:

$X_{check\_m\_midsup} = 29.7\ m$ Coordinate for control calculations - bending moment over midsupport

$X_{check\_m\_span} = 13.246\ m$ Coordinate for control calculations - bending moment in span

$X_{check\_v\_endsup} = 1.4\ m$ Coordinate for control calculations - shear force over end support

$X_{check\_v\_midsup} = 29.7\ m$ Coordinate for control calculations - shear force over midsupport

5.1 Load Combinations

The loads should be combined according to STR/GEO and 6.10a or 6.10b dependent on which case gives the worst load effects. The load combinations are presented below.

6.10a, all parts in CSC1 or 2

Permanent loads	sup	inf	Unfavorable	Favorable
Self-weight	1.0	1.0	$\gamma_d \cdot 1.35 \cdot sup$	$1.0 \cdot inf$
Surfacing	1.1	0.9	$\gamma_d \cdot 1.35 \cdot sup$	$1.0 \cdot inf$
1st Shrinkage	1.0	1.0	$\gamma_d \cdot 1.35 \cdot sup$	$1.0 \cdot inf$
2nd Shrinkage	1.0	1.0	$\gamma_d \cdot 0.0 \cdot sup$	$0.0 \cdot inf$
2nd Creep	1.0	1.0	$\gamma_d \cdot 0.0 \cdot sup$	$0.0 \cdot inf$
Variable loads	Ψ_0		**Main load**	**Other load**
Traffic loads	0.75		$\gamma_d \cdot 1.5 \cdot \Psi_0$	$\gamma_d \cdot 1.5 \cdot \Psi_0$
Acceleration	0.75		$\gamma_d \cdot 1.5 \cdot 0.6 \cdot \Psi_0$	$\gamma_d \cdot 1.5 \cdot \Psi_0$
Temperature	0.6		$\gamma_d \cdot 0.0 \cdot \Psi_0$	$\gamma_d \cdot 0.0 \cdot \Psi_0$

6.10a, some parts in CSC3 or 4

Permanent loads	sup	inf	Unfavorable	Favorable
Self-weight	1.0	1.0	$\gamma_d \cdot 1.35 \cdot sup$	$1.0 \cdot inf$
Surfacing	1.1	0.9	$\gamma_d \cdot 1.35 \cdot sup$	$1.0 \cdot inf$
1st Shrinkage	1.0	1.0	$\gamma_d \cdot 1.35 \cdot sup$	$1.0 \cdot inf$
2nd Shrinkage	1.0	1.0	$\gamma_d \cdot 1.0 \cdot sup$	$1.0 \cdot inf$
2nd Creep	1.0	1.0	$\gamma_d \cdot 1.35 \cdot sup$	$1.0 \cdot inf$
Variable loads	Ψ_0		**Main load**	**Other load**
Traffic loads	0.75		$\gamma_d \cdot 1.5 \cdot \Psi_0$	$\gamma_d \cdot 1.5 \cdot \Psi_0$
Acceleration	0.75		$\gamma_d \cdot 1.5 \cdot 0.6 \cdot \Psi_0$	$\gamma_d \cdot 1.5 \cdot \Psi_0$
Temperature	0.6		$\gamma_d \cdot 1.5 \cdot \Psi_0$	$\gamma_d \cdot 1.5 \cdot \Psi_0$

6.10b, all parts in CSC1 or 2

Permanent loads	sup	inf	Unfavorable	Favorable
Self-weight	1.0	1.0	$\gamma_d \cdot 0.89 \cdot 1.35 \cdot sup$	$1.0 \cdot inf$
Surfacing	1.1	0.9	$\gamma_d \cdot 0.89 \cdot 1.35 \cdot sup$	$1.0 \cdot inf$
1st Shrinkage	1.0	1.0	$\gamma_d \cdot 0.89 \cdot 1.35 \cdot sup$	$0.0 \cdot inf$
2nd Shrinkage	1.0	1.0	$\gamma_d \cdot 0.0 \cdot sup$	$0.0 \cdot inf$
2nd Creep	1.0	1.0	$\gamma_d \cdot 0.0 \cdot sup$	$0.0 \cdot inf$
Variable loads	Ψ_0		**Main load**	**Other load**
Traffic loads	0.75		$\gamma_d \cdot 1.5$	$\gamma_d \cdot 1.5 \cdot \Psi_0$
Acceleration	0.75		$\gamma_d \cdot 1.5 \cdot 0.6$	$\gamma_d \cdot 1.5 \cdot \Psi_0$
Temperature	0.6		$\gamma_d \cdot 0.0$	$\gamma_d \cdot 0.0 \cdot \Psi_0$

6.10b, some parts in CSC3 or 4

Permanent loads	sup	inf	Unfavorable	Favorable
Self-weight	1.0	1.0	$\gamma_d \cdot 0.89 \cdot 1.35 \cdot sup$	$1.0 \cdot inf$
Surfacing	1.1	0.9	$\gamma_d \cdot 0.89 \cdot 1.35 \cdot sup$	$1.0 \cdot inf$
1st Shrinkage	1.0	1.0	$\gamma_d \cdot 0.89 \cdot 1.35 \cdot sup$	$1.0 \cdot inf$
2nd Shrinkage	1.0	1.0	$\gamma_d \cdot 1.0 \cdot sup$	$1.0 \cdot inf$
2nd Creep	1.0	1.0	$\gamma_d \cdot 0.89 \cdot 1.35 \cdot sup$	$1.0 \cdot inf$
Variable loads	Ψ_0		**Main load**	**Other load**
Traffic loads	0.75		$\gamma_d \cdot 1.5$	$\gamma_d \cdot 1.5 \cdot \Psi_0$
Acceleration	0.75		$\gamma_d \cdot 1.5 \cdot 0.6$	$\gamma_d \cdot 1.5 \cdot \Psi_0$
Temperature	0.6		$\gamma_d \cdot 1.5$	$\gamma_d \cdot 1.5 \cdot \Psi_0$

5.1.1 Bending moment

Bending moment in the ultimate limit state

$M_{d.ULS.6.10a}(x)$ Design bending moment effect from all loads, combined according to STR/GEO 6.10a

$M_{d.ULS.6.10b}(x)$ Design bending moment effect from all loads, combined according to STR/GEO 6.10b

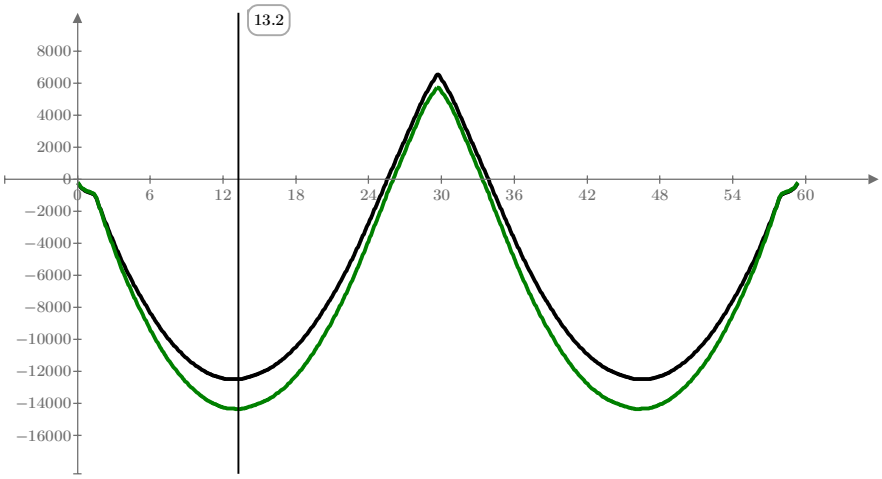

$X\ (m)$

$M_{d.ULS.6.10a.span}(X)\ (m \cdot kN)$

$M_{d.ULS.6.10b.span}(X)\ (kN \cdot m)$

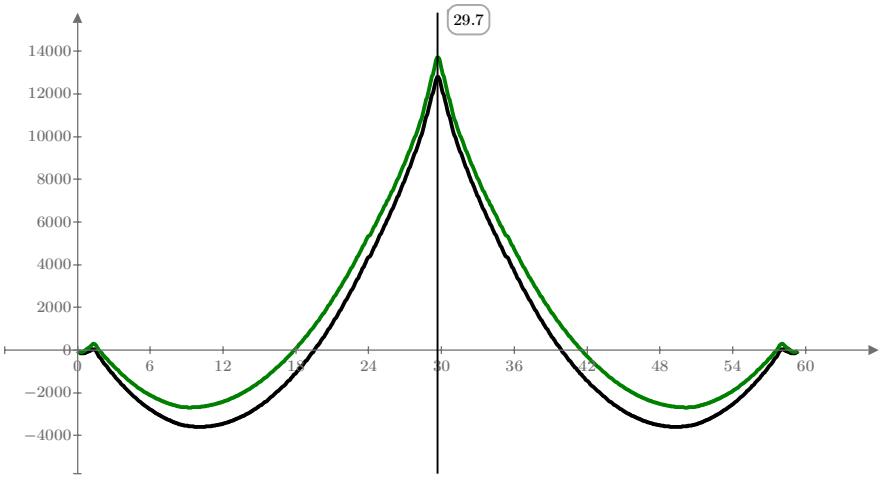

$X\ (m)$

$M_{d.ULS.6.10a.midsup}(X)\ (m \cdot kN)$

$M_{d.ULS.6.10b.midsup}(X)\ (kN \cdot m)$

The load combination according to STR/GEO 6.10b gives the dimensioning bending moment and will therefore be used for the capacity calculations.

$LoadComb := \text{“6.10b”}$ Load combination that gives worst load effects

5.2 Load Effects

Loads that give unfavorable moment in span

$M_{d.perm}(x)$ Bending moment from permanent loads

$M_{d.min.tr}(x)$ Bending moment from min traffic loads

$M_{d.temp.min}(x)$ Bending moment from min temperature loads

$M_{d.1.cs}(x)$ Bending moment from first order effects from shrinkage

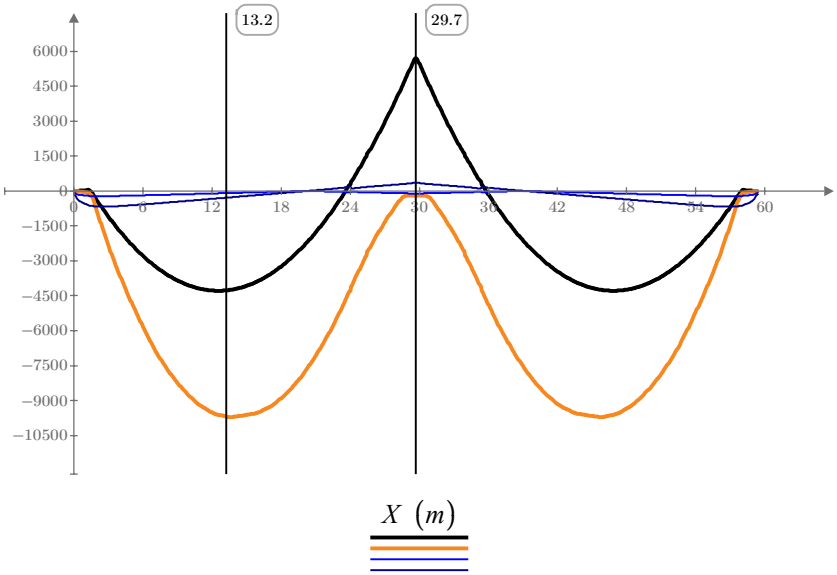

Loads that give unfavorable moment over support

Second order effects from creep and both first and second order effects from shrinkage will only be acconted for when it gives an unfavorable effects in the capacity checks, i.e over the supports regions.

$M_{d.perm}(x)$	Bending moment from permanent loads
$M_{d.max.tr}(x)$	Bending moment from max traffic loads
$M_{d.temp.max}(x)$	Bending moment from max temperature loads
$M_{d.1.cs}(x)$	Bending moment from first order effects from shrinkage
$M_{d.2.cs}(x)$	Bending moment from second order effects from shrinkage
$M_{d.creep}(x)$	Bending moment from second order effects from creep

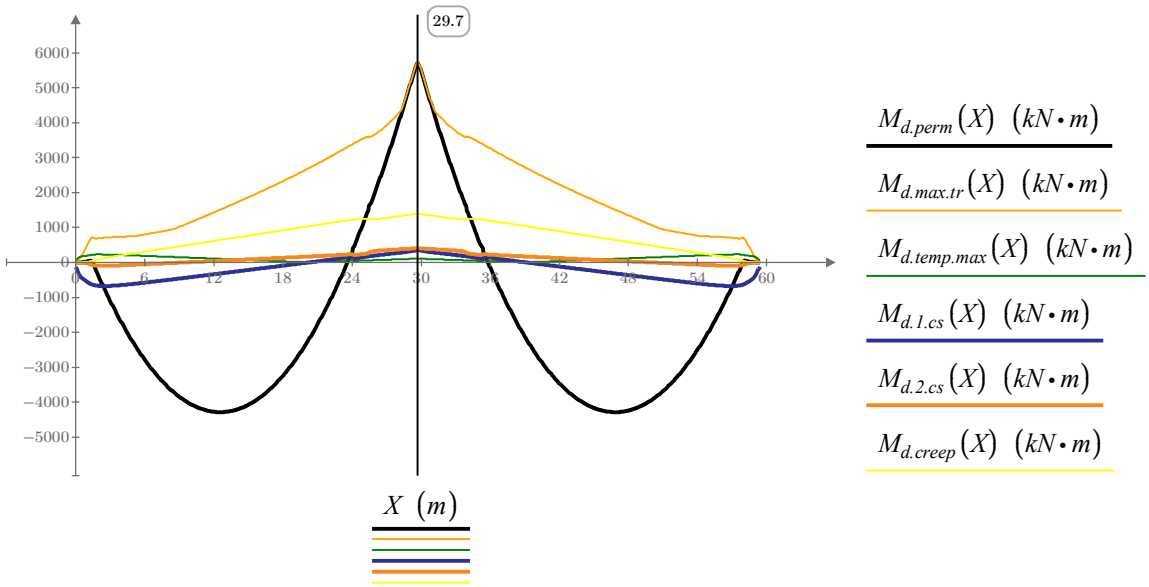

Axial force in the ultimate limit state

$N_{d.perm}(x)$	Normal force from permanent loads
$N_{d.min.tr}(x)$	Min normal force from multi components loads
$N_{d.max.tr}(x)$	Max normal force from multi components loads
$N_{d.temp.min}(x)$	Min normal force from temperature loads
$N_{d.temp.max}(x)$	Max normal force from temperature loads
$N_{d.1.cs}(x)$	Normal force from shrinkage

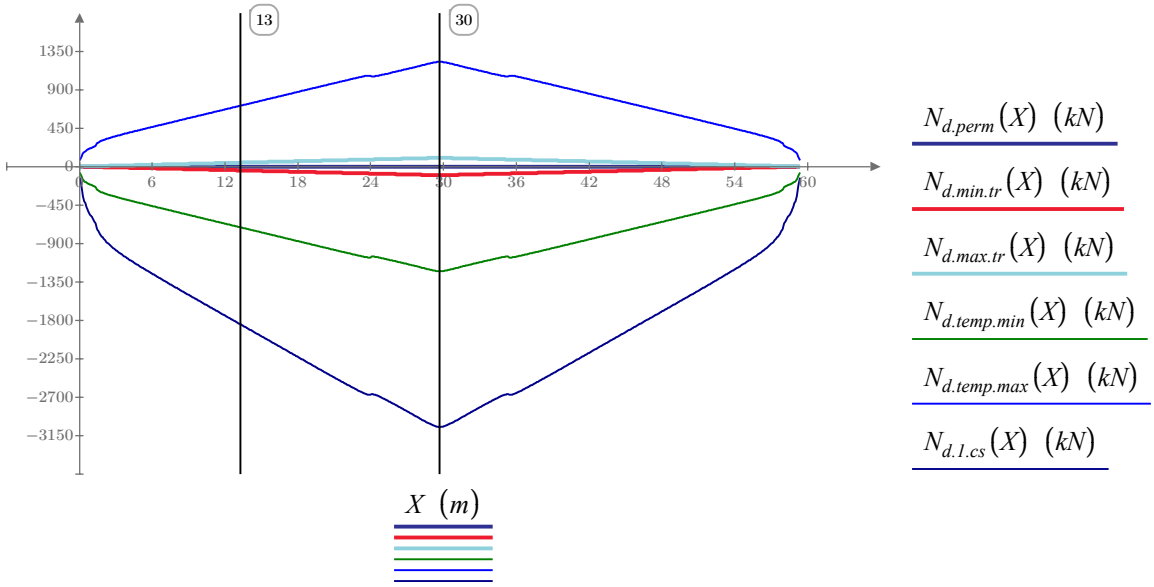

Shear force in the ultimate limit state

$V_{d.per}(x)$ Shear force from permanent loads

$V_{d.tr}(x)$ Shear force from multi components loads

$V_{d.temp}(x)$ Shear force from temperature loads

$V_{d.cs}(x)$ Shear force from shrinkage

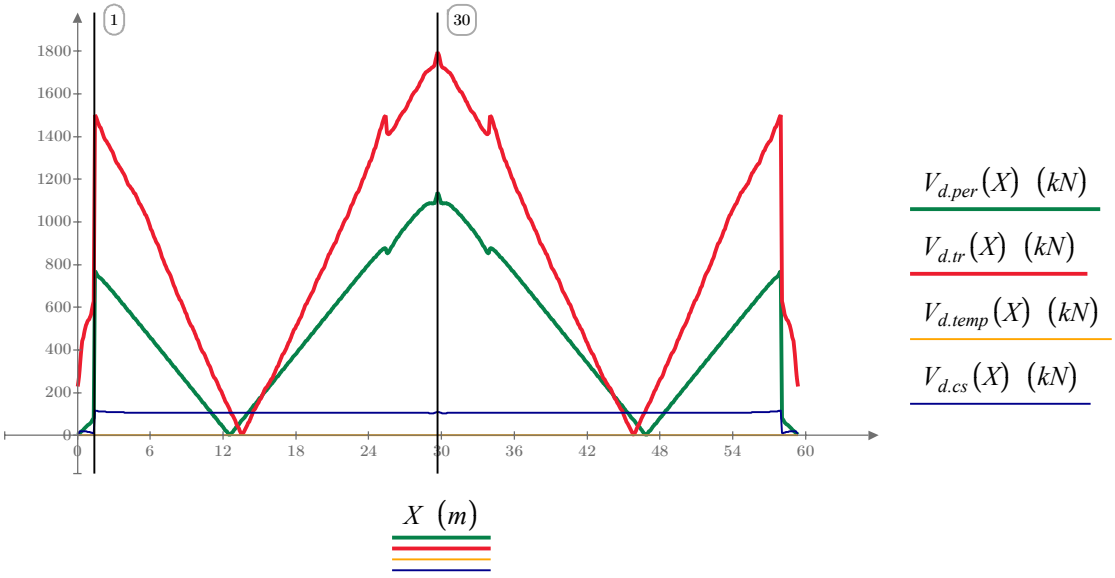

$$V_{d.ULS}(x) := \overrightarrow{V_{d.per}(x) + V_{d.tr}(x) + V_{d.temp}(x) + V_{d.cs}(x)}$$

$V_{d.ULS}(X_{check\_v\_endsup}) = 2391\ kN$ Maximum shear force over end support

$V_{d.ULS}(X_{check\_v\_midsup}) = 3041\ kN$ Maximum shear force over mid support

Second order effects in the ultimate limit state

The second order effects from shrinkage and creep that arises due to the continuous system have an unfavourable effect over the internal support. These effects will therefore only be accounted for when calculating the capacity of the cross section over support and not in span. The moment and normal force from the second order effects are plotted below.

$M_{d.creep}(x)$ Moment from second order effects of creep (Appendix X)

$M_{d.2.cs}(x)$ Moment from second order effects of shrinkage (Appendix X)

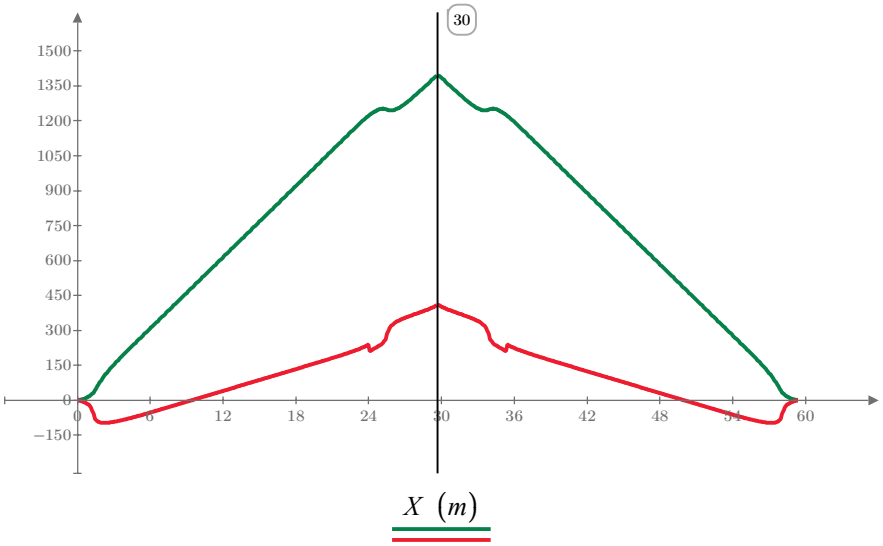

$M_{d.creep}(X)\ (kN \cdot m)$

$M_{d.2.cs}(X)\ (kN \cdot m)$

$N_{d.creep}(x)$ Normal force from second order effects of creep (Appendix X)

$N_{d.2.cs}(x)$ Normal force from second order effects of shrinkage (Appendix X)

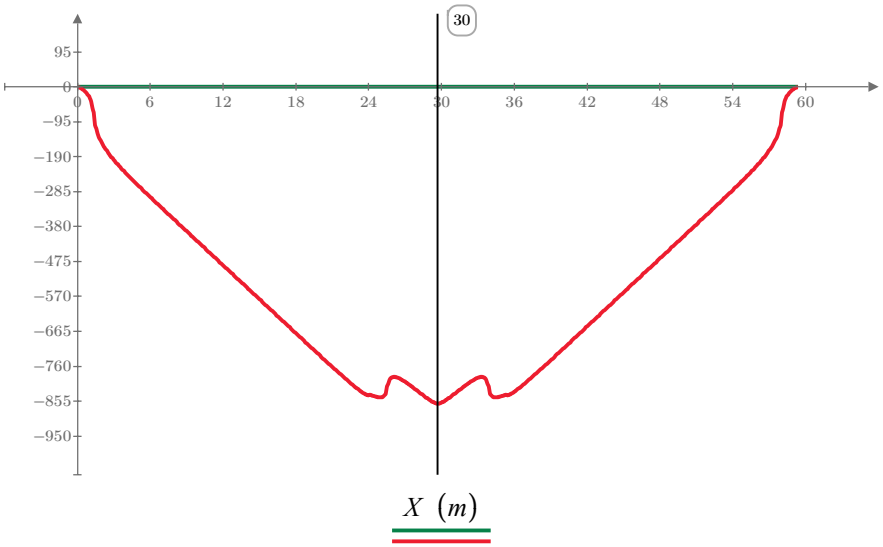

$N_{d.creep}(X)\ (kN)$

$N_{d.2.cs}(X)\ (kN)$

5.3 Cross-sectional constants

Effective concrete width along the bridge

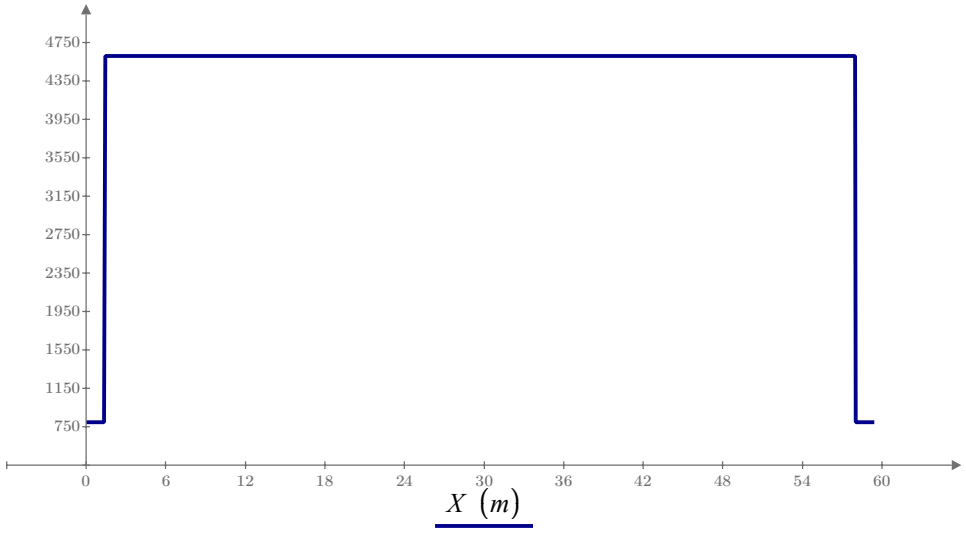

$b_{eff.c}(X)\ (mm)$

Effective with of top flange along the bridge with reduction due to shear lag

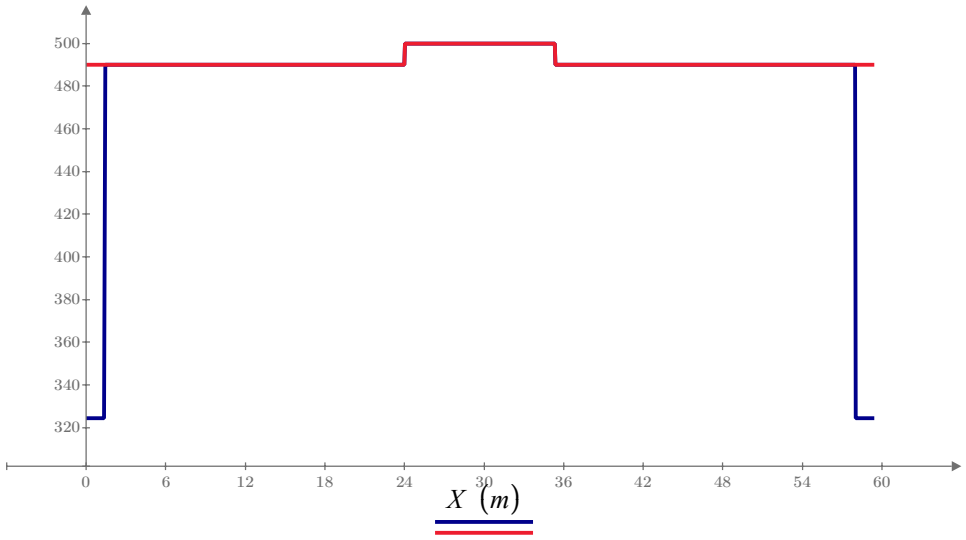

$b_{eff.s}(X)\ (mm)$

$b_{tf}(X)\ (mm)$

Effective reinforcement area where the concrete is considered as cracked

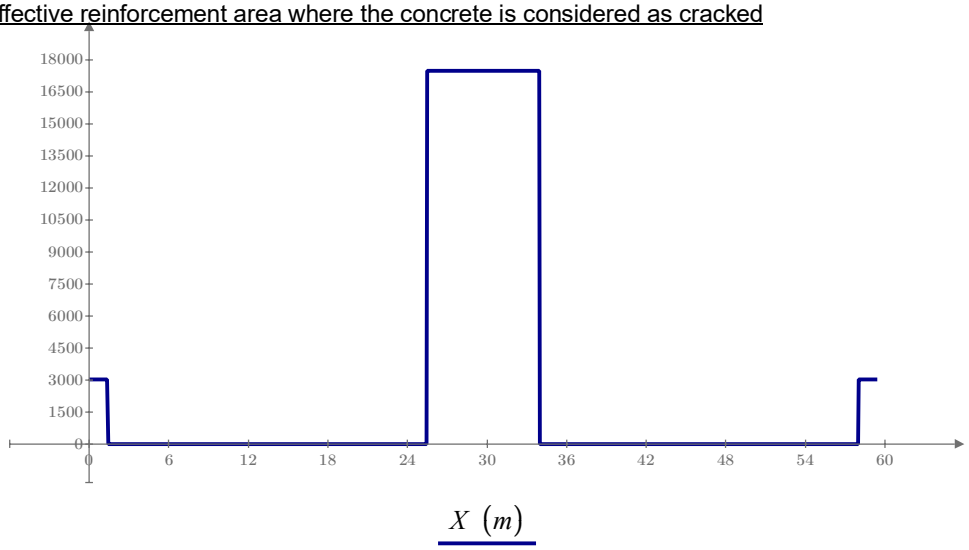

$A_{re}(X)\ (mm^2)$

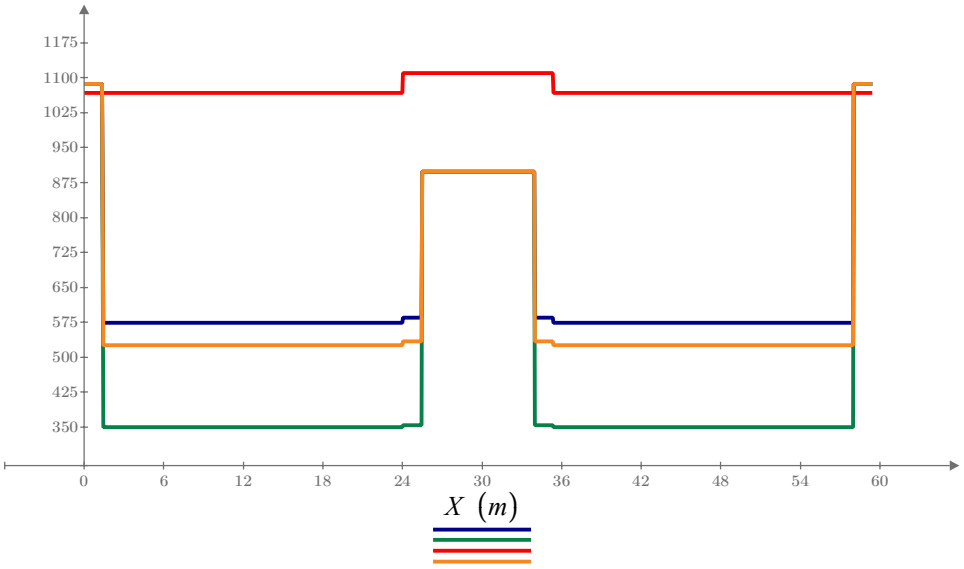

$z_{tp.comp.long}(X)\ \ (mm)$

$z_{tp.comp.short}(X)\ \ (mm)$

$z_{tp.steel}(X)\ \ (mm)$

$z_{tp.comp.cs}(X)\ \ (mm)$

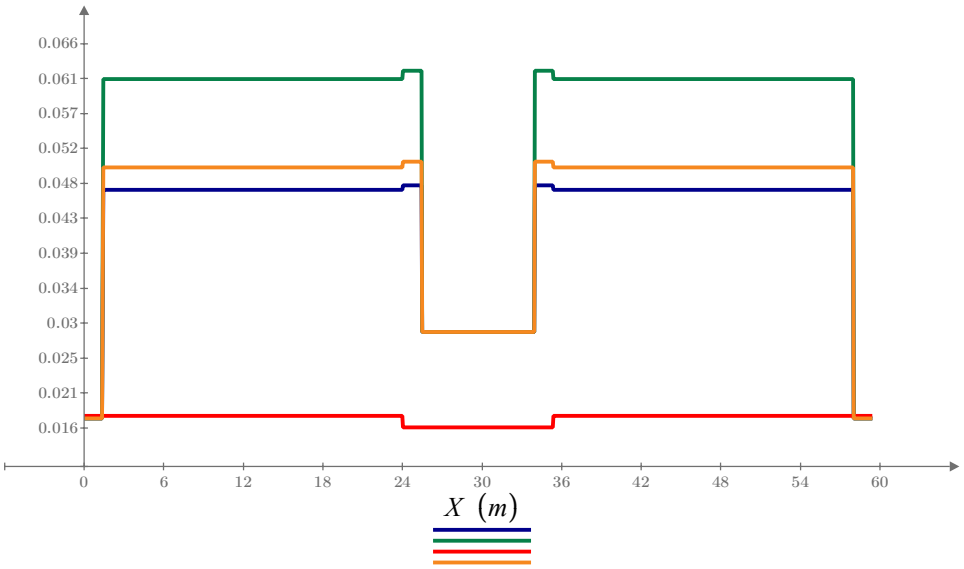

$I_{y.comp.long}(X)\ \ (m^4)$

$I_{y.comp.short}(X)\ \ (m^4)$

$I_{y.steel}(X)\ \ (m^4)$

$I_{y.comp.cs}(X)\ \ (m^4)$

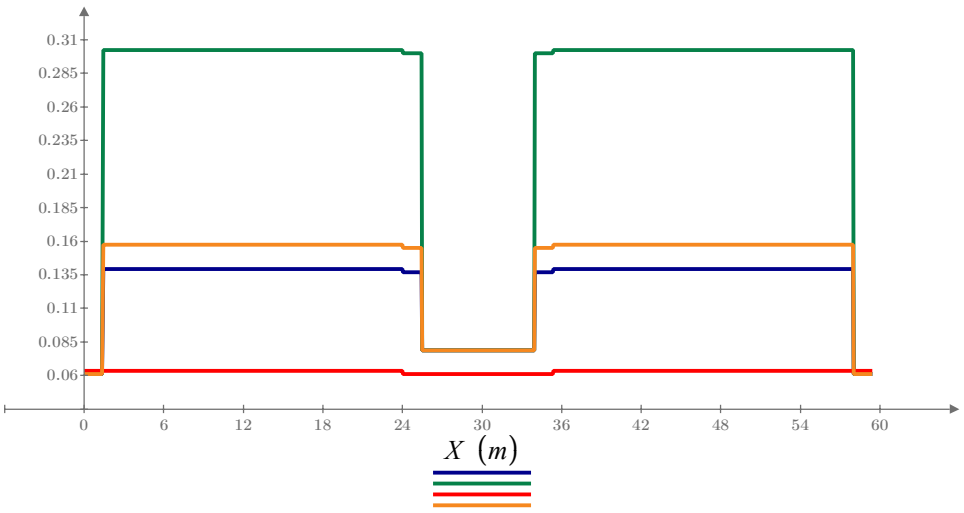

$A_{comp.long}(X)\ \ (m^2)$

$A_{comp.short}(X)\ \ (m^2)$

$A_{steel}(X)\ \ (m^2)$

$A_{comp.cs}(X)\ \ (m^2)$

The cross-sectional constants are checked at two locations, one in span and one over the internal support in order to verify the constants in the graphs above.

Span section

At this location, the concrete deck is assumed to be uncracked and composite action is obtained between the concrete and the steel girders.

$b_{ef.con} := b_{eff.c}\left(X_{check\_m\_span}\right) = 4611\ mm$ — Effective width of concrete deck

$A_{ef.con} := b_{ef.con} \cdot t_{deck} = 1.476\ m^2$ — Effective area of concrete deck

$I_{y.ef.con} := \frac{b_{ef.con} \cdot t_{deck}^{3}}{12} = 0.013\ m^4$ — Effective moment of inertia around y-axis

$I_{z.ef.con} := \frac{b_{ef.con}^{3} \cdot t_{deck}}{12} = 2.615\ m^4$ — Effective moment of inertia around z-axis

$b_{ef.steel} := b_{eff.s}\left(X_{check\_m\_span}\right) = 490\ mm$ — Effective width of steel top flange with with regard to shear lag

$bfb := b_{bf}\left(X_{check\_m\_span}\right) = 720\ mm$ — Width of bottom flange

$tfb := t_{bf}\left(X_{check\_m\_span}\right) = 40\ mm$ — Thickness of bottom flange

$tft := t_{tf}\left(X_{check\_m\_span}\right) = 32\ mm$ — Thickness of top flange

$hw := h_w\left(X_{check\_m\_span}\right) = 1178\ mm$ — Web height

$tw := t_w\left(X_{check\_m\_span}\right) = 16\ mm$ — Web thickness

$h := h_{beam}\left(X_{check\_m\_span}\right) = 1250\ mm$ — Height of beam

Steel cross-section

$A_s := b_{ef.steel} \cdot tft + tw \cdot hw + bfb \cdot tfb = 0.063\ m^2$

$A_{steel}\left(X_{check\_m\_span}\right) = 0.063\ m^2$

$$z_{tp.s} := \frac{b_{ef.steel} \cdot tft \cdot \left(t_{deck} + \frac{tft}{2}\right) + hw \cdot tw \cdot \left(t_{deck} + tft + \frac{hw}{2}\right) + bfb \cdot tfb \cdot \left(t_{deck} + tft + hw + \frac{tfb}{2}\right)}{A_s} = 1068\ mm$$

$z_{tp.steel}\left(X_{check\_m\_span}\right) = 1068\ mm$

$$I_{y.s} := \frac{b_{ef.steel} \cdot tft^3}{12} + b_{ef.steel} \cdot tft \cdot \left(z_{tp.s} - t_{deck} - \frac{tft}{2}\right)^2 + \frac{bfb \cdot tfb^3}{12} + bfb \cdot tfb \cdot \left(t_{deck} + h - \frac{tfb}{2} - z_{tp.s}\right)^2 + \frac{tw \cdot hw^3}{12} + tw \cdot hw \cdot \left(t_{deck} + tft + \frac{hw}{2} - z_{tp.s}\right)^2 = 0.0176\ m^4$$

$I_{y.steel}\left(X_{check\_m\_span}\right) = 0.0176\ m^4$

$$I_{z.s} := \frac{b_{ef.steel}{}^3 \cdot tft}{12} + \frac{bfb^3 \cdot tfb}{12} + \frac{tw^3 \cdot hw}{12} = 0.00156\ m^4$$

$I_{z.steel}\left(X_{check\_m\_span}\right) = 0.00156\ m^4$

Short-term composite section

$n_{L.short} = 6.18$

$$A_{c.short} := \frac{A_{ef.con}}{n_{L.short}} + A_s = 0.302\ m^2$$

$A_{comp.short}\left(X_{check\_m\_span}\right) = 0.302\ m^2$

$$z_{tp.c.short} := \frac{A_s \cdot z_{tp.s} + \frac{A_{ef.con}}{n_{L.short}} \cdot \frac{t_{deck}}{2}}{A_{c.short}} = 350\ mm$$

$z_{tp.comp.short}\left(X_{check\_m\_span}\right) = 350\ mm$

$$I_{y.c.short} := I_{y.s} + \frac{I_{y.ef.con}}{n_{L.short}} + \frac{A_{ef.con}}{n_{L.short}} \cdot \left(z_{tp.c.short} - \frac{t_{deck}}{2}\right)^2 + A_s \cdot \left(z_{tp.s} - z_{tp.c.short}\right)^2 = 0.061\ m^4$$

$I_{y.comp.short}\left(X_{check\_m\_span}\right) = 0.061\ m^4$

$$I_{z.c.short} := I_{z.s} + \frac{I_{z.ef.con}}{n_{L.short}} = 0.425\ m^4$$

$I_{z.comp.short}\left(X_{check\_m\_span}\right) = 0.425\ m^4$

Long-term composite section

$n_{L.long} = 19.49$

$$A_{c.long} := \frac{A_{ef.con}}{n_{L.long}} + A_s = 0.139\ m^2$$

$A_{comp.long}\left(X_{check\_m\_span}\right) = 0.139\ m^2$

$$z_{tp.c.long} := \frac{A_s \cdot z_{tp.s} + \frac{A_{ef.con}}{n_{L.long}} \cdot \frac{t_{deck}}{2}}{A_{c.long}} = 574\ mm$$

$z_{tp.comp.long}\left(X_{check\_m\_span}\right) = 574\ mm$

$$I_{y.c.long} := I_{y.s} + \frac{I_{y.ef.con}}{n_{L.long}} + \frac{A_{ef.con}}{n_{L.long}} \cdot \left(z_{tp.c.long} - \frac{t_{deck}}{2}\right)^2 + A_s \cdot \left(z_{tp.s} - z_{tp.c.long}\right)^2 = 0.047\ m^4$$

$I_{y.comp.long}\left(X_{check\_m\_span}\right) = 0.047\ m^4$

$$I_{z.c.short} := I_{z.s} + \frac{I_{z.ef.con}}{n_{L.long}} = 0.136\ m^4$$

$I_{z.comp.long}\left(X_{check\_m\_span}\right) = 0.136\ m^4$

Shrinkage composite section

$n_{L.cs} = 15.71$

$$A_{c.cs} := \frac{A_{ef.con}}{n_{L.cs}} + A_s = 0.157\ m^2$$

$A_{comp.cs}\left(X_{check\_m\_span}\right) = 0.157\ m^2$

$$z_{tp.c.cs} := \frac{A_s \cdot z_{tp.s} + \frac{A_{ef.con}}{n_{L.cs}} \cdot \frac{t_{deck}}{2}}{A_{c.cs}} = 526\ mm$$

$z_{tp.comp.cs}\left(X_{check\_m\_span}\right) = 526\ mm$

$$I_{y.c.cs} := I_{y.s} + \frac{I_{y.ef.con}}{n_{L.cs}} + \frac{A_{ef.con}}{n_{L.cs}} \cdot \left(z_{tp.c.cs} - \frac{t_{deck}}{2}\right)^2 = 0.05\ m^4 + A_s \cdot \left(z_{tp.s} - z_{tp.c.cs}\right)^2$$

$I_{y.comp.cs}\left(X_{check\_m\_span}\right) = 0.05\ m^4$

$$I_{z.c.cs} := I_{z.s} + \frac{I_{z.ef.con}}{n_{L.cs}} = 0.168\ m^4$$

$I_{z.comp.cs}\left(X_{check\_m\_span}\right) = 0.168\ m^4$

Support section

Over the support, the concrete deck is assumed to be cracked and therefore composite action is obtained between the reinforcement and the steel girders.

$A_{rein} := A_{re}\left(X_{check\_m\_midsup}\right) = 17493\ mm^2$ — Reinforcement area over the support

$b_{ef.steel} := b_{eff.s}\left(X_{check\_m\_midsup}\right) = 500\ mm$ — Effective width of steel top flange with with regard to shear lag

$bfb := b_{bf}\left(X_{check\_m\_midsup}\right) = 740\ mm$ — Width of bottom flange

$tfb := t_{bf}\left(X_{check\_m\_midsup}\right) = 40\ mm$ — Thickness of bottom flange

$tft := t_{tf}\left(X_{check\_m\_midsup}\right) = 25\ mm$ — Thickness of top flange

$hw := h_w\left(X_{check\_m\_midsup}\right) = 1185\ mm$ — Height of top flange

$h := h_{beam}\left(X_{check\_m\_midsup}\right) = 1250\ mm$ — Height of beam

Steel cross-section

$$A_s := b_{ef.steel} \cdot tft + tw \cdot hw + bfb \cdot tfb = 0.061\ m^2$$

$$A_{steel}\left(X_{check\_m\_midsup}\right) = 0.061\ m^2$$

$$z_{tp.s} := \frac{b_{ef.steel} \cdot tft \cdot \left(t_{deck} + \frac{tft}{2}\right) + hw \cdot tw \cdot \left(t_{deck} + tft + \frac{hw}{2}\right) + bfb \cdot tfb \cdot \left(t_{deck} + tft + hw + \frac{tfb}{2}\right)}{A_s} = 1111\ mm$$

$$z_{tp.steel}\left(X_{check\_m\_midsup}\right) = 1111\ mm$$

$$I_{y.s} := \frac{b_{ef.steel} \cdot tft^3}{12} + b_{ef.steel} \cdot tft \cdot \left(z_{tp.s} - t_{deck} - \frac{tft}{2}\right)^2 = 0.0161\ m^4$$
$$+ \frac{bfb \cdot tfb^3}{12} + bfb \cdot tfb \cdot \left(t_{deck} + h - \frac{tfb}{2} - z_{tp.s}\right)^2$$
$$+ \frac{tw \cdot hw^3}{12} + tw \cdot hw \cdot \left(t_{deck} + tft + \frac{hw}{2} - z_{tp.s}\right)^2$$

$$I_{y.steel}\left(X_{check\_m\_midsup}\right) = 0.0161\ m^4$$

$$I_{z.s} := \frac{b_{ef.steel}^{\ 3} \cdot tft}{12} + \frac{bfb^3 \cdot tfb}{12} + \frac{tw^3 \cdot hw}{12} = 0.00161\ m^4$$

$$I_{z.steel}\left(X_{check\_m\_midsup}\right) = 0.00161\ m^4$$

Short-term composite section

$$n_{L.short} = 6.18$$

$$A_{c.short} := A_{rein} + A_s = 0.079\ m^2$$

$$A_{comp.short}\left(X_{check\_m\_midsup}\right) = 0.079\ m^2$$

$$z_{tp.c.short} := \frac{A_s \cdot z_{tp.s} + A_{rein} \cdot \frac{t_{deck}}{2}}{A_{c.short}} = 899\ mm$$

$$z_{tp.comp.short}\left(X_{check\_m\_midsup}\right) = 899\ mm$$

$$I_{y.c.short} := A_{rein} \cdot \left(z_{tp.c.short} - \frac{t_{deck}}{2}\right)^2 + I_{y.s} = 0.0284\ m^4$$
$$+ A_s \cdot \left(z_{tp.s} - z_{tp.c.short}\right)^2$$

$$I_{y.comp.short}\left(X_{check\_m\_midsup}\right) = 0.0284\ m^4$$

$$I_{z.c.short} := I_{z.s} = 0.00161\ m^4$$

$$I_{z.comp.short}\left(X_{check\_m\_midsup}\right) = 0.00161\ m^4$$

Long-term composite section

$n_{L.long} = 19.49$

$A_{c.long} := A_{rein} + A_s = 0.079\ m^2$ $\quad A_{comp.long}\left(X_{check\_m\_midsup}\right) = 0.079\ m^2$

$z_{tp.c.long} := \dfrac{A_s \cdot z_{tp.s} + A_{rein} \cdot \frac{t_{deck}}{2}}{A_{c.long}} = 899\ mm$ $\quad z_{tp.comp.long}\left(X_{check\_m\_midsup}\right) = 899\ mm$

$I_{y.c.long} := A_{rein} \cdot \left(z_{tp.c.long} - \frac{t_{deck}}{2}\right)^2 + I_{y.s} + A_s \cdot \left(z_{tp.s} - z_{tp.c.long}\right)^2 = 0.028\ m^4$ $\quad I_{y.comp.long}\left(X_{check\_m\_midsup}\right) = 0.028\ m^4$

$I_{z.c.short} := I_{z.s} = 0.00161\ m^4$ $\quad I_{z.comp.long}\left(X_{check\_m\_midsup}\right) = 0.00161\ m^4$

Shrinkage composite section

$n_{L.cs} = 15.71$

$A_{c.cs} := A_{rein} + A_s = 0.079\ m^2$ $\quad A_{comp.cs}\left(X_{check\_m\_midsup}\right) = 0.079\ m^2$

$z_{tp.c.cs} := \dfrac{A_s \cdot z_{tp.s} + A_{rein} \cdot \frac{t_{deck}}{2}}{A_{c.cs}} = 899\ mm$ $\quad z_{tp.comp.cs}\left(X_{check\_m\_midsup}\right) = 899\ mm$

$I_{y.c.cs} := A_{rein} \cdot \left(z_{tp.c.cs} - \frac{t_{deck}}{2}\right)^2 + I_{y.s} + A_s \cdot \left(z_{tp.s} - z_{tp.c.cs}\right)^2 = 0.0284\ m^4$ $\quad I_{y.comp.cs}\left(X_{check\_m\_midsup}\right) = 0.0284\ m^4$

$I_{z.c.cs} := I_{z.s} = 0.00161\ m^4$ $\quad I_{z.comp.cs}\left(X_{check\_m\_midsup}\right) = 0.00161\ m^4$

5.4 Stresses in steel cross-section over support

The stresses are calculated for each load with respective cross-sectional constants. The stresses are summarized by the superposition rule.

5.4.1 Stresses due to variable (short term) loads

5.4.1.1 Traffic loads

$M := M_{d.max.tr}\left(X_{check\_m\_midsup}\right) = 5758\ kN \cdot m$ Bending moment

$N := N_{d.max.tr}\left(X_{check\_m\_midsup}\right) = 101.526\ kN$ Normal force

$A := A_{comp.short}\left(X_{check\_m\_midsup}\right) = 0.079\ m^2$ Cross-sectional area

$I := I_{y.comp.short}\left(X_{check\_m\_midsup}\right) = 0.028\ m^4$ Moment of inertia

$z := z_{tp.comp.short}\left(X_{check\_m\_midsup}\right) = 899\ mm$ Center of gravity from top of concrete deck

$h := h_{beam}\left(X_{check\_m\_midsup}\right) = 1250\ mm$ Height of girder

$t_b := t_{bf}\left(X_{check\_m\_midsup}\right) = 40\ mm$ Thickness of bottom flange

$t_t := t_{tf}\left(X_{check\_m\_midsup}\right) = 25\ mm$ Thickness of top flange

$\sigma_{s.t} := \frac{N}{A} + \frac{M}{I} \cdot \left(t_{deck} - z\right) = -116.2\ MPa$ = $\sigma_{s.t.tr}\left(X_{check\_m\_midsup}\right) = -116.2\ MPa$ Stresses in top flange from short term loads

$\sigma_{s.b} := \frac{N}{A} + \frac{M}{I} \cdot \left(t_{deck} + h - z\right) = 137.5\ MPa$ = $\sigma_{s.b.tr}\left(X_{check\_m\_midsup}\right) = 137.5\ MPa$ Stresses in bottom flange from short term loads

5.4.1.2 Temperature loads

$M_{max} := M_{d.temp.max}\left(X_{check\_m\_midsup}\right) = 113\ kN \cdot m$ Bending moment imposed on steel section

$N_{max} := N_{d.temp.max}\left(X_{check\_m\_midsup}\right) = 1227\ kN$ Normal force imposed on steel section

$M_{min} := M_{d.temp.min}\left(X_{check\_m\_midsup}\right) = -114\ kN \cdot m$ Bending moment imposed on steel section

$N_{min} := N_{d.temp.min}\left(X_{check\_m\_midsup}\right) = -1228\ kN$ Normal force imposed on steel section

$A := A_{steel}\left(X_{check\_m\_midsup}\right) = 0.061\ m^2$ Cross-sectional area - steel section

$I := I_{y.steel}\left(X_{check\_m\_midsup}\right) = 0.016\ m^4$ Moment of inertia - steel section

$z := z_{tp.steel}\left(X_{check\_m\_midsup}\right) = 1111\ mm$ Center of gravity from top of concrete deck - steel section

$h := h_{beam}\left(X_{check\_m\_midsup}\right) = 1250\ mm$ Height of girder

$\sigma_{s.t.min} := \frac{N_{min}}{A} + \frac{M_{max}}{I} \cdot \left(t_{deck} - z\right) = -25.7\ MPa$ = $\sigma_{s.t.temp.min}\left(X_{check\_m\_midsup}\right) = -25.7\ MPa$

$\sigma_{s.t.max} := \frac{N_{max}}{A} + \frac{M_{min}}{I} \cdot \left(t_{deck} - z\right) = 25.7\ MPa$ = $\sigma_{s.t.temp.max}\left(X_{check\_m\_midsup}\right) = 25.7\ MPa$

$\sigma_{s.t} := min\left(\sigma_{s.t.max}, \sigma_{s.t.min}\right) = -25.7\ MPa$ $\sigma_{s.t.temp}(x) := \sigma_{s.t.temp.min}(x)$

$\sigma_{s.b.min} := \frac{N_{min}}{A} + \frac{M_{max}}{I} \cdot \left(t_{deck} + h - z\right) = -16.9\ MPa$ = $\sigma_{s.b.temp.min}\left(X_{check\_m\_midsup}\right) = -16.9\ MPa$

$\sigma_{s.b.max} := \frac{N_{max}}{A} + \frac{M_{min}}{I} \cdot \left(t_{deck} + h - z\right) = 16.8\ MPa$ = $\sigma_{s.b.temp.max}\left(X_{check\_m\_midsup}\right) = 16.8\ MPa$

$\sigma_{s.b} := max\left(\sigma_{s.b.max}, \sigma_{s.b.min}\right) = 16.8\ MPa$ $\sigma_{s.b.temp}(x) := \sigma_{s.b.temp.max}(x)$

5.4.2 Stresses due to additional permanent loads

$M := M_{d.perm}\left(X_{check\_m\_midsup}\right) = 5717\ kN \cdot m$ Bending moment

$I := I_{y.comp.long}\left(X_{check\_m\_midsup}\right) = 0.028\ m^4$ Moment of inertia

$z := z_{tp.comp.long}\left(X_{check\_m\_midsup}\right) = 899\ mm$ Center of gravity from top of concrete deck

$h := h_{beam}\left(X_{check\_m\_midsup}\right) = 1250\ mm$ Height of girder

$t_b := t_{bf}\left(X_{check\_m\_midsup}\right) = 40\ mm$ Thickness of bottom flange

$t_t := t_{tf}\left(X_{check\_m\_midsup}\right) = 25\ mm$ Thickness of top flange

$\sigma_{s.t} := \frac{M}{I} \cdot \left(t_{deck} - z\right) = -116.7\ MPa$ = $\sigma_{s.t.perm}\left(X_{check\_m\_midsup}\right) = -116.7\ MPa$ Stresses in top flange from additional permanent loads

$\sigma_{s.b} := \frac{M}{I} \cdot \left(t_{deck} + h - z\right) = 135.3\ MPa$ = $\sigma_{s.b.perm}\left(X_{check\_m\_midsup}\right) = 135.3\ MPa$ Stresses in bottom flange from additional permanent loads

5.4.3 Stresses due to shrinkage, first order effects

Over the support, the concrete is considered as cracked and therefore the normal forces due to shrinkage in the steel cross-section is equal to 0.

$M := M_{d.1.cs}\left(X_{check\_m\_midsup}\right) = 356\ kN \cdot m$ Bending moment imposed on steel section

$A := A_{steel}\left(X_{check\_m\_midsup}\right) = 0.061\ m^2$ Cross-sectional area - steel section

$I := I_{y.steel}\left(X_{check\_m\_midsup}\right) = 0.016\ m^4$ Moment of inertia - steel section

$z := z_{tp.steel}\left(X_{check\_m\_midsup}\right) = 1111\ mm$ Center of gravity from top of concrete deck - steel section

$h := h_{beam}\left(X_{check\_m\_midsup}\right) = 1250\ mm$ Height of girder

$\sigma_{s.t} := \frac{M}{I} \cdot \left(t_{deck} - z\right) = -17.52\ MPa$ = $\sigma_{s.t.shrink}\left(X_{check\_m\_midsup}\right) = -17.52\ MPa$ Stresses in top flange due to shrinkage

$\sigma_{s.b} := \frac{M}{I} \cdot \left(t_{deck} + h - z\right) = 10.2\ MPa$ = $\sigma_{s.b.shrink}\left(X_{check\_m\_midsup}\right) = 10.2\ MPa$ Stresses in lower flange due to shrinkage

5.4.4 Stresses due to shrinkage, second order effects

Over the support, the concrete is considered as cracked and therefore the normal forces due to the second order effects of shrinkage in the steel cross-section is equal to 0.

$M := M_{d.2.cs}\left(X_{check\_m\_midsup}\right) = 409\ kN \cdot m$ Bending moment imposed on steel section

$A := A_{steel}\left(X_{check\_m\_midsup}\right) = 0.061\ m^2$ Cross-sectional area - steel section

$I := I_{y.steel}\left(X_{check\_m\_midsup}\right) = 0.016\ m^4$ Moment of inertia - steel section

$z := z_{tp.steel}\left(X_{check\_m\_midsup}\right) = 1111\ mm$ Center of gravity from top of concrete deck - steel section

$t_t := t_{tf}\left(X_{check\_m\_midsup}\right) = 25\ mm$

$h := h_{beam}\left(X_{check\_m\_midsup}\right) = 1250\ mm$ Height of girder

$\sigma_{s.t} := \frac{M}{I} \cdot \left(t_{deck} - z\right) = -20.12\ MPa$ = $\sigma_{s.t.shrink.2}\left(X_{check\_m\_midsup}\right) = -20.12\ MPa$ Stresses in upper flange due to shrinkage

$\sigma_{s.b} := \frac{M}{I} \cdot \left(t_{deck} + h - z\right) = 11.7\ MPa$ = $\sigma_{s.b.shrink.2}\left(X_{check\_m\_midsup}\right) = 11.7\ MPa$ Stresses in bottom flange due to shrinkage

5.4.5 Stresses due to creep, second order effects

$M := M_{d.creep}\left(X_{check\_m\_midsup}\right) = 1395\ kN \cdot m$ Bending moment

$N := N_{d.creep}\left(X_{check\_m\_midsup}\right) = 0\ N$ Normal force

$I := I_{y.comp.long}\left(X_{check\_m\_midsup}\right) = 0.028\ m^4$ Moment of inertia

$A := A_{comp.long}\left(X_{check\_m\_midsup}\right) = 0.08\ m^2$ Cross-sectional area - composite section

$z := z_{tp.comp.long}\left(X_{check\_m\_midsup}\right) = 899\ mm$ Center of gravity from top concrete deck

$h := h_{beam}\left(X_{check\_m\_midsup}\right) = 1250\ mm$ Height of girder

$\sigma_{s.t} := \frac{N}{A} + \frac{M}{I} \cdot \left(t_{deck} - z\right) = -28.5\ MPa$ = $\sigma_{s.t.creep}\left(X_{check\_m\_midsup}\right) = -28.5\ MPa$ Stresses in top flange from additional permanent loads

$\sigma_{s.b} := \frac{N}{A} + \frac{M}{I} \cdot \left(t_{deck} + h - z\right) = 33\ MPa$ = $\sigma_{s.b.creep}\left(X_{check\_m\_midsup}\right) = 33\ MPa$ Stresses in bottom flange from additional permanent loads

5.4.6 Summary of stresses

Stresses in top flange over support

$$\sigma_{s.t.support}(x) := \sigma_{s.t.tr}(x) + \sigma_{s.t.perm}(x) + \sigma_{s.t.temp}(x) + \sigma_{s.t.shrink}(x) + \sigma_{s.t.shrink.2}(x) + \sigma_{s.t.creep}(x)$$

Stresses in bottom flange over support

$$\sigma_{s.b.support}(x) := \sigma_{s.b.tr}(x) + \sigma_{s.b.perm}(x) + \sigma_{s.b.temp}(x) + \sigma_{s.b.shrink}(x) + \sigma_{s.b.shrink.2}(x) + \sigma_{s.b.creep}(x)$$

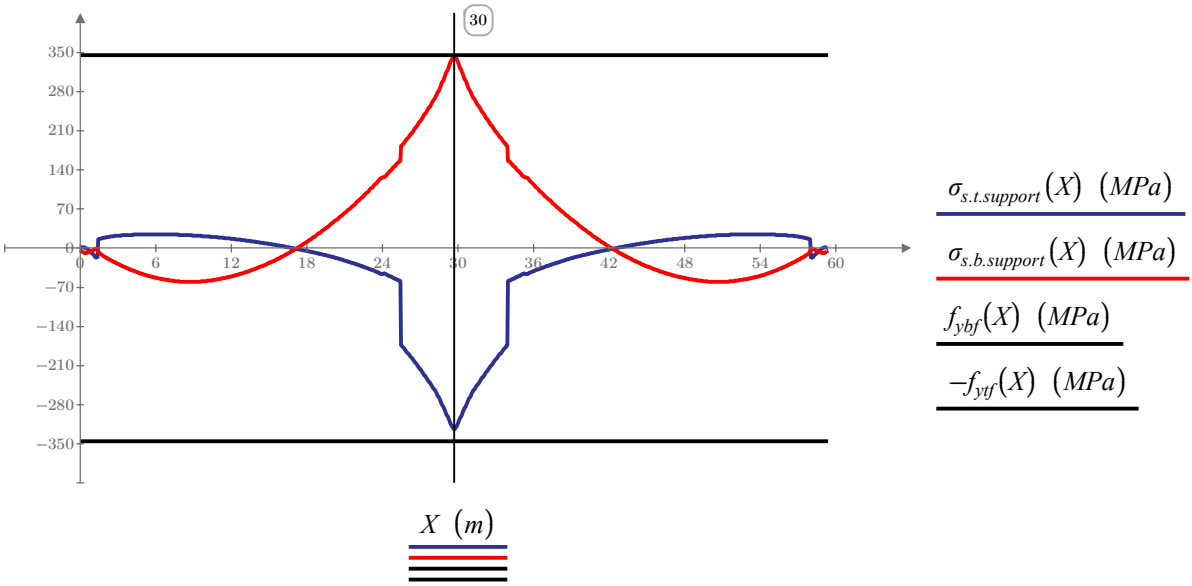

$$\eta_{\sigma.t.max} := max\left(\frac{\sigma_{s.t.support}(X)}{-f_{ytf}(X)}\right) = 94\%$$

Maximum utilization rate - top flange

$$\eta_{\sigma.b.max} := max\left(\frac{\sigma_{s.b.support}(X)}{f_{ybf}(X)}\right) = 100\%$$

Maximum utilization rate - bottom flange

5.5 Stresses in steel cross-section in span

The stresses are calculated for each load with respective cross-sectional constants. The stresses are summarized by the superposition rule.

5.5.1 Stresses due to variable (short term) loads

5.5.1.1 Traffic loads

$M := M_{d.min.tr}\left(X_{check\_m\_span}\right) = -9691\ kN \cdot m$ Bending moment

$N := N_{d.min.tr}\left(X_{check\_m\_span}\right) = -45\ kN$ Normal force

$A := A_{comp.short}\left(X_{check\_m\_span}\right) = 0.302\ m^2$ Cross-sectional area

$I := I_{y.comp.short}\left(X_{check\_m\_span}\right) = 0.061\ m^4$ Moment of inertia

$z := z_{tp.comp.short}\left(X_{check\_m\_span}\right) = 350\ mm$ Center of gravity from top of concrete deck

$h := h_{beam}\left(X_{check\_m\_span}\right) = 1250\ mm$ Height of girder

$t_b := t_{bf}\left(X_{check\_m\_span}\right) = 40\ mm$ Thickness of bottom flange

$t_t := t_{tf}\left(X_{check\_m\_span}\right) = 32\ mm$ Thickness of top flange

$\sigma_{s.t} := \frac{N}{A} + \frac{M}{I} \cdot \left(t_{deck} - z\right) = 4.7\ MPa$ = $\sigma_{s.t.tr}\left(X_{check\_m\_span}\right) = 4.7\ MPa$ Stresses in top flange from short term loads

$\sigma_{s.b} := \frac{N}{A} + \frac{M}{I} \cdot \left(t_{deck} + h - z\right) = -194.2\ MPa$ = $\sigma_{s.b.tr}\left(X_{check\_m\_span}\right) = -194.2\ MPa$ Stresses in bottom flange from short term loads

5.5.1.2 Temperature loads

$M_{max} := M_{d.temp.max}\left(X_{check\_m\_span}\right) = 93\ kN \cdot m$ Bending moment imposed on steel section

$N_{max} := N_{d.temp.max}\left(X_{check\_m\_span}\right) = 711\ kN$ Normal force imposed on steel section

$M_{min} := M_{d.temp.min}\left(X_{check\_m\_span}\right) = -93\ kN \cdot m$ Bending moment imposed on steel section

$N_{min} := N_{d.temp.min}\left(X_{check\_m\_span}\right) = -711\ kN$ Normal force imposed on steel section

$A := A_{steel}\left(X_{check\_m\_span}\right) = 0.063\ m^2$ Cross-sectional area - steel section

$I := I_{y.steel}\left(X_{check\_m\_span}\right) = 0.018\ m^4$ Moment of inertia - steel section

$z := z_{tp.steel}\left(X_{check\_m\_span}\right) = 1068\ mm$ Center of gravity from top of concrete deck - steel section

$h := h_{beam}\left(X_{check\_m\_span}\right) = 1250\ mm$ Height of girder

$\sigma_{s.t.min} := \frac{N_{min}}{A} + \frac{M_{max}}{I} \cdot \left(t_{deck} - z\right) = -15.18\ MPa =$ $\sigma_{s.t.temp.min}\left(X_{check\_m\_span}\right) = -15.18\ MPa$

$\sigma_{s.t.max} := \frac{N_{max}}{A} + \frac{M_{min}}{I} \cdot \left(t_{deck} - z\right) = 15.19\ MPa$ = $\sigma_{s.t.temp.max}\left(X_{check\_m\_span}\right) = 15.19\ MPa$

$\sigma_{s.t} := max\left(\sigma_{s.t.max}, \sigma_{s.t.min}\right) = 15.19\ MPa$ $\sigma_{s.t.temp}(x) := \sigma_{s.t.temp.max}(x)$

$\sigma_{s.b.min} := \frac{N_{min}}{A} + \frac{M_{max}}{I} \cdot \left(t_{deck} + h - z\right) = -8.6\ MPa$ = $\sigma_{s.b.temp.min}\left(X_{check\_m\_span}\right) = -8.6\ MPa$

$\sigma_{s.b.max} := \frac{N_{max}}{A} + \frac{M_{min}}{I} \cdot \left(t_{deck} + h - z\right) = 8.6\ MPa$ = $\sigma_{s.b.temp.max}\left(X_{check\_m\_span}\right) = 8.6\ MPa$

$\sigma_{s.b} := min\left(\sigma_{s.b.max}, \sigma_{s.b.min}\right) = -8.6\ MPa$ $\sigma_{s.b.temp}(x) := \sigma_{s.b.temp.min}(x)$

5.5.2 Stresses due to additional permanent loads

$M := M_{d.perm}\left(X_{check\_m\_span}\right) = -4270\ kN \cdot m$ Bending moment

$I := I_{y.comp.long}\left(X_{check\_m\_span}\right) = 0.047\ m^4$ Moment of inertia

$z := z_{tp.comp.long}\left(X_{check\_m\_span}\right) = 574\ mm$ Center of gravity from top of concrete deck

$h := h_{beam}\left(X_{check\_m\_span}\right) = 1250\ mm$ Height of girder

$t_b := t_{bf}\left(X_{check\_m\_span}\right) = 40\ mm$ Thickness of bottom flange

$t_t := t_{tf}\left(X_{check\_m\_span}\right) = 32\ mm$ Thickness of top flange

$\sigma_{s.t} := \frac{M}{I} \cdot \left(t_{deck} - z\right) = 23.2\ MPa$ = $\sigma_{s.t.perm}\left(X_{check\_m\_span}\right) = 23.2\ MPa$ Stresses in top flange from additional permanent loads

$\sigma_{s.b} := \frac{M}{I} \cdot \left(t_{deck} + h - z\right) = -91.16\ MPa$ = $\sigma_{s.b.perm}\left(X_{check\_m\_span}\right) = -91.16\ MPa$ Stresses in bottom flange from additional permanent loads

5.5.3 Stresses due to shrinkage

$M := M_{d.1.cs}\left(X_{check\_m\_span}\right) = -288\ kN \cdot m$ Bending moment imposed on steel section

$N := N_{d.1.cs}\left(X_{check\_m\_span}\right) = -1847\ kN$ Normal force imposed on steel section

$A := A_{steel}\left(X_{check\_m\_span}\right) = 0.063\ m^2$ Cross-sectional area - steel section

$I := I_{y.steel}\left(X_{check\_m\_span}\right) = 0.018\ m^4$ Moment of inertia - steel section

$z := z_{tp.steel}\left(X_{check\_m\_span}\right) = 1068\ mm$ Center of gravity from top of concrete deck - steel section

$h := h_{beam}\left(X_{check\_m\_span}\right) = 1250\ mm$ Height of girder

$\sigma_{s.t} := \frac{N}{A} + \frac{M}{I} \cdot \left(t_{deck} - z\right) = -16.9\ MPa$ = $\sigma_{s.t.shrink}\left(X_{check\_m\_span}\right) = -16.9\ MPa$ Stresses in top flange due to shrinkage

$\sigma_{s.b} := \frac{N}{A} + \frac{M}{I} \cdot \left(t_{deck} + h - z\right) = -37.4\ MPa$ = $\sigma_{s.b.shrink}\left(X_{check\_m\_span}\right) = -37.4\ MPa$ Stresses in bottom flange due to shrinkage

5.5.4 Summary of stresses

Stresses in top flange over support

$$\sigma_{s.t.span}(x) := \sigma_{s.t.tr}(x) + \sigma_{s.t.perm}(x) + \sigma_{s.t.shrink}(x) + \sigma_{s.t.temp}(x)$$ Stresses in top flange in span

Stresses in bottom flange over support

$$\sigma_{s.b.span}(x) := \sigma_{s.b.tr}(x) + \sigma_{s.b.perm}(x) + \sigma_{s.b.shrink}(x) + \sigma_{s.b.temp}(x)$$ Stresses in bottom flange in span

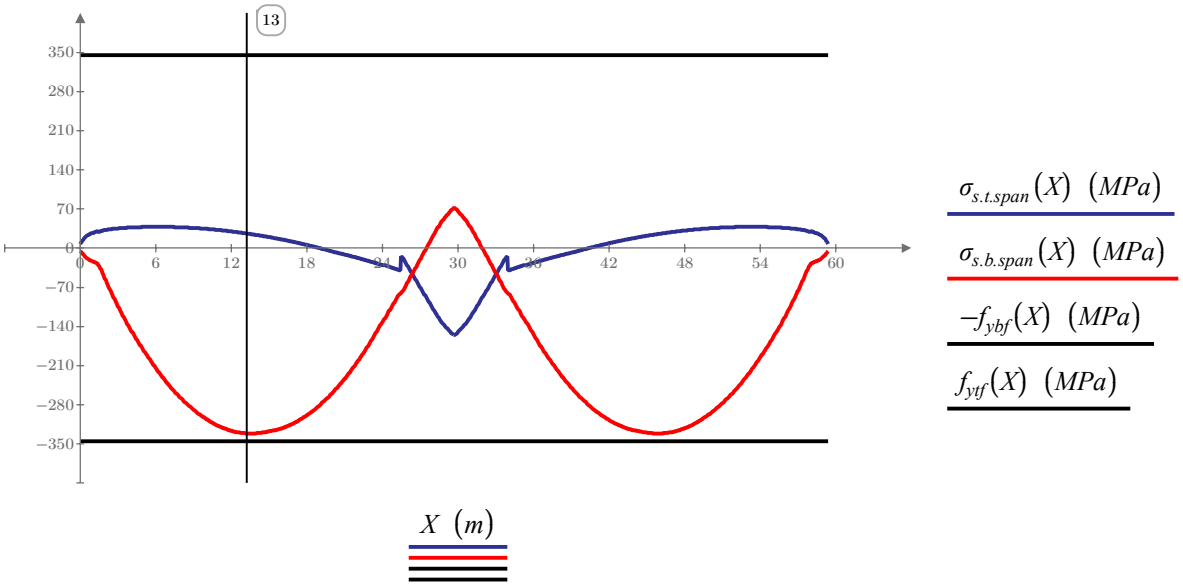

$$\eta_{\sigma.t.max} := max\left(\frac{\sigma_{s.t.span}(X)}{f_{ytf}(X)}\right) = 11\%$$ Maximum utilization rate - top flange

$$\eta_{\sigma.b.max} := max\left(\frac{\sigma_{s.b.span}(X)}{-f_{ybf}(X)}\right) = 96\%$$ Maximum utilization rate - bottom flange

5.6 Shear capacity

The shear capacity of the flat steel girder is calculated according to SS-EN 1993-1-5, 5.

Check if shear resistance control is necessary

$$\varepsilon := \varepsilon_w\left(X_{check\_v\_midsup}\right) = 0.814$$

$$\eta := 1.2$$

SS-EN 1993-1-5 (2) Note 2, same for carbon and stainless steel

$$f_w := f_{yw}\left(X_{check\_v\_midsup}\right) = 355\ MPa$$

$$hw := h_w\left(X_{check\_v\_midsup}\right) = 1185\ mm$$

$$tw := t_w\left(X_{check\_v\_midsup}\right) = 16\ mm$$

$$k_{\tau.v} := \left\| \begin{array}{l} \text{if } \frac{l_{cr.support}}{hw} \geq 1 \\ \quad out \leftarrow 5.34 + 4 \cdot \left(\frac{hw}{l_{cr.support}}\right)^2 \\ \text{else} \\ \quad out \leftarrow 4 + 5.34 \cdot \left(\frac{hw}{l_{cr.support}}\right)^2 \end{array} \right\| = 5.691$$

SS-EN 1993-1-5 A.3, no longitudinal stiffeners

Carbon steel, SS-EN 1993-1-5 5.1(2), for stiffened webs

$$Shearbuckling\_check_v := \left\| \begin{array}{l} \text{if } \frac{hw}{tw} > \frac{31}{\eta} \cdot \varepsilon \cdot \sqrt{k_{\tau.v}} \\ \quad out \leftarrow \text{“Check needed”} \\ \text{else} \\ \quad out \leftarrow \text{“No check needed!”} \end{array} \right\| = \text{“Check needed”}$$

Contribution from web

$$\sigma_{E.v} := 190000\ MPa \cdot \left(\frac{tw}{hw}\right)^2 = 35\ MPa$$

SS-EN 1991-1-5, Bilaga A

$$\tau_{cr.v} := k_{\tau.v} \cdot \sigma_{E.v} = 197\ MPa$$

SS-EN 1993-1-5 5.3(3), Critical buckling stress

$$\lambda_{w.v} := 0.76 \cdot \sqrt{\frac{f_w}{\tau_{cr.v}}} = 1.02$$

SS-EN 1993-1-5 5.3(3)

$$\chi_{w.v} := \left\| \begin{array}{l} \text{if } \lambda_{w.v} < \frac{0.83}{\eta} \\ \quad \left\| out \leftarrow \eta \right. \\ \text{else if } \frac{0.83}{\eta} \le \lambda_{w.v} < 1.08 \\ \quad \left\| out \leftarrow \frac{0.83}{\lambda_{w.v}} \right. \\ \text{else} \\ \quad \left\| out \leftarrow \frac{0.83}{\lambda_{w.v}} \right. \end{array} \right\| = 0.8138$$

SS-EN 1991-1-5 5.3, Table 5.1 Non-rigid end post

$$V_{Ed} := V_{d.ULS}\left(X_{check\_v\_midsup}\right) = 3041\ kN$$

$$V_{Rd} := \frac{\chi_{w.v} \cdot f_w \cdot hw \cdot tw}{\sqrt{3} \cdot \gamma_{M1}} = 3163\ kN \quad = \quad V_{Rd.w}\left(X_{check\_v\_midsup}\right) = 3163\ kN$$

Shear stress capacity

$$n_{V.w} := \frac{V_{Ed}}{V_{Rd}} = 96\% \qquad n_V\left(X_{check\_v\_midsup}\right) = 96\%$$

Maximum utilization rate

5.7 Interaction between moment and shear

The interaction between moment and shear force needs to be done close to internal supports since the web is utilized for both bending and shear. Worst case is the combination of maximum moment over support with associated shear force.

$$M_{f.Rd.tf}(x) := \overrightarrow{\frac{t_{tf}(x) \cdot b_{tf}(x) \cdot f_{ytf}(x)}{\gamma_{M0}} \cdot \left(z_{tp.comp.short}(x) - \frac{t_{tf}(x)}{2} - t_{deck} \right)}$$

$$M_{f.Rd.bf}(x) := \overrightarrow{\frac{t_{bf}(x) \cdot b_{bf}(x) \cdot f_{ybf}(x)}{\gamma_{M0}} \cdot \left(\left(t_{deck} + h_{beam}(x) - \frac{t_{bf}(x)}{2} \right) - z_{tp.comp.short}(x) \right)}$$

$$M_{f.Rd.re}(x) := \overrightarrow{\frac{A_{re}(x) \cdot f_{yk}}{\gamma_{M0}} \cdot \left(z_{tp.comp.short}(x) - \frac{t_{deck}}{2} \right)}$$

$$M_{f.Rd}(x) := \overrightarrow{M_{f.Rd.tf}(x) + M_{f.Rd.bf}(x) + M_{f.Rd.re}(x)}$$

Moment capacity of the flanges and reinforcement

$$h_{w.part1}(x) := \overrightarrow{z_{tp.comp.short}(x) - t_{deck} - t_{tf}(x)}$$

Height of the web above the neutral axis

$$h_{w.part2}(x) := \overrightarrow{t_{deck} + h_{beam}(x) - z_{tp.comp.short}(x)}$$

Height of the web below the neutral axis

$$M_{pl.Rd.w1}(x) := \overrightarrow{\frac{t_w(x) \cdot h_{w.part1}(x) \cdot f_{yw}(x)}{\gamma_{M0}} \cdot \left(\frac{h_{w.part1}(x)}{2} \right)}$$

$$M_{pl.Rd.w2}(x) := \overrightarrow{\frac{t_w(x) \cdot h_{w.part2}(x) \cdot f_{yw}(x)}{\gamma_{M0}} \cdot \left(\frac{h_{w.part2}(x)}{2} \right)}$$

$$M_{pl.Rd.tf}(x) := \overrightarrow{\frac{t_{tf}(x) \cdot b_{tf}(x) \cdot f_{ytf}(x)}{\gamma_{M0}} \cdot \left(z_{tp.comp.short}(x) - \frac{t_{tf}(x)}{2} - t_{deck} \right)}$$

$$M_{pl.Rd.bf}(x) := \overrightarrow{\frac{t_{bf}(x) \cdot b_{bf}(x) \cdot f_{ybf}(x)}{\gamma_{M0}} \cdot \left(\left(t_{deck} + h_{beam}(x) - \frac{t_{bf}(x)}{2} \right) - z_{tp.comp.short}(x) \right)}$$

$$M_{pl.Rd.re}(x) := \overrightarrow{\frac{A_{re}(x) \cdot f_{yk}}{\gamma_{M0}} \cdot \left(z_{tp.comp.short}(x) - \frac{t_{deck}}{2} \right)}$$

$$M_{pl.Rd}(x) := \overrightarrow{M_{pl.Rd.w1}(x) + M_{pl.Rd.w2}(x) + M_{pl.Rd.tf}(x) + M_{pl.Rd.bf}(x) + M_{pl.Rd.re}(x)}$$

Moment capacity of the composite section over support

$$M_{Ed.ULS.support}\left(X_{check\_v\_midsup}\right) = 14420 \ kN \cdot m$$

Maximum moment over support

$$V_{Ed.ULS.interaction}\left(X_{check\_v\_midsup}\right) = 2423 \ kN$$

Associated shear force to maximum moment over support

$$\eta_1 := \frac{M_{Ed.ULS.support}\left(X_{check\_v\_midsup}\right)}{M_{pl.Rd}\left(X_{check\_v\_midsup}\right)} = 0.8145$$

$$\eta_3 := \frac{V_{Ed.ULS.interaction}\left(X_{check\_v\_midsup}\right)}{V_{Rd.w}\left(X_{check\_v\_midsup}\right)} = 0.766$$

$$n_{int} := \eta_1 + \left(1 - \frac{M_{f.Rd}\left(X_{check\_v\_midsup}\right)}{M_{pl.Rd}\left(X_{check\_v\_midsup}\right)}\right) \cdot \left(2 \cdot \eta_3 - 1\right)^2 = 0.849 \qquad < 1 \qquad \text{Utilization rate, interaction}$$

5.8 Lateral torsional buckling of compressed flange over support

Due to composite action with compressed top flange in span, the check of LT-buckling of compressed flange is only necessary over support where the bottom flange is in compression. The check of LT-buckling is preformed according to the simplified method, SS-EN 1993-1-4 5.4.2.1.

$$\alpha_{LT} := \left\| \begin{array}{l} \text{if } t_{bf}\left(X_{check\_m\_midsup}\right) \le 40\ mm \\ \quad \| \ 0.49 \\ \text{else if } t_{bf}\left(X_{check\_m\_midsup}\right) > 40\ mm \\ \quad \| \ 0.76 \end{array} \right\| = 0.49$$

SS-EN 1993-1-1 Table 6.2, buckling around z-z

$l_{cr.support} = 4\ m$ — Distance between the cross-beams

$b_f := b_{bf}\left(X_{check\_m\_midsup}\right) = 740\ mm$ — Width of bottom flange

$t_f := t_{bf}\left(X_{check\_m\_midsup}\right) = 40\ mm$ — Thickness of bottom flange

$E_s = 210\ GPa$ — Modulus of elasticity

$f_{yb} := f_{ybf}\left(X_{check\_m\_midsup}\right) = 345\ MPa$ — Proof strength

$I_{zf} := \frac{b_f^{3} \cdot t_f}{12} = 0.001\ m^4$ — Moment of inertia, top flange

$N_{crLT} := \frac{\pi^2 \cdot E_s \cdot I_{zf}}{l_{cr.support}^{2}} = 174974\ kN$ — Critical buckling load

$\lambda_{LT\_l} := \sqrt{\frac{b_f \cdot t_f \cdot f_{yb}}{N_{crLT}}} = 0.242$ — SS-EN 1993-1-4 5.4.2.1 Equation 5.9

$\Phi_{LT\_l} := 0.5 \cdot \left(1 + \alpha_{LT} \cdot \left(\lambda_{LT\_l} - 0.2\right) + \lambda_{LT\_l}^{2}\right) = 0.54$ — SS-EN 1993-1-4 5.4.2.1 Equation 5.7

$\chi_{LT\_l} := min\left(\frac{1}{\Phi_{LT\_l} + \sqrt{\Phi_{LT\_l}^{2} - \lambda_{LT\_l}^{2}}}, 1\right) = 0.979$ = $\chi_{LT.b}\left(X_{check\_m\_midsup}\right) = 0.979$

SS-EN 1993-1-4 5.4.2.1 Equation 5.6

$k_{fl} := 1.1$ — Increase in capacity due to simlified method used, SS-EN 1993-1-1 6.3.2.4 (2)B

$\sigma_{Rd.b.LT\_l} := \frac{k_{fl} \cdot \chi_{LT\_l} \cdot f_{yb}}{\gamma_{M1}} = 371\ MPa$ = $\sigma_{Rd.b.LT}\left(X_{check\_m\_midsup}\right) = 371\ MPa$

5.8.1 Check of lateral torsional buckling

$\sigma_{Rd.b.LT}(X)$ Capacity of the bottom flange against LT- buckling

$\sigma_{s.b.support}(X)$ Maximum stress in the bottom flange over support

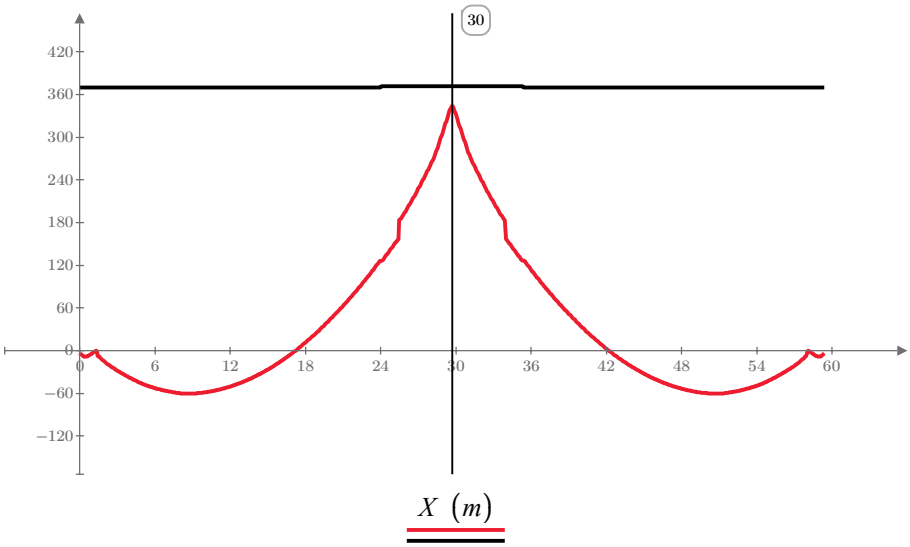

$\sigma_{s.b.support}(X)$ (MPa)

$\sigma_{Rd.b.LT}(X)$ (MPa)

$$\eta_{max} := \frac{\sigma_{s.b.support}\left(X_{check\_m\_midsup}\right)}{\sigma_{Rd.b.LT}\left(X_{check\_m\_midsup}\right)} = 93\%$$

Maximum utilization rate of the steel cross-section

6 Fatigue

The check for fatigue of welds and plates is carried out according to SS-EN 1993-2 and SS-EN 1993-1-9 using the lambda method. Fatigue load model 3 gives the worst fatigue effects and are therefore used for the verifications on fatigue.

Bending moment from Fatigue load model 3

$M_{FAT.max}(x)$ Maximum design bending moment from Fatigue load model 3

$M_{FAT.min}(x)$ Minimum design bending moment from Fatigue load model 3

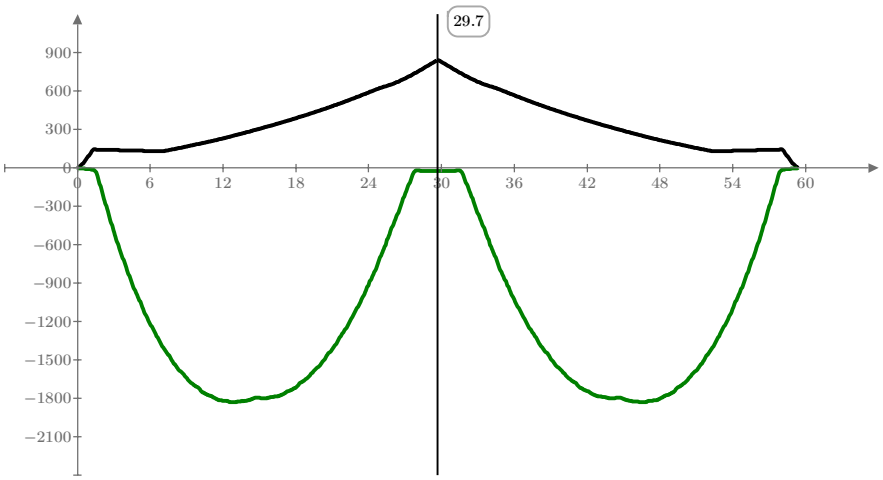

$M_{FAT.max}(X)\ \ (kN \cdot m)$

$M_{FAT.min}(X)\ \ (kN \cdot m)$

Shear force from Fatigue load model 3

$V_{FAT}(x)$ Shear force from Fatigue load model 3

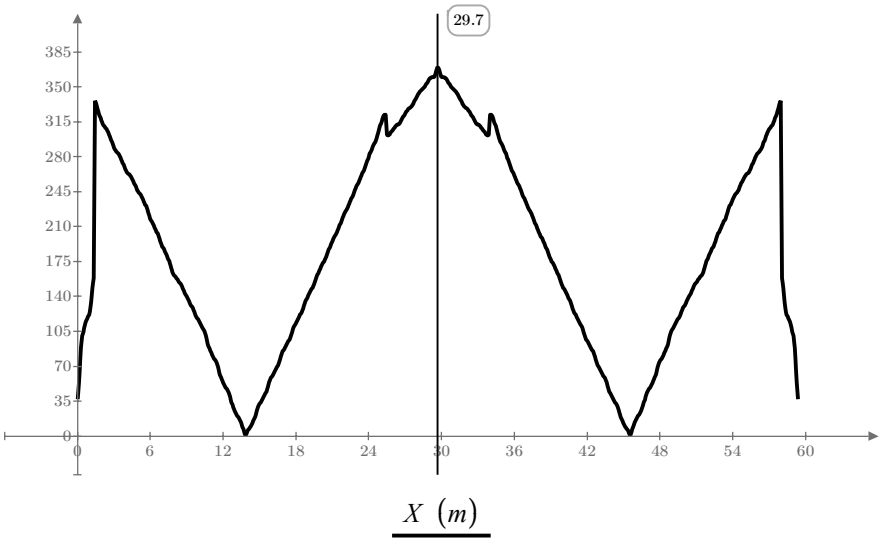

$V_{FAT}(X)\ \ (kN)$

Stress width from Fatigue load model 3

$\Delta\sigma_{e.tf}(x)$ Maximum stress width in the top flange along the length of the beam

$\Delta\sigma_{e.bf}(x)$ Maximum stress width in the bottom flange along the length of the beam

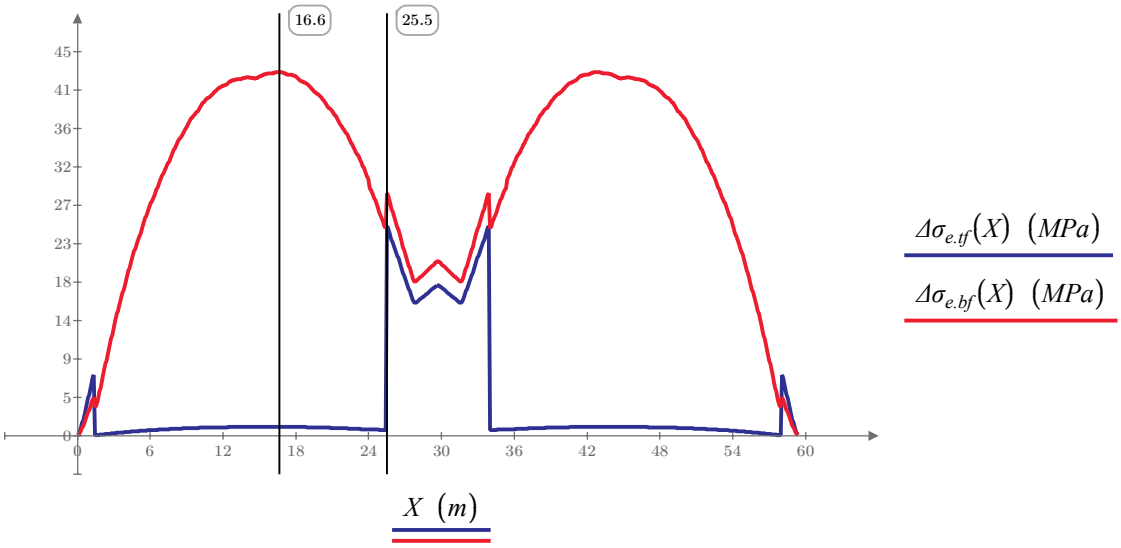

6.1 λ-method

$$\gamma_{Ff} \cdot \Delta\sigma_E < \frac{\Delta\sigma_c}{\gamma_{mf}}$$

$$\Delta\sigma_E = \lambda_f \cdot \phi \cdot \Delta\sigma$$

$\gamma_{Ff} := 1.0$ SS-EN 1993-2 9.3 (1)

$\gamma_{Mf} := 1.35$ SS-EN 1993-1-9 Table 3.1

$L_{span} = \begin{bmatrix} 28 \\ 28 \end{bmatrix} m$ Span length of bridge

$Q_{m1} := 445\ kN$ Krav Brobyggande E.3.1 (f)

$Q_{m1tdok} := 410\ kN$ Krav Brobyggande E.3.1 (f)

$Q_0 := 480\ kN$ SS-EN 1993-2 9.5.2 (3)

$N_{obs} := 0.05 \cdot 10^6$ SS-EN 1991-2 4.6.1 Table 4.5

$N_0 := 0.5 \cdot 10^6$ SS-EN 1993-2 9.5.2 (3)

$N_{year} := 80$

Critical length for shear force SS-EN 1993-2 9.5.2 (b)

$L_{CR.span} := max\left(L_{span}\right) \cdot 0.4 = 11.32\ m$

$L_{CR.sup} := max\left(L_{span}\right) = 28\ m$

$\lambda_{1V.span} := 2.55 - 0.7 \cdot \left(\frac{L_{CR.span} - 10\ m}{70\ m}\right) = 2.54$ Shear force in span SS-EN 1993-2 9.5.2 Figure 9.5

$\lambda_{1V.sup} := \left\| \begin{array}{l} \text{if } L_{CR.sup} \le 30\ m \\ \quad j \leftarrow 2.0 - 0.3 \cdot \left(\frac{L_{CR.sup} - 10\ m}{20\ m}\right) \\ \text{else if } L_{CR.sup} > 30\ m \\ \quad j \leftarrow 1.7 + 0.5 \cdot \left(\frac{L_{CR.sup} - 30\ m}{50\ m}\right) \\ j \end{array} \right| = 1.73$ Shear force over support SS-EN 1993-2 9.5.2 Figure 9.5

Critical length for moment SS-EN 1993-2 9.5.2 (a)

$L_{CR.span} := max\left(L_{span}\right) = 28.3\ m$

$L_{CR.sup} := \frac{L_{span}(0) + L_{span}(1)}{2} = 28\ m$

$\lambda_{1M.span} := 2.55 - 0.7 \cdot \left(\frac{L_{CR.span} - 10\ m}{70\ m}\right) = 2.37$ Moment in span SS-EN 1993-2 9.5.2 Figure 9.5

$\lambda_{1M.sup} := \left\| \begin{array}{l} \text{if } L_{CR.sup} \le 30\ m \\ \quad \left\| j \leftarrow 2.0 - 0.3 \cdot \left(\frac{L_{CR.sup} - 10\ m}{20\ m}\right) \right. \\ \text{else if } L_{CR.sup} > 30\ m \\ \quad \left\| j \leftarrow 1.7 + 0.5 \cdot \left(\frac{L_{CR.sup} - 30\ m}{50\ m}\right) \right. \\ j \end{array} \right\| = 1.73$ Moment over support SS-EN 1993-2 9.5.2 Figure 9.5

Critical length for reaction forces SS-EN 1993-2 9.5.2 (a)

$L_{CR.sup} := L_{span}(0) + L_{span}(1) = 57\ m$

$\lambda_{1R.sup} := \left\| \begin{array}{l} \text{if } L_{CR.sup} \le 30\ m \\ \quad \left\| j \leftarrow 2.0 - 0.3 \cdot \left(\frac{L_{CR.sup} - 10\ m}{20\ m}\right) \right. \\ \text{else if } L_{CR.sup} > 30\ m \\ \quad \left\| j \leftarrow 1.7 + 0.5 \cdot \left(\frac{L_{CR.sup} - 30\ m}{50\ m}\right) \right. \\ j \end{array} \right\| = 1.97$ Moment over support SS-EN 1993-2 9.5.2 Figure 9.5

$\lambda_2 := \frac{Q_{m1}}{Q_0} \cdot \left(\frac{N_{obs}}{N_0}\right)^{\frac{1}{5}} = 0.58$ SS-EN 1993-2 9.5.2 Equation 9.10

$\lambda_3 := \left(\frac{N_{year}}{100}\right)^{\frac{1}{5}} = 0.96$ SS-EN 1993-2 9.5.2 Equation 9.11

$\lambda_4 := 1.0$ TSFS 2018:57 27ch. $3

$L_{span} := max\left(L_{span}\right) = 28\ m$

$$\lambda_{max.span} := \left\| \begin{array}{l} \text{if } L_{span} \le 25\ m \\ \quad \left\| j \leftarrow 2.5 - 0.5 \cdot \left(\frac{L_{span} - 10\ m}{15\ m} \right) \right. \\ \text{else if } L_{span} > 25\ m \\ \quad \left\| j \leftarrow 2.0 \right. \\ j \end{array} \right\| = 2$$

$$\lambda_{max.sup} := \left\| \begin{array}{l} \text{if } L_{span} \ge 30\ m \\ \quad \left\| j \leftarrow 1.8 + 0.9 \cdot \left(\frac{L_{span} - 30\ m}{50\ m} \right) \right. \\ \text{else if } L_{span} < 30\ m \\ \quad \left\| j \leftarrow 1.8 \right. \\ j \end{array} \right\| = 1.8$$

$\lambda_{m.sup} := min\left(\lambda_{1M.sup} \cdot \lambda_2 \cdot \lambda_3 \cdot \lambda_4, \lambda_{max.sup}\right) = 0.97$ SS-EN 1993-2 9.5.2 Equation 9.9

$\lambda_{m.span} := min\left(\lambda_{1M.span} \cdot \lambda_2 \cdot \lambda_3 \cdot \lambda_4, \lambda_{max.span}\right) = 1.32$ SS-EN 1993-2 9.5.2 Equation 9.9

$\lambda_{V.sup} := min\left(\lambda_{1V.sup} \cdot \lambda_2 \cdot \lambda_3 \cdot \lambda_4, \lambda_{max.sup}\right) = 0.97$ SS-EN 1993-2 9.5.2 Equation 9.9

$\lambda_{V.span} := min\left(\lambda_{1V.span} \cdot \lambda_2 \cdot \lambda_3 \cdot \lambda_4, \lambda_{max.span}\right) = 1.42$ SS-EN 1993-2 9.5.2 Equation 9.9

$\lambda_{R.sup} := min\left(\lambda_{1R.sup} \cdot \lambda_2 \cdot \lambda_3 \cdot \lambda_4, \lambda_{max.sup}\right) = 1.1$ SS-EN 1993-2 9.5.2 Equation 9.9

6.2 Fatigue in steel parts

Cross-section change - Butt weld between bottom flanges

$X_{check\_fat\_1} := X_{check\_secChange} = 24.04\ m$ Location of cross-section change

$k_s(x) := \left(\frac{25\ mm}{t_{bf}(x)}\right)^{0.2}$ Size effect SS-EN 1993-1-9 7.2.2, due to different thickness of plates

$\Delta\sigma_c := 112\ MPa$ Fatigue class c112 SS-EN 1993-1-9 Table 8.3 (4)

$\sigma_{max}(x) := \frac{M_{FAT.max}(x)}{I_{y.comp.short}(x)} \cdot \left(h_{beam}(x) + t_{deck} - z_{tp.comp.short}(x)\right)$ Normal stresses in bottom flange, from max moment

$\sigma_{min}(x) := \frac{M_{FAT.min}(x)}{I_{y.comp.short}(x)} \cdot \left(h_{beam}(x) + t_{deck} - z_{tp.comp.short}(x)\right)$ Normal stresses in bottom flange, from min moment

$\Delta\sigma_e(x) := \lambda_{m.span} \cdot \left|\sigma_{max}(x) - \sigma_{min}(x)\right|$

$\Delta\sigma_e\left(X_{check\_fat\_1}\right) = 39\ MPa$

$\Delta\sigma_{c.red}(x) := k_s(x) \cdot \frac{\Delta\sigma_c}{\gamma_{Mf}}$ Fatigue strength SS-EN 1993-1-9 Eq: 7.1

$\Delta\sigma_{c.red}\left(X_{check\_fat\_1}\right) = 76\ MPa$

$\eta_{fat\_1} := \frac{\Delta\sigma_e\left(X_{check\_fat\_1}\right)}{\Delta\sigma_{c.red}\left(X_{check\_fat\_1}\right)} = 51\%$ Utilization ratio

Joint - Butt weld between bottom flanges

$X_{check\_fat\_2} := 12\ m$ Location of joint

$k_s(x) := \left(\frac{25\ mm}{t_{bf}(x)}\right)^{0.2}$ Size effect SS-EN 1993-1-9 7.2.2

$\Delta\sigma_c := 112\ MPa$ Fatigue class c112 SS-EN 1993-1-9 Table 8.3 (2)

$\sigma_{max}(x) := \frac{M_{FAT.max}(x)}{I_{y.comp.short}(x)} \cdot \left(h_{beam}(x) + t_{deck} - z_{tp.comp.short}(x)\right)$ Normal stresses in bottom flange, from max moment

$\sigma_{min}(x) := \frac{M_{FAT.min}(x)}{I_{y.comp.short}(x)} \cdot \left(h_{beam}(x) + t_{deck} - z_{tp.comp.short}(x)\right)$ Normal stresses in bottom flange, from min moment

$$\Delta\sigma_e(x) := \lambda_{m.span} \cdot |\sigma_{max}(x) - \sigma_{min}(x)|$$

$$\Delta\sigma_e(X_{check\_fat\_2}) = 54\ MPa$$

$$\Delta\sigma_{c.red}(x) := k_s(x) \cdot \frac{\Delta\sigma_c}{\gamma_{Mf}}$$ Fatigue strength SS-EN 1993-1-9 Eq: 7.1

$$\Delta\sigma_{c.red}(X_{check\_fat\_2}) = 76\ MPa$$

$$\eta_{fat\_2} := \frac{\Delta\sigma_e(X_{check\_fat\_2})}{\Delta\sigma_{c.red}(X_{check\_fat\_2})} = 72\%$$ Utilization ratio

Lower flange to stiffener in span

$$X_{check\_fat\_3} := 1.4\ m + 2 \cdot l_{cr.span} = 13\ m$$ Find the location of the transverse beam that gives the highest stress width

$$\Delta\sigma_c := 80\ MPa$$ Fatigue class c80 SS-EN 1993-1-9 Table 8.4 (7)

$$\sigma_{max}(x) := \frac{M_{FAT.max}(x)}{I_{y.comp.short}(x)} \cdot (h_{beam}(x) + t_{deck} - t_{bf}(x) - z_{tp.comp.short}(x))$$ Normal stresses in bottom flange, from max moment

$$\sigma_{min}(x) := \frac{M_{FAT.min}(x)}{I_{y.comp.short}(x)} \cdot (h_{beam}(x) + t_{deck} - t_{bf}(x) - z_{tp.comp.short}(x))$$ Normal stresses in bottom flange, from min moment

$$\Delta\sigma_e(x) := \lambda_{m.span} \cdot |\sigma_{max}(x) - \sigma_{min}(x)|$$

$$\Delta\sigma_e(X_{check\_fat\_3}) = 54\ MPa$$

$$\Delta\sigma_{c.red}(x) := \frac{\Delta\sigma_c}{\gamma_{Mf}}$$ Fatigue strength SS-EN 1993-1-9 Eq: 7.1

$$\Delta\sigma_{c.red}(X_{check\_fat\_3}) = 59\ MPa$$

$$\eta_{fat\_3} := \frac{\Delta\sigma_e(X_{check\_fat\_3})}{\Delta\sigma_{c.red}(X_{check\_fat\_3})} = 90\%$$ Utilization ratio

Effect of studs at top flange

$$X_{check\_fat\_4} := X_{check\_max.tf} = 25.5\ m$$ Location with largest stress width at top flange

$$\Delta\sigma_c := 80\ MPa$$ Fatigue class c80 SS-EN 1993-1-9 Table 8.5 (9)

$$\sigma_{max}(x) := \frac{M_{FAT.max}(x)}{I_{y.comp.short}(x)} \cdot \left(t_{deck} - z_{tp.comp.short}(x)\right)$$

Normal stresses in bottom flange, from max moment

$$\sigma_{min}(x) := \frac{M_{FAT.min}(x)}{I_{y.comp.short}(x)} \cdot \left(t_{deck} - z_{tp.comp.short}(x)\right)$$

Normal stresses in bottom flange, from min moment

$$\Delta\sigma_e(x) := \lambda_{m.span} \cdot \left|\sigma_{max}(x) - \sigma_{min}(x)\right|$$

$$\Delta\sigma_e\left(X_{check\_fat\_4}\right) = 33\ MPa$$

$$\Delta\sigma_{c.red}(x) := \frac{\Delta\sigma_c}{\gamma_{Mf}}$$

Fatigue strength SS-EN 1993-1-9 Eq: 7.1

$$\Delta\sigma_{c.red}\left(X_{check\_fat\_4}\right) = 59\ MPa$$

$$\eta_{fat\_4} := \frac{\Delta\sigma_e\left(X_{check\_fat\_4}\right)}{\Delta\sigma_{c.red}\left(X_{check\_fat\_4}\right)} = 55\%$$

Utilization ratio

6.3 Fatigue in welds

Check at support

$X_{check\_fat\_5} := X_{check\_m\_midsup} = 29.7\ m$

Check bottom flange fillet weld, web

$a := a_{weld.bot} = 7\ mm$

$\Delta\tau_{c\_ll\_tab} := 100\ MPa$ Fatigue class c80 m=5 SS-EN 1993-1-9 Table 8.2 (5)

$\Delta\tau_{e\_ll}(x) := \frac{V_{FAT}(x) \cdot S_{bw\_short.sup}(x) \cdot \lambda_{V.sup}}{I_{y.comp.short}(x) \cdot 2 \cdot a}$ Shear stresses in weld

$\Delta\tau_{e\_ll}(X_{check\_fat\_5}) = 17.334\ MPa$

$\Delta\tau_{c\_ll} := \frac{\Delta\tau_{c\_ll\_tab}}{\gamma_{Mf}} = 74\ MPa$ Fatigue strength SS-EN 1993-1-9 Eq: 7.1

$\eta_{fat\_5} := \frac{\Delta\tau_{e\_ll}(X_{check\_fat\_5})}{\Delta\tau_{c\_ll}} = 23\%$ Utilization ratio

Vertical load on web, see section 7.1

$\Delta\tau_{c\_L} := 100\ MPa$ Fatigue class c36 m=3 SS-EN 1993-1-9 Table 8.5 (8)

$\Delta\sigma_{c\_L} := 100\ MPa$ Fatigue class c36 m=3 SS-EN 1993-1-9 Table 8.5 (8)

$b_{bearing} := 535\ mm$ Width of bearing plate

$R := 260\ kN$ Reaction force from Fatigue load model 3

$\Delta\sigma_L := \frac{R}{2 \cdot \sqrt{2} \cdot a \cdot b_{bearing}} = 25\ MPa$ Normal stresses perpendicular to weld

$\Delta\tau_L := \Delta\sigma_L = 25\ MPa$ Shear stresses perpendicular to weld

$\Delta\sigma_{wf} := \lambda_{R.sup} \cdot \sqrt{\Delta\sigma_L^{\,2} + \Delta\tau_L^{\,2}} = 38\ MPa$ SS-EN 1993-1-9 5 (6)

$\eta_{fat\_6} := \frac{\Delta\sigma_{wf}}{\Delta\sigma_{c\_L}} = 38\%$ Utilization ratio

$\eta_{fat\_7} := \left(\frac{\Delta\sigma_{wf}}{\Delta\sigma_{c\_L}}\right)^3 + \left(\frac{\Delta\tau_{e\_ll}(X_{check\_fat\_5})}{\Delta\tau_{c\_ll}}\right)^5 = 6\%$ Utilization ratio

6.4 Fatigue utilization

$\eta_{fat\_1} = 51\%$	Check cross-section change, butt weld between bottom flanges
$\eta_{fat\_2} = 72\%$	Check joint in span, butt weld between bottom flanges
$\eta_{fat\_3} = 90\%$	Check lower flange to stiffener in span
$\eta_{fat\_4} = 55\%$	Check effect of studs at top flange
$\eta_{fat\_5} = 23\%$	Check bottom flange to web from shear forces, at internal support
$\eta_{fat\_6} = 38\%$	Check bottom flange to web from reaction forces, at internal support
$\eta_{fat\_7} = 6\%$	Check combined shear and normal stresses at internal support

7 Servicability limit state

7.1 Deflection from traffic loads

$\delta_{tr}(X)$ Calculated deflection retrieved from Birgade/Plus

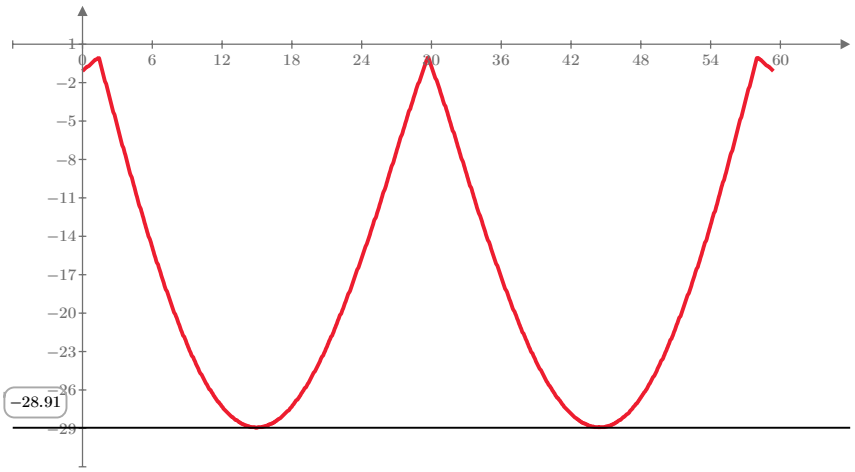

$\delta_{tr}(X)\ \ (mm)$

$X\ \ (m)$

$\delta_{tr.max} := min\left(\delta_{tr}(X)\right) = -28.91\ mm$ Maximum deflection caused by trafic loads

$L_{span} = 28.3\ m$ Span length

$\delta_{tr.all} := \frac{L_{span}}{400} = 71\ mm$ Allowed displacement - Krav Brobyggande B.3.4.2.2

$\eta_{\delta} := \frac{|\delta_{tr.max}|}{\delta_{tr.all}} = 41\%$ Utilization rate - allowed deflection

$\delta_{tr\_end} := \delta_{tr}(0\ m) = -1.08\ mm$ Vertical displacement at free end

$\delta_{tr\_end.all} := 5\ mm$ Allowed vertical displacement at free end - Krav Brobyggande B.3.4.2.2

$\textbf{if}\left(|\delta_{tr\_end}| \le \delta_{tr\_end.all}, \text{“OK”}, \text{“NOT OK”}\right) = \text{“OK”}$

7.2 Deflection from long-term loads and shrinkage

$$\delta_{tot}(X) := \delta_{long}(X) + \delta_{cs}(X)$$

$\delta_{tot}(X)$	Total deflection
$\delta_{long}(X)$	Deflection from permanent loads
$\delta_{cs}(X)$	Deflection from shrinkage

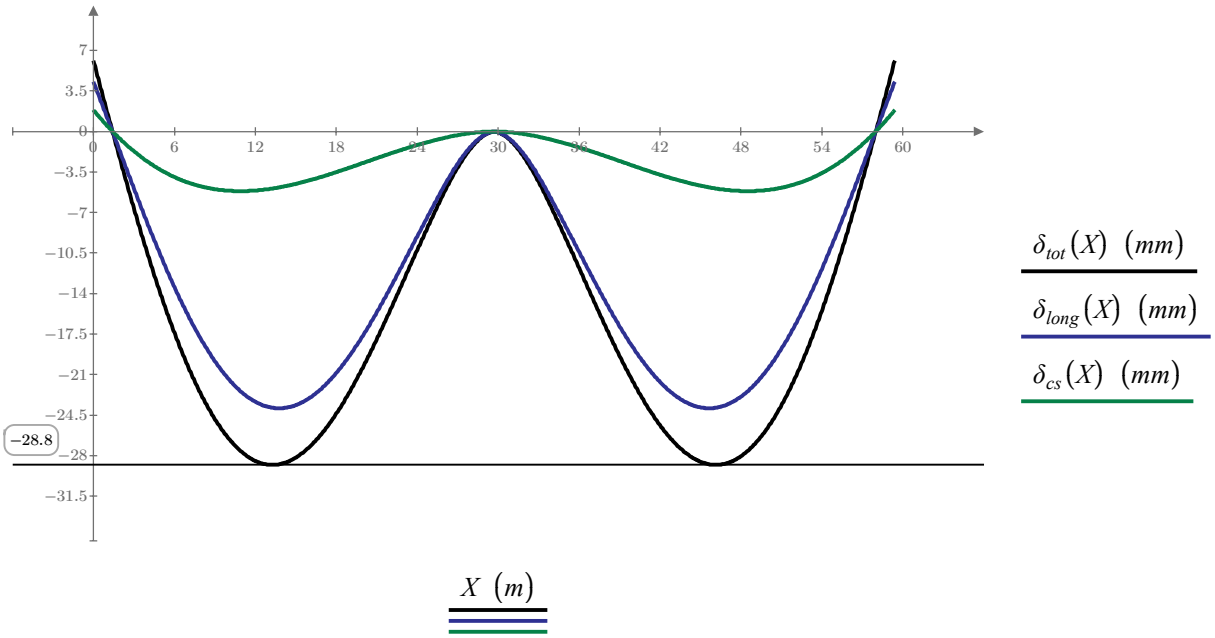

7.3 Deflection from casting loads

$\delta_{cast}(X)$ Deflection from casting loads

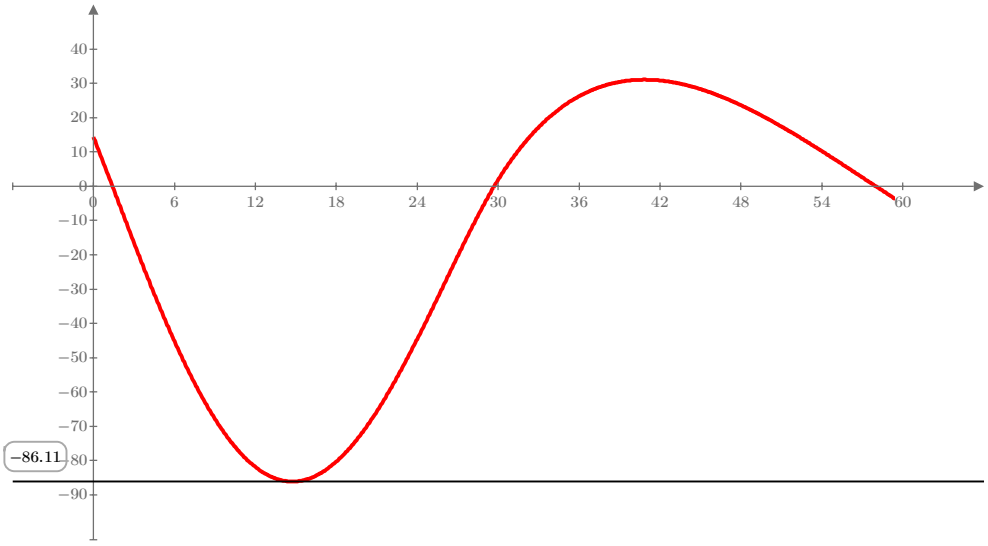

$\delta_{cast}(X)\ \ (mm)$

$X\ \ (m)$

7.4 Web breathing

The subsection is considered to be a stiffened plate. The check of web breathing is performed according to SS-EN 1993-2, 7.4.

$$Breathing\_check := \left\| \begin{array}{l} \text{if } \dfrac{h_w\left(\dfrac{L_{bridge}}{2}\right)}{t_w\left(\dfrac{L_{bridge}}{2}\right)} > 30 + 4 \cdot \dfrac{L_{span}}{m} \\ \quad \| \; out \leftarrow \text{“Check breathing”} \\ \text{else} \\ \quad \| \; out \leftarrow \text{“OK!”} \end{array} \right\| = \text{“OK!”}$$

SS-EN 1993-2 7.4 (2) Eq: 7.5

D

Case study 1: Design with corrugated web in stainless steel

1 Material

1.1 Stainless steel girder

The choosen steel grade is duplex stainless steel 1.4162. Material strengths are presented below for different thicknesses.

$f_{y\_8mm} = 530\ MPa$ Proof strength for $t \leq 8\ mm$ - SS- EN 1993-1-4:2006/A1:2015

$f_{u\_8mm} = 700\ MPa$ Ultimate strength for $t \leq 8\ mm$ - SS- EN 1993-1-4:2006/A1:2015

$f_{y\_13.5mm} = 480\ MPa$ Proof strength for $t \leq 13.5\ mm$ - SS- EN 1993-1-4:2006/A1:2015

$f_{u\_13.5mm} = 680\ MPa$ Ultimate strength for $t \leq 13.5\ mm$ - SS- EN 1993-1-4:2006/A1:2015

$f_{y\_75mm} = 450\ MPa$ Proof strength for $t \leq 75\ mm$ - SS- EN 1993-1-4:2006/A1:2015

$f_{u\_75mm} = 650\ MPa$ Ultimate strength for $t \leq 75\ mm$ - SS- EN 1993-1-4:2006/A1:2015

For Duplex stainless steel, the limits for thin plates differ. The limits for yield and ultimate strength are presented below.

$f_{y\_6.4mm} := 530\ MPa$ Proof strength for $t \leq 6.4\ mm$ - SS- EN 1993-1-4:2006/A1:2015

$f_{y\_10mm} := 480\ MPa$ Proof strength for $t \leq 10\ mm$ - SS- EN 1993-1-4:2006/A1:2015

$f_{ytf} := f_{y\_75mm} = 450\ MPa$ $f_{utf} := f_{u\_75mm} = 650\ MPa$ Choosen strength in top flange

$f_{ybf} := f_{y\_75mm} = 450\ MPa$ $f_{ubf} := f_{u\_75mm} = 650\ MPa$ Choosen strength in bottom flange

$f_{yw} := f_{y\_10mm} = 480\ MPa$ $f_{uw} := f_{u\_13.5mm} = 680\ MPa$ Choosen strength in web

$E_s = 200\ GPa$ Modulus of elasticity - SS-EN 1993-1-4 2.1.3 (1)

$\varepsilon_{ft} := \sqrt{\frac{235}{f_{ytf}} \cdot \frac{E_s}{210000}} = 0.71$ SS-EN 1993-1-4 5.2.2 Table 5.2

$\varepsilon_{fb} := \sqrt{\frac{235}{f_{ybf}} \cdot \frac{E_s}{210000}} = 0.71$ SS-EN 1993-1-4 5.2.2 Table 5.2

$\varepsilon_w := \sqrt{\frac{235}{f_{yw}} \cdot \frac{E_s}{210000}} = 0.68$ SS-EN 1993-1-4 5.2.2 Table 5.2

$\gamma_{M0} := 1.0$ Partial coefficient considering the resistance of the cross-section -TSFS 18 ch 2 §

$\gamma_{M1} := 1.0$ Partial coefficient considering the resistance of members to instability -TSFS 18 ch 2 §

$\gamma_{M2} := 1.2$ Partial coefficient considering the resistance of the cross-section in tension to fracture -TSFS 18 ch 2 §

$\alpha_s = 13 \cdot 10^{-6}$ Thermal expansion coefficient for stainless steel

1.2 Concrete slab

The design of the concrete slab is neglected in this master thesis. In order to calculate loads from shrinkage and creep some material parameters are necessary to include.

1.2.1 Concrete

The choosen concrete class is C35/45.

$f_{ck} = 35\ MPa$	Compressive strength - SS- EN 1992-1-1 Table 3.1
$f_{cm} = 43\ MPa$	Mean compressive strength - SS- EN 1992-1-1 Table 3.1
$f_{ctm} = 3.2\ MPa$	Mean tensile strength - SS- EN 1992-1-1 Table 3.1
$f_{ctk.0.05} = 2.2\ MPa$	5% fractile tensile strength - SS- EN 1992-1-1 Table 3.1
$E_{cm} = 34\ GPa$	Youngs modulus - SS- EN 1992-1-1 Table 3.1
$\gamma_c := 1.5$	Partial safety factor concrete (Permanent and variable loads) - SS- EN 1992-1-1 Table .2.1N
$\gamma_{cE} := 1.2$	Partial safety factor concrete (Accidental loads) - SS- EN 1992-1-1 Table 2.1N
$\alpha_{cc} := 1.0$	Accounting for longterm effects on the compressive strength - TSFS 2018:57 14 ch 3 §
$\alpha_{ct} := 1.0$	Accounting for longterm effects on the tensile strength - TSFS 2018:57 14 ch 3 §
$f_{cd} := \alpha_{cc} \cdot \frac{f_{ck}}{\gamma_c} = 23.3\ MPa$	Design compressive stength
$f_{ctd} := \alpha_{ct} \cdot \frac{f_{ctk.0.05}}{\gamma_c} = 1.47\ MPa$	Design tensile stength
$\alpha_c = 10 \cdot 10^{-6}$	Thermal expansion coefficient for concrete

1.2.1.1 Final shrinkage strain

$u := 2\ w_{deck} + 2\ t_{deck} = 19.640\ m$ Is the perimeter of the cross-section in contact with the atmosphere

$A_c = 3.040\ m^2$ Area of full concrete deck section

$h_0 := \frac{2 \cdot A_c}{u} = 310\ mm$ Equivalent thickness

$t_y := 80 years$ Length of service life in years

$t := 29200\ day$ Length of service life in days

$f_{cm} = 43\ MPa$ Mean compressive strength

$t_s := 1\ day$ Age of concrete by the start of drying shrinkage process

$RH := 80\%$ Krav Brobyggande B.3.1.5

$$\beta_{ds} := \frac{\frac{t - t_s}{day}}{\left(\frac{t - t_s}{day}\right) + 0.04 \cdot \sqrt{\left(\frac{h_0}{1\ mm}\right)^3}} = 0.993$$ SS-EN 1992-1-1 3.1.4 Equation 3.10

$$k_h := \begin{cases} 0.85 - \left(\frac{h_0}{mm} - 200\right) \cdot 0.001 & \text{if } 200\ mm \le h_0 < 300\ mm \\ 0.75 - \left(\frac{h_0}{mm} - 300\right) \cdot 0.0005 & \text{else if } 300\ mm \le h_0 < 500\ mm \\ 0.7 & \text{else if } h_0 \ge 500\ mm \\ 1.0 & \text{else} \end{cases} = 0.75$$ SS-EN 1992-1-1 3.1.4 table 3.3

$RH_0 := 100\%$

$\alpha_{ds1} := 4$ SS-EN 1992-1-1 Appendix B.2 (1), Cementclass N

$\alpha_{ds2} := 0.12$ SS-EN 1992-1-1 Appendix B.2 (1), Cementclass N

$$\beta_{RH} := 1.55 \cdot \left(1 - \left(\frac{RH}{RH_0}\right)^3\right) = 0.76$$ SS-EN 1992-1-1 Appendix B.2 equation B12

$f_{cmo} := 10\ MPa$ SS-EN 1992-1-1 Appendix B.2 (1)

$\varepsilon_{cd.0} := 0.85 \cdot \left(\left(220 + 110 \cdot \alpha_{ds1} \right) \cdot e^{\left(-\alpha_{ds2} \cdot \frac{f_{cm}}{f_{cmo}} \right)} \right) \cdot 10^{-6} \cdot \beta_{RH} = 2.53 \cdot 10^{-4}$ SS-EN 1992-1-1 Appendix B.2 equation B11

$\varepsilon_{cd} := \beta_{ds} \cdot k_h \cdot \varepsilon_{cd.0} = 1.87 \cdot 10^{-4}$ Drying shrinkage - SS-EN 1992-1-1 3.1.4 Equation 3.9

$\varepsilon_{ca0} := 2.5 \cdot \left(\frac{f_{ck} - f_{cmo}}{MPa} \right) \cdot 10^{-6} = 6.3 \cdot 10^{-5}$ SS-EN 1992-1-1 3.1.4 Equation 3.12

$\beta_{as} := 1 - e^{\left(-0.2 \cdot \sqrt{\frac{t - t_s}{day}} \right)} = 1.0$ SS-EN 1992-1-1 3.1.4 Equation 3.13

$\varepsilon_{ca} := \beta_{as} \cdot \varepsilon_{ca0} = 6.25 \cdot 10^{-5}$ Autogenous shrinkage - SS-EN 1992-1-1 3.1.4 Equation 3.11

$\varepsilon_{cs} := \varepsilon_{ca} + \varepsilon_{cd} = 2.5 \cdot 10^{-4}$ Total shrinkage - SS-EN 1992-1-1 3.1.4 Equation 3.8

1.2.1.2 Creep function

Creep for the concrete are calculated according to SS-EN 1992-1-1 Annex B.

$RH := 80$ — [%] - Relative humidity in the ambient air

t_0 — [days] - Time for first loading

$u := 2\ w_{deck} + 2\ t_{deck} = 19.640\ m$ — Is the perimeter of the cross-section in contact with the atmosphere

$A_c = 3.040\ m^2$ — Area of full concrete deck section

$$h_0 := \frac{2 \cdot A_c}{u} = 310\ mm$$ — SS- EN 1992-1-1 B.1 (B.6)

$$\alpha_1 := \left(\frac{35\ MPa}{f_{cm}}\right)^{0.7} = 0.87$$ — SS- EN 1992-1-1 B.1 (B.8c)

$$\alpha_2 := \left(\frac{35\ MPa}{f_{cm}}\right)^{0.2} = 0.96$$ — SS- EN 1992-1-1 B.1 (B.8c)

$$\varphi_{RH} := \begin{cases} \left(1 + \frac{1 - \frac{RH}{100}}{0.1 \cdot \sqrt[3]{\frac{h_0}{mm}}} \cdot \alpha_1\right) \cdot \alpha_2 & \text{if } f_{cm} > 35\ MPa \\ \left(1 + \frac{1 - \frac{RH}{100}}{0.1 \cdot \sqrt[3]{\frac{h_0}{mm}}}\right) & \text{else} \end{cases} = 1.21$$ — SS- EN 1992-1-1 B.1 (B.3a,b)

$$\beta_{fcm} := \frac{16.8}{\sqrt{\frac{f_{cm}}{MPa}}} = 2.6$$ — SS- EN 1992-1-1 B.1 (B.4)

$$\beta_{t0}(t_0) := \frac{1}{0.1 + \left(\frac{t_0}{day}\right)^{0.2}}$$ — SS- EN 1992-1-1 B.1 (B.5)

$\varphi_0(t_0) := \varphi_{RH} \cdot \beta_{fcm} \cdot \beta_{t0}(t_0)$ — Nominal creep value - SS- EN 1992-1-1 B.1 (B.2)

$\varphi_{\infty\_cs} := \varphi_0(1\ day) = 2.81$ — Final creep value for shrinkage (t= 1 day) - SS-EN 1994-2 5.4.2.2 (4)

$\varphi_{\infty\_perm} := \varphi_0(7\ day) = 1.96$ — Final creep value for permanent loads (t= 7 day) - SS-EN 1994-2 5.4.2.2

1.2.2 Reinforcement

The reinforcement used for the case study is B500B.

$f_{yk} = 500\ MPa$ — Yield strength

$E_{rs} := 200\ GPa$ — SS- EN 1994-2 3.2(2)

$\gamma_s := 1.15$ — Permanent and variable loads SS- EN 1992-1-1 Table 2.1N

$\gamma_{sfat} := 1.15$ — Fatigue loading SS- EN 1992-1-1 Table 2.1N

$\gamma_{sA} := 1.0$ — Accidental loading SS- EN 1992-1-1 Table 2.1N

$f_{yd} := \frac{f_{yk}}{\gamma_s} = 435\ MPa$ — Design yield strength - SS-EN 1990 6.3.3

1.2.3 Modular ratios

Modular ratios are calculated according to SS-EN 1994-2, 5.4.2.2, Equation (5.6).

$n_0 := \frac{E_s}{E_{cm}} = 5.88$ — Modular ratio between stainless steel and concrete

$\varphi_{L\_perm} := 1.1$ — Creep factor depending on the load durance for permanent loads - SS- EN 1994-2 5.4.2.2

$\varphi_{L\_cs} := 0.55$ — Creep factor depending on the load durance for shrinkage - SS- EN 1994-2 5.4.2.2

$n_{L.short} := n_0 \cdot (1 + 0 \cdot 0) = 5.9$ — Modular ratio for short-term loads and temperature

$n_{L.long} := n_0 \cdot (1 + \varphi_{L\_perm} \cdot \varphi_{\infty\_perm}) = 18.6$ — Modular ratio for permanent loads (excl. shrinkage)

$n_{L.cs} := n_0 \cdot (1 + \varphi_{L\_cs} \cdot \varphi_{\infty\_cs}) = 14.96$ — Modular ratio for shrinkage

$$n_L := \begin{bmatrix} n_{L.long} \\ n_{L.short} \\ n_{L.cs} \end{bmatrix} = \begin{bmatrix} 18.56 \\ 5.88 \\ 14.96 \end{bmatrix}$$

2 System

The system consists of two steel girders with a concrete slab on top.

2.1 Primary system - longitudinal

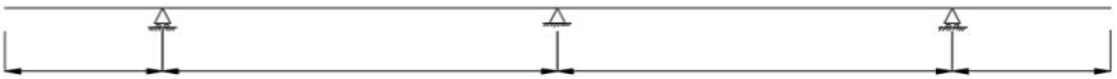

$l_{console.1} = 1.40\ m$ $L_{span_1} = 28.30\ m$ $L_{span_2} = 28.30\ m$ $l_{console.2} = 1.40\ m$

The longitudinal system consists of two steel beams spanning over several spans. The steel girder change in cross-section over the internal supports. The cross-section changes are located according to the coordinates below.

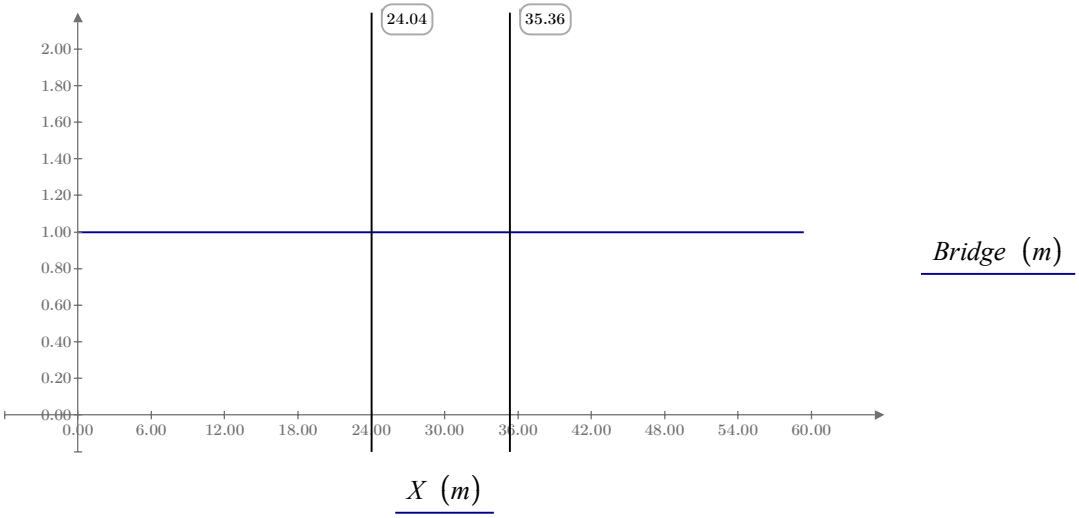

2.1.1 Cross-section dimensions

2.1.1.1 Beam type 1

Steel beam type 1 is located in the spans .

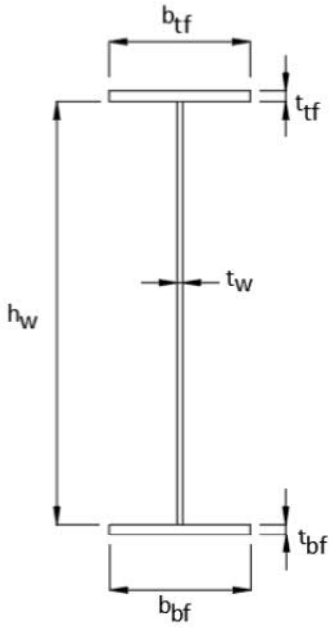

$b_{tf}(X_{span}) = 460\ mm$	Width top flange
$t_{tf}(X_{span}) = 30\ mm$	Thickness top flange
$h_w(X_{span}) = 1180\ mm$	Height web
$t_w(X_{span}) = 9\ mm$	Thickness tweb
$b_{bf}(X_{span}) = 770\ mm$	Width bottom flange
$t_{bf}(X_{span}) = 40\ mm$	Thickness bottom flange

2.1.1.2 Beam type 2

Steel beam type 2 is located over the internal support area.

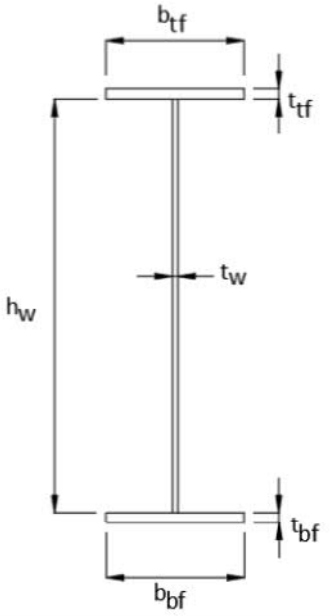

$b_{tf}(X_{support}) = 380\ mm$	Width top flange
$t_{tf}(X_{support}) = 30\ mm$	Thickness top flange
$h_w(X_{support}) = 1183\ mm$	Height web
$t_w(X_{support}) = 9\ mm$	Thickness tweb
$b_{bf}(X_{support}) = 640\ mm$	Width bottom flange
$t_{bf}(X_{support}) = 37\ mm$	Thickness bottom flange

2.1.1.3 Corrugation parameters

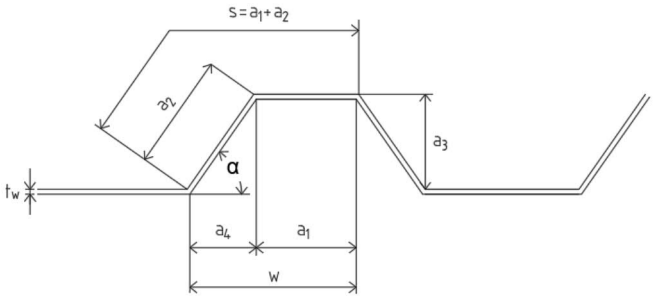

$a_{c1} = 70\ mm$ Flat-fold length

$\alpha_c = 36\ deg$ Corrugation angle

$a_{c3} = 40\ mm$ Corrugation depth

$a_{c2} := \frac{a_{c3}}{\sin(\alpha_c \cdot deg)} = 68\ mm$ Length of angled part

$a_{c4} := \frac{a_{c3}}{\tan(\alpha_c \cdot deg)} = 55\ mm$ Length of hypopythis

$s_c := a_{c1} + a_{c2} = 138\ mm$ Length of corrugation

$w_c := a_{c1} + a_{c4} = 125\ mm$ Straight length

$r_c := \frac{s_c}{w_c} = 1.104$ Factor for increased length due to corrugation

2.2 Secondary system - transversal

The secondary system consists of a reinforced concrete deck with dimensions presented below.

2.2.1 Concrete

$t_{deck} = 0.32\ m$ Height of concrete deck

$w_{deck} = 9.50\ m$ Total width of concrete deck

2.2.2 Reinforcement

The reinforcement is assumed to be located in the center of the concrete deck.

$\phi_{rein} = 16\ mm$ Dimension of reinforcement bar

$s_{rein} = 106\ mm$ CC-distance between bars

$n_{rein} = 2$ Number of layers

3 Loads

Here, the loads included in the system analysis in Brigade/Plus are presented.

$L_{bridge} := 59.4\ m$ — Bridge length

$cc_{beams} := 5.3\ m$ — CC-distance between main girders

$h_{girder} := 1.250\ m$ — Height of girder

$t_{deck} := 0.32\ m$ — Thickness of concrete deck

$h_{edgebeam} := 0.7\ m$ — Height of edge beam

$w_{deck} := 9.5\ m$ — Width of bridge deck

3.1 Permanent loads

3.1.1 Steel beams

$\rho_{steel} := 7700\ \frac{kg}{m^3}$ — Density of stainless steel

3.1.2 Concrete deck

$\rho_{con.w} := 26\ \frac{kN}{m^3}$ — Wet concrete used for calaculations during construction stage

$\rho_{con} := 25\ \frac{kN}{m^3}$ — Dry concrete used for calaculations during service stage

3.1.3 Coating

$t_{cov} := 100\ mm$ — Thickness of coating

$\rho_{cov} := 23\ \frac{kN}{m^3}$ — Weight of coating

$g_{cov} := t_{cov} \cdot \rho_{cov} = 2300\ \frac{N}{m^2}$ — Uniformly distributed load from coating

3.1.4 Rails

$g_{rails} := 0.5 \ \frac{kN}{m}$

Line load due to railings located on the edgebeams

3.1.5 Shrinkage

$\varepsilon_{cs} = 2.50 \cdot 10^{-4}$

Final shrinkage strain

$M_{as} := 213.51 \ kN \cdot m$

Average span moment working on the steel section due to first order effects of shrinkage

3.1.6 Creep, 2nd order

$M_0 := 3732.27 \ kN \cdot m$

Maximum short term moment in span due to permanent loads

3.2 Variable loads

3.2.1 Braking and acceleration force

Trafikverket vehicles

$A_{tr} := 180 \ kN$

$B_{tr} := 300 \ kN$

$$Br := max\left(\begin{bmatrix} 0.88 \\ 1 \\ 1.1 \\ 1.17 \\ 1.32 \\ 0.44 + 1.32 + 0.44 + 1.32 \\ 0.55 + 1 + 1.32 \\ 0.44 + 1.1 + 1.1 + 0.66 \\ 0.44 + 1.32 + 0.44 + 1.32 \\ 0.55 + 1 + 1.32 \\ 0.44 + 1.1 + 1.1 + 0.66 \\ 0.33 + 1 + 1.32 \\ 0.55 + 0.55 + 0.55 + 0.33 + 0.12 \end{bmatrix} \cdot B_{tr}\right) = 1056.00 \ kN$$

$Q_{1k\_tr} := min\left(0.35 \cdot Br, 500 \ kN\right) = 369.60 \ kN$

$q_{br.tr} := \frac{Q_{1k\_tr}}{2 \cdot L_{bridge}} = 3.11 \ \frac{kN}{m}$

Braking/acceleration load from Trafikverket vehicle

3.2.2 Temperature load

$T_0 := 10$

$T_{min} := -35$ Minimum temperature for Borås kommun, TSFS 2018:57

$T_{max} := 35$ Maximum temperature for Borås kommun, TSFS 2018:57

$T_{e.min} := T_{min} + 4 = -31$

$T_{e.max} := T_{max} + 4 = 39$

3.2.3 Wind load

$h_{vehicle} := 2\ m$

$d_{tot} := h_{girder} + t_{deck} + t_{cov} + h_{vehicle} = 3.67\ m$

$\rho_{air} := 1.25\ \frac{kg}{m^3}$

$v_b := 25\ \frac{m}{s}$

$q_p := 0.79\ \frac{kN}{m^2}$ Terrain category II, assumed height 8m. TSFS 2018:57 Table 7.1

$q_b := \frac{1}{2} \cdot \rho_{air} \cdot v_b^{\ 2} = 0.39\ \frac{kN}{m^2}$ SS-EN 1991-1-4 4.5, Eq.4.10

$c_e := \frac{q_p}{q_b} = 2.02$ SS-EN 1991-1-4 4.5, Eq.4.9

$\frac{w_{deck}}{d_{tot}} = 2.59$

$c_{fx} := 1.65$ SS-EN 1991-1-4, Figure 8.3

$C_w := c_e \cdot c_{fx} = 3.34$ Form factor for force on superstructure in x-direction

Wind load on structure

$d_{bridge} := h_{girder} + h_{edgebeam} + 0.6\ m = 2.55\ m$ SS-EN 1991-1-4, Table 8.1

$F_{w.bridge} := q_p \cdot c_{fx} \cdot d_{bridge} = 3.32\ \frac{kN}{m}$ Horizontal component per meter bridge

$z := d_{bridge} - (h_{girder} + t_{deck}) = 0.98\ m$

$$q_{bridge} := \frac{F_{w.bridge} \cdot \left(\frac{d_{bridge}}{2} - z \right)}{cc_{beams}} = 0.185 \ \frac{kN}{m}$$

Wind load on structure

Wind load on vehicle

$d_{vehicle} := h_{vehicle} = 2.0 \ m$

SS-EN 1991-1-4, Table 8.1

$$F_{w.vehicle} := q_p \cdot c_{fx} \cdot d_{vehicle} = 2.607 \ \frac{kN}{m}$$

$$q_{vehicle} := \frac{F_{w.vehicle} \cdot \left(\frac{d_{vehicle}}{2} \right)}{cc_{beams}} = 0.492 \ \frac{kN}{m}$$

Wind load on vehicle

4 Capacity checks during construction

The capacity check that is carried out in this chapter is bending moment capacity with respect to lateral torsional buckling in the construction stage togheter with maximum stresses in the cross-section.

Because the checks are performed by using vectors and closed areas, controll-caluclations are showed for the governing coordinates. Critical points are presented in blue below:

$X_{check\_m\_midsup} = 29.7\ m$	Coordinate for control calculations - Bending moment over mid support
$X_{check\_m\_span} = 13.84\ m$	Coordinate for control calculations - Bending moment in span
$X_{check\_v\_midsup} = 29.641\ m$	Coordinate for control calculations - Shear force over mid support
$X_{check\_v\_endsup} = 1.426\ m$	Coordinate for control calculations - shear force end support

4.1 Load Combinations

The loads should be combined according to STR/GEO and 6.10a or 6.10b dependent on which case that gives the worst load effects. The load combinations are presented below.

STR/GEO 6.10a

Permanent loads	**sup**	**inf**	**Unfavorable**	**Favorable**
Self-weight	1.0	1.0	$\gamma_d \cdot 1.35 \cdot sup$	$1.0 \cdot inf$
Surfacing	1.1	0.9	$\gamma_d \cdot 1.35 \cdot sup$	$1.0 \cdot inf$
Variable loads	Ψ_0		**Main load**	**Other load**
Wind loads	1.0		$\gamma_d \cdot 1.5 \cdot \Psi_0$	$\gamma_d \cdot 1.5 \cdot \Psi_0$

STR/GEO 6.10b

Permanent loads	**sup**	**inf**	**Unfavorable**	**Favorable**
Self-weight	1.0	1.0	$\gamma_d \cdot 0.89 \cdot 1.35 \cdot sup$	$1.0 \cdot inf$
Surfacing	1.1	0.9	$\gamma_d \cdot 0.89 \cdot 1.35 \cdot sup$	$1.0 \cdot inf$
Variable loads	Ψ_0		**Main load**	**Other load**
Wind loads	1.0		$\gamma_d \cdot 1.5$	$\gamma_d \cdot 1.5 \cdot \Psi_0$

4.2 Load effects

Load effects are retrieved from Brigade/Plus. During construction stage two different casting scenarios are calculated in order to see the worst effect. One scenario is when the casting load is located in one span the other with casting load located in two spans.

Bending moment, casting loads in one span

$M_{d.LC1.6.10.a}$ Bending moment from casting loads in 1 span, load combination 6.10a
$M_{d.LC1.6.10.b}$ Bending moment from casting loads in 1 span, load combination 6.10b

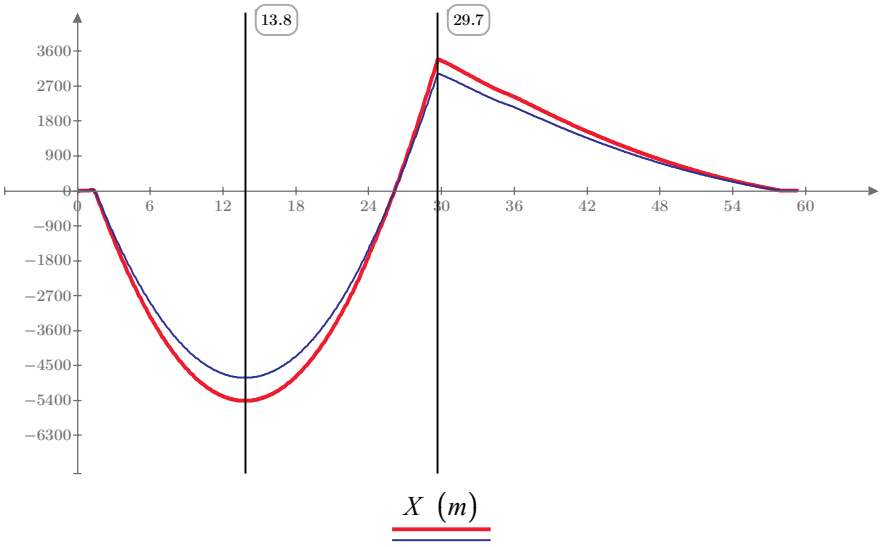

$M_{d.LC1.6.10.a}(X)\ \ (kN \cdot m)$

$M_{d.LC1.6.10.b}(X)\ \ (kN \cdot m)$

Bending moment, casting loads in two span

$M_{d.LC2.6.10.a}$ Bending moment from casting loads in 2 spans, load combination 6.10a
$M_{d.LC2.6.10.b}$ Bending moment from casting loads in 2 spans, load combination 6.10b

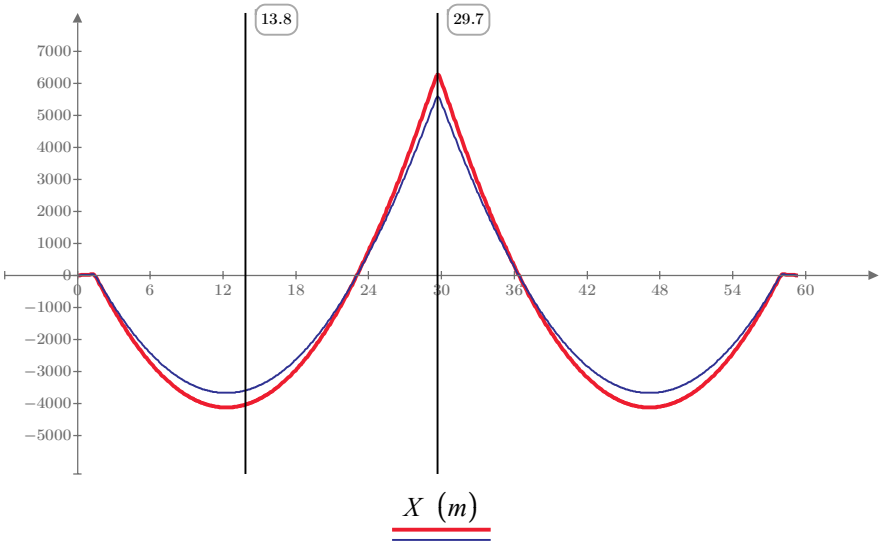

$M_{d.LC2.6.10.a}(X)\ \ (kN \cdot m)$

$M_{d.LC2.6.10.b}(X)\ \ (kN \cdot m)$

Shear force, load effect from loads in one span

$V_{d.LC1.6.10.a}$ Shear force from casting loads in 1 span, load combination 6.10a

$V_{d.LC1.6.10.b}$ Shear force from casting loads in 1 span, load combination 6.10b

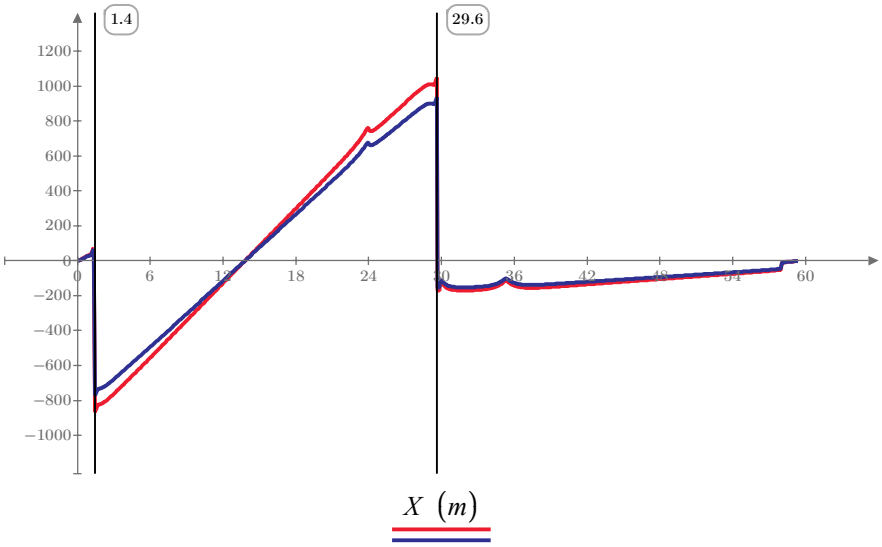

$V_{d.LC1.6.10.a}(X)$ (kN)

$V_{d.LC1.6.10.b}(X)$ (kN)

Shear force, load effect from loads in two span

$V_{d.LC2.6.10.a}$ Shear force from casting loads in 2 spans, load combination 6.10a

$V_{d.LC2.6.10.b}$ Shear force from casting loads in 2 spans, load combination 6.10b

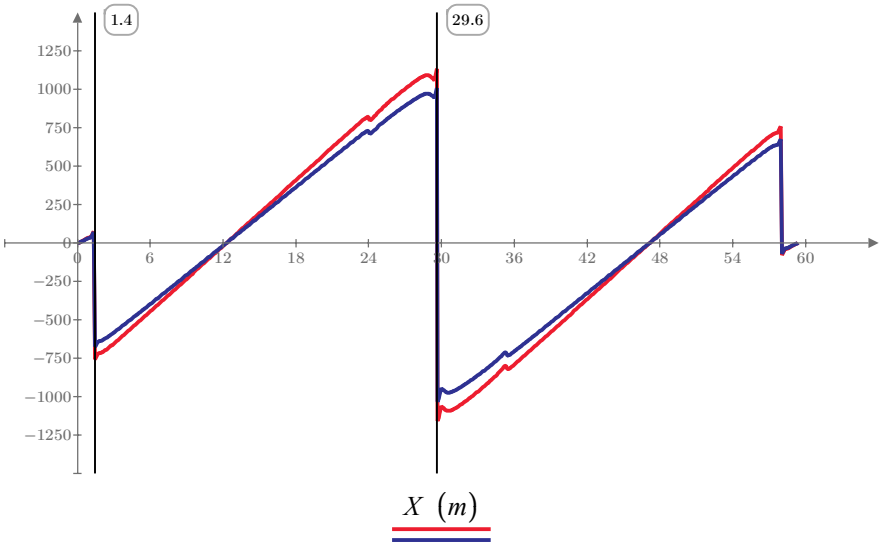

$V_{d.LC2.6.10.a}(X)$ (kN)

$V_{d.LC2.6.10.b}(X)$ (kN)

$LoadComb := \text{“6.10a”}$ Load combination that gives worst load effects

4.3 Cross-section classification

The cross-section classes is determined according to SS-EN 1993 1-4 5.2.2 with updated limits from SS-EN 1993-1-4:2006/A1:2015. The corrugated web does not contribute to the axial stiffness and classification of the web is therefore not necessary

$a_{weld.top} = 7\ mm$ Weld thickness between top flange and web

$a_{weld.bot} = 7\ mm$ Weld thickness between bottom flange and web

$c_w(x) := h_w(x) - \sqrt{2} \cdot a_{weld.top} - \sqrt{2} \cdot a_{weld.bot}$ Distance between welded toes on web.

$$c_{tf}(x) := \left\| \begin{array}{l} \text{if } \frac{(a_{c1} + a_{c4}) \cdot a_{c3}}{(a_{c1} + 2 \cdot a_{c4}) \cdot b_{tf}(x)} < 0.14 \\ \quad \left\| \frac{b_{tf}(x)}{2} - \frac{t_w(x)}{2} - \sqrt{2} \cdot a_{weld.top} \right. \\ \text{else} \\ \quad \left\| \frac{b_{tf}(x)}{2} + \frac{a_{c3}}{2} - \frac{t_w(x)}{2} - \sqrt{2} \cdot a_{weld.top} \right. \end{array} \right.$$

Length of the outstand part of top flange. *"Commentary and worked examples to EN 1993-1-5 Plated structural elements" (Johansson, Maquoi, Sedlacek, Müller, and Beg, 2007)*

$$c_{bf}(x) := \left\| \begin{array}{l} \text{if } \frac{(a_{c1} + a_{c4}) \cdot a_{c3}}{(a_{c1} + 2 \cdot a_{c4}) \cdot b_{bf}(x)} < 0.14 \\ \quad \left\| \frac{b_{bf}(x)}{2} - \frac{t_w(x)}{2} - \sqrt{2} \cdot a_{weld.bot} \right. \\ \text{else} \\ \quad \left\| \frac{b_{bf}(x)}{2} + \frac{a_{c3}}{2} - \frac{t_w(x)}{2} - \sqrt{2} \cdot a_{weld.bot} \right. \end{array} \right.$$

Length of the outstand part of bottom flange. *"Commentary and worked examples to EN 1993-1-5 Plated structural elements" (Johansson, Maquoi, Sedlacek, Müller, and Beg, 2007)*

Cross-section class, top flange

$E_s = 200\ GPa$ Modulus of elasticity

$f_{ytf} = 450\ MPa$ Proof strength of top flange

$\varepsilon_{tf} = 0.71$

$$csc_{tf}(x) := \left\| \begin{array}{l} \text{if } \frac{c_{tf}(x)}{t_{tf}(x)} \le 9\ \varepsilon_{tf} \\ \quad \left\| \text{“csc1”} \right. \\ \text{else if } 9\ \varepsilon_{tf} < \frac{c_{tf}(x)}{t_{tf}(x)} \le 10\ \varepsilon_{tf} \\ \quad \left\| \text{“csc2”} \right. \\ \text{else if } 10\ \varepsilon_{tf} < \frac{c_{tf}(x)}{t_{tf}(x)} \le 14\ \varepsilon_{tf} \\ \quad \left\| \text{“csc3”} \right. \\ \text{else} \\ \quad \left\| \text{“csc4”} \right. \end{array} \right.$$

Cross-section class top flange

$csc_{tf}(X_{check\_m\_midsup}) = \text{“csc1”}$ Cross-section class at $X_{check\_m\_midsup} = 29.700\ m$

$csc_{tf}(X_{check\_m\_span}) = \text{“csc3”}$ Cross-section class at $X_{check\_m\_span} = 13.840\ m$

$csc_{tf}(X_{check\_v\_midsup}) = \text{“csc1”}$ Cross-section class at $X_{check\_v\_midsup} = 29.641\ m$

$csc_{tf}(X_{check\_v\_endsup}) = \text{“csc3”}$ Cross-section class at $X_{check\_v\_endsup} = 1.426\ m$

Cross-section class, bottom flange

$E_s = 200\ GPa$ Modulus of elasticity

$f_{ybf} = 450\ MPa$ Proof strength of bottom flange

$\varepsilon_{bf} = 0.71$

$$csc_{bf}(x) := \begin{cases} \text{if } \dfrac{c_{bf}(x)}{t_{bf}(x)} \le 9\ \varepsilon_{bf} \\ \quad \text{“csc1”} \\ \text{else if } 9\ \varepsilon_{bf} < \dfrac{c_{bf}(x)}{t_{bf}(x)} \le 10\ \varepsilon_{bf} \\ \quad \text{“csc2”} \\ \text{else if } 10\ \varepsilon_{bf} < \dfrac{c_{bf}(x)}{t_{bf}(x)} \le 14\ \varepsilon_{bf} \\ \quad \text{“csc3”} \\ \text{else} \\ \quad \text{“csc4”} \end{cases}$$

Cross-section class bottom flange

$csc_{bf}(X_{check\_m\_midsup}) = \text{“csc3”}$ Cross-section class at $X_{check\_m\_midsup} = 29.700\ m$

$csc_{bf}(X_{check\_m\_span}) = \text{“csc3”}$ Cross-section class at $X_{check\_m\_span} = 13.840\ m$

$csc_{bf}(X_{check\_v\_midsup}) = \text{“csc3”}$ Cross-section class at $X_{check\_v\_midsup} = 29.641\ m$

$csc_{bf}(X_{check\_v\_endsup}) = \text{“csc3”}$ Cross-section class at $X_{check\_v\_endsup} = 1.426\ m$

4.4 Lateral torsional buckling of compressed flanges

The compressed flanges are controlled against LT-buckling according to the simplified method, SS-EN 1993-1-4 5.4.2.1.

Compressed top flange in span

$\alpha_{LT} := 0.76$ — Buckling curve d for stainless steel

$l_{cr.span} = 6\ m$ — Distance between the cross-beams

$b_t := b_{tf}\left(X_{check\_m\_span}\right) = 460\ mm$ — Width of top flange

$t_t := t_{tf}\left(X_{check\_m\_span}\right) = 30\ mm$ — Thickness of top flange

$E_s = 200\ GPa$ — Modulus of elasticity

$f_{ytf} = 450\ MPa$ — Proof strength

$I_{zt} := \frac{b_t^{\,3} \cdot t_t}{12} = 0.00024\ m^4$ — Moment of inertia, top flange

$N_{crLT} := \frac{\pi^2 \cdot E_s \cdot I_{zt}}{l_{cr.span}^{\,2}} = 13343\ kN$ — Critical buckling load

$\lambda_{LT\_t} := \sqrt{\frac{b_t \cdot t_t \cdot f_{ytf}}{N_{crLT}}} = 0.682$ — SS-EN 1993-1-4 5.4.2.1 Equation 5.9

$\Phi_{LT\_t} := 0.5 \cdot \left(1 + \alpha_{LT} \cdot \left(\lambda_{LT\_t} - 0.2\right) + \lambda_{LT\_t}^{\,2}\right) = 0.92$ — SS-EN 1993-1-4 5.4.2.1 Equation 5.7

$\chi_{LT\_t} := min\left(\frac{1}{\Phi_{LT\_t} + \sqrt{\Phi_{LT\_t}^{\,2} - \lambda_{LT\_t}^{\,2}}}, 1\right) = 0.655$ = $\chi_{LT}\left(X_{check\_m\_span}\right) = 0.655$ — SS-EN 1993-1-4 5.4.2.1 Equation 5.6

$h_{w\_t} := h_w\left(X_{check\_m\_span}\right) = 1180\ mm$ — Height of web

$t_b := t_{bf}\left(X_{check\_m\_span}\right) = 40\ mm$ — Thickness of bottom flange

$k_{fl} := 1.1$ — Increase in capacity due to simlified method used, SS-EN 1993-1-1 6.3.2.4 (2)B

$M_{Rd.t.LT\_t} := \frac{b_t \cdot t_t \cdot k_{fl} \cdot \chi_{LT\_t} \cdot f_{ytf}}{\gamma_{M1}} \left(h_{w\_t} + \frac{t_t + t_b}{2}\right) = 5435\ kN \cdot m$ = $M_{Rd.t.LT}\left(X_{check\_m\_span}\right) = 5435\ kN \cdot m$

SS-EN 1993-1-5 D.2.1 Equation D.1

Compressed bottom flange over support

$\alpha_{LT} := 0.76$ — Stainless steel, SS-EN 1993-1-4 Table 5.3

$l_{cr.support} = 4\ m$ — Distance between the cross-beams

$b_b := b_{bf}\left(X_{check\_m\_midsup}\right) = 640\ mm$ — Width of bottom flange

$t_b := t_{bf}\left(X_{check\_m\_midsup}\right) = 37\ mm$ — Thickness of bottom flange

$E_s = 200\ GPa$ — Modulus of elasticity

$f_{ybf} = 450\ MPa$ — Proof strength

$I_{zb} := \frac{b_b^{\,3} \cdot t_b}{12} = 0.00081\ m^4$ — Moment of inertia, bottom flange

$N_{crLT} := \frac{\pi^2 \cdot E_s \cdot I_{zb}}{l_{cr.support}^{\,2}} = 99717\ kN$ — Critical buckling load

$\lambda_{LT\_b} := \sqrt{\frac{b_b \cdot t_b \cdot f_{ybf}}{N_{crLT}}} = 0.327$ — SS-EN 1993-1-4 5.4.2.1 Equation 5.9

$\Phi_{LT\_b} := 0.5 \cdot \left(1 + \alpha_{LT} \cdot \left(\lambda_{LT\_b} - 0.2\right) + \lambda_{LT\_b}^{\,2}\right) = 0.6$ — SS-EN 1993-1-4 5.4.2.1 Equation 5.7

$\chi_{LT\_b} := min\left(\frac{1}{\Phi_{LT\_b} + \sqrt{\Phi_{LT\_b}^{\,2} - \lambda_{LT\_b}^{\,2}}}, 1\right) = 0.904$ = $\chi_{LT}\left(X_{check\_m\_midsup}\right) = 0.904$ — SS-EN 1993-1-4 5.4.2.1 Equation 5.6

$h_{w\_b} := h_w\left(X_{check\_m\_midsup}\right) = 1183\ mm$ — Height of web

$t_t := t_{tf}\left(X_{check\_m\_midsup}\right) = 30\ mm$ — Thickness of top flange

$k_{fl} := 1.1$ — Increase in capacity due to simlified method used, SS-EN 1993-1-1 6.3.2.4 (2)B

$M_{Rd.b.LT\_l} := \frac{b_b \cdot t_b \cdot k_{fl} \cdot \chi_{LT\_b} \cdot f_{ybf}}{\gamma_{M1}} \left(h_{w\_b} + \frac{t_t + t_b}{2}\right) = 12884\ kN \cdot m$ = $M_{Rd.b.LT}\left(X_{check\_m\_midsup}\right) = 12884\ kN \cdot m$

SS-EN 1993-1-5 D.2.1 Equation D.1

4.4.1 Check of lateral torsional buckling

$M_{Rd.t.LT}(X)$	Capacity of the top flange against LT- buckling during casting
$M_{Rd.b.LT}(X)$	Capacity of the bottom flange against LT- buckling during casting
$M_{d.ULS.LC1}(X)$	Load effects during casting, worst case over support
$M_{d.ULS.LC2}(X)$	Load effects during casting, worst case in span

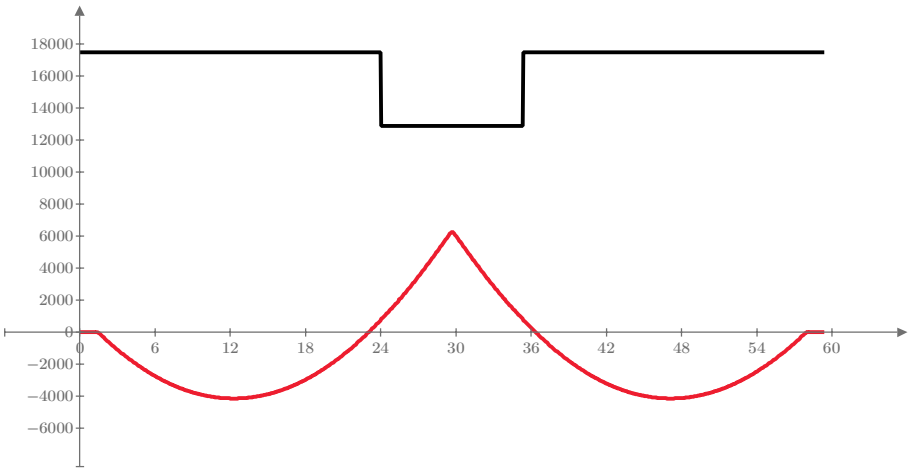

$M_{d.ULS.LC2}(X)\ \ (kN \cdot m)$

$M_{Rd.b.LT}(X)\ \ (kN \cdot m)$

$X\ \ (m)$

$$\eta_{max} := max\left(\frac{M_{d.ULS.LC2}(X)}{M_{Rd.b.LT}(X)}\right) = 49\%$$

Maximum utilization rate of the bottom flange during casting

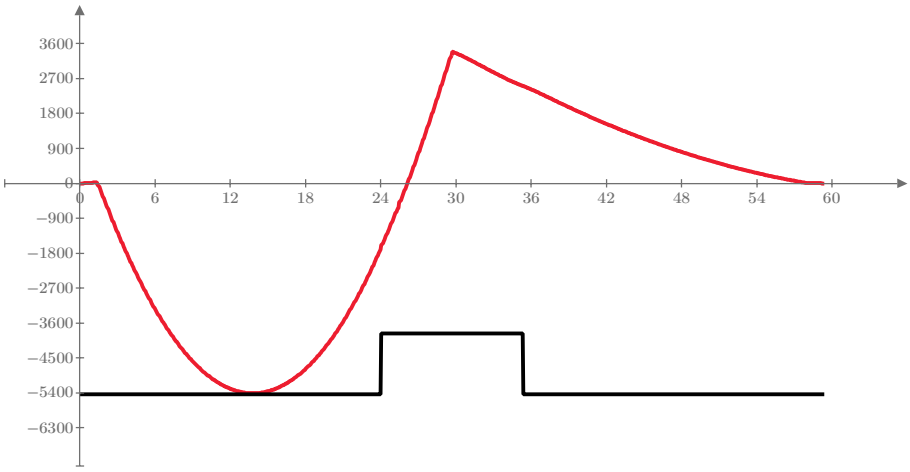

$M_{d.ULS.LC1}(X)\ \ (kN \cdot m)$

$-M_{Rd.t.LT}(X)\ \ (kN \cdot m)$

$X\ \ (m)$

$$\eta_{min} := max\left(\frac{M_{d.ULS.LC1}(X)}{-M_{Rd.t.LT}(X)}\right) = 100\%$$

Maximum utilization rate of top flange during casting

4.5 Stresses in steel cross-section

The stresses in the top and bottom flange from loads during construction are compared to the yield strength of steel girders to verify that the steel girders can withstand the stresses alone before composite action with concrete is achieved.

Top flange, in span

$M := M_{d.ULS.LC1}\left(X_{check\_m\_span}\right) = -5409\ kN \cdot m$ Load effect at midspan

$I := I_{y.steel}\left(X_{check\_m\_span}\right) = 0.014\ m^4$ Moment of inertia at midspan

$z := \left(t_{deck} + \frac{t_{tf}\left(X_{check\_m\_span}\right)}{2}\right) - z_{tp.steel}\left(X_{check\_m\_span}\right) = -0.839\ m$ Centre of gravity at midspan maesured from the top of the concrete deck

$\sigma := \frac{M}{I} \cdot z = 323\ MPa$ = $\sigma_{stf\_ULS\_cast}\left(X_{check\_m\_span}\right) = 323\ MPa$

$\sigma_{stf\_ULS\_cast}(X)$ Stresses in top flange during construction stage.

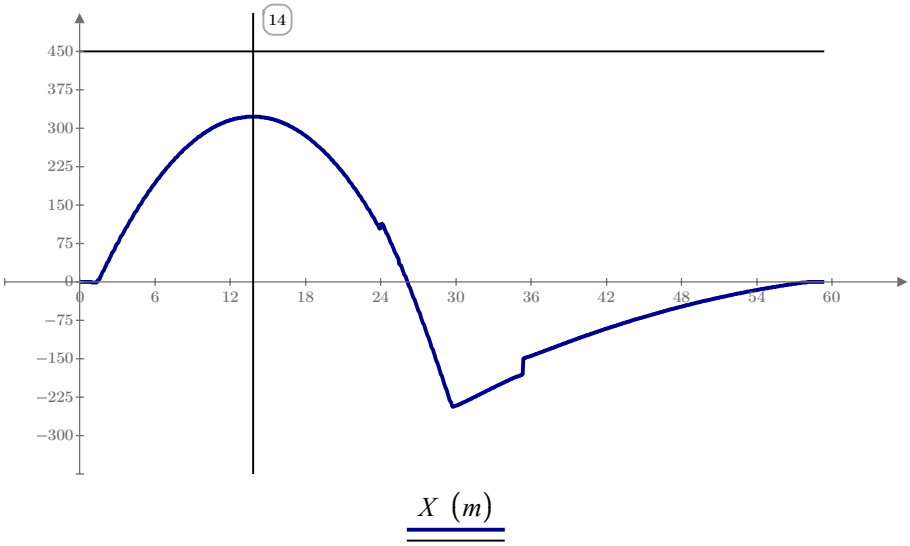

$\frac{\sigma_{stf\_ULS\_cast}(X)\ (MPa)}{f_{ytf.x}(X)\ (MPa)}$

$\eta_{max} := max\left(\frac{\sigma_{stf\_ULS\_cast}(X)}{f_{ytf}}\right) = 72\%$

Bottom flange, in span

$M := M_{d.ULS.LC1}\left(X_{check\_m\_span}\right) = -5409\ kN \cdot m$ Load effect at midspan

$I := I_{y.steel}\left(X_{check\_m\_span}\right) = 0.014\ m^4$ Moment of inertia at midspan

$z := t_{deck} + h_{beam}\left(X_{check\_m\_span}\right) - \frac{t_{bf}\left(X_{check\_m\_span}\right)}{2} - z_{tp.steel}\left(X_{check\_m\_span}\right) = 0.376\ m$ Centre of gravity at midspan measured from the top of concrete deck

$\sigma := \frac{M}{I} \cdot z = -144\ MPa$ = $\sigma_{sbf\_ULS\_cast}\left(X_{check\_m\_span}\right) = -144\ MPa$

$\sigma_{sbf\_ULS\_cast}(X)$ Stresses in bottom flange during construction stage.

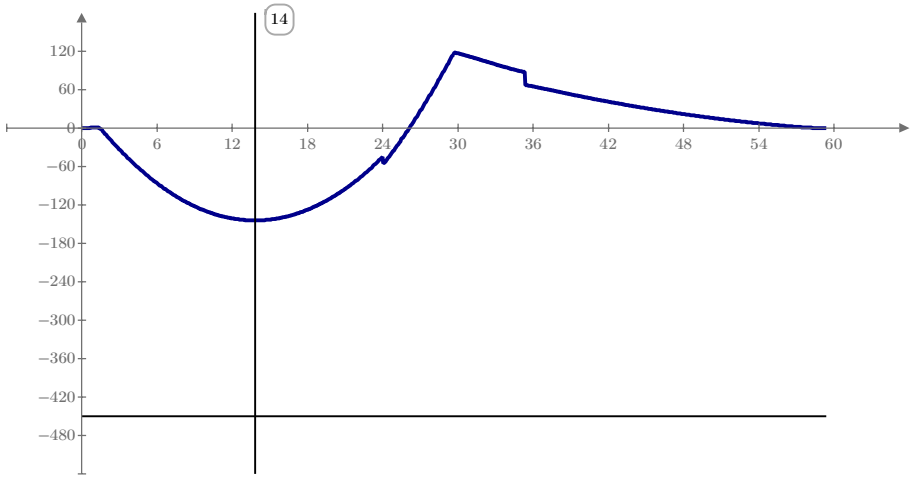

$X\ (m)$

$\sigma_{sbf\_ULS\_cast}(X)\ (MPa)$

$-f_{ybf.x}(X)\ (MPa)$

$\eta_{max} := max\left(\frac{\sigma_{sbf\_ULS\_cast}(X)}{-f_{ybf}}\right) = 32\%$

Top flange, over midsupport

$M := M_{d.ULS.LC2}\left(X_{check\_m\_midsup}\right) = 6274\ kN \cdot m$ Load effect at midsupport

$I := I_{y.steel}\left(X_{check\_m\_midsup}\right) = 0.011\ m^4$ Moment of inertia at midsupport

$z := \left(t_{deck} + \frac{t_{tf}\left(X_{check\_m\_midsup}\right)}{2}\right) - z_{tp.steel}\left(X_{check\_m\_midsup}\right) = -0.8212\ m$ Centre of gravity at midsupport maesured from the top of the concrete deck

$\sigma := \frac{M}{I} \cdot z = -452\ MPa$ = $\sigma_{stf\_ULS\_cast}\left(X_{check\_m\_midsup}\right) = -452\ MPa$

$\sigma_{stf\_ULS\_cast}(X)$ Stresses in the top flange during construction stage.

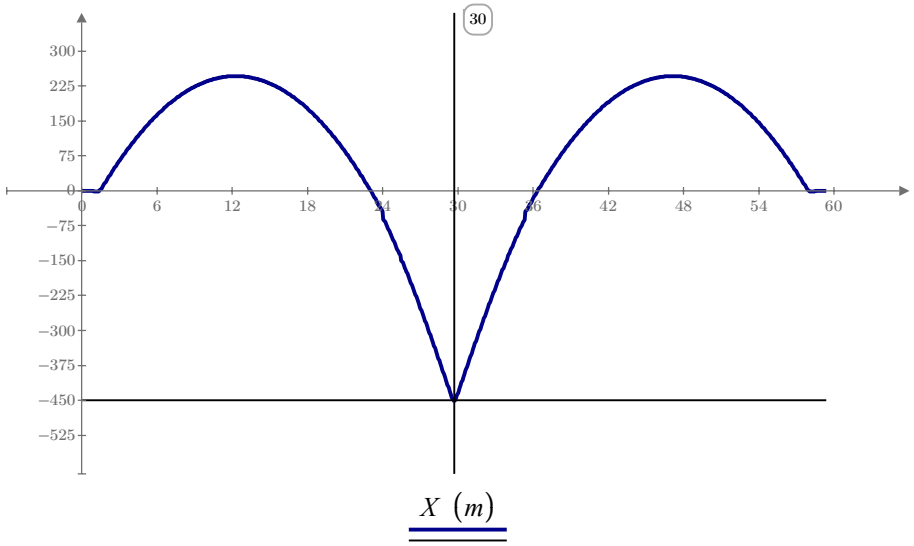

$\sigma_{stf\_ULS\_cast}(X)\ (MPa)$

$-f_{ytf.x}(X)\ (MPa)$

$\eta_{max} := max\left(\frac{\sigma_{stf\_ULS\_cast}(X)}{-f_{ytf}}\right) = 101\%$

Bottom flange, over midsupport

$M := M_{d.ULS.LC2}\left(X_{check\_m\_midsup}\right) = 6274\ kN \cdot m$ Load effect at midsupport

$I := I_{y.steel}\left(X_{check\_m\_midsup}\right) = 0.011\ m^4$ Moment of inertia at midsupport

$z := t_{deck} + h_{beam}\left(X_{check\_m\_midsup}\right) - \frac{t_{bf}\left(X_{check\_m\_midsup}\right)}{2} - z_{tp.steel}\left(X_{check\_m\_midsup}\right) = 0.395\ m$ Centre of gravity at midsupport measured from the top of the concrete deck

$\sigma := \frac{M}{I} \cdot z = 218\ MPa$ = $\sigma_{sbf\_ULS\_cast}\left(X_{check\_m\_midsup}\right) = 218\ MPa$

$\sigma_{sbf\_ULS\_cast}(X)$ Stresses in bottom during construction stage.

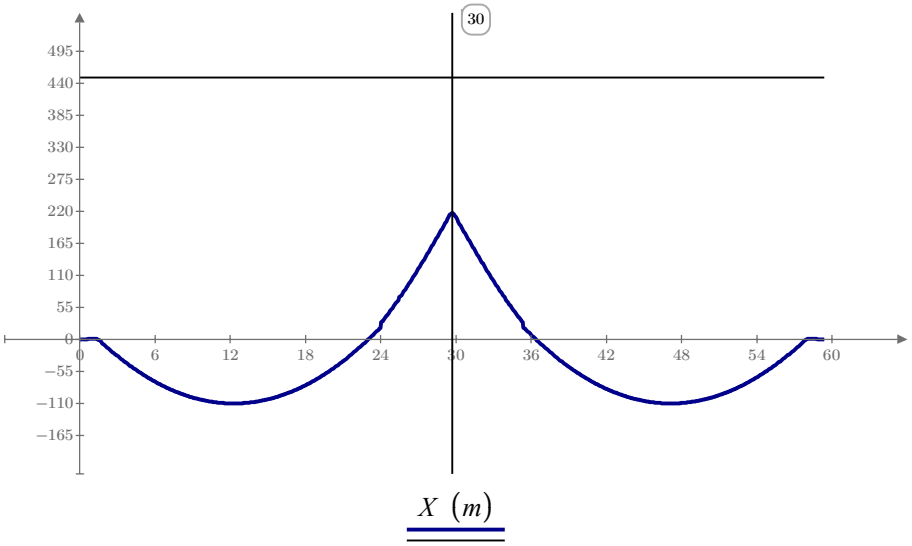

$\sigma_{sbf\_ULS\_cast}(X)\ (MPa)$

$f_{ybf.x}(X)\ (MPa)$

$\eta_{max} := max\left(\frac{\sigma_{sbf\_ULS\_cast}(X)}{f_{ybf}}\right) = 48\%$

5 Capacity checks - Ultimate limit state

The capacity checks that are to be carried out in this chapter are bending moment capacity and shear capacity. Flanges are assumed to carry all the bending and the corrugated web are designed to carry the shear force, i.e Interaction between bending moment and shear force is not checked.

Because the checks are performed by using vectors and closed areas, controll-caluclations are showed for the governing coordinates. Critical points are presented in blue below:

$X_{check\_m\_midsup} = 29.7\ m$ Coordinate for control calculations - bending moment over midsupport

$X_{check\_m\_span} = 13.306\ m$ Coordinate for control calculations - bending moment in span

$X_{check\_v\_midsup} = 29.7\ m$ Coordinate for control calculations - bending moment over midsupport

$X_{check\_v\_endsup} = 1.4\ m$ Coordinate for control calculations - bending moment over endsupport

5.1 Load Combinations

The loads should be combined according to STR/GEO and 6.10a or 6.10b dependent on which case that gives the worst load effects. The load combinations are presented below.

6.10a, all parts in CSC1 or 2

Permanent loads	sup	inf	Unfavorable	Favorable
Self-weight	1.0	1.0	$\gamma_d \cdot 1.35 \cdot sup$	$1.0 \cdot inf$
Surfacing	1.1	0.9	$\gamma_d \cdot 1.35 \cdot sup$	$1.0 \cdot inf$
1st Shrinkage	1.0	1.0	$\gamma_d \cdot 1.35 \cdot sup$	$1.0 \cdot inf$
2nd Shrinkage	1.0	1.0	$\gamma_d \cdot 0.0 \cdot sup$	$0.0 \cdot inf$
2nd Creep	1.0	1.0	$\gamma_d \cdot 0.0 \cdot sup$	$0.0 \cdot inf$
Variable loads	Ψ_0		**Main load**	**Other load**
Traffic loads	0.75		$\gamma_d \cdot 1.5 \cdot \Psi_0$	$\gamma_d \cdot 1.5 \cdot \Psi_0$
Acceleration	0.75		$\gamma_d \cdot 1.5 \cdot 0.6 \cdot \Psi_0$	$\gamma_d \cdot 1.5 \cdot \Psi_0$
Temperature	0.6		$\gamma_d \cdot 0.0 \cdot \Psi_0$	$\gamma_d \cdot 0.0 \cdot \Psi_0$

6.10a, some part in CSC3 or 4

Permanent loads	sup	inf	Unfavorable	Favorable
Self-weight	1.0	1.0	$\gamma_d \cdot 1.35 \cdot sup$	$1.0 \cdot inf$
Surfacing	1.1	0.9	$\gamma_d \cdot 1.35 \cdot sup$	$1.0 \cdot inf$
1st Shrinkage	1.0	1.0	$\gamma_d \cdot 1.35 \cdot sup$	$1.0 \cdot inf$
2nd Shrinkage	1.0	1.0	$\gamma_d \cdot 1.0 \cdot sup$	$1.0 \cdot inf$
2nd Creep	1.0	1.0	$\gamma_d \cdot 1.35 \cdot sup$	$1.0 \cdot inf$
Variable loads	Ψ_0		**Main load**	**Other load**
Traffic loads	0.75		$\gamma_d \cdot 1.5 \cdot \Psi_0$	$\gamma_d \cdot 1.5 \cdot \Psi_0$
Acceleration	0.75		$\gamma_d \cdot 1.5 \cdot 0.6 \cdot \Psi_0$	$\gamma_d \cdot 1.5 \cdot \Psi_0$
Temperature	0.6		$\gamma_d \cdot 1.5 \cdot \Psi_0$	$\gamma_d \cdot 1.5 \cdot \Psi_0$

6.10b, all parts in CSC1 or 2

Permanent loads	sup	inf	Unfavorable	Favorable
Self-weight	1.0	1.0	$\gamma_d \cdot 0.89 \cdot 1.35 \cdot sup$	$1.0 \cdot inf$
Surfacing	1.1	0.9	$\gamma_d \cdot 0.89 \cdot 1.35 \cdot sup$	$1.0 \cdot inf$
1st Shrinkage	1.0	1.0	$\gamma_d \cdot 0.89 \cdot 1.35 \cdot sup$	$0.0 \cdot inf$
2nd Shrinkage	1.0	1.0	$\gamma_d \cdot 0.0 \cdot sup$	$0.0 \cdot inf$
2nd Creep	1.0	1.0	$\gamma_d \cdot 0.0 \cdot sup$	$0.0 \cdot inf$
Variable loads	Ψ_0		**Main load**	**Other load**
Traffic loads	0.75		$\gamma_d \cdot 1.5$	$\gamma_d \cdot 1.5 \cdot \Psi_0$
Acceleration	0.75		$\gamma_d \cdot 1.5 \cdot 0.6$	$\gamma_d \cdot 1.5 \cdot \Psi_0$
Temperature	0.6		$\gamma_d \cdot 0.0$	$\gamma_d \cdot 0.0 \cdot \Psi_0$

6.10b, some part in CSC3 or 4

Permanent loads	sup	inf	Unfavorable	Favorable
Self-weight	1.0	1.0	$\gamma_d \cdot 0.89 \cdot 1.35 \cdot sup$	$1.0 \cdot inf$
Surfacing	1.1	0.9	$\gamma_d \cdot 0.89 \cdot 1.35 \cdot sup$	$1.0 \cdot inf$
1st Shrinkage	1.0	1.0	$\gamma_d \cdot 0.89 \cdot 1.35 \cdot sup$	$1.0 \cdot inf$
2nd Shrinkage	1.0	1.0	$\gamma_d \cdot 1.0 \cdot sup$	$1.0 \cdot inf$
2nd Creep	1.0	1.0	$\gamma_d \cdot 0.89 \cdot 1.35 \cdot sup$	$1.0 \cdot inf$
Variable loads	Ψ_0		**Main load**	**Other load**
Traffic loads	0.75		$\gamma_d \cdot 1.5$	$\gamma_d \cdot 1.5 \cdot \Psi_0$
Acceleration	0.75		$\gamma_d \cdot 1.5 \cdot 0.6$	$\gamma_d \cdot 1.5 \cdot \Psi_0$
Temperature	0.6		$\gamma_d \cdot 1.5$	$\gamma_d \cdot 1.5 \cdot \Psi_0$

5.1.1 Bending moment

Bending moment in the ultimate limit state

$M_{d.ULS.6.10a.midsup}(x)$ Design bending moment from all loads, combined according to STR/GEO 6.10a

$M_{d.ULS.6.10b.midsup}(x)$ Design bending moment from all loads, combined according to STR/GEO 6.10b

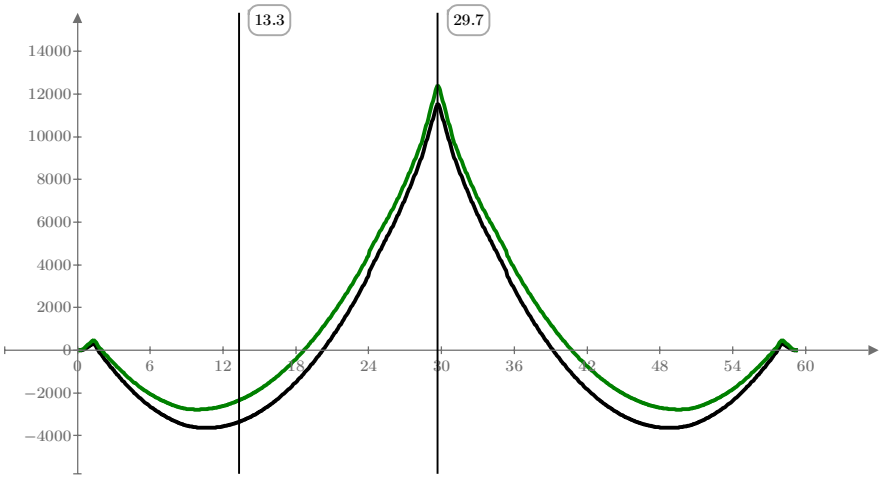

$M_{d.ULS.6.10a.midsup}(X)$ $(m \cdot kN)$

$M_{d.ULS.6.10b.midsup}(X)$ $(kN \cdot m)$

$M_{d.ULS.6.10a.span}(x)$ Design bending moment from all loads, combined according to STR/GEO 6.10a

$M_{d.ULS.6.10b.span}(x)$ Design bending moment from all loads, combined according to STR/GEO 6.10b

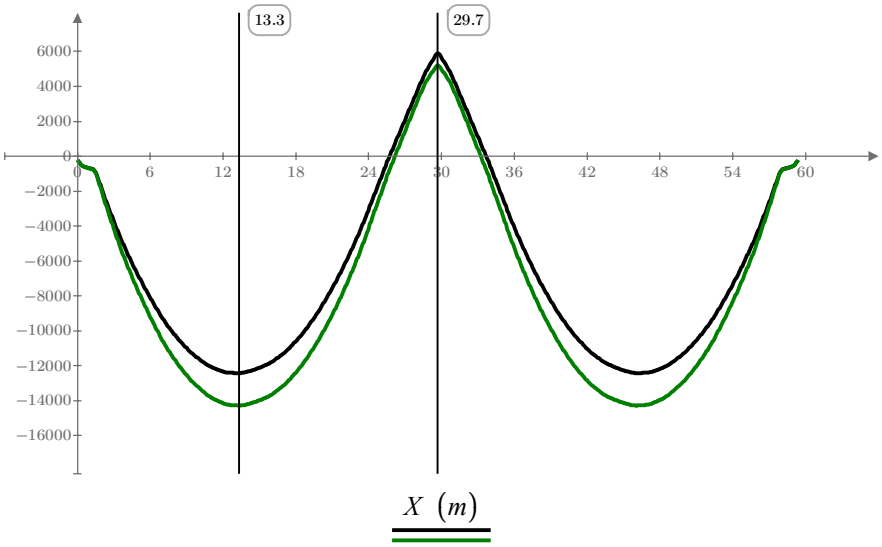

$M_{d.ULS.6.10a.span}(X)$ $(m \cdot kN)$

$M_{d.ULS.6.10b.span}(X)$ $(kN \cdot m)$

The load combination according to STR/GEO 6.10b gives the dimensioning bending moment and will therefore be used for the capacity calculations.

$LoadComb := \text{“6.10b”}$ Load combination that gives worst load effects

5.2 Load Effects

Loads that gives unfavorable moment in span

$M_{d.perm}(x)$ Bending moment from permanent loads

$M_{d.min.tr}(x)$ Bending moment from min traffic loads

$M_{d.temp.min}(x)$ Bending moment from min temperature loads

$M_{d.1.cs}(x)$ Bending moment from first order effects from shrinkage

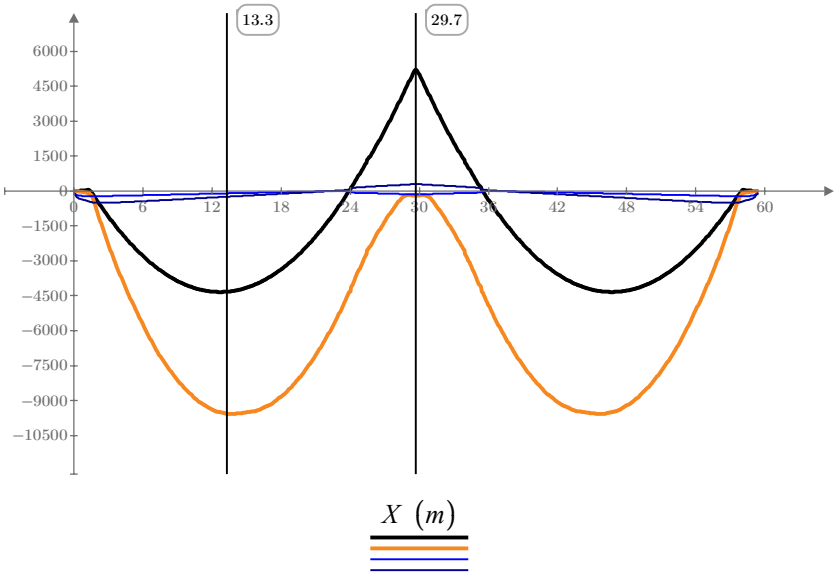

Loads that gives unfavorable moment over support

Second order effects from creep and both first and second order effects from shrinkage will only be acconted for when it gives an unfavorable effects in the capacity checks, i.e over the supports regions.

$M_{d.perm}(x)$ Bending moment from permanent loads

$M_{d.max.tr}(x)$ Bending moment from max traffic loads

$M_{d.temp.max}(x)$ Bending moment from max temperature loads

$M_{d.1.cs}(x)$ Bending moment from first order effects from shrinkage

$M_{d.2.cs}(x)$ Bending moment from second order effects from shrinkage

$M_{d.creep}(x)$ Bending moment from second order effects from creep

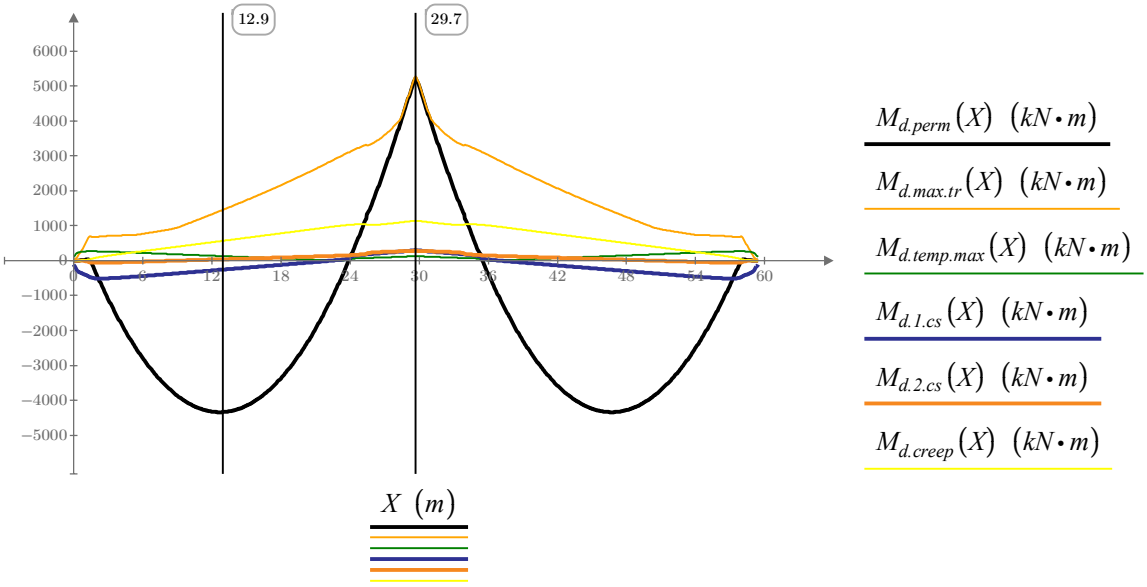

Axial force in the ultimate limit state

$N_{d.perm}(x)$	Normal force from permanent loads
$N_{d.min.tr}(x)$	Min normal force from multi components loads
$N_{d.max.tr}(x)$	Max normal force from multi components loads
$N_{d.temp.min}(x)$	Min normal force from temperature loads
$N_{d.temp.max}(x)$	Max normal force from temperature loads
$N_{d.1.cs}(x)$	Normal force from shrinkage

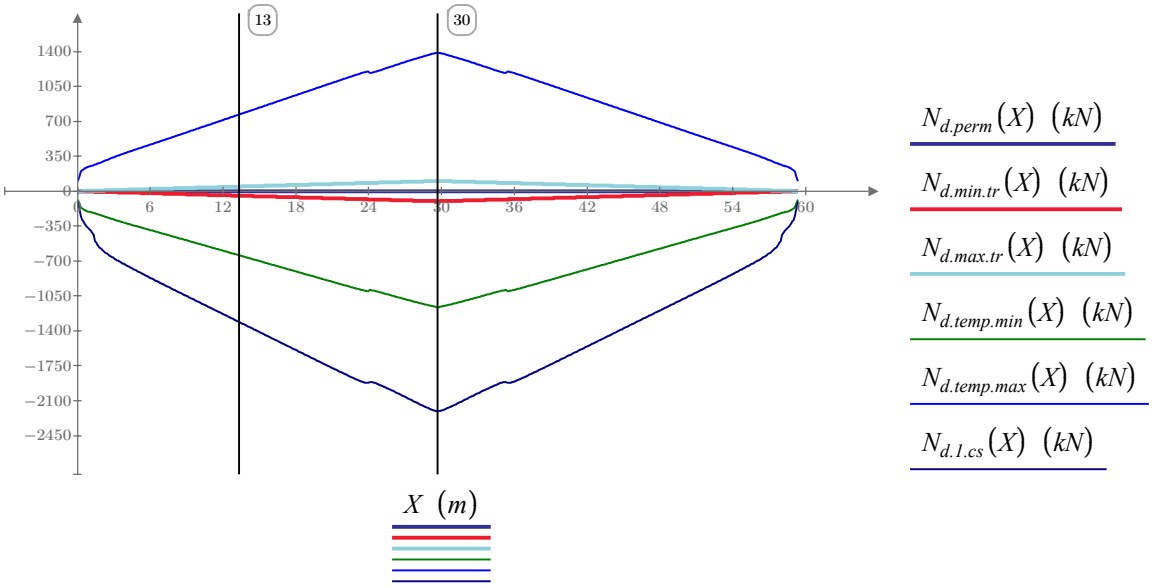

Shear force in the ultimate limit state

$V_{d.per}(x)$ Shear force from permanent loads

$V_{d.tr}(x)$ Shear force from multi components loads

$V_{d.temp}(x)$ Shear force from temperature loads

$V_{d.cs}(x)$ Shear force from shrinkage

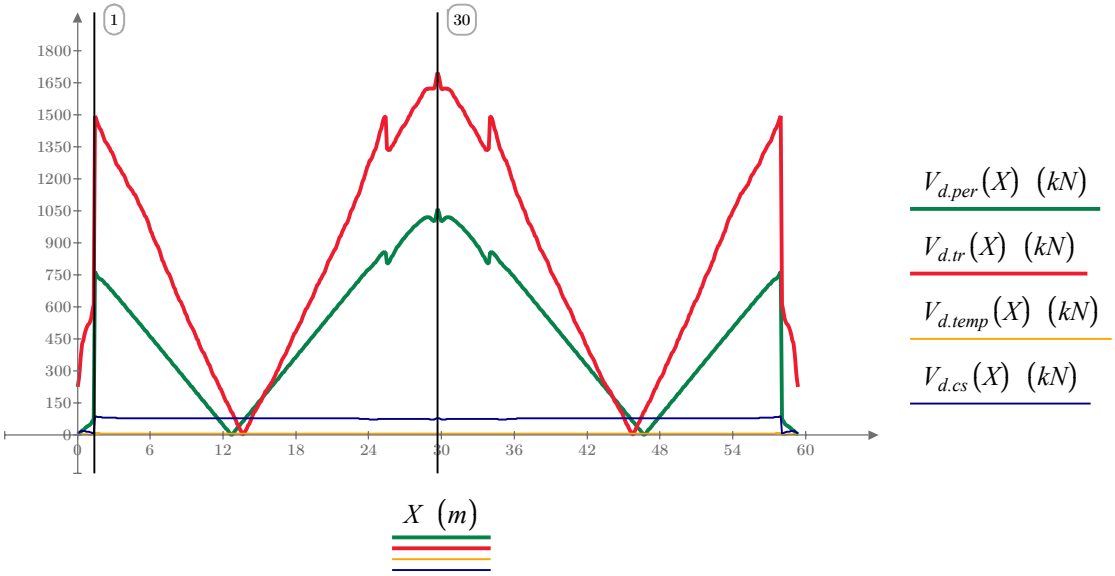

$$V_{d.ULS}(x) := \overrightarrow{V_{d.per}(x) + V_{d.tr}(x) + V_{d.temp}(x) + V_{d.cs}(x)}$$

$V_{d.ULS}(X_{check\_v\_endsup}) = 2363\ kN$ Maximum shear force over end support

$V_{d.ULS}(X_{check\_v\_midsup}) = 2847\ kN$ Maximum shear force over mid support

Second order effects in the ultimate limit state

The second order effects from shrinkage and creep that arises due to the continuous system have an unfavourable effect over the internal support. These effects will therefore be accounted for when calculating the capacity of the cross section over support and not in span. The moment and normal force from the second order effects are plotted below.

$M_{d.creep}(x)$ Moment from second order effects of creep

$M_{d.2.cs}(x)$ Moment from second order effects of shrinkage

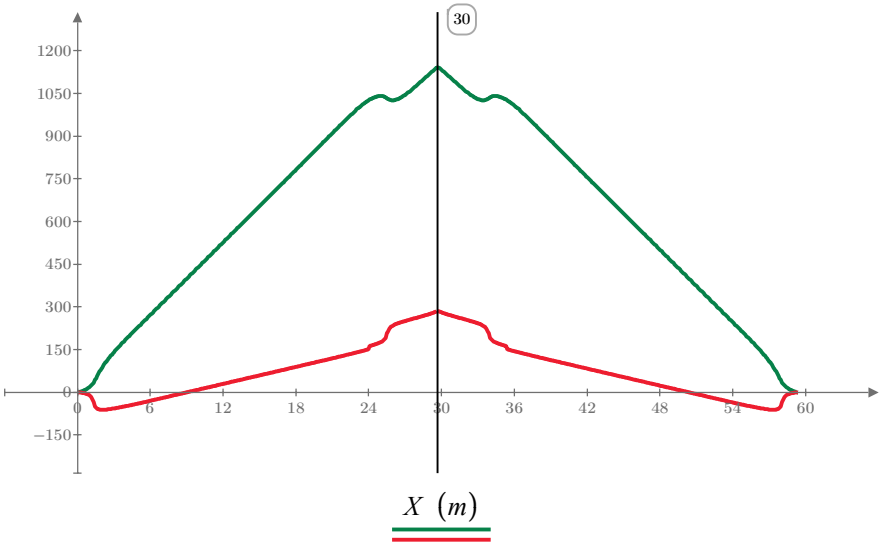

$M_{d.creep}(X)$ $(kN \cdot m)$

$M_{d.2.cs}(X)$ $(kN \cdot m)$

$N_{d.creep}(x)$ Normal force from second order effects of creep

$N_{d.2.cs}(x)$ Normal force from second order effects of shrinkage

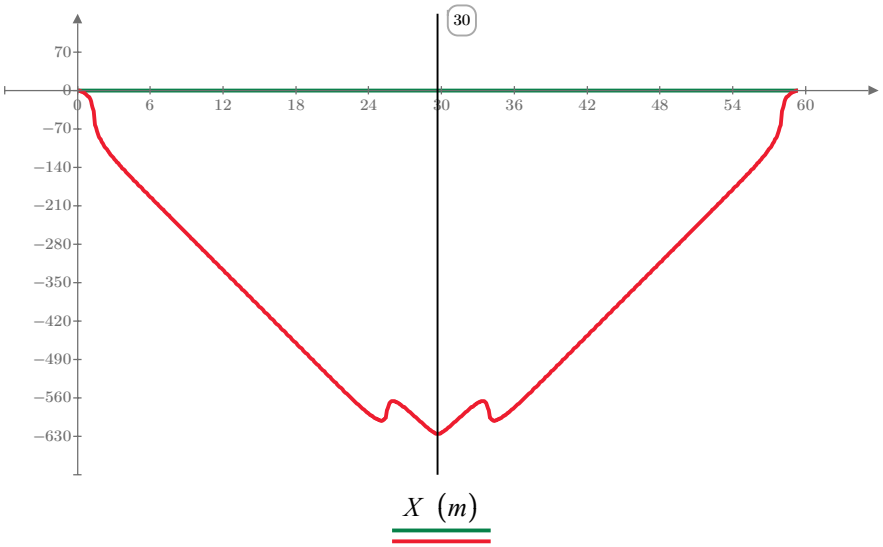

$N_{d.creep}(X)$ (kN)

$N_{d.2.cs}(X)$ (kN)

5.3 Cross-sectional constants

Effective concrete width along the bridge

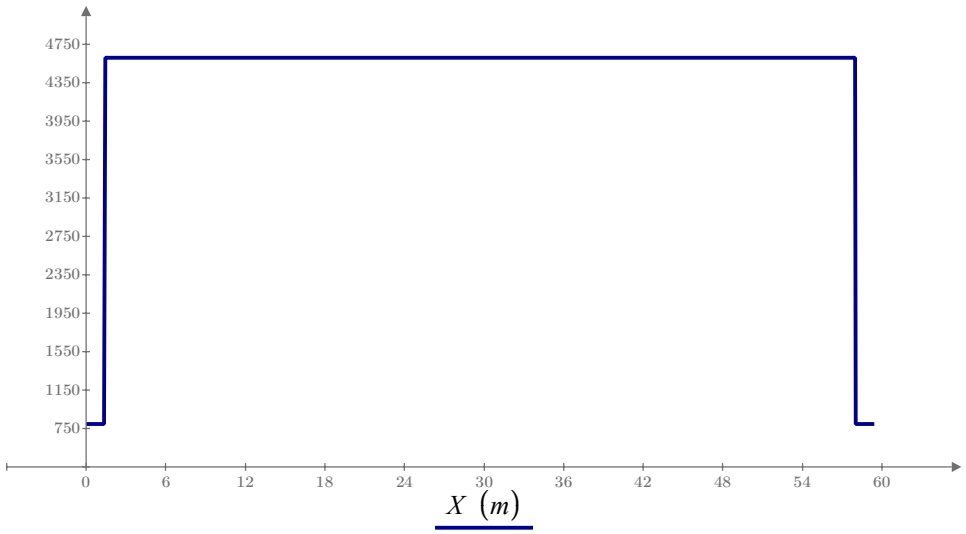

$b_{eff.c}(X)\ \ (mm)$

Effective with of top flange along the bridge with reduction due to shear lag

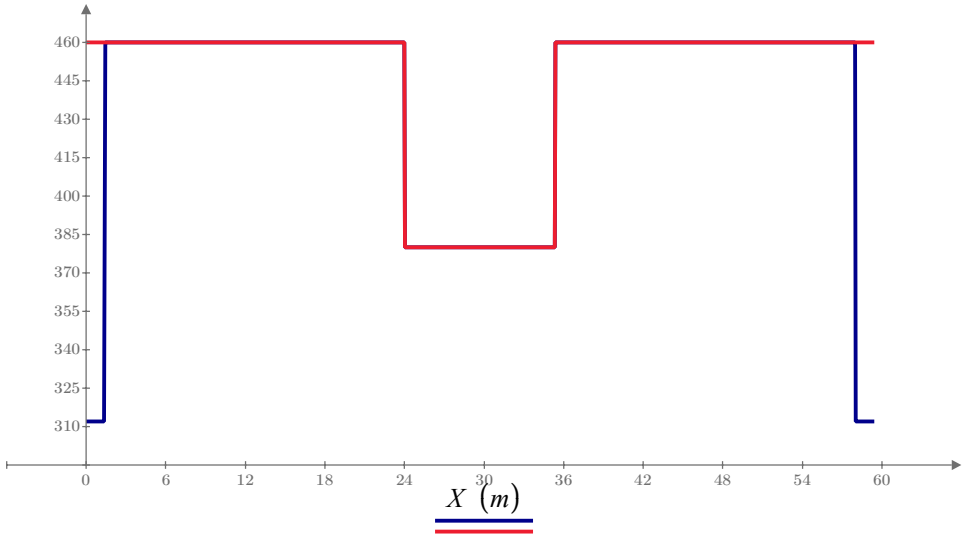

$b_{eff.s}(X)\ \ (mm)$

$b_{tf}(X)\ \ (mm)$

Effective reinforcement area where the concrete is considered as cracked

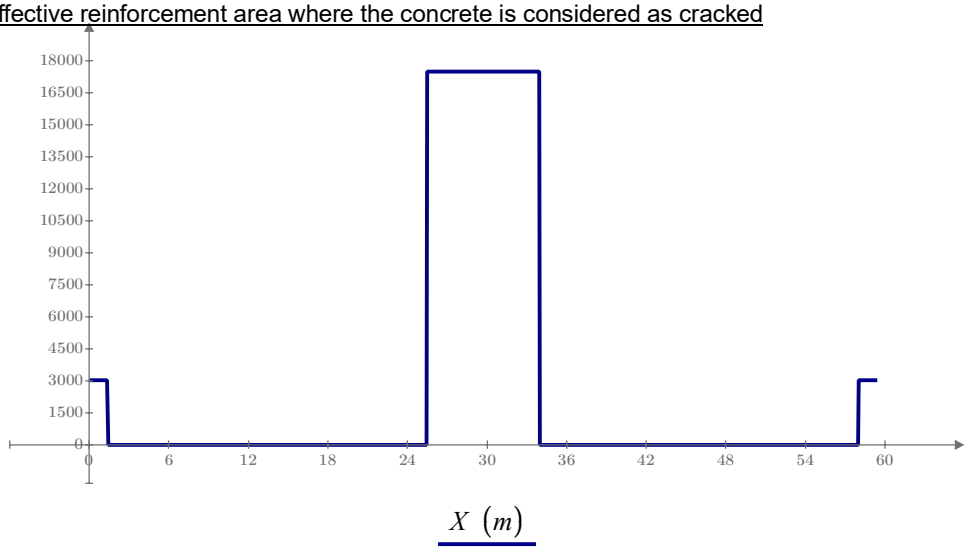

$A_{re}(X)\ \ (mm^2)$

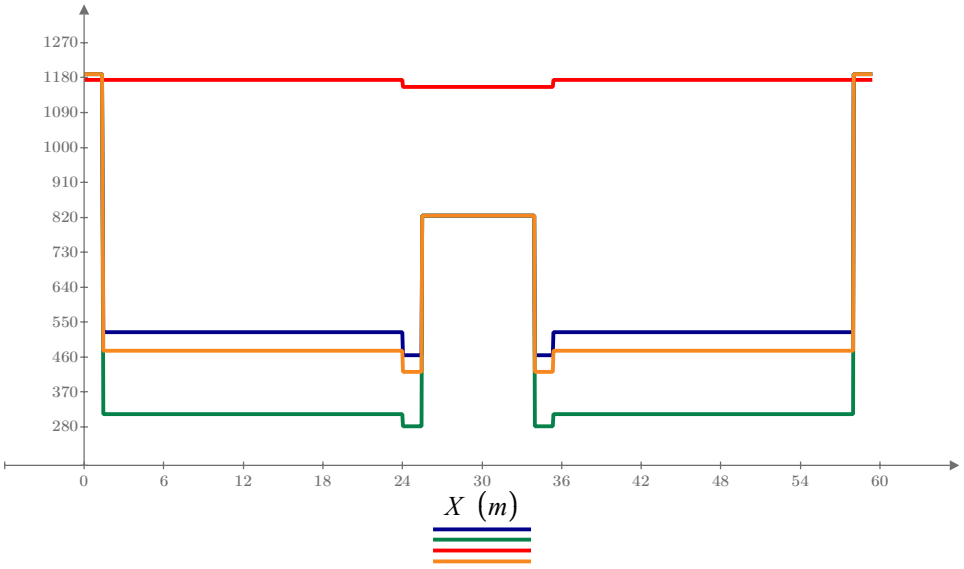

$z_{tp.comp.long}(X)$ (mm)

$z_{tp.comp.short}(X)$ (mm)

$z_{tp.steel}(X)$ (mm)

$z_{tp.comp.cs}(X)$ (mm)

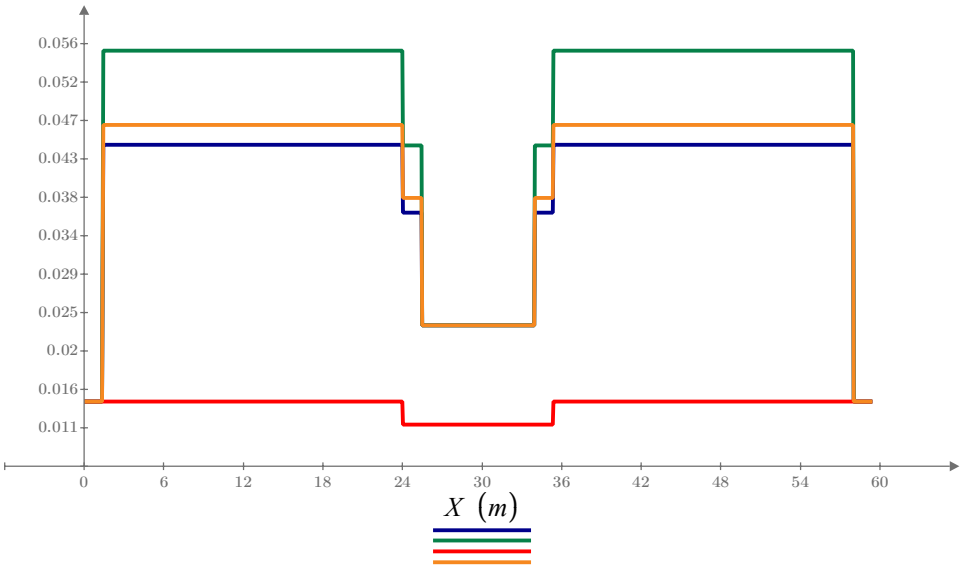

$I_{y.comp.long}(X)$ $\langle m^4 \rangle$

$I_{y.comp.short}(X)$ $\langle m^4 \rangle$

$I_{y.steel}(X)$ $\langle m^4 \rangle$

$I_{y.comp.cs}(X)$ $\langle m^4 \rangle$

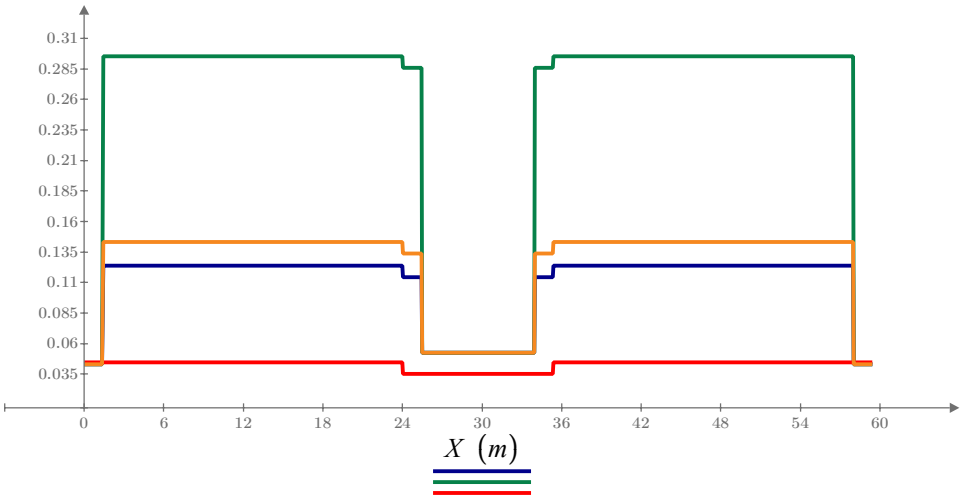

$A_{comp.long}(X)$ $\langle m^2 \rangle$

$A_{comp.short}(X)$ $\langle m^2 \rangle$

$A_{steel}(X)$ $\langle m^2 \rangle$

$A_{comp.cs}(X)$ $\langle m^2 \rangle$

The cross-sectional constants are checked at two locations, one in span and one over the internal support in order to verify the constants in the graphs above.

Span section

At this location, the concrete deck is assumed to be uncracked and composite action is obtained between the concrete and the steel girders.

$b_{ef.con} := b_{eff.c}\left(X_{check\_m\_span}\right) = 4611\ mm$ — Effective width of concrete deck

$A_{ef.con} := b_{ef.con} \cdot t_{deck} = 1.476\ m^2$ — Effective area of concrete deck

$I_{y.ef.con} := \frac{b_{ef.con} \cdot t_{deck}^{3}}{12} = 0.013\ m^4$ — Effective moment of inertia around y-axis

$I_{z.ef.con} := \frac{b_{ef.con}^{3} \cdot t_{deck}}{12} = 2.615\ m^4$ — Effective moment of inertia around z-axis

$b_{ef.steel} := b_{eff.s}\left(X_{check\_m\_span}\right) = 460\ mm$ — Effective width of steel top flange with with regard to shear lag

$bfb := b_{bf}\left(X_{check\_m\_span}\right) = 770\ mm$ — Width of bottom flange

$tfb := t_{bf}\left(X_{check\_m\_span}\right) = 40\ mm$ — Thickness of bottom flange

$tft := t_{tf}\left(X_{check\_m\_span}\right) = 30\ mm$ — Thickness of top flange

$hw := h_w\left(X_{check\_m\_span}\right) = 1180\ mm$ — Height of top flange

$h := h_{beam}\left(X_{check\_m\_span}\right) = 1250\ mm$ — Height of beam

Steel cross-section

$A_s := b_{ef.steel} \cdot tft + bfb \cdot tfb = 0.045\ m^2$

$A_{steel}\left(X_{check\_m\_span}\right) = 0.045\ m^2$

$$z_{tp.s} := \frac{b_{ef.steel} \cdot tft \cdot \left(t_{deck} + \frac{tft}{2}\right) + bfb \cdot tfb \cdot \left(t_{deck} + tft + hw + \frac{tfb}{2}\right)}{A_s} = 1174\ mm$$

$z_{tp.steel}\left(X_{check\_m\_span}\right) = 1174\ mm$

$$I_{y.s} := \frac{b_{ef.steel} \cdot tft^3}{12} + b_{ef.steel} \cdot tft \cdot \left(z_{tp.s} - t_{deck} - \frac{tft}{2}\right)^2 = 0.014\ m^4$$
$$+ \frac{bfb \cdot tfb^3}{12} + bfb \cdot tfb \cdot \left(t_{deck} + h - \frac{tfb}{2} - z_{tp.s}\right)^2$$

$I_{y.steel}\left(X_{check\_m\_span}\right) = 0.014\ m^4$

$$I_{z.s} := \frac{b_{ef.steel}^{3} \cdot tft}{12} + \frac{bfb^3 \cdot tfb}{12} = 0.00177\ m^4$$

$I_{z.steel}\left(X_{check\_m\_span}\right) = 0.00177\ m^4$

Short-term composite section

$n_{L.short} = 5.88$

$$A_{c.short} := \frac{A_{ef.con}}{n_{L.short}} + A_s = 0.295\ m^2$$

$A_{comp.short}(X_{check\_m\_span}) = 0.295\ m^2$

$$z_{tp.c.short} := \frac{A_s \cdot z_{tp.s} + \frac{A_{ef.con}}{n_{L.short}} \cdot \frac{t_{deck}}{2}}{A_{c.short}} = 313\ mm$$

$z_{tp.comp.short}(X_{check\_m\_span}) = 313\ mm$

$$I_{y.c.short} := I_{y.s} + \frac{I_{y.ef.con}}{n_{L.short}} + \frac{A_{ef.con}}{n_{L.short}} \cdot \left(z_{tp.c.short} - \frac{t_{deck}}{2}\right)^2 + A_s \cdot \left(z_{tp.s} - z_{tp.c.short}\right)^2 = 0.055\ m^4$$

$I_{y.comp.short}(X_{check\_m\_span}) = 0.055\ m^4$

$$I_{z.c.short} := I_{z.s} + \frac{I_{z.ef.con}}{n_{L.short}} = 0.446\ m^4$$

$I_{z.comp.short}(X_{check\_m\_span}) = 0.446\ m^4$

Long-term composite section

$n_{L.long} = 18.56$

$$A_{c.long} := \frac{A_{ef.con}}{n_{L.long}} + A_s = 0.124\ m^2$$

$A_{comp.long}(X_{check\_m\_span}) = 0.124\ m^2$

$$z_{tp.c.long} := \frac{A_s \cdot z_{tp.s} + \frac{A_{ef.con}}{n_{L.long}} \cdot \frac{t_{deck}}{2}}{A_{c.long}} = 524\ mm$$

$z_{tp.comp.long}(X_{check\_m\_span}) = 524\ mm$

$$I_{y.c.long} := I_{y.s} + \frac{I_{y.ef.con}}{n_{L.long}} + \frac{A_{ef.con}}{n_{L.long}} \cdot \left(z_{tp.c.long} - \frac{t_{deck}}{2}\right)^2 + A_s \cdot \left(z_{tp.s} - z_{tp.c.long}\right)^2 = 0.044\ m^4$$

$I_{y.comp.long}(X_{check\_m\_span}) = 0.044\ m^4$

$$I_{z.c.short} := I_{z.s} + \frac{I_{z.ef.con}}{n_{L.long}} = 0.143\ m^4$$

$I_{z.comp.long}(X_{check\_m\_span}) = 0.143\ m^4$

Shrinkage composite section

$n_{L.cs} = 14.96$

$$A_{c.cs} := \frac{A_{ef.con}}{n_{L.cs}} + A_s = 0.143\ m^2$$

$$A_{comp.cs}\left(X_{check\_m\_span}\right) = 0.143\ m^2$$

$$z_{tp.c.cs} := \frac{A_s \cdot z_{tp.s} + \frac{A_{ef.con}}{n_{L.cs}} \cdot \frac{t_{deck}}{2}}{A_{c.cs}} = 476\ mm$$

$$z_{tp.comp.cs}\left(X_{check\_m\_span}\right) = 476\ mm$$

$$I_{y.c.cs} := I_{y.s} + \frac{I_{y.ef.con}}{n_{L.cs}} + \frac{A_{ef.con}}{n_{L.cs}} \cdot \left(z_{tp.c.cs} - \frac{t_{deck}}{2}\right)^2 + A_s \cdot \left(z_{tp.s} - z_{tp.c.cs}\right)^2 = 0.046\ m^4$$

$$I_{y.comp.cs}\left(X_{check\_m\_span}\right) = 0.046\ m^4$$

$$I_{z.c.cs} := I_{z.s} + \frac{I_{z.ef.con}}{n_{L.cs}} = 0.176\ m^4$$

$$I_{z.comp.cs}\left(X_{check\_m\_span}\right) = 0.176\ m^4$$

Support section

Over the support, the concrete deck is assumed to be cracked and therefore composite action is obtained between the reinforcement and the steel girders.

$A_{rein} := A_{re}\left(X_{check\_m\_midsup}\right) = 17493\ mm^2$ — Reinforcement area over the support

$b_{ef.steel} := b_{eff.s}\left(X_{check\_m\_midsup}\right) = 380\ mm$ — Effective width of steel top flange with with regard to shear lag

$bfb := b_{bf}\left(X_{check\_m\_midsup}\right) = 640\ mm$ — Width of bottom flange

$tfb := t_{bf}\left(X_{check\_m\_midsup}\right) = 37\ mm$ — Thickness of bottom flange

$tft := t_{tf}\left(X_{check\_m\_midsup}\right) = 30\ mm$ — Thickness of top flange

$hw := h_w\left(X_{check\_m\_midsup}\right) = 1183\ mm$ — Height of top flange

$h := h_{beam}\left(X_{check\_m\_midsup}\right) = 1250\ mm$ — Height of beam

Steel cross-section

$$A_s := b_{ef.steel} \cdot tft + bfb \cdot tfb = 0.035\ m^2$$

$$A_{steel}\left(X_{check\_m\_midsup}\right) = 0.035\ m^2$$

$$z_{tp.s} := \frac{b_{ef.steel} \cdot tft \cdot \left(t_{deck} + \frac{tft}{2}\right) + bfb \cdot tfb \cdot \left(t_{deck} + tft + hw + \frac{tfb}{2}\right)}{A_s} = 1156\ mm$$

$$z_{tp.steel}\left(X_{check\_m\_midsup}\right) = 1156\ mm$$

$$I_{y.s} := \frac{b_{ef.steel} \cdot tft^3}{12} + b_{ef.steel} \cdot tft \cdot \left(z_{tp.s} - t_{deck} - \frac{tft}{2}\right)^2 = 0.011\ m^4$$
$$+ \frac{bfb \cdot tfb^3}{12} + bfb \cdot tfb \cdot \left(t_{deck} + h - \frac{tfb}{2} - z_{tp.s}\right)^2$$

$$I_{y.steel}\left(X_{check\_m\_midsup}\right) = 0.011\ m^4$$

$$I_{z.s} := \frac{b_{ef.steel}^{\ 3} \cdot tft}{12} + \frac{bfb^3 \cdot tfb}{12} = 0.00095\ m^4$$

$$I_{z.steel}\left(X_{check\_m\_midsup}\right) = 0.00095\ m^4$$

Short-term composite section

$$n_{L.short} = 5.88$$

$$A_{c.short} := A_{rein} + A_s = 0.053\ m^2$$

$$A_{comp.short}\left(X_{check\_m\_midsup}\right) = 0.053\ m^2$$

$$z_{tp.c.short} := \frac{A_s \cdot z_{tp.s} + A_{rein} \cdot \frac{t_{deck}}{2}}{A_{c.short}} = 825\ mm$$

$$z_{tp.comp.short}\left(X_{check\_m\_midsup}\right) = 825\ mm$$

$$I_{y.c.short} := A_{rein} \cdot \left(z_{tp.c.short} - \frac{t_{deck}}{2}\right)^2 + I_{y.s} = 0.023\ m^4$$
$$+ A_s \cdot \left(z_{tp.s} - z_{tp.c.short}\right)^2$$

$$I_{y.comp.short}\left(X_{check\_m\_midsup}\right) = 0.023\ m^4$$

$$I_{z.c.short} := I_{z.s} = 0.00095\ m^4$$

$$I_{z.comp.short}\left(X_{check\_m\_midsup}\right) = 0.00095\ m^4$$

Long-term composite section

$n_{L.long} = 18.56$

$A_{c.long} := A_{rein} + A_s = 0.053\ m^2$ $\quad A_{comp.long}\left(X_{check\_m\_midsup}\right) = 0.053\ m^2$

$z_{tp.c.long} := \dfrac{A_s \cdot z_{tp.s} + A_{rein} \cdot \dfrac{t_{deck}}{2}}{A_{c.long}} = 825\ mm$ $\quad z_{tp.comp.long}\left(X_{check\_m\_midsup}\right) = 825\ mm$

$I_{y.c.long} := A_{rein} \cdot \left(z_{tp.c.long} - \dfrac{t_{deck}}{2}\right)^2 + I_{y.s} = 0.023\ m^4$ $\quad I_{y.comp.long}\left(X_{check\_m\_midsup}\right) = 0.023\ m^4$

$+ A_s \cdot \left(z_{tp.s} - z_{tp.c.long}\right)^2$

$I_{z.c.short} := I_{z.s} = 0.00095\ m^4$ $\quad I_{z.comp.long}\left(X_{check\_m\_midsup}\right) = 0.00095\ m^4$

Shrinkage composite section

$n_{L.cs} = 14.96$

$A_{c.cs} := A_{rein} + A_s = 0.053\ m^2$ $\quad A_{comp.cs}\left(X_{check\_m\_midsup}\right) = 0.053\ m^2$

$z_{tp.c.cs} := \dfrac{A_s \cdot z_{tp.s} + A_{rein} \cdot \dfrac{t_{deck}}{2}}{A_{c.cs}} = 825\ mm$ $\quad z_{tp.comp.cs}\left(X_{check\_m\_midsup}\right) = 825\ mm$

$I_{y.c.cs} := A_{rein} \cdot \left(z_{tp.c.cs} - \dfrac{t_{deck}}{2}\right)^2 + I_{y.s} = 0.023\ m^4$ $\quad I_{y.comp.cs}\left(X_{check\_m\_midsup}\right) = 0.023\ m^4$

$+ A_s \cdot \left(z_{tp.s} - z_{tp.c.cs}\right)^2$

$I_{z.c.cs} := I_{z.s} = 0.00095\ m^4$ $\quad I_{z.comp.cs}\left(X_{check\_m\_midsup}\right) = 0.00095\ m^4$

5.4 Stresses in steel cross-section over support

The stresses are calculated for each load with respective cross-sectional constants. The stresses are summarized by the superposition rule.

5.4.1 Stresses due to variable (short term) loads

The variale loads that are included in the system analysis for the global system are traffic and temperature loads.

5.4.1.1 Traffic loads

$M := M_{d.max.tr}\left(X_{check\_m\_midsup}\right) = 5288\ kN \cdot m$ Bending moment

$N := N_{d.max.tr}\left(X_{check\_m\_midsup}\right) = 102\ kN$ Normal force

$A := A_{comp.short}\left(X_{check\_m\_midsup}\right) = 0.053\ m^2$ Cross-sectional area

$I := I_{y.comp.short}\left(X_{check\_m\_midsup}\right) = 0.023\ m^4$ Moment of inertia

$z := z_{tp.comp.short}\left(X_{check\_m\_midsup}\right) = 825\ mm$ Center of gravity from top of concrete deck

$h := h_{beam}\left(X_{check\_m\_midsup}\right) = 1250\ mm$ Height of girder

$t_b := t_{bf}\left(X_{check\_m\_midsup}\right) = 37\ mm$ Thickness of bottom flange

$t_t := t_{tf}\left(X_{check\_m\_midsup}\right) = 30\ mm$ Thickness of top flange

$\sigma_{s.t} := \frac{N}{A} + \frac{M}{I} \cdot \left(t_{deck} - z\right) = -114.2\ MPa$ = $\sigma_{s.t.tr}\left(X_{check\_m\_midsup}\right) = -114.2\ MPa$ Stresses in top flange from short term loads

$\sigma_{s.b} := \frac{N}{A} + \frac{M}{I} \cdot \left(t_{deck} + h - z\right) = 173.5\ MPa$ = $\sigma_{s.b.tr}\left(X_{check\_m\_midsup}\right) = 173.5\ MPa$ Stresses in bottom flange from short term loads

5.4.1.2 Temperature loads

$M_{max} := M_{d.temp.max}\left(X_{check\_m\_midsup}\right) = 129\ kN \cdot m$ Bending moment imposed on steel section

$N_{max} := N_{d.temp.max}\left(X_{check\_m\_midsup}\right) = 1387\ kN$ Normal force imposed on steel section

$M_{min} := M_{d.temp.min}\left(X_{check\_m\_midsup}\right) = -155\ kN \cdot m$ Bending moment imposed on steel section

$N_{min} := N_{d.temp.min}\left(X_{check\_m\_midsup}\right) = -1161\ kN$ Normal force imposed on steel section

$A := A_{steel}\left(X_{check\_m\_midsup}\right) = 0.035\ m^2$ Cross-sectional area - steel section

$I := I_{y.steel}\left(X_{check\_m\_midsup}\right) = 0.011\ m^4$ Moment of inertia - steel section

$z := z_{tp.steel}\left(X_{check\_m\_midsup}\right) = 1156\ mm$ Center of gravity from top of concrete deck- steel section

$h := h_{beam}\left(X_{check\_m\_midsup}\right) = 1250\ mm$ Height of girder

$\sigma_{s.t.min} := \frac{N_{min}}{A} + \frac{M_{max}}{I} \cdot \left(t_{deck} - z\right) = -42.6\ MPa$ = $\sigma_{s.t.temp.min}\left(X_{check\_m\_midsup}\right) = -42.6\ MPa$

$\sigma_{s.t.max} := \frac{N_{max}}{A} + \frac{M_{min}}{I} \cdot \left(t_{deck} - z\right) = 50.9\ MPa$ = $\sigma_{s.t.temp.max}\left(X_{check\_m\_midsup}\right) = 50.9\ MPa$

$\sigma_{s.t} := min\left(\sigma_{s.t.max}, \sigma_{s.t.min}\right) = -42.6\ MPa$ $\sigma_{s.t.temp}(x) := \sigma_{s.t.temp.min}(x)$

$\sigma_{s.b.min} := \frac{N_{min}}{A} + \frac{M_{max}}{I} \cdot \left(t_{deck} + h - z\right) = -28.4\ MPa$ = $\sigma_{s.b.temp.min}\left(X_{check\_m\_midsup}\right) = -28.4\ MPa$

$\sigma_{s.b.max} := \frac{N_{max}}{A} + \frac{M_{min}}{I} \cdot \left(t_{deck} + h - z\right) = 33.9\ MPa$ = $\sigma_{s.b.temp.max}\left(X_{check\_m\_midsup}\right) = 33.9\ MPa$

$\sigma_{s.b} := max\left(\sigma_{s.b.max}, \sigma_{s.b.min}\right) = 33.9\ MPa$ $\sigma_{s.b.temp}(x) := \sigma_{s.b.temp.max}(x)$

5.4.2 Stresses due to permanent loads

$M := M_{d.perm}\left(X_{check\_m\_midsup}\right) = 5219\ kN \cdot m$ Bending moment

$I := I_{y.comp.long}\left(X_{check\_m\_midsup}\right) = 0.023\ m^4$ Moment of inertia

$z := z_{tp.comp.long}\left(X_{check\_m\_midsup}\right) = 825\ mm$ Center of gravity from top of concrete deck

$h := h_{beam}\left(X_{check\_m\_midsup}\right) = 1250\ mm$ Height of girder

$t_b := t_{bf}\left(X_{check\_m\_midsup}\right) = 37\ mm$ Thickness of bottom flange

$t_t := t_{tf}\left(X_{check\_m\_midsup}\right) = 30\ mm$ Thickness of top flange

$\sigma_{s.t} := \frac{M}{I} \cdot \left(t_{deck} - z\right) = -114.6\ MPa$ = $\sigma_{s.t.perm}\left(X_{check\_m\_midsup}\right) = -114.6\ MPa$ Stresses in top flange from additional permanent loads

$\sigma_{s.b} := \frac{M}{I} \cdot \left(t_{deck} + h - z\right) = 169.3\ MPa$ = $\sigma_{s.b.perm}\left(X_{check\_m\_midsup}\right) = 169.3\ MPa$ Stresses in bottom flange from additional permanent loads

5.4.3 Stresses due to shrinkage, first order effects

Over the support, the concrete is considered as cracked and therefore the normal forces due to shrinkage in the steel cross-section is equal to 0.

$M := M_{d.1.cs}\left(X_{check\_m\_midsup}\right) = 303\ kN \cdot m$ Bending moment imposed on steel section

$A := A_{steel}\left(X_{check\_m\_midsup}\right) = 0.035\ m^2$ Cross-sectional area - steel section

$I := I_{y.steel}\left(X_{check\_m\_midsup}\right) = 0.011\ m^4$ Moment of inertia - steel section

$z := z_{tp.steel}\left(X_{check\_m\_midsup}\right) = 1156\ mm$ Center of gravity from top of concrete deck- steel section

$h := h_{beam}\left(X_{check\_m\_midsup}\right) = 1250\ mm$ Height of girder

$\sigma_{s.t} := \frac{M}{I} \cdot \left(t_{deck} - z\right) = -22.23\ MPa$ = $\sigma_{s.t.shrink}\left(X_{check\_m\_midsup}\right) = -22.23\ MPa$ Stresses in top flange due to shrinkage

$\sigma_{s.b} := \frac{M}{I} \cdot \left(t_{deck} + h - z\right) = 11\ MPa$ = $\sigma_{s.b.shrink}\left(X_{check\_m\_midsup}\right) = 11\ MPa$ Stresses in lower flange due to shrinkage

5.4.4 Stresses due to shrinkage, second order effects

Over the support, the concrete is considered as cracked and therefore the normal forces due to the second order effects of shrinkage in the steel cross-section is equal to 0.

$M := M_{d.2.cs}\left(X_{check\_m\_midsup}\right) = 285\ kN \cdot m$ Bending moment imposed on steel section

$A := A_{steel}\left(X_{check\_m\_midsup}\right) = 0.035\ m^2$ Cross-sectional area - steel section

$I := I_{y.steel}\left(X_{check\_m\_midsup}\right) = 0.011\ m^4$ Moment of inertia - steel section

$z := z_{tp.steel}\left(X_{check\_m\_midsup}\right) = 1156\ mm$ Center of gravity from top of concrete deck - steel section

$t_t := t_{tf}\left(X_{check\_m\_midsup}\right) = 30\ mm$

$h := h_{beam}\left(X_{check\_m\_midsup}\right) = 1250\ mm$ Height of girder

$\sigma_{s.t} := \frac{M}{I} \cdot \left(t_{deck} - z\right) = -20.94\ MPa$ = $\sigma_{s.t.shrink.2}\left(X_{check\_m\_midsup}\right) = -20.94\ MPa$ Stresses in top flange due to shrinkage

$\sigma_{s.b} := \frac{M}{I} \cdot \left(t_{deck} + h - z\right) = 10.4\ MPa$ = $\sigma_{s.b.shrink.2}\left(X_{check\_m\_midsup}\right) = 10.4\ MPa$ Stresses in bottom flange due to shrinkage

5.4.5 Stresses due to second order effects of creep

$M := M_{d.creep}\left(X_{check\_m\_midsup}\right) = 1142\ kN \cdot m$ Bending moment

$N := N_{d.creep}\left(X_{check\_m\_midsup}\right) = 0\ N$ Normal force

$I := I_{y.comp.long}\left(X_{check\_m\_midsup}\right) = 0.023\ m^4$ Moment of inertia

$A := A_{comp.long}\left(X_{check\_m\_midsup}\right) = 0.05\ m^2$ Cross-sectional area - composite section

$z := z_{tp.comp.long}\left(X_{check\_m\_midsup}\right) = 825\ mm$ Center of gravity from top of concrete deck

$h := h_{beam}\left(X_{check\_m\_midsup}\right) = 1250\ mm$ Height of girder

$\sigma_{s.t} := \frac{N}{A} + \frac{M}{I} \cdot \left(t_{deck} - z\right) = -25.1\ MPa$ = $\sigma_{s.t.creep}\left(X_{check\_m\_midsup}\right) = -25.1\ MPa$ Stresses in top flange from additional permanent loads

$\sigma_{s.b} := \frac{N}{A} + \frac{M}{I} \cdot \left(t_{deck} + h - z\right) = 37.1\ MPa$ = $\sigma_{s.b.creep}\left(X_{check\_m\_midsup}\right) = 37.1\ MPa$ Stresses in bottom flange from additional permanent loads

5.4.6 Summary of stresses over support

Stresses in top flange over support

$$\sigma_{s.t.support}(x) := \sigma_{s.t.tr}(x) + \sigma_{s.t.perm}(x) + \sigma_{s.t.temp}(x) + \sigma_{s.t.shrink}(x) + \sigma_{s.t.shrink.2}(x) + \sigma_{s.t.creep}(x)$$

Stresses in bottom flange over support

$$\sigma_{s.b.support}(x) := \sigma_{s.b.tr}(x) + \sigma_{s.b.perm}(x) + \sigma_{s.b.temp}(x) + \sigma_{s.b.shrink}(x) + \sigma_{s.b.shrink.2}(x) + \sigma_{s.b.creep}(x)$$

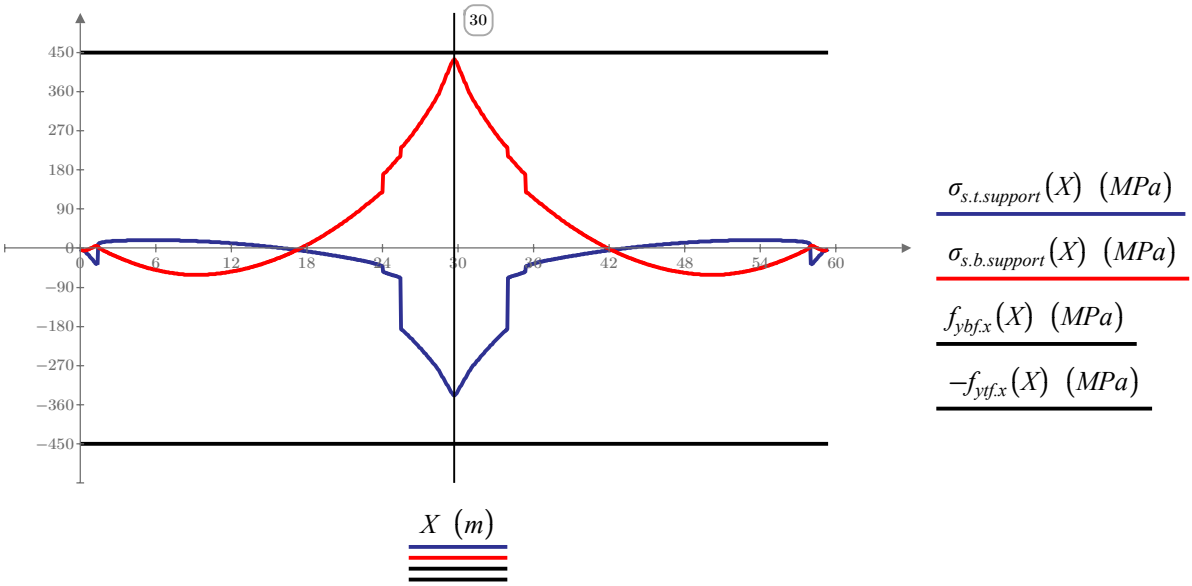

$$\eta_{\sigma.t.max} := max\left(\frac{\sigma_{s.t.support}(X)}{-f_{ytf.x}(X)}\right) = 75\%$$

Maximum utilization rate - top flange

$$\eta_{\sigma.b.max} := max\left(\frac{\sigma_{s.b.support}(X)}{f_{ybf.x}(X)}\right) = 97\%$$

Maximum utilization rate - bottom flange

5.5 Stresses in steel cross-section in span

The stresses are calculated for each load with respective cross-sectional constants. The stresses are summarized by the superposition rule.

5.5.1 Stresses due to variable (short term) loads

The variale loads that are included in the system analysis for the global system are traffic and temperature loads.

5.5.1.1 Traffic loads

$M := M_{d.min.tr}\left(X_{check\_m\_span}\right) = -9573\ kN \cdot m$ Bending moment

$N := N_{d.min.tr}\left(X_{check\_m\_span}\right) = -46\ kN$ Normal force

$A := A_{comp.short}\left(X_{check\_m\_span}\right) = 0.295\ m^2$ Cross-sectional area

$I := I_{y.comp.short}\left(X_{check\_m\_span}\right) = 0.055\ m^4$ Moment of inertia

$z := z_{tp.comp.short}\left(X_{check\_m\_span}\right) = 313\ mm$ Center of gravity from top of concrete deck

$h := h_{beam}\left(X_{check\_m\_span}\right) = 1250\ mm$ Height of girder

$t_b := t_{bf}\left(X_{check\_m\_span}\right) = 40\ mm$ Thickness of bottom flange

$t_t := t_{tf}\left(X_{check\_m\_span}\right) = 30\ mm$ Thickness of top flange

$\sigma_{s.t} := \frac{N}{A} + \frac{M}{I} \cdot \left(t_{deck} - z\right) = -1.4\ MPa$ = $\sigma_{s.t.tr}\left(X_{check\_m\_span}\right) = -1.4\ MPa$ Stresses in top flange from short term loads

$\sigma_{s.b} := \frac{N}{A} + \frac{M}{I} \cdot \left(t_{deck} + h - z\right) = -218.3\ MPa$ = $\sigma_{s.b.tr}\left(X_{check\_m\_span}\right) = -218.3\ MPa$ Stresses in bottom flange from short term loads

5.5.1.2 Temperature loads

$M_{max} := M_{d.temp.max}\left(X_{check\_m\_span}\right) = 124\ kN \cdot m$ Bending moment imposed on steel section

$N_{max} := N_{d.temp.max}\left(X_{check\_m\_span}\right) = 767\ kN$ Normal force imposed on steel section

$M_{min} := M_{d.temp.min}\left(X_{check\_m\_span}\right) = -104\ kN \cdot m$ Bending moment imposed on steel section

$N_{min} := N_{d.temp.min}\left(X_{check\_m\_span}\right) = -642\ kN$ Normal force imposed on steel section

$A := A_{steel}\left(X_{check\_m\_span}\right) = 0.045\ m^2$ Cross-sectional area - steel section

$I := I_{y.steel}\left(X_{check\_m\_span}\right) = 0.014\ m^4$ Moment of inertia - steel section

$z := z_{tp.steel}\left(X_{check\_m\_span}\right) = 1174\ mm$ Center of gravity from top of concrete deck - steel section

$h := h_{beam}\left(X_{check\_m\_span}\right) = 1250\ mm$ Height of girder

$\sigma_{s.t.min} := \frac{N_{min}}{A} + \frac{M_{max}}{I} \cdot \left(t_{deck} - z\right) = -21.91\ MPa =$ $\sigma_{s.t.temp.min}\left(X_{check\_m\_span}\right) = -21.91\ MPa$

$\sigma_{s.t.max} := \frac{N_{max}}{A} + \frac{M_{min}}{I} \cdot \left(t_{deck} - z\right) = 23.49\ MPa$ = $\sigma_{s.t.temp.max}\left(X_{check\_m\_span}\right) = 23.49\ MPa$

$\sigma_{s.t} := max\left(\sigma_{s.t.max}, \sigma_{s.t.min}\right) = 23.49\ MPa$ $\sigma_{s.t.temp}(x) := \sigma_{s.t.temp.max}(x)$

$\sigma_{s.b.min} := \frac{N_{min}}{A} + \frac{M_{max}}{I} \cdot \left(t_{deck} + h - z\right) = -10.9\ MPa$ = $\sigma_{s.b.temp.min}\left(X_{check\_m\_span}\right) = -10.9\ MPa$

$\sigma_{s.b.max} := \frac{N_{max}}{A} + \frac{M_{min}}{I} \cdot \left(t_{deck} + h - z\right) = 14.3\ MPa$ = $\sigma_{s.b.temp.max}\left(X_{check\_m\_span}\right) = 14.3\ MPa$

$\sigma_{s.b} := min\left(\sigma_{s.b.max}, \sigma_{s.b.min}\right) = -10.9\ MPa$ $\sigma_{s.b.temp}(x) := \sigma_{s.b.temp.min}(x)$

5.5.2 Stresses due to permanent loads

$M := M_{d.perm}\left(X_{check\_m\_span}\right) = -4326\ kN \cdot m$ Bending moment

$I := I_{y.comp.long}\left(X_{check\_m\_span}\right) = 0.044\ m^4$ Moment of inertia

$z := z_{tp.comp.long}\left(X_{check\_m\_span}\right) = 524\ mm$ Center of gravity from top of concrete deck

$h := h_{beam}\left(X_{check\_m\_span}\right) = 1250\ mm$ Height of girder

$t_b := t_{bf}\left(X_{check\_m\_span}\right) = 40\ mm$ Thickness of bottom flange

$t_t := t_{tf}\left(X_{check\_m\_span}\right) = 30\ mm$ Thickness of top flange

$\sigma_{s.t} := \frac{M}{I} \cdot \left(t_{deck} - z\right) = 20\ MPa$ = $\sigma_{s.t.perm}\left(X_{check\_m\_span}\right) = 20\ MPa$ Stresses in top flange from additional permanent loads

$\sigma_{s.b} := \frac{M}{I} \cdot \left(t_{deck} + h - z\right) = -102.49\ MPa$ = $\sigma_{s.b.perm}\left(X_{check\_m\_span}\right) = -102.49\ MPa$ Stresses in bottom flange from additional permanent loads

5.5.3 Stresses due to shrinkage, first order effect

$M := M_{d.1.cs}\left(X_{check\_m\_span}\right) = -247\ kN \cdot m$ Bending moment imposed on steel section

$N := N_{d.1.cs}\left(X_{check\_m\_span}\right) = -1310\ kN$ Normal force imposed on steel section

$A := A_{steel}\left(X_{check\_m\_span}\right) = 0.045\ m^2$ Cross-sectional area - steel section

$I := I_{y.steel}\left(X_{check\_m\_span}\right) = 0.014\ m^4$ Moment of inertia - steel section

$z := z_{tp.steel}\left(X_{check\_m\_span}\right) = 1174\ mm$ Center of gravity from top of the concrete deck - steel section

$h := h_{beam}\left(X_{check\_m\_span}\right) = 1250\ mm$ Height of girder

$\sigma_{s.t} := \frac{N}{A} + \frac{M}{I} \cdot \left(t_{deck} - z\right) = -14.4\ MPa$ = $\sigma_{s.t.shrink}\left(X_{check\_m\_span}\right) = -14.4\ MPa$ Stresses in top flange due to shrinkage

$\sigma_{s.b} := \frac{N}{A} + \frac{M}{I} \cdot \left(t_{deck} + h - z\right) = -36.3\ MPa$ = $\sigma_{s.b.shrink}\left(X_{check\_m\_span}\right) = -36.3\ MPa$ Stresses in bottom flange due to shrinkage

5.5.4 Summary of stresses in span

Stresses in top flange over support

$\sigma_{s.t.span}(x) := \sigma_{s.t.tr}(x) + \sigma_{s.t.perm}(x) + \sigma_{s.t.shrink}(x) + \sigma_{s.t.temp}(x)$ Stresses in top flange in span

Stresses in bottom flange over support

$\sigma_{s.b.span}(x) := \sigma_{s.b.tr}(x) + \sigma_{s.b.perm}(x) + \sigma_{s.b.shrink}(x) + \sigma_{s.b.temp}(x)$ Stresses in bottom flange in span

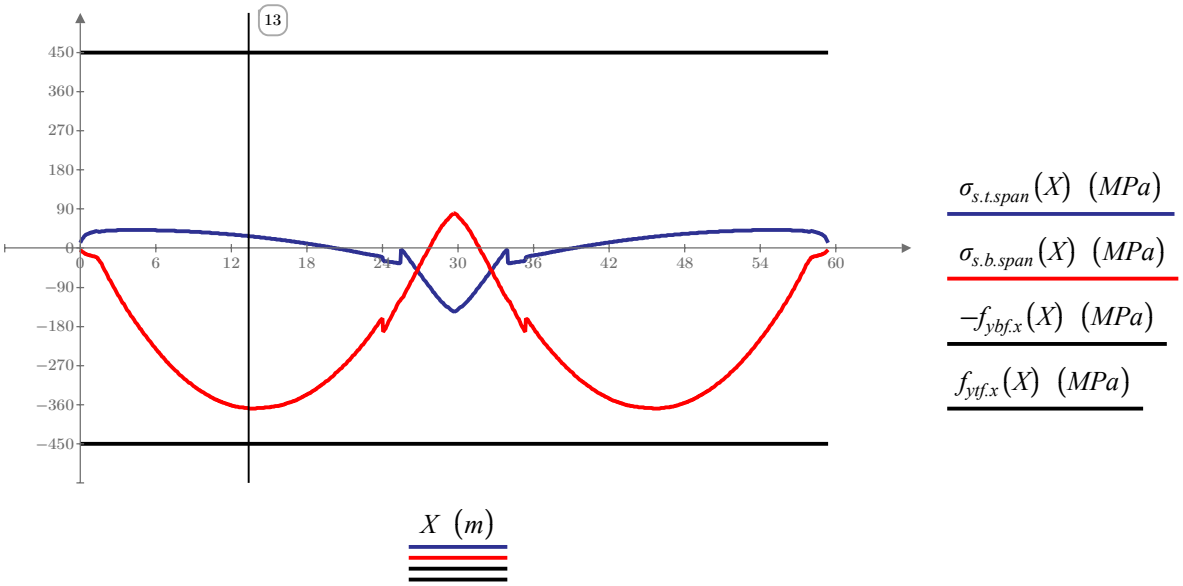

$\eta_{\sigma.t.max} := max\left(\frac{\sigma_{s.t.span}(X)}{f_{ytf.x}(X)}\right) = 9\%$ Maximum utilization rate - top flange

$\eta_{\sigma.b.max} := max\left(\frac{\sigma_{s.b.span}(X)}{-f_{ybf.x}(X)}\right) = 82\%$ Maximum utilization rate - bottom flange

5.6 Shear capacity

The shear capacity of the corrugated steel girder is calculated according to SS-EN 1993-1-5, Appendix D.
The shear capacity is checked at two locations, end-support and midsupport.

Local buckling factor

$a_{c1} = 70\ mm$ $a_{c2} = 68\ mm$ — Corrugation geometries

$w_c := a_{c1} + a_{c4} = 125\ mm$ — Straight length of corrugation

$s_c := a_{c1} + a_{c2} = 138\ mm$ — Total length of corrugation

$a_{cmax} := max\left(a_{c1}, a_{c2}\right) = 70\ mm$ — SS-EN 1993-1-5 D.2.2.(2)

$tw := t_w\left(X_{check\_v\_midsup}\right) = 9\ mm$ — Web thickness

$\tau_{cr} := 4.83 \cdot E_s \cdot \left(\frac{tw}{a_{cmax}}\right)^2 = 15969\ MPa$ — SS-EN 1993-1-5 D.2.2.(2) Equation D.7

$\lambda_c := \sqrt{\frac{f_{yw}}{\tau_{cr} \cdot \sqrt{3}}} = 0.132$ — SS-EN 1993-1-5 D.2.2.(2) Equation D.6

$\chi_l := min\left(\frac{1.15}{0.9 + \lambda_c}, 1\right) = 1.00$ = $\chi_{c.l}\left(X_{check\_v\_midsup}\right) = 1.00$ — Reduction factor local buckling - SS-EN 1993-1-5 D.2.2.(2) Equation D.5

Global buckling factor

$D_X := \frac{E_s \cdot tw^3}{12 \cdot \left(1 - v^2\right)} \cdot \frac{w_c}{s_c} = 12\ kN \cdot m$ — SS-EN 1993-1-5 D.2.2.(3)

$D_Z := \frac{E_s \cdot tw \cdot {a_{c3}}^2}{12} \cdot \frac{\left(3\ a_{c1} + a_{c2}\right)}{w_c} = 534\ kN \cdot m$ — SS-EN 1993-1-5 D.2.2.(3)

$hw := h_w\left(X_{check\_v\_midsup}\right) = 1183\ mm$ — Web height

$\tau := \frac{32.4}{tw \cdot hw^2} \cdot \sqrt[4]{D_X \cdot {D_Z}^3} = 533\ MPa$ — SS-EN 1993-1-5 D.2.2.(3) Equation D.10

$\lambda := \sqrt{\frac{f_{yw}}{\tau \cdot \sqrt{3}}} = 0.72$ — SS-EN 1993-1-5 D.2.2.(3) Equation D.9

$\chi_g := min\left(\frac{1.5}{0.5 + \lambda^2}, 1\right) = 1.00$ = $\chi_{c.g}\left(X_{check\_v\_midsup}\right) = 1.00$ — Global buckling factor SS-EN 1993-1-5 D.2.2.(3) Equation D.8

$\chi_C := min\left(\chi_g, \chi_l\right) = 1$ = $\chi_c\left(X_{check\_v\_midsup}\right) = 1.00$ — SS-EN 1993-1-5 D.2.2

$$V_{Rd} := \chi_C \cdot \frac{f_{yw}}{\gamma_{M1} \cdot \sqrt{3}} \cdot hw \cdot tw = 2951\ kN \quad = \quad V_{Rdw}\left(X_{check\_v\_midsup}\right) = 2951\ kN$$

SS-EN 1993-1-5 D.2.2.(1) Eq.D.4

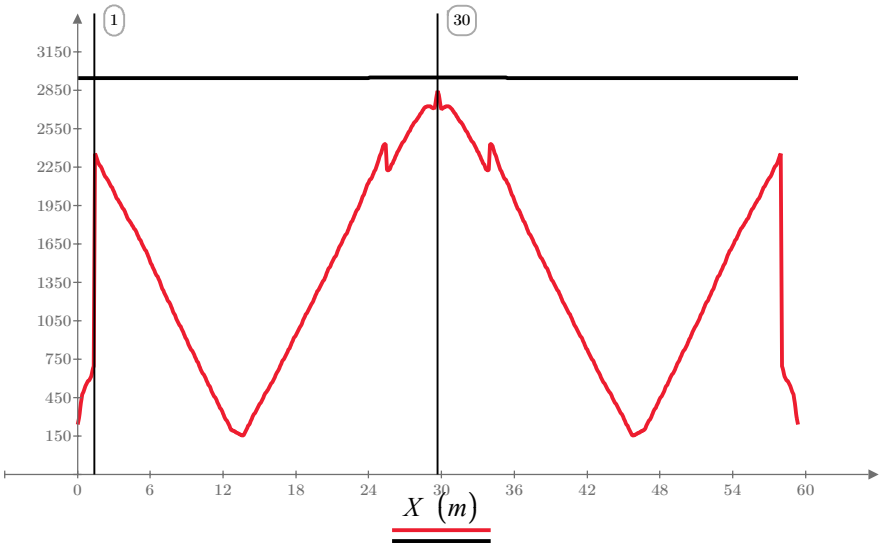

$V_{d.ULS}(X)\ \ (kN)$

$V_{Rdw}(X)\ \ (kN)$

$$\eta_{V.midsup} := \frac{V_{d.ULS}\left(X_{check\_v\_midsup}\right)}{V_{Rdw}\left(X_{check\_v\_midsup}\right)} = 96\%$$

Maximum utilization rate over midsupport

$$\eta_{V.endsup} := \frac{V_{d.ULS}\left(X_{check\_v\_endsup}\right)}{V_{Rdw}\left(X_{check\_v\_endsup}\right)} = 80\%$$

Maximum utilization rate over endsupport

5.7 Lateral torsional buckling of compressed bottom flange over support

Due to composite action with compressed top flange in span the check of LT-buckling of compressed flange is only necessary over support were the bottom flange is in compression. The check of LT-buckling is preformed according to the simplified method, SS-EN 1993-1-4 5.4.2.1.

$\alpha_{LT} := 0.76$ — Stainless steel, SS-EN 1993-1-4 Table 5.3

$l_{cr.support} = 4\ m$ — Distance between the cross-beams

$b_f := b_{bf}\left(X_{check\_m\_midsup}\right) = 640\ mm$ — Width of lower flange

$t_f := t_{bf}\left(X_{check\_m\_midsup}\right) = 37\ mm$ — Thickness of lower flange

$E_s = 200\ GPa$ — Modulus of elasticity

$f_{ybf} = 450\ MPa$ — Proof strength

$I_{zb} := \frac{b_f^{3} \cdot t_b}{12} = 0.001\ m^4$ — Moment of inertia, lower flange

$N_{crLT} := \frac{\pi^2 \cdot E_s \cdot I_{zb}}{l_{cr.support}^{2}} = 107802\ kN$ — Critical buckling load

$\lambda_{LT\_b} := \sqrt{\frac{b_f \cdot t_b \cdot f_{ybf}}{N_{crLT}}} = 0.327$ — SS-EN 1993-1-4 5.4.2.1 Equation 5.9

$\Phi_{LT\_b} := 0.5 \cdot \left(1 + \alpha_{LT} \cdot \left(\lambda_{LT\_b} - 0.2\right) + \lambda_{LT\_b}^{2}\right) = 0.6$ — SS-EN 1993-1-4 5.4.2.1 Equation 5.7

$\chi_{LT\_b} := min\left(\frac{1}{\Phi_{LT\_b} + \sqrt{\Phi_{LT\_b}^{2} - \lambda_{LT\_b}^{2}}}, 1\right) = 0.904$ = $\chi_{LT}\left(X_{check\_m\_midsup}\right) = 0.904$

SS-EN 1993-1-4 5.4.2.1 Equation 5.6

$h_{w\_b} := h_w\left(X_{check\_m\_midsup}\right) = 1183\ mm$ — Height of web

$t_t := t_{tf}\left(X_{check\_m\_midsup}\right) = 30\ mm$ — Thickness of top flange

$k_{fl} := 1.1$ — Increase in capacity due to simlified method used, SS-EN 1993-1-1 6.3.2.4 (2)B

$\sigma_{Rd.b.LT\_mid} := \frac{k_{fl} \cdot \chi_{LT\_b} \cdot f_{ybf}}{\gamma_{M1}} = 447\ MPa$ = $\sigma_{Rd.b.LT}\left(X_{check\_m\_midsup}\right) = 447\ MPa$

5.7.1 Check of lateral torsional buckling of compressed flange

$\sigma_{s.b.support}(X)$ Stresses in bottom flange from loads during service stage

$\sigma_{Rd.b.LT}(X)$ Capacity of the bottom flange against LT- buckling

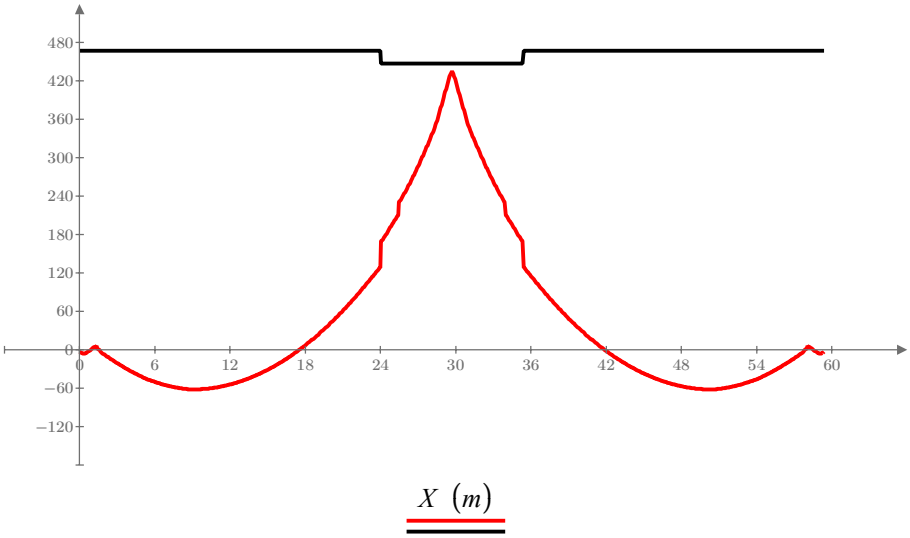

$\sigma_{s.b.support}(X)\ (MPa)$

$\sigma_{Rd.b.LT}(X)\ (MPa)$

$$\eta_{max} := max\left(\frac{\sigma_{s.b.support}(X)}{\sigma_{Rd.b.LT}(X)}\right) = 97\%$$

Maximum utilization rate of LT-buckling of bottom flange over support

6 Fatigue

The check for fatigue of welds and plates is carried out according to SS-EN 1993-2 and SS-EN 1993-1-9 using the lambda method. Fatigue load model 3 gives the worst fatigue effects and are therefore used for the verifications on fatigue.

Bending moment from Fatigue load model 3

$M_{FAT.max}(x)$ Maximum design bending moment from Fatigue load model 3

$M_{FAT.min}(x)$ Minimum design bending moment from Fatigue load model 3

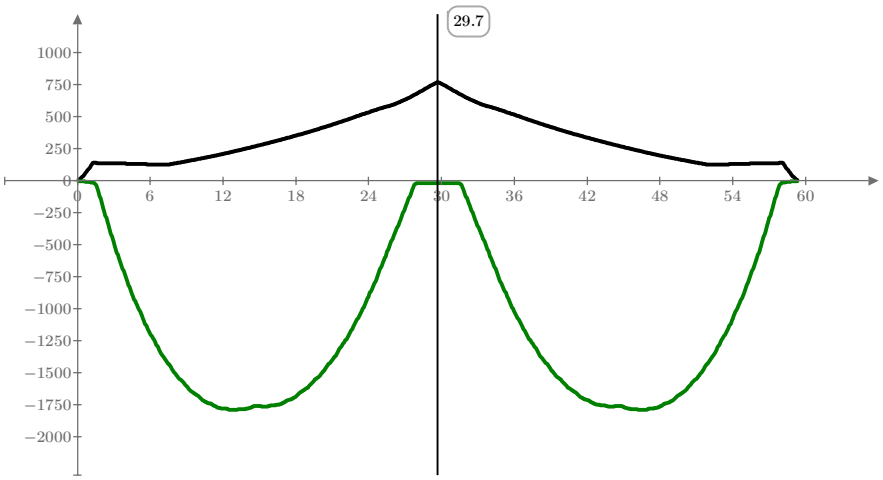

$M_{FAT.max}(X)\ \ (kN \cdot m)$

$M_{FAT.min}(X)\ \ (kN \cdot m)$

Shear force from Fatigue load model 3

$V_{FAT}(x)$ Shear force from Fatigue load model 3

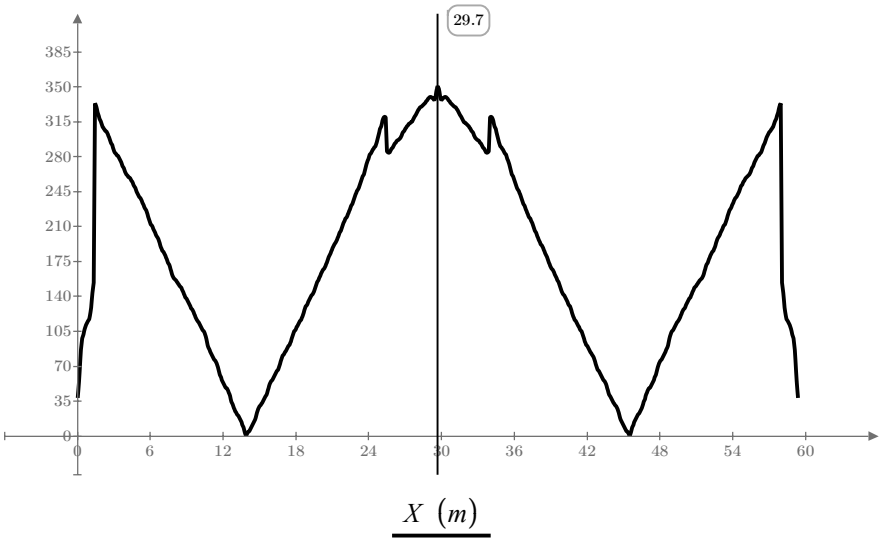

$V_{FAT}(X)\ \ (kN)$

Stress width from Fatigue load model 3

$\Delta\sigma_{e.tf}(x)$ Maximum stress width in the top flange along the length of the beam

$\Delta\sigma_{e.bf}(x)$ Maximum stress width in the bottom flange along the length of the beam

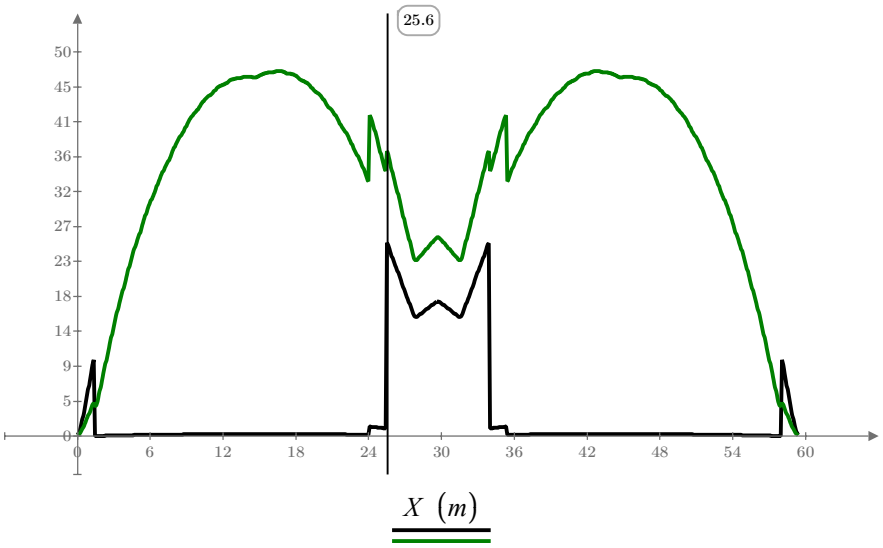

6.1 λ-method

$$\gamma_{Ff} \cdot \Delta\sigma_E < \frac{\Delta\sigma_c}{\gamma_{mf}}$$

$$\Delta\sigma_E = \lambda_f \cdot \phi \cdot \Delta\sigma$$

$\gamma_{Ff} := 1.0$ SS-EN 1993-2 9.3 (1)

$\gamma_{Mf} := 1.35$ SS-EN 1993-1-9 Table 3.1

$L_{span} = \begin{bmatrix} 28 \\ 28 \end{bmatrix} m$ Span length of bridge

$Q_{m1} := 445\ kN$ Krav Brobyggande E.3.1 (f)

$Q_{m1tdok} := 410\ kN$ Krav Brobyggande E.3.1 (f)

$Q_0 := 480\ kN$ SS-EN 1993-2 9.5.2 (3)

$N_{obs} := 0.05 \cdot 10^6$ SS-EN 1991-2 4.6.1 Table 4.5

$N_0 := 0.5 \cdot 10^6$ SS-EN 1993-2 9.5.2 (3)

$N_{year} := 80$

Critical length for shear force SS-EN 1993-2 9.5.2 (b)

$L_{CR.span} := max\left(L_{span}\right) \cdot 0.4 = 11.32\ m$

$L_{CR.sup} := max\left(L_{span}\right)$

$\lambda_{1V.span} := 2.55 - 0.7 \cdot \left(\frac{L_{CR.span} - 10\ m}{70\ m}\right) = 2.54$ Shear force span SS-EN 1993-2 9.5.2 Figure 9.5

$\lambda_{1V.sup} := \left\| \begin{array}{l} \text{if } L_{CR.sup} \le 30\ m \\ \quad j \leftarrow 2.0 - 0.3 \cdot \left(\frac{L_{CR.sup} - 10\ m}{20\ m}\right) \\ \text{else if } L_{CR.sup} > 30\ m \\ \quad j \leftarrow 1.7 + 0.5 \cdot \left(\frac{L_{CR.sup} - 30\ m}{50\ m}\right) \\ j \end{array} \right| = 1.73$ Shear force support SS-EN 1993-2 9.5.2 Figure 9.5

Critical length for moment SS-EN 1993-2 9.5.2 (a)

$L_{CR.span} := max\left(L_{span}\right) = 28.3\ m$

$L_{CR.sup} := \frac{L_{span}(0) + L_{span}(1)}{2} = 28\ m$

$\lambda_{1M.span} := 2.55 - 0.7 \cdot \left(\frac{L_{CR.span} - 10\ m}{70\ m}\right) = 2.37$ Moment in span SS-EN 1993-2 9.5.2 Figure 9.5

$\lambda_{1M.sup} := \left\| \begin{array}{l} \text{if } L_{CR.sup} \le 30\ m \\ \quad \left\| j \leftarrow 2.0 - 0.3 \cdot \left(\frac{L_{CR.sup} - 10\ m}{20\ m}\right) \right. \\ \text{else if } L_{CR.sup} > 30\ m \\ \quad \left\| j \leftarrow 1.7 + 0.5 \cdot \left(\frac{L_{CR.sup} - 30\ m}{50\ m}\right) \right. \\ j \end{array} \right\| = 1.73$ Moment over support SS-EN 1993-2 9.5.2 Figure 9.5

Critical length for reaction forces SS-EN 1993-2 9.5.2 (a)

$L_{CR.sup} := L_{span}(0) + L_{span}(1) = 57\ m$

$\lambda_{1R.sup} := \left\| \begin{array}{l} \text{if } L_{CR.sup} \le 30\ m \\ \quad \left\| j \leftarrow 2.0 - 0.3 \cdot \left(\frac{L_{CR.sup} - 10\ m}{20\ m}\right) \right. \\ \text{else if } L_{CR.sup} > 30\ m \\ \quad \left\| j \leftarrow 1.7 + 0.5 \cdot \left(\frac{L_{CR.sup} - 30\ m}{50\ m}\right) \right. \\ j \end{array} \right\| = 1.97$ Moment over support SS-EN 1993-2 9.5.2 Figure 9.5

$\lambda_2 := \frac{Q_{m1}}{Q_0} \cdot \left(\frac{N_{obs}}{N_0}\right)^{\frac{1}{5}} = 0.58$ SS-EN 1993-2 9.5.2 Equation 9.10

$\lambda_3 := \left(\frac{N_{year}}{100}\right)^{\frac{1}{5}} = 0.96$ SS-EN 1993-2 9.5.2 Equation 9.11

$\lambda_4 := 1.0$ TSFS 2018:57 27ch. $3

$$L_{span} := max\left(L_{span}\right) = 28\ m$$

$$\lambda_{max.span} := \left\| \begin{array}{l} \text{if } L_{span} \le 25\ m \\ \quad \left\| j \leftarrow 2.5 - 0.5 \cdot \left(\frac{L_{span} - 10\ m}{15\ m} \right) \right. \\ \text{else if } L_{span} > 25\ m \\ \quad \left\| j \leftarrow 2.0 \right. \\ j \end{array} \right\| = 2$$

$$\lambda_{max.sup} := \left\| \begin{array}{l} \text{if } L_{span} \ge 30\ m \\ \quad \left\| j \leftarrow 1.8 + 0.9 \cdot \left(\frac{L_{span} - 30\ m}{50\ m} \right) \right. \\ \text{else if } L_{span} < 30\ m \\ \quad \left\| j \leftarrow 1.8 \right. \\ j \end{array} \right\| = 1.8$$

$\lambda_{m.sup} := min\left(\lambda_{1M.sup} \cdot \lambda_2 \cdot \lambda_3 \cdot \lambda_4, \lambda_{max.sup}\right) = 0.97$ SS-EN 1993-2 9.5.2 Equation 9.9

$\lambda_{m.span} := min\left(\lambda_{1M.span} \cdot \lambda_2 \cdot \lambda_3 \cdot \lambda_4, \lambda_{max.span}\right) = 1.32$ SS-EN 1993-2 9.5.2 Equation 9.9

$\lambda_{V.sup} := min\left(\lambda_{1V.sup} \cdot \lambda_2 \cdot \lambda_3 \cdot \lambda_4, \lambda_{max.sup}\right) = 0.97$ SS-EN 1993-2 9.5.2 Equation 9.9

$\lambda_{V.span} := min\left(\lambda_{1V.span} \cdot \lambda_2 \cdot \lambda_3 \cdot \lambda_4, \lambda_{max.span}\right) = 1.42$ SS-EN 1993-2 9.5.2 Equation 9.9

$\lambda_{R.sup} := min\left(\lambda_{1R.sup} \cdot \lambda_2 \cdot \lambda_3 \cdot \lambda_4, \lambda_{max.sup}\right) = 1.1$ SS-EN 1993-2 9.5.2 Equation 9.9

6.1.1 Fatigue in steel parts

Cross-section change - Butt weld between bottom flanges

$X_{check\_fat\_1} := X_{check\_secChange} = 24\ m$ — Location of cross-section change

$k_s(x) := \left(\frac{25\ mm}{t_{bf}(x)}\right)^{0.2}$ — Size effect SS-EN 1993-1-9 7.2.2, due to different thickness of plates

$\Delta\sigma_c := 112\ MPa$ — Fatigue class c112 SS-EN 1993-1-9 Table 8.3 (4)

$\sigma_{max}(x) := \frac{M_{FAT.max}(x)}{I_{y.comp.short}(x)} \cdot \left(h_{beam}(x) + t_{deck} - z_{tp.comp.short}(x)\right)$ — Normal stresses in bottom flange, from max moment

$\sigma_{min}(x) := \frac{M_{FAT.min}(x)}{I_{y.comp.short}(x)} \cdot \left(h_{beam}(x) + t_{deck} - z_{tp.comp.short}(x)\right)$ — Normal stresses in bottom flange, from min moment

$\Delta\sigma_e(x) := \lambda_{m.span} \cdot \left|\sigma_{max}(x) - \sigma_{min}(x)\right|$

$\Delta\sigma_e\left(X_{check\_fat\_1}\right) = 51\ MPa$

$\Delta\sigma_{c.red}(x) := k_s(x) \cdot \frac{\Delta\sigma_c}{\gamma_{Mf}}$ — Fatigue strength SS-EN 1993-1-9 Eq: 7.1

$\Delta\sigma_{c.red}\left(X_{check\_fat\_1}\right) = 76\ MPa$

$\eta_{fat\_1} := \frac{\Delta\sigma_e\left(X_{check\_fat\_1}\right)}{\Delta\sigma_{c.red}\left(X_{check\_fat\_1}\right)} = 66\%$ — Utilization ratio

Joint - Butt weld between bottom flanges

$X_{check\_fat\_2} := 12\ m$ — Location of joint

$k_s(x) := \left(\frac{25\ mm}{t_{bf}(x)}\right)^{0.2}$ — Size effect SS-EN 1993-1-9 7.2.2

$\Delta\sigma_c := 112\ MPa$ — Fatigue class c112 SS-EN 1993-1-9 Table 8.3 (2)

$\sigma_{max}(x) := \frac{M_{FAT.max}(x)}{I_{y.comp.short}(x)} \cdot \left(h_{beam}(x) + t_{deck} - z_{tp.comp.short}(x)\right)$ — Normal stresses in bottom flange, from max moment

$\sigma_{min}(x) := \frac{M_{FAT.min}(x)}{I_{y.comp.short}(x)} \cdot \left(h_{beam}(x) + t_{deck} - z_{tp.comp.short}(x)\right)$ — Normal stresses in bottom flange, from min moment

$$\Delta\sigma_e(x) := \lambda_{m.span} \cdot |\sigma_{max}(x) - \sigma_{min}(x)|$$

$$\Delta\sigma_e(X_{check\_fat\_2}) = 60\ MPa$$

$$\Delta\sigma_{c.red}(x) := k_s(x) \cdot \frac{\Delta\sigma_c}{\gamma_{Mf}}$$ Fatigue strength SS-EN 1993-1-9 Eq: 7.1

$$\Delta\sigma_{c.red}(X_{check\_fat\_2}) = 76\ MPa$$

$$\eta_{fat\_2} := \frac{\Delta\sigma_e(X_{check\_fat\_2})}{\Delta\sigma_{c.red}(X_{check\_fat\_2})} = 79\%$$ Utilization ratio

Lower flange to stiffener in span

$$X_{check\_fat\_3} := 13.4\ m$$ Find the location of the transverse beam that gives the highest stress width

$$\Delta\sigma_c := 80\ MPa$$ Fatigue class c80 SS-EN 1993-1-9 Table 8.4 (7)

$$\sigma_{max}(x) := \frac{M_{FAT.max}(x)}{I_{y.comp.short}(x)} \cdot (h_{beam}(x) + t_{deck} - t_{bf}(x) - z_{tp.comp.short}(x))$$ Normal stresses in bottom flange, from max moment

$$\sigma_{min}(x) := \frac{M_{FAT.min}(x)}{I_{y.comp.short}(x)} \cdot (h_{beam}(x) + t_{deck} - t_{bf}(x) - z_{tp.comp.short}(x))$$ Normal stresses in bottom flange, from min moment

$$\Delta\sigma_e(x) := \lambda_{m.span} \cdot |\sigma_{max}(x) - \sigma_{min}(x)|$$

$$\Delta\sigma_e(X_{check\_fat\_3}) = 59\ MPa$$

$$\Delta\sigma_{c.red}(x) := \frac{\Delta\sigma_c}{\gamma_{Mf}}$$ Fatigue strength SS-EN 1993-1-9 Eq: 7.1

$$\Delta\sigma_{c.red}(X_{check\_fat\_3}) = 59\ MPa$$

$$\eta_{fat\_3} := \frac{\Delta\sigma_e(X_{check\_fat\_3})}{\Delta\sigma_{c.red}(X_{check\_fat\_3})} = 100\%$$ Utilization ratio

Effect of studs at top flange

$$X_{check\_fat\_4} := X_{check\_max.tf} = 25.5\ m$$ Location with largest stress width at top flange

$$\Delta\sigma_c := 80\ MPa$$ Fatigue class c80 SS-EN 1993-1-9 Table 8.5 (9)

$$\sigma_{max}(x) := \frac{M_{FAT.max}(x)}{I_{y.comp.short}(x)} \cdot (t_{deck} - z_{tp.comp.short}(x))$$ Normal stresses in bottom flange, from max moment

$$\sigma_{min}(x) := \frac{M_{FAT.min}(x)}{I_{y.comp.short}(x)} \cdot (t_{deck} - z_{tp.comp.short}(x))$$ Normal stresses in bottom flange, from min moment

$$\Delta\sigma_e(x) := \lambda_{m.span} \cdot |\sigma_{max}(x) - \sigma_{min}(x)|$$

$$\Delta\sigma_e\left(X_{check\_fat\_4}\right) = 33\ MPa$$

$$\Delta\sigma_{c.red}(x) := \frac{\Delta\sigma_c}{\gamma_{Mf}}$$ Fatigue strength SS-EN 1993-1-9 Eq: 7.1

$$\Delta\sigma_{c.red}\left(X_{check\_fat\_4}\right) = 59\ MPa$$

$$\eta_{fat\_4} := \frac{\Delta\sigma_e\left(X_{check\_fat\_4}\right)}{\Delta\sigma_{c.red}\left(X_{check\_fat\_4}\right)} = 56\%$$ Utilization ratio

6.1.2 Fatigue in welds

Check at support

$$X_{check\_fat\_5} := X_{check\_m\_midsup} = 29.7\ m$$

Check bottom flange fillet weld, web

$$a := a_{weld.bot} = 7\ mm$$

$$\Delta\tau_{c\_ll\_tab} := 100\ MPa$$ Fatigue class c80 m=5 SS-EN 1993-1-9 Table 8.2 (5)

$$\Delta\tau_{e\_ll}(x) := \frac{V_{FAT}(x) \cdot S_{bw\_short.sup}(x) \cdot \lambda_{V.sup}}{I_{y.comp.short}(x) \cdot 2 \cdot a}$$ Shear stresses in weld

$$\Delta\tau_{e\_ll}\left(X_{check\_fat\_5}\right) = 18.1\ MPa$$

$$\Delta\tau_{c\_ll} := \frac{\Delta\tau_{c\_ll\_tab}}{\gamma_{Mf}} = 74\ MPa$$ Fatigue strength SS-EN 1993-1-9 Eq: 7.1

$$\eta_{fat\_5} := \frac{\Delta\tau_{e\_ll}\left(X_{check\_fat\_5}\right)}{\Delta\tau_{c\_ll}} = 24\%$$ Utilization ratio

Vertical load on web

$$\Delta\tau_{c\_L} := 100\ MPa$$ Fatigue class c36 m=3 SS-EN 1993-1-9 Table 8.5 (8)

$$\Delta\sigma_{c\_L} := 100\ MPa$$ Fatigue class c36 m=3 SS-EN 1993-1-9 Table 8.5 (8)

$$b_{bearing} := 535\ mm$$ Width of bearing plate

$$R := 510\ kN$$ Reaction force from Fatigue load model 3

$$\Delta\sigma_L := \frac{R}{2 \cdot \sqrt{2} \cdot a \cdot b_{bearing}} = 48\ MPa$$ Normal stresses perpendicular to weld

$\Delta\tau_L := \Delta\sigma_L = 48\ MPa$ Shear stresses perpendicular to weld

$\Delta\sigma_{wf} := \lambda_{R.sup} \cdot \sqrt{\Delta\sigma_L^{\,2} + \Delta\tau_L^{\,2}} = 75\ MPa$ SS-EN 1993-1-9 5 (6)

$\eta_{fat\_6} := \frac{\Delta\sigma_{wf}}{\Delta\sigma_{c\_L}} = 75\%$ Utilization ratio

$\eta_{fat\_7} := \left(\frac{\Delta\sigma_{wf}}{\Delta\sigma_{c\_L}}\right)^3 + \left(\frac{\Delta\tau_{e\_ll}\left(X_{check\_fat\_5}\right)}{\Delta\tau_{c\_ll}}\right)^5 = 42\%$ Utilization ratio

6.1.3 Fatigue utilization

$\eta_{fat\_1} = 66\%$ Check cross-section change, butt weld between bottom flanges

$\eta_{fat\_2} = 79\%$ Check joint in span, butt weld between bottom flanges

$\eta_{fat\_3} = 100\%$ Check lower flange to stiffener in span

$\eta_{fat\_4} = 56\%$ Check effect of studs at top flange

$\eta_{fat\_5} = 24\%$ Check bottom flange to web from shear forces, at internal support

$\eta_{fat\_6} = 75\%$ Check bottom flange to web from reaction forces, at internal support

$\eta_{fat\_7} = 42\%$ Check combined shear and normal stresses at internal support

7 Deflection checks - servicability limit state

7.1 Secant modulus of elasticity

The non-linear behavior of stainless steel can be accounted for by using a secant modulus of elasticity.

$$E_{s.ser} = \frac{E_{s.1} + E_{s.2}}{2}$$

$E_{s.1}$ Secant modulus corresponding to the stress in the tensile flange (bottom)

$E_{s.2}$ Secant modulus corresponding to the stress in the compression flange (top)

$$E_{s.i}(\sigma, f_y, n) := \frac{E_s}{1 + 0.002 \cdot \frac{E_s}{f_y} \cdot \left(\frac{\sigma}{f_y}\right)^n}$$

Equation for calculating the secant modulus (top- or bottom flange)

$SteelGrade := \text{“1.4162”}$

Used stainless steel

$n := 5$

Ramberg- Osgood parameter for the specific steel grade - SS-EN 1993-1-4 Table 4.1.

7.1.1 Calculation of stresses and secant modulus of elasticity

Short-term loads

$$\sigma_{SLS\_tr.tf}(x) := \overrightarrow{\frac{N_{SLS.short}(x)}{A_{comp.short}(x)} + \frac{M_{SLS.short}(x)}{I_{y.comp.short}(x)} \cdot \left(t_{deck} - z_{tp.comp.short}(x)\right)}$$

$$\sigma_{SLS\_tr.bf}(x) := \overrightarrow{\frac{N_{SLS.short}(x)}{A_{comp.short}(x)} + \frac{M_{SLS.short}(x)}{I_{y.comp.short}(x)} \cdot \left(t_{deck} + h_{beam}(x) - z_{tp.comp.short}(x)\right)}$$

$\sigma_{tr.max\_tf} := max\left(\sigma_{SLS\_tr.tf}(X)\right) = 27.02\ MPa$ $\sigma_{tr.max\_bf} := -min\left(\sigma_{SLS\_tr.bf}(X)\right) = 109.32\ MPa$

$$E_{s.defl} := \frac{E_{s.i}\left(\sigma_{tr.max\_tf}, f_{ytf}, n\right) + E_{s.i}\left(\sigma_{tr.max\_bf}, f_{ybf}, n\right)}{2} = 199.92\ GPa$$

Casting loads

Casting load in 1 span

$$\sigma_{SLS\_cast.tf1}(x) := \overrightarrow{\frac{N_{SLS.LC1}(x)}{A_{steel}(x)} + \frac{M_{SLS.LC1}(x)}{I_{y.steel}(x)} \cdot \left(t_{deck} - z_{tp.steel}(x)\right)}$$

$$\sigma_{SLS\_cast.bf1}(x) := \overrightarrow{\frac{N_{SLS.LC1}(x)}{A_{steel}(x)} + \frac{M_{SLS.LC1}(x)}{I_{y.steel}(x)} \cdot \left(t_{deck} + h_{beam}(x) - z_{tp.steel}(x)\right)}$$

$\sigma_{cast.max\_tf1} := max\left(\sigma_{SLS\_cast.tf1}(X)\right) = 242.98\ MPa$ $\sigma_{cast.max\_bf1} := -min\left(\sigma_{SLS\_cast.bf1}(X)\right) = 112.65\ MPa$

$$E_{s.cast1} := \frac{E_{s.i}\left(\sigma_{cast.max\_tf1}, f_{ytf}, n\right) + E_{s.i}\left(\sigma_{cast.max\_bf1}, f_{ybf}, n\right)}{2} = 195.99\ GPa$$

Casting load in 2 span

$$\sigma_{SLS\_cast.tf2}(x) := \overrightarrow{\frac{N_{SLS.LC2}(x)}{A_{steel}(x)} + \frac{M_{SLS.LC2}(x)}{I_{y.steel}(x)} \cdot \left(t_{deck} - z_{tp.steel}(x)\right)}$$

$$\sigma_{SLS\_cast.bf2}(x) := \overrightarrow{\frac{N_{SLS.LC2}(x)}{A_{steel}(x)} + \frac{M_{SLS.LC2}(x)}{I_{y.steel}(x)} \cdot \left(t_{deck} + h_{beam}(x) - z_{tp.steel}(x)\right)}$$

$\sigma_{cast.max\_tf2} := max\left(\sigma_{SLS\_cast.tf2}(X)\right) = 185.5\ MPa$ $\sigma_{cast.max\_bf2} := -min\left(\sigma_{SLS\_cast.bf2}(X)\right) = 86\ MPa$

$$E_{s.cast2} := \frac{E_{s.i}\left(\sigma_{cast.max\_tf2}, f_{ytf}, n\right) + E_{s.i}\left(\sigma_{cast.max\_bf2}, f_{ybf}, n\right)}{2} = 198.93\ GPa$$

$$E_{s.cast} := max\left(E_{s.cast1}, E_{s.cast2}\right) = 198.93\ GPa$$

Permanent loads

$$\sigma_{SLS\_per.tf}(x) := \overrightarrow{\frac{N_{SLS.long}(x)}{A_{comp.long}(x)} + \frac{M_{SLS.long}(x)}{I_{y.comp.long}(x)} \cdot \left(t_{deck} - z_{tp.comp.long}(x)\right)}$$

$$\sigma_{SLS\_per.bf}(x) := \overrightarrow{\frac{N_{SLS.long}(x)}{A_{comp.long}(x)} + \frac{M_{SLS.long}(x)}{I_{y.comp.long}(x)} \cdot \left(t_{deck} + h_{beam}(x) - z_{tp.comp.long}(x)\right)}$$

$$\sigma_{perm.max\_tf} := max\left(\sigma_{SLS\_per.tf}(X)\right) = 16.43\ MPa \qquad \sigma_{perm.max\_bf} := -min\left(\sigma_{SLS\_per.bf}(X)\right) = 84\ MPa$$

$$E_{s.perm} := \frac{E_{s.i}\left(\sigma_{perm.max\_tf}, f_{ytf}, n\right) + E_{s.i}\left(\sigma_{perm.max\_bf}, f_{ybf}, n\right)}{2} = 199.98\ GPa$$

Shrinkage, first order effects

$$\sigma_{SLS\_1.cs.tf}(x) := \overrightarrow{\frac{N_{SLS.1.cs}(x)}{A_{steel}(x)} + \frac{M_{SLS.1.cs}(x)}{I_{y.steel}(x)} \cdot \left(t_{deck} - z_{tp.steel}(x)\right)}$$

$$\sigma_{SLS\_1.cs.bf}(x) := \overrightarrow{\frac{N_{SLS.1.cs}(x)}{A_{steel}(x)} + \frac{M_{SLS.1.cs}(x)}{I_{y.steel}(x)} \cdot \left(t_{deck} + h_{beam}(x) - z_{tp.steel}(x)\right)}$$

$$\sigma_{1.cs.max\_tf} := max\left(\sigma_{SLS\_1.cs.tf}(X)\right) = 14.98\ MPa \qquad \sigma_{1.cs.max\_bf} := -min\left(\sigma_{SLS\_1.cs.bf}(X)\right) = 43.43\ MPa$$

$$E_{s.1.cs} := \frac{E_{s.i}\left(\sigma_{1.cs.max\_tf}, f_{ytf}, n\right) + E_{s.i}\left(\sigma_{1.cs.max\_bf}, f_{ybf}, n\right)}{2} = 200.00\ GPa$$

Shrinkage, second order effects

$$\sigma_{SLS\_2.cs.tf}(x) := \overrightarrow{\frac{N_{SLS.2.cs}(x)}{A_{steel}(x)} + \frac{M_{SLS.2.cs}(x)}{I_{y.steel}(x)} \cdot \left(t_{deck} - z_{tp.steel}(x)\right)}$$

$$\sigma_{SLS\_2.cs.bf}(x) := \overrightarrow{\frac{N_{SLS.2.cs}(x)}{A_{steel}(x)} + \frac{M_{SLS.2.cs}(x)}{I_{y.steel}(x)} \cdot \left(t_{deck} + h_{beam}(x) - z_{tp.steel}(x)\right)}$$

$$\sigma_{2.cs.max\_tf} := max\left(\sigma_{SLS\_2.cs.tf}(X)\right) = 1.79\ MPa \qquad \sigma_{2.cs.max\_bf} := -min\left(\sigma_{SLS\_2.cs.bf}(X)\right) = 10.91\ MPa$$

$$E_{s.2.cs} := \frac{E_{s.i}\left(\sigma_{2.cs.max\_tf}, f_{ytf}, n\right) + E_{s.i}\left(\sigma_{2.cs.max\_bf}, f_{ybf}, n\right)}{2} = 200.00\ GPa$$

Creep

$$\sigma_{SLS\_creep.tf}(x) := \overrightarrow{\frac{N_{SLS.creep}(x)}{A_{comp.long}(x)} + \frac{M_{SLS.creep}(x)}{I_{y.comp.long}(x)} \cdot \left(t_{deck} - z_{tp.comp.long}(x)\right)}$$

$$\sigma_{SLS\_creep.bf}(x) := \overrightarrow{\frac{N_{SLS.creep}(x)}{A_{comp.long}(x)} + \frac{M_{SLS.creep}(x)}{I_{y.comp.long}(x)} \cdot \left(t_{deck} + h_{beam}(x) - z_{tp.comp.long}(x)\right)}$$

$$\sigma_{creep.max\_tf} := max\left(\sigma_{SLS\_creep.tf}(X)\right) = -0.02\ MPa \quad \sigma_{creep.max\_bf} := -min\left(\sigma_{SLS\_creep.bf}(X)\right) = -0.01\ MPa$$

$$E_{s.defl} := \frac{E_{s.i}\left(\sigma_{creep.max\_tf}, f_{ytf}, n\right) + E_{s.i}\left(\sigma_{creep.max\_bf}, f_{ybf}, n\right)}{2} = 200.00\ GPa$$

7.2 Deflection from traffic loads

$\delta_{tr}(X)$ Calculated deflection retrieved from Brigade/Plus

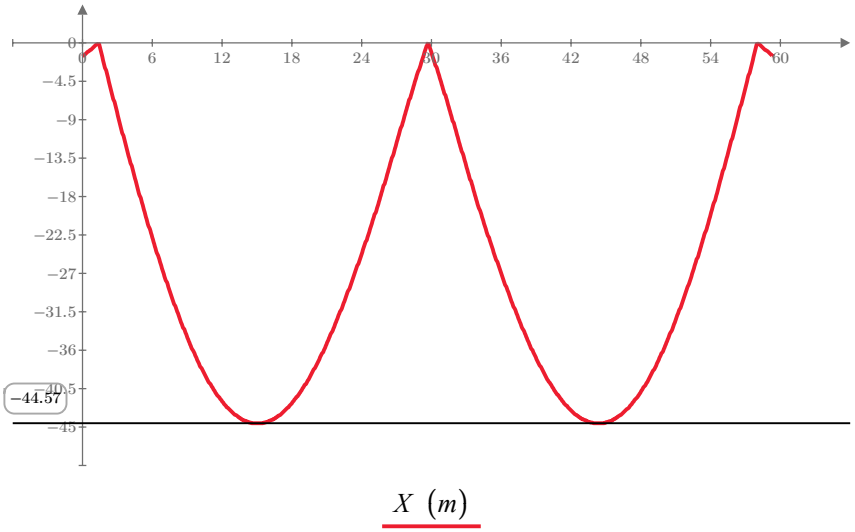

$$\delta_{tr.max} := min\left(\delta_{tr}(X)\right) \cdot \frac{E_s}{E_{s.defl}} = -44.57\ mm$$

Maximum deflection caused by trafic loads

$L_{span} = 28.3\ m$

Span length

$$\delta_{tr.all} := \frac{L_{span}}{400} = 71\ mm$$

Allowed displacement - Krav Brobyggande B.3.4.2.2

$$\eta_\delta := \frac{\left|\delta_{tr.max}\right|}{\delta_{tr.all}} = 63\%$$

Utilization rate - allowed deflection

$$\delta_{tr\_end} := \delta_{tr}(0\ m) \cdot \frac{E_s}{E_{s.defl}} = -1.59\ mm$$

Vertical displacement at free end

$\delta_{tr\_end.all} := 5\ mm$

Allowed vertical displacement at free end
- Krav Brobyggande B.3.4.2.2

if $\left(\left|\delta_{tr\_end}\right| \le \delta_{tr\_end.all}, \text{“OK”}, \text{“NOT OK”}\right) = \text{“OK”}$

7.3 Deflection from long-term loads and shrinkage

$$\delta_{tot}(X) := \delta_{long}(X) \cdot \frac{E_s}{E_{s.perm}} + \delta_{cs}(X) \cdot \frac{E_s}{E_{s.1.cs}}$$

$\delta_{tot}(X)$	Total deflection including weighing of secant modulus of elasticity
$\delta_{long}(X)$	Deflection from permanent loads
$\delta_{cs}(X)$	Deflection from shrinkage

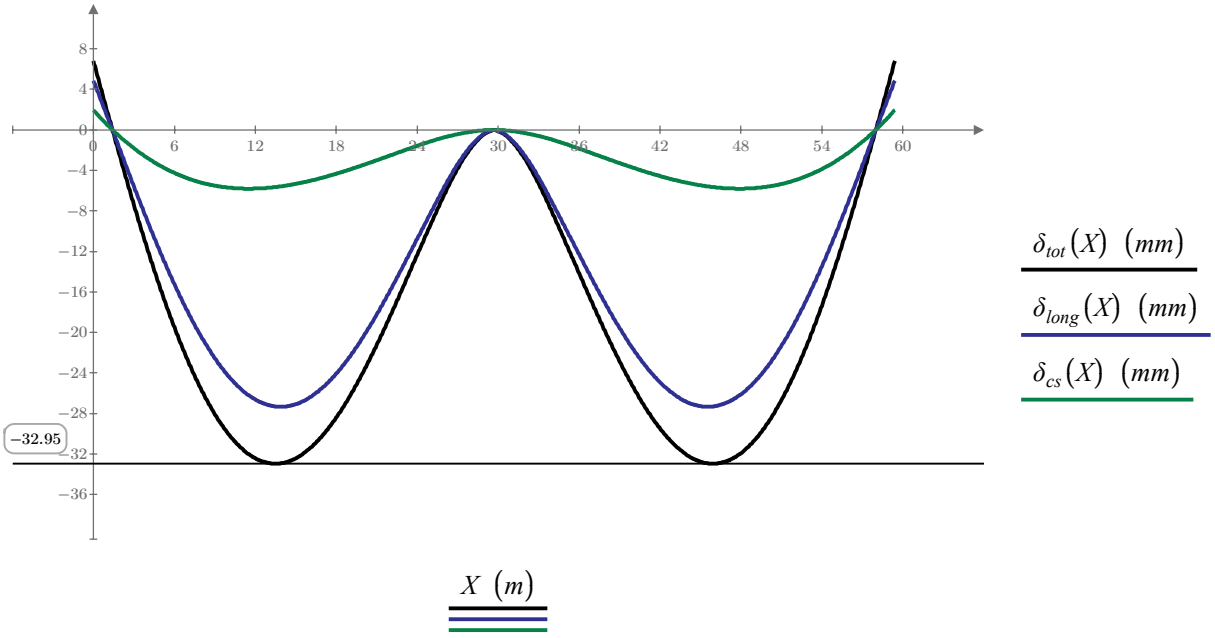

7.4 Deflection from casting loads

$$\delta_{tot}(X) := \delta_{cast}(X) \cdot \frac{E_s}{E_{s.cast}}$$

$\delta_{tot}(X)$	Total deflection including weighing of secant modulus of elasticity
$\delta_{cast}(X)$	Deflection from casting loads

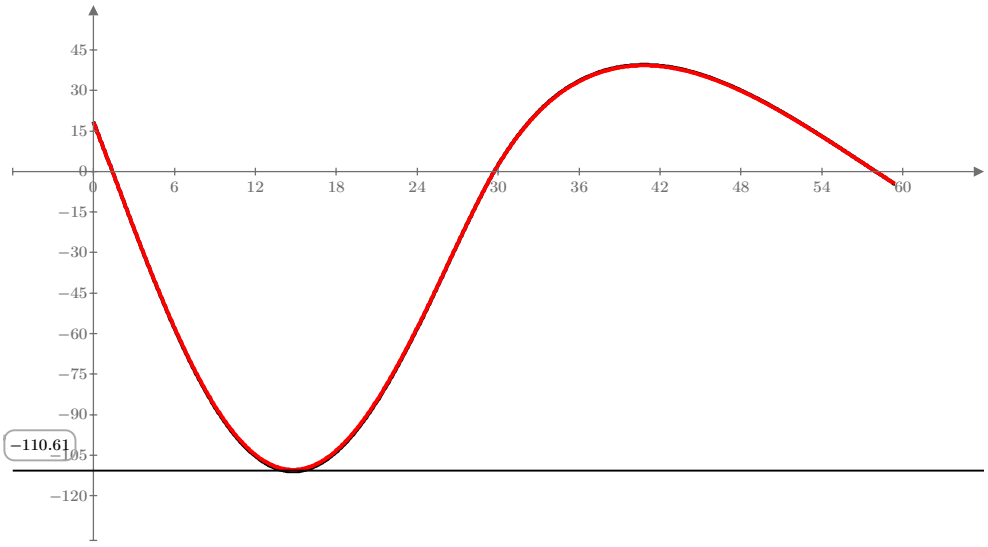

$\delta_{tot}(X)\ \ (mm)$

$\delta_{cast}(X)\ \ (mm)$

$X\ \ (m)$

7.5 Web breathing

The check of web breathing is perfomed on the largest subsection of corrugation.The check is performed according to SS-EN 1993-2, 7.4. Because of the accordion effect of the corrugation $\sigma_{x.ED.ser}$ is set to zero and the shear stresses will be governing for the check of web breathing. The check will therefor only be perfomed over the internal support were the cross-section is assumed to be cracked.

$$Breathing\_check := \left\| \begin{array}{l} \text{if } \frac{h_w\left(X_{check\_m\_span}\right)}{t_w\left(X_{check\_m\_span}\right)} > 30 + 4 \cdot \frac{L_{span}}{m} \\ \quad \left\| out \leftarrow \text{“Check breathing”} \right. \\ \text{else} \\ \quad \left\| out \leftarrow \text{“OK!”} \right. \end{array} \right\| = \text{“OK!”}$$

SS-EN 1993-2 7.4 (2) Eq: 7.5

8 Material savings

The amount of material used for the steel griders using corrugated web in stainless steel are compared to the bridge with flat web in carbon steel.

8.1 Main girder

Savings are presented for the full bridge. The extra length from corrugation are included by a factor that increases the volume of the web.

$V_{flat\_S355} = 3.74\ m^3$ — Steel volume - girder with flat web, S355

$V_{flat\_S460} = 3.28\ m^3$ — Steel volume - girder with flat web, S460

$V_{corrugated} = 3.24\ m^3$ — Steel volume - girder with corrugated web, stainless steel

$m_{flat\_S355} := 7850\ \frac{kg}{m^3} \cdot V_{flat\_S355} = 29.3\ 10^3 \cdot kg$ — Weight of girder - flat web, S355

$m_{flat\_S460} := 7850\ \frac{kg}{m^3} \cdot V_{flat\_S460} = 25.8\ 10^3 \cdot kg$ — Weight of girder - flat web, S460

$m_{corrugated} := 7700\ \frac{kg}{m^3} \cdot V_{corrugated} = 24.9\ 10^3 \cdot kg$ — Weight of girder - corrugated web, stainless steel

Corrugated web in stainless steel compared to flat web in S460

$\eta_{girder} := 1 - \frac{m_{corrugated}}{m_{flat\_S460}} = 3\%$ — Material saving [%] - compared to stainless corrugated web

$\Delta m_{saving\_max} := m_{flat\_S460} - m_{corrugated} = 0.83\ 10^3\ kg$ — Material saving [kg]

Corrugated web in stainless steel compared to flat web in S355

$\eta_{girder} := 1 - \frac{m_{corrugated}}{m_{flat\_S355}} = 15\%$ — Material saving [%] - compared to stainless corrugated web

$\Delta m_{saving\_max} := m_{flat\_S355} - m_{corrugated} = 4.39\ 10^3\ kg$ — Material saving [kg]

E

Stress distribution

E.1 Case study 1

Table E.1: Stresses in flat web in carbon steel S355, h=1250mm

Load	**Top flange [MPa]**	**Bottom flange [MPa]**
Traffic loads	-116.2	137.5
Permanent loads	-116.7	135.3
Temperature loads	-25.7	16.8
1st Shrinkage loads	-17.5	10.2
2nd Shrinkage loads	-20.1	11.7
2nd Creep loads	-28.5	33.0
Total	-324.7 MPa	344.5 MPa

Table E.2: Stresses in flat web in carbon steel S460, h=1250mm

Load	**Top flange [MPa]**	**Bottom flange [MPa]**
Traffic loads	-124.8	170.1
Permanent loads	-124.0	165.4
Temperature loads	-29.5	18.5
1st Shrinkage loads	-20.7	11.9
2nd Shrinkage loads	-22.2	12.7
2nd Creep loads	-29.6	39.4
Total	-350.8 MPa	418.0 MPa

Table E.3: Stresses in corrugated web in stainless steel, h=1250mm

Load	**Top flange [MPa]**	**Bottom flange [MPa]**
Traffic loads	-114.8	166.6
Permanent loads	-114.6	159.3
Temperature loads	-42.6	33.9
1st Shrinkage loads	-22.2	11.0
2nd Shrinkage loads	-21.0	10.4
2nd Creep loads	-25.1	37.1
Total	-340.3 MPa	428.3 MPa

E.2 Case study 2

Table E.4: Stresses in flat web in S355, h=1750mm

Load	**Top flange [MPa]**	**Bottom flange [MPa]**
Traffic loads	-109.5	135.5
Permanent loads	-105.3	127.4
Temperature loads	-25.8	17.1
1st Shrinkage loads	-17.2	10.0
2nd Shrinkage loads	-22.2	12.9
2nd Creep loads	-24.5	29.6
Total	-304.5 MPa	332.5 MPa

Table E.5: Stresses in flat web in S460, h=1750mm

Load	**Top flange [MPa]**	**Bottom flange [MPa]**
Traffic loads	-107.6	169.8
Permanent loads	-103.9	159.9
Temperature loads	-29.1	17.6
1st Shrinkage loads	-21.0	14.6
2nd Shrinkage loads	-23.3	16.3
2nd Creep loads	-23.7	36.5
Total	-308.6 MPa	414.7 MPa

Table E.6: Stresses in corrugated web in stainless steel, h=1750mm

Load	**Top flange [MPa]**	**Bottom flange [MPa]**
Traffic loads	-98.1	172.3
Permanent loads	-93.9	158.9
Temperature loads	-46.4	35.9
1st Shrinkage loads	-25.6	11.8
2nd Shrinkage loads	-22.8	10.5
2nd Creep loads	-18.1	30.7
Total	-304.9 MPa	420.1 MPa

F

Simplified LCA-analysis

Simplified LCA provided by F. Syu (2021-05-21) in collaboration with Master's thesis *Comparative life cycle analysis for bridges made of conventional steel and stainless steel in the early design phases: Developing a parametric multi-perspective approach.*

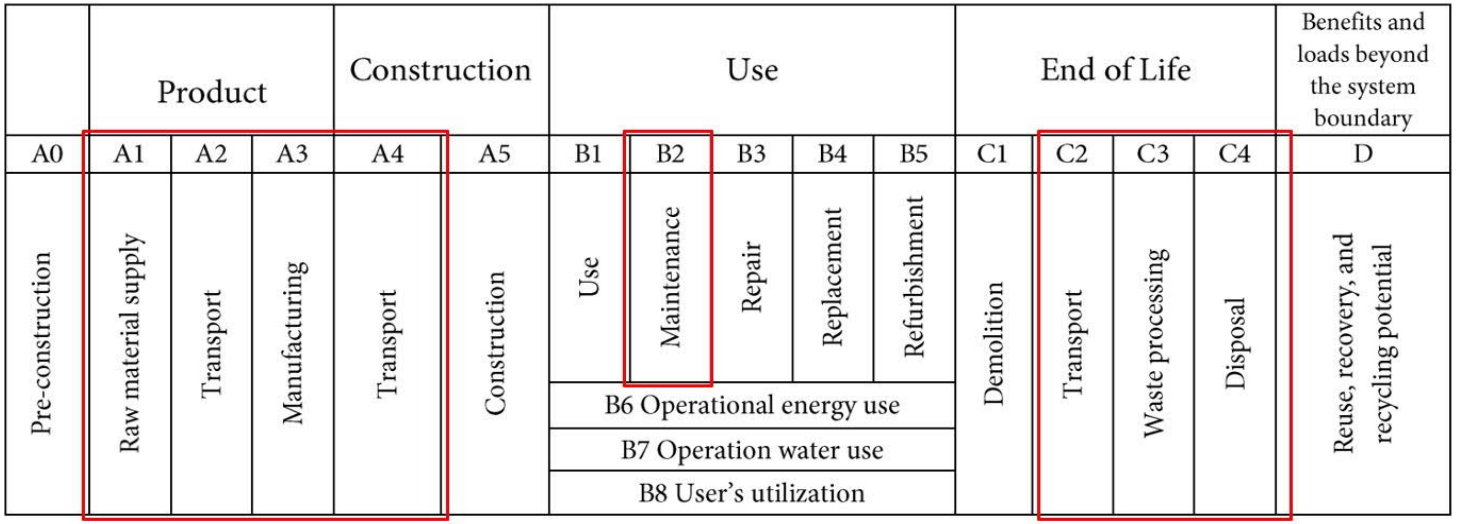

Alternative	Service Year	BridgeLength_m	BridgeSpanLength_m	BridgeWidth_m	Welding_Length_m	Painting_Area_m2
s460	80	59,4	28,3	9,5	238	658
s355	80	59,4	28,3	9,5	238	658
stainless steel	80	59,4	28,3	9,5	270	0

Assumptions

Product stage	Density(kg*m-3)	kg CO2e/kg	Data source:
steel s460_SSAB	7850	2,71	https://www.ssab.com/download-center?dcFilter=environmentalpr&dcSearch#sort=%40customorder%20descending&f:document=[3f0a0e364ca54f74a30faff866bd87ff]
steel s355_SSAB	7850	2,71	https://www.ssab.com/download-center?dcFilter=environmentalpr&dcSearch#sort=%40customorder%20descending&f:document=[3f0a0e364ca54f74a30faff866bd87ff]
stainless steel	7700	2,74	https://www.outokumpu.com/en/sustainability/sustainable-solutions/environmental-product-declarations
steel_reinforcement_bars	7850	0,7	https://klimatkalkyl-pub.ea.trafikverket.se/Klimatkalkyl/Modell
welds_filler metal_s355	7850	2,3	https://link.springer.com/content/pdf/10.1007/s11367-019-01621-x.pdf
welds_filler metal_s460	7850	2,3	https://link.springer.com/content/pdf/10.1007/s11367-019-01621-x.pdf
welds_filler metal_stainless_steel	7700	4,5	https://link.springer.com/content/pdf/10.1007/s11367-019-01621-x.pdf
concrete_plant	2523	0,166	https://klimatkalkyl-pub.ea.trafikverket.se/Klimatkalkyl/Modell
paint	1400	3,41	https://www.epd-norge.no/getfile.php/1316585-1608215319/EPDer/Byggevarer/Maling/NEPD-2596-1317_Hardtop-XP--Jotun-UAE-Ltd--LLC-.pdf

Process	kg CO2e/m	Data source:
welding_steel_s355	4,4	https://link.springer.com/content/pdf/10.1007/s11367-019-01621-x.pdf
welding_steel_s460	6,75	https://link.springer.com/content/pdf/10.1007/s11367-019-01621-x.pdf
welding_stainless_steel	6,09	https://link.springer.com/content/pdf/10.1007/s11367-019-01621-x.pdf

Pickling for stainless steel has been considered in the stainless steel EPD

Construction stage

Transportation	Railway_km	Truck_national_km	Truck_regional_km	Truck_local_km	
steel s460	1000	200	100	40	
steel s355	1000	200	100	40	
stainless steel	1000	200	100	40	
steel_reinforcement_bars	500	300	0	40	
welds_filler metal_s355	0	500	0	0	
welds_filler metal_s460	0	500	0	0	
welds_filler metal_stainless_steel	0	500	0	0	
concrete_plant	0	0	0	35	
paint	0	400	0	40	

Approach	Fuel efficiency	unit	kg CO2e/tkm
Railway	8,33E-05	MWh*tkm	0,001
Truck_national	2,83E-02	L*tkm-1	0,079
Truck_local	7,09E-02	L*tkm-1	0,198
Truck_regional	4,25E-02	L*tkm-1	0,119

Data source: Trafikverket; https://klimatkalkyl-pub.ea.trafikverket.se/Klimatkalkyl/Modell

Use stage

Remedial action		Intervals (Year)	Action time (Year)	Reference Quantity		
Structural member	Description			From	Unit	%
Steel superstructure						
	Paint Improvement		10	Steel External surface area	m^2	10
	Partial repaint		20	Steel External surface area	m^2	20
	Paint Improvement		30	Steel External surface area	m^2	10
	Repaint		40	Steel External surface area	m^2	100
	Paint Improvement		50	Steel External surface area	m^2	10
	Partial repaint		60	Steel External surface area	m^2	30
	Paint Improvement		70	Steel External surface area	m^2	10
Stainless Steele Beams		1	100	If right Quality is used, no paint actions are needed		

Data source: Trafikverket

paint consumption 0,666 kg/m2 https://www.epd-norge.no/getfile.php/1316585-1608215319/EPDer/Byggevarer/Maling/NEPD-2596-1317_Hardtop-XP--Jotun-UAE-Ltd--LLC-.pdf

end of life stage	kg CO2e/kg	Dismantling material	Approach	Fuel efficien unit	kg CO2e/tkm
incineration_paint	3,510	Transportation distance_km	Truck_local	0,07 L*tkm-1	0,20
recycle_concrete	0,016	150			
recycle_asphalt	0,014				
recycle_metal_steel	0,045				
recycle_metal_stainless_steel	0,045				
recycle_metal_reinforcement_bars	0,057				

Data source: Ecoinvent, Trafikverket; https://klimatkalkyl-pub.ea.trafikverket.se/Klimatkalkyl/Modell

Flat web - S460

Indicator Name	Unit	product	construction	use	eol	whole life cycle
Climate_greenhouse_emission_equivalent	kg CO2e	222652	5490	2872	27211	258225

Product stage

Process_Category	Process_Name	kg CO2e
material supply	concrete_plant	74732
material supply	paint	1494
material supply	steel_reinforcement_bars	11764
material supply	steel_s460_2.71kgCO2_SAAB_Nordic	132636
material supply	welds_steel_s460	420
Processing	Welding	1607

Construction stage

Process_Category	Process_Name	kg CO2e
machine_operation	machinary operation	0
transportation	Worker commute	0
transportation	material from market to construction site	5490
transportation	temparary structure return	0

Use stage

Process_Category	Process_Name	kg CO2e
machine_operation	construction machinary	0
transportation	material from market to construction site	33
transportation	replaced elements from site to treatment plant	0
EOL_treatment	treatment of replaced elements	0
material supply	paint	2839

EoI stage

Process_Category	Process_Name	kg CO2e
machine_operation	dismantling operation	0
transportation	dismantling material from bridge site to treatment site	15374
EOL_treatment	incineration_paint	1538
EOL_treatment	recycle_concrete	7139
EOL_treatment	recycle_metal_reinforcement_bars	956
EOL_treatment	recycle_metal_steel	2204

Flat web - S355

Indicator Name	Unit	product	construction	use	eol	whole life cycle
Climate_greenhouse_emission_equivalent	kg CO2e	237152	5694	2872	27626	273344

Product stage

Process_Category	Process_Name	kg CO2e
material supply	concrete_plant	74732
material supply	paint	1494
material supply	steel_reinforcement_bars	11764
material supply	steel_s355_2.71kgCO2_SAAB_Nordic	147695
material supply	welds_steel_s355	420
Processing	Welding	1047

Construction stage

Process_Category	Process_Name	kg CO2e
machine_operation	machinary operation	0
transportation	Worker commute	0
transportation	material from market to construction site	5694
transportation	temparary structure return	0

Use stage

Process_Category	Process_Name	kg CO2e
machine_operation	construction machinary	0
transportation	material from market to construction site	33
transportation	replaced elements from site to treatment plant	0
EOL_treatment	treatment of replaced elements	0
material supply	paint	2839

Eol stage

Process_Category	Process_Name	kg CO2e
machine_operation	dismantling operation	0
transportation	dismantling material from bridge site to treatment site	15539
EOL_treatment	incineration_paint	1538
EOL_treatment	recycle_concrete	7139
EOL_treatment	recycle_metal_reinforcement_bars	956
EOL_treatment	recycle_metal_stainless_steel	2445
EOL_treatment	recycle_metal_steel	8

Corrugated web - stainless steel

Indicator Name	Unit	product	construction	use	eol	whole life cycle
Climate_greenhouse_emission_equivalent	kg CO2e	215096	5365	0	25442	245903

Product stage

Process_Category	Process_Name	kg CO2e
material supply	concrete_plant	74732
material supply	stainless_steel_2.74kgCO2_Outokumpu_Nordic	126040
material supply	steel_reinforcement_bars	11764
material supply	welds_stainless_steel	917
Processing	Welding	1644

Construction stage

Process_Category	Process_Name	kg CO2e
machine_operation	machinary operation	0
transportation	Worker commute	0
transportation	material from market to construction site	5365
transportation	temparary structure return	0

Use stage

Process_Category	Process_Name	kg CO2e
machine_operation	construction machinary	0
transportation	material from market to construction site	0
transportation	replaced elements from site to treatment plant	0
EOL_treatment	treatment of replaced elements	0
material supply	No Material input	0

EoI stage

Process_Category	Process_Name	kg CO2e
machine_operation	dismantling operation	0
transportation	dismantling material from bridge site to treatment site	15274
EOL_treatment	recycle_concrete	7139
EOL_treatment	recycle_metal_reinforcement_bars	956
EOL_treatment	recycle_metal_stainless_steel	2073

Comparison

Alternatives	Unit	product	construction	use	eol	wholeLifeCycle
s460	kg CO2e	222652	5490	2872	27211	258225
s355	kg CO2e	237152	5694	2872	27626	273344
stainless steel	kg CO2e	215096	5365	0	25442	245903

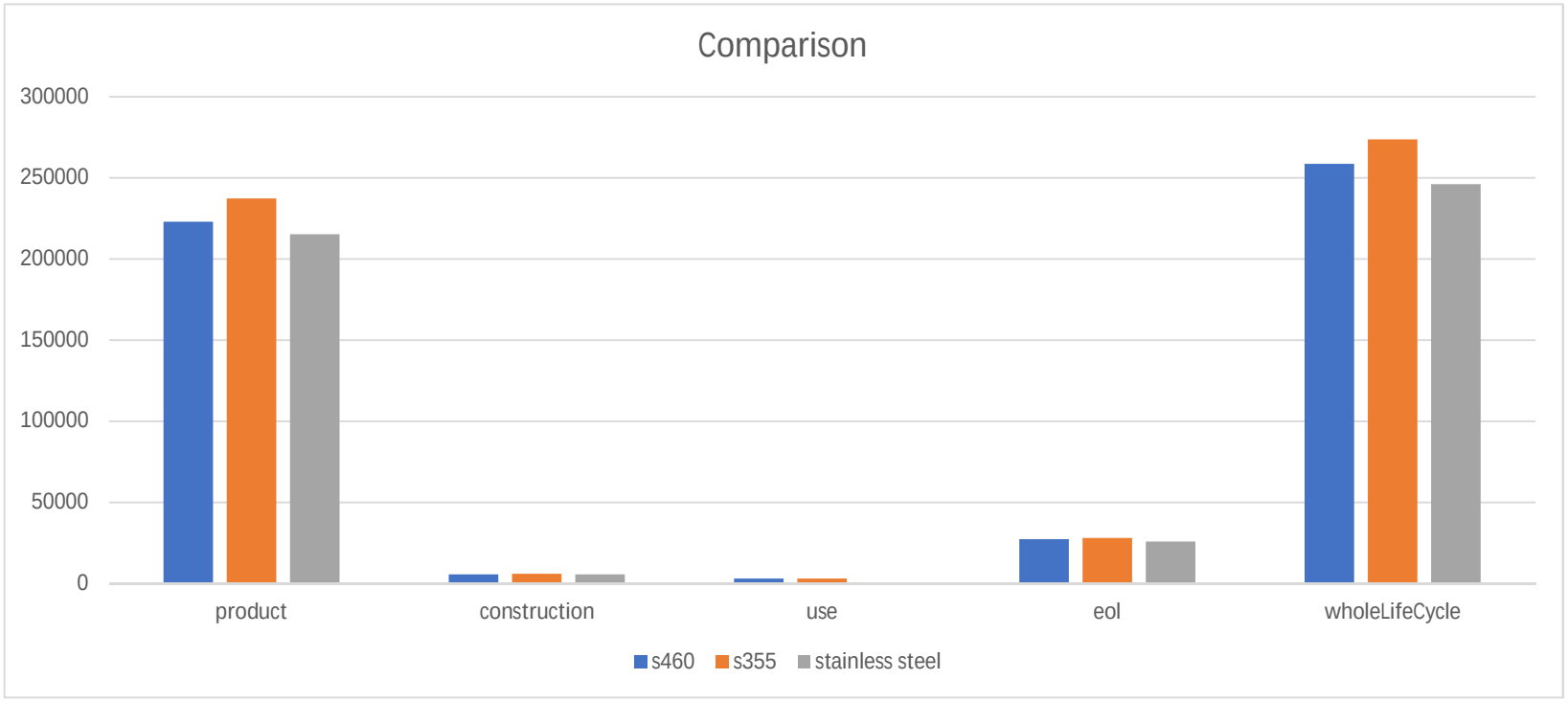

Sensitivity analysis

s460

IndicatorName	Unit	product	construction	use	eol	wholeLifeCycle	carbon emission of steel (kg CO2e/ kg steel S460)	product	constructic	use	eol	wholeLifeCycle
Climate_greenhous	kg CO2e	114488	5490	2872	27211	150061	0,5	76%	4%	2%	18%	100%
Climate_greenhous	kg CO2e	138960	5490	2872	27211	174533	1	80%	3%	2%	16%	100%
Climate_greenhous	kg CO2e	163431	5490	2872	27211	199004	1,5	82%	3%	1%	14%	100%
Climate_greenhous	kg CO2e	187903	5490	2872	27211	223476	2	84%	2%	1%	12%	100%
Climate_greenhous	kg CO2e	212374	5490	2872	27211	247947	2,5	86%	2%	1%	11%	100%
Climate_greenhous	kg CO2e	236846	5490	2872	27211	272419	3	87%	2%	1%	10%	100%
Climate_greenhous	kg CO2e	261317	5490	2872	27211	296890	3,5	88%	2%	1%	9%	100%
Climate_greenhous	kg CO2e	285789	5490	2872	27211	321362	4	89%	2%	1%	8%	100%
Climate_greenhous	kg CO2e	310260	5490	2872	27211	345833	4,5	90%	2%	1%	8%	100%
Climate_greenhous	kg CO2e	334732	5490	2872	27211	370305	5	90%	1%	1%	7%	100%

S355

IndicatorName	Unit	product	construction	use	eol	wholeLifeCycle	carbon emission of steel (kg CO2e/ kg steel S355)	product	constructic	use	eol	wholeLifeCycle
Climate_greenhous	kg CO2e	116707	5694	2872	27626	152899	0,5	76%	4%	2%	18%	100%
Climate_greenhous	kg CO2e	143957	5694	2872	27626	180149	1	80%	3%	2%	15%	100%
Climate_greenhous	kg CO2e	171207	5694	2872	27626	207399	1,5	83%	3%	1%	13%	100%
Climate_greenhous	kg CO2e	198457	5694	2872	27626	234649	2	85%	2%	1%	12%	100%
Climate_greenhous	kg CO2e	225707	5694	2872	27626	261899	2,5	86%	2%	1%	11%	100%
Climate_greenhous	kg CO2e	252957	5694	2872	27626	289149	3	87%	2%	1%	10%	100%
Climate_greenhous	kg CO2e	280207	5694	2872	27626	316399	3,5	89%	2%	1%	9%	100%
Climate_greenhous	kg CO2e	307457	5694	2872	27626	343649	4	89%	2%	1%	8%	100%
Climate_greenhous	kg CO2e	334707	5694	2872	27626	370899	4,5	90%	2%	1%	7%	100%
Climate_greenhous	kg CO2e	361957	5694	2872	27626	398149	5	91%	1%	1%	7%	100%

stainless steel

IndicatorName	Unit	product	construction	use	eol	wholeLifeCycle	carbon emission of steel (kg CO2e/ kg stainless steel)	product	constructic	use	eol	wholeLifeCycle
Climate_greenhous	kg CO2e	112056	5365	0	25442	142863	0,5	78%	4%	0%	18%	100%
Climate_greenhous	kg CO2e	135056	5365	0	25442	165863	1	81%	3%	0%	15%	100%
Climate_greenhous	kg CO2e	158056	5365	0	25442	188863	1,5	84%	3%	0%	13%	100%
Climate_greenhous	kg CO2e	181056	5365	0	25442	211863	2	85%	3%	0%	12%	100%
Climate_greenhous	kg CO2e	204056	5365	0	25442	234863	2,5	87%	2%	0%	11%	100%
Climate_greenhous	kg CO2e	227056	5365	0	25442	257863	3	88%	2%	0%	10%	100%
Climate_greenhous	kg CO2e	250056	5365	0	25442	280863	3,5	89%	2%	0%	9%	100%
Climate_greenhous	kg CO2e	273056	5365	0	25442	303863	4	90%	2%	0%	8%	100%
Climate_greenhous	kg CO2e	296056	5365	0	25442	326863	4,5	91%	2%	0%	8%	100%
Climate_greenhous	kg CO2e	319056	5365	0	25442	349863	5	91%	2%	0%	7%	100%

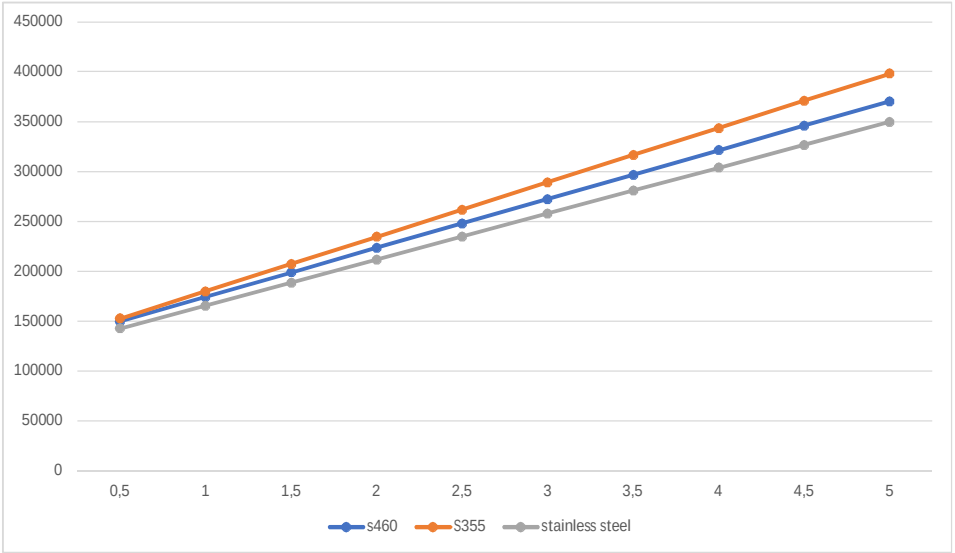

DEPARTMENT OF ARCHITECTURE AND CIVIL ENGINEERING
CHALMERS UNIVERSITY OF TECHNOLOGY
Gothenburg, Sweden 2021
www.chalmers.se

CHALMERS
UNIVERSITY OF TECHNOLOGY